UNIVERSITÀ
DEGLI STUDI
DI PADOVA

Sede Amministrativa: Università degli Studi di Padova

Dipartimento *Territorio e Sistemi Agro-Forestali*

SCUOLA DI DOTTORATO DI RICERCA IN : Territorio, Ambiente, Risorse, Salute
INDIRIZZO : Ecologia
CICLO : XXV

POST-FIRE RESTORATION IN ALPINE ENVIRONMENT: FROM THE MICROSITE TO THE LANDSCAPE

MULTI-SCALE APPROACH FOR THE DEFINITION OF MITIGATION STRATEGIES

Direttore della Scuola : prof. Mario Aristide Lenzi
Coordinatore d'indirizzo : prof. Tommaso Anfodillo
Supervisore : dott. Emanuele Lingua
Correlatore : dott. Raffaella Marzano

Dottorando : Enrico Marcolin

To my family and Franco, a brother for me.

POST-FIRE RESTORATION IN ALPINE ENVIRONMENT: FROM THE MICROSITE TO THE LANDSCAPE:

Multi-Scale Approach for the Definition of Mitigation Strategies

by

Enrico Marcolin

A DISSERTATION

submitted to

University of Padova

in partial fulfillment of
the requirements for the
degree of
Doctor of Philosophy

Presented January 31, 2013

Contents

CHAPTER 5

Chapter 1 – General Introduction

Fire in forest stands is the result of combining fuel availability, meteorological conditions and source of ignition. In many ecosystems, fire plays an important role in regulating and shaping forest structure. In general, fire may cause loss of vegetation, successional change of species, alteration of the resource availability for both fauna and flora (DeBano et al., 1998; Núñez et al., 2008). Fire severity summarizes ecosystem changes (physical, chemical and biological) induced by the passage of fire (White et al., 1996). High severity of fire is strongly correlated with the lack of vegetation cover, enhancing the impact of rainfall on bare soil, leading to runoff and erosion (Cocke et al., 2005). Post-fire regeneration depends on fire severity and environmental constrains such as availability of light, water, nutrients and seeds (Greene et al., 2005). In addition to this, post-fire recovery process of the ecosystems undergoes to the current climate change scenarios of increasing risk of wildfires and others severe disturbances induced by the greater frequency of extreme climatic events (Running, 2006).

Resistance of the ecosystem to the changes and rate of recovery to the pre-fire conditions (resilience) are features to consider for planning post-fire actions (McCann, 2000; Proença et al., 2010). However, evaluating the economic value of the wood, the degrees of hydro-geological risk and the pattern of fire severity, make the range of post-fire interventions rather wide (Beschta et al., 2004; Spanos et al., 2005; Foster and Orwig, 2006; Noss and Lindenmayer, 2006). Post-fire restoration activities should consider several factors, such as the characteristics of vegetation before the event, the concentration of residual ash, mineralization rate affecting the nutrient cycle, climatic factors, the influence of fauna living in the ecosystem (Rosario Nuñez et al., 2003; Hille and den Ouden, 2004; Casady et al., 2009; Puerta-Piñero et al., 2010). Characteristics of the stand affected by fire and restoration objectives should drive to a proper restoration planning. However, restoration activities have been frequently planned without a proper evaluation of ecological and economic consequences (Leverkus et al., 2012). Altering physico-chemical factors of the ecosystem, restoration activities can severely limit vegetation recovery (Beschta et al., 2004; Ordóñez et al., 2005; Noss and Lindenmayer, 2006). Salvage logging (felling and removal of burnt trees) is a common post-fire practice applied worldwide, sometimes coupled to artificial plantations (McIver and Starr, 2001; Beschta et al., 2004; Beghin et al., 2010). In order to keep safety slopes (i.e. tree-fall accidents) and for the extraction of valuable wood products, salvage logging has become the most common post-fire practice. The massive application of salvage logging as exclusive post-fire management practice has been the focus of an intense scientific debate (DellaSala et al., 2006; Noss and Lindenmayer, 2006; Lindenmayer et al., 2008) concerning the ecological consequences of salvage interventions on regeneration establishment and survival (Donato et al., 2006). In this context, restoration practices alternative or complementary to salvage logging emphasize the role of burnt wood in improving the availability of “safe sites”, where regeneration can find positive microclimatic conditions (Purdy et al., 2002; Greene et al., 2007; de Chantal et al., 2009; Legras et al., 2010). The variability in functions, species composition and ecological niches in the forests of the Alps, bonded with a wide range of environmental and

climatic variables, makes it difficult to define the plans of proper mitigation measures. Actually, in the alpine environment there are few information of restoration outcomes, especially in regard to wildfire involving spread surfaces. Recent studies focusing comparisons between active restoration techniques with no intervention strategies, highlighted in these latter a greater efficiency in terms of costs, species diversity and vegetation recovery (Jonášová et al., 2006; Beghin et al., 2010; Leverkus et al., 2012). This research fits into this context bringing further elements of knowledge focused on post-fire management in alpine environment.

The main objectives of this thesis were:

• to analyze post-fire recovery dynamics and their relationship with fire severity and restoration activities;

• to evaluate the role of deadwood on regeneration establishment and survival;

• to assess the impact of different post-fire management practices on forest recovery.

In order to deepen the knowledge on the role of fire towards forest dynamics, this research proposes a series of studies in whom the recovery processes of vegetation are explored through methods of integrated analysis, using different spatial- and temporal-scale approaches (Figure 1.1).

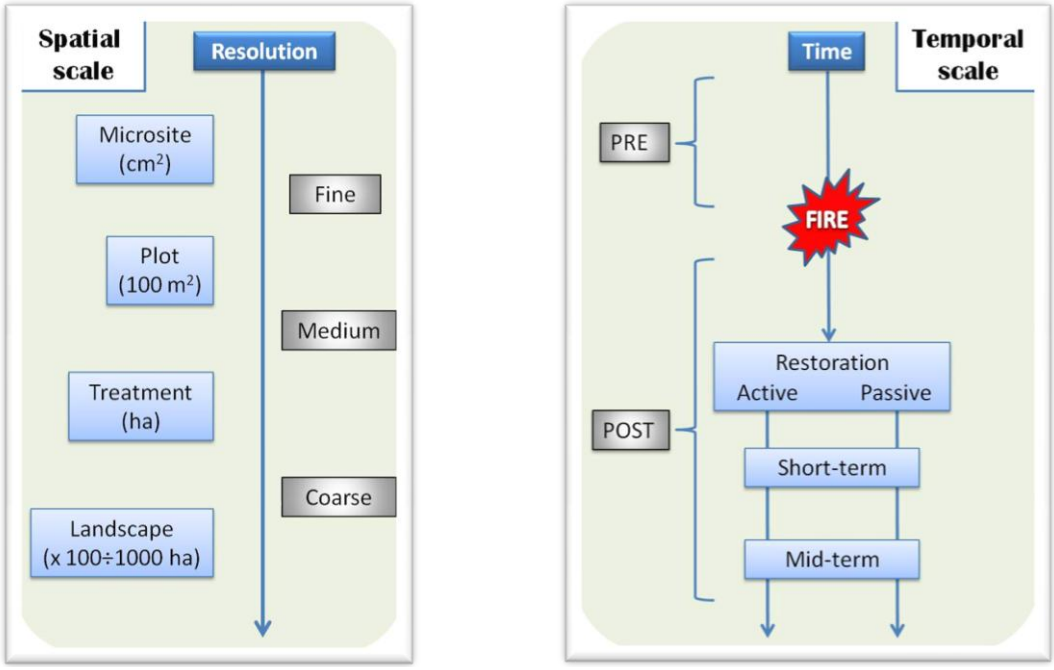

Figure 1.1 - Flowchart resuming the different spatial and temporal scales of analysis approached in the study. Each chapter take advantage of different combinations of investigation scales.

A suitable spatial scale can be potentially identified for a specific process (Levin, 1992), but wildfire typically affects a mountain forest at many scales. Fire severity and seed dispersal capabilities may

define key spatial scales for regeneration (Wiens, 1989), whose recovery relies on patchily distributed biological legacies (Franklin et al., 2000). Aiming at identifying the factors that mostly influence the dynamics of vegetation recovery, a single spatial scale taking into account microsite characteristics, regeneration and environmental patterns in the burnt area could not be selected a-priori. Capability to detect ecological patterns is a function of both the extent and the resolution of an investigation (O'Neill et al., 1988). Since regeneration process is sensitive to several environmental factors at different scales, a multi-scale approach allows to overcome the insufficient information available on actual pattern of vegetation recovery (Wiens, 1989).
The achievement of the targets planned by restoration management implies a post-intervention assessment of the recovery process over the time. Identification at-broad scale of areas with low resilience (high vulnerability) to wildfires or unexpected shifts of species composition over the time, may further improve post-fire restoration actions.

The research has been carried on two study areas located in the Italian Alps where restoration activities were applied after major forest fires. Both fires burnt wide surfaces of pine forests located over slopes southern exposed and characterized by harsh conditions (dry environment with high solar radiation exposure) through the growing season. The two study sites were:

- a forest of *Pinus nigra* and *Pinus sylvestris* situated in the South-Eastern Dolomites (Cellina valley, Friuli Venezia Giulia) where the study focuses on the effects of fire severity and post-fire management on the recovery process in medium-term (Figure 1.3), since the forest fire occurred in 1997;

- a forest of *Pinus sylvestris* located in the Western Alps (Aosta Valley) affected by a wildfire in 2005, enabling to assess, at short term, the effects of restoration activities on regeneration establishment, survival and potential changes in microclimate in the managed areas (Figure 1.2).

This thesis includes four investigations performed following different spatio-temporal approaches (Figure 1.1).

In the second chapter, one of the most wide burnt forest of the Alps is analyzed (Cellina valley). Different scales of investigations allow to gather an overview of the area with punctual observations all over the burnt forest 13 years after the fire and 10 years after the interventions. A broad-scale analysis was carried out by means of Remote Sensing techniques which enabled a spatio-temporal scan of the whole area from the pre-fire conditions (1994) to the 2010.

The third chapter concerns a forest affected by a stand-replacing fire in Aosta valley. The study was performed in permanent monitoring areas where different post-fire restoration practices were applied. The experimental design allowed to combine observations at-microsite scale with sampling descriptions of regeneration processes carried at-treatment scale.

Chapter four includes a Remote Sensing analysis of the burnt area in Aosta valley. Field investigations were combined to a RS-dataset describing at a broad scale the experimental area.

Chapter five concerns an experimental study of the main environmental parameters affecting the regeneration establishment and survival of the site located in Aosta valley. The study reports outcomes of a field campaign performed during summer 2011 among the monitoring areas managed with different post-fire interventions.

Each chapter includes a final discussion of the main results. The study carried in Cellina valley includes the conclusions related to the site as well, whereas “General Conclusions” reports the most relevant outcomes from the whole research, highlighting the different scales of analysis.

Most of analysis were performed using GIS supports on geographic databases provided by Aosta Valley Region and Friuli Venezia-Giulia Region. Investigations at-broad scale used Remote Sensing satellite imagery from Landsat Thematic Mapper (TM) and Enhanced Thematic Mapper plus (ETM+) archives. An airborne LiDAR (laser Light Detection and Ranging) scan of the burnt area in Aosta valley site (summer 2011) provided an additional high-resolution information layer.

Figure 1.2 - Landscape view of the burnt area in the Bourra site (Aosta valley - image taken in 2007).

Figure 1.3 - Views of the burnt area in Cellina valley (images taken in 2010).
(Above) - within the M.te Lupo site an area subjected to passive restoration; there are still visible many standing dead trees.
(Left) - a detailed view of a steep slope subjected to active restoration in the Arcola site.

References

Beghin, R., Lingua, E., Garbarino, M., Lonati, M., Bovio, G., Motta, R., Marzano, R., 2010. *Pinus sylvestris* forest regeneration under different post-fire restoration practices in the northwestern Italian Alps. Ecological Engineering 36, 1365–1372.

Beschta, R.L., Rhodes, J.J., Kauffman, J.B., Gresswell, R.E., Minshall, G.W., Karr, J.R., Perry, D. a., Hauer, F.R., Frissell, C. a., 2004. Postfire Management on Forested Public Lands of the Western United States. Conservation Biology 18, 957–967.

Casady, G.M., Leeuwen, W.J.D., Marsh, S.E., 2009. Evaluating Post-wildfire Vegetation Regeneration as a Response to Multiple Environmental Determinants. Environmental Modeling & Assessment 15, 295–307.

De Chantal, M., Lilja-Rothsten, S., Peterson, C., Kuuluvainen, T., Vanha-Majamaa, I., Puttonen, P., 2009. Tree regeneration before and after restoration treatments in managed boreal Picea abies stands. Applied Vegetation Science 12, 131–143.

Cocke, A.E., Fulé, P.Z., Crouse, J.E., 2005. Comparison of burn severity assessments using Differenced Normalized Burn Ratio and ground data. International Journal of Wildland Fire 14, 189.

DeBano, L., Neary, D., Ffolliott, P., 1998. Fire Effects on Ecosystems. Wiley.

DellaSala, D.A., Karr, J.R., Schoennagel, T., Perry, D., Noss, R.F., Lindenmayer, D., Beschta, R., Hutto, R.L., Swanson, M.E., Evans, J., 2006. Post-fire logging debate ignores many issues. Science 314, 51–2.

Donato, D.C., Fontaine, J.B., Campbell, J.L., Robinson, W.D., Kauffman, J.B., Law, B.E., 2006. Post-wildfire logging hinders regeneration and increases fire risk. Science (New York, N.Y.) 311, 352.

Foster, D.R., Orwig, D. a., 2006. Preemptive and Salvage Harvesting of New England Forests: When Doing Nothing Is a Viable Alternative. Conservation Biology 20, 959–970.

Franklin, J.F., Lindenmayer, D., MacMahon, J.A., McKee, A., Magnuson, J., Perry, D.A., Waide, R., Foster, D., 2000. Threads of Continuity. There are immense differences between even-aged silvicultural disturbances (especially clearcutting) and natural disturbances, such as windthrow, wildfire, and even volcanic eruptions. Conservation in Practice 1, 8–17.

Greene, D.F., Macdonald, S.E., Cumming, S., Swift, L., 2005. Seedbed variation from the interior through the edge of a large wildfire in Alberta. Canadian Journal of Forest Research 35, 1640–1647.

Greene, D.F., Macdonald, S.E., Haeussler, S., Domenicano, S., Noël, J., Jayen, K., Charron, I., Gauthier, S., Hunt, S., Gielau, E.T., Bergeron, Y., Swift, L., 2007. The reduction of organic-layer depth by wildfire in the North American boreal forest and its effect on tree recruitment by seed. Canadian Journal of Forest Research 37, 1012–1023.

Hille, M., Den Ouden, J., 2004. Improved recruitment and early growth of Scots pine (*Pinus sylvestris* L.) seedlings after fire and soil scarification. European Journal of Forest Research 123, 213–218.

Jonášová, M., Van Hees, A., Prach, K., 2006. Rehabilitation of monotonous exotic coniferous plantations: A case study of spontaneous establishment of different tree species. Ecological Engineering 28, 141–148.

Legras, E.C., Vander Wall, S.B., Board, D.I., 2010. The role of germination microsite in the establishment of sugar pine and Jeffrey pine seedlings. Forest Ecology and Management 260, 806–813.

Leverkus, A.B., Puerta-Piñero, C., Guzmán-Álvarez, J.R., Navarro, J., Castro, J., 2012. Post-fire salvage logging increases restoration costs in a Mediterranean mountain ecosystem. New Forests 43, 601–613.

Levin, S.A., 1992. The Problem of Pattern and Scale in Ecology: The Robert H. MacArthur Award Lecture. Ecology 73, 1943–1967.

Lindenmayer, D.B., Burton, P.J., Franklin, J.F., 2008. Salvage Logging and Its Ecological Consequences. Island Press.

McCann, K.S., 2000. The diversity-stability debate. Nature 405, 228–33.

McIver, J.D., Starr, L., 2001. A Literature Review on the Environmental Effects of Postfire Logging. Western Journal of Applied Forestry 16, 159–168.

Noss, F., Lindenmayer, D.B., 2006. Special Section: The Ecological Effects of Salvage Logging after Natural Disturbance. Conservation Biology 20, 946–948.

Núñez, M., Calvo, L., Pando Fernández, V., Bravo, F., 2008. Floristic changes induced by fire on" *Pinus sylvestris*" plantations in northwest of Spain. Investigación agraria. Sistemas y recursos forestales 17, 168–177.

Ordóñez, J.L., Retana, J., Espelta, J.M., 2005. Effects of tree size, crown damage, and tree location on post-fire survival and cone production of *Pinus nigra* trees. Forest Ecology and Management 206, 109–117.

O'Neill, R. V., Milne, B.T., Turner, M.G., Gardner, R.H., 1988. Resource utilization scales and landscape pattern. Landscape Ecology 2, 63–69.

Proença, V., Pereira, H.M., Vicente, L., 2010. Resistance to wildfire and early regeneration in natural broadleaved forest and pine plantation. Acta Oecologica 36, 626–633.

Puerta-Piñero, C., Sánchez-Miranda, a., Leverkus, a., Castro, J., 2010. Management of burnt wood after fire affects post-dispersal acorn predation. Forest Ecology and Management 260, 345–352.

Purdy, B.G., Macdonald, S.E., Dale, M.R.T., 2002. The regeneration niche of white spruce following fire in the mixedwood boreal forest. Silva Fennica 36, 289–306.

Rosario Nuñez, M., Bravo, F., Calvo, L., 2003. Predicting the probability of seed germination in *Pinus sylvestris* L. and four competitor shrub species after fire. Annals of Forest Science 60, 75–81.

Running, S.W., 2006. Climate change. Is global warming causing more, larger wildfires? Science (New York, N.Y.) 313, 927–8.

Spanos, I., Raftoyannis, Y., Goudelis, G., Xanthopoulou, E., Samara, T., Tsiontsis, A., 2005. Effects of Postfire Logging on Soil and Vegetation Recovery in a *Pinus halepensis* Mill. Forest of Greece. Plant and Soil 278, 171–179.

White, J.D., Ryan, K.C., Key, C.C., Running, S.W., 1996. Remote sensing of forest fire severity and vegetation recovery. The International Journal of Wildland Fire 6, 125–136.

Wiens, J.A., 1989. Spatial scaling in ecology. Functional Ecology 3, 385–397.

Chapter 2

Role of fire severity and effects of post-fire restoration in a burnt forest of the Alps: a Remote Sensing analysis.

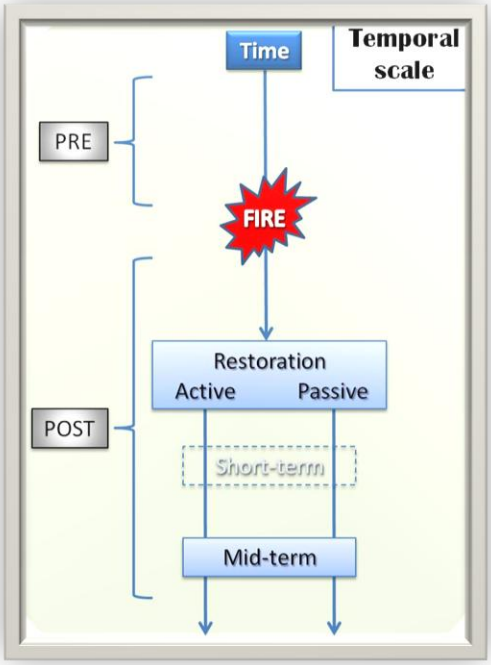

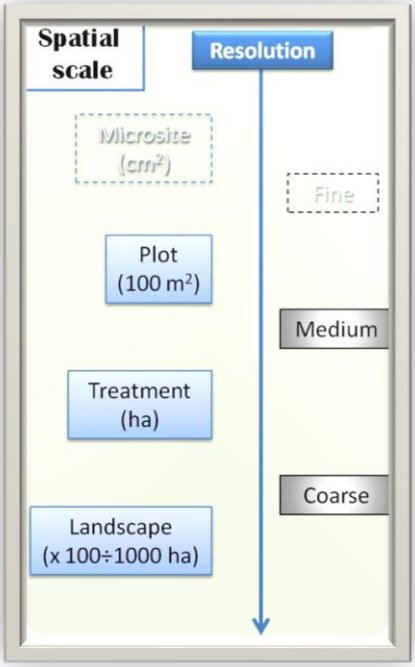

Introduction

In the last centuries, the anthropic activities have led to a diminished importance of natural disturbance as a regulator agent of the forest dynamics in the Alps. Wind-throw, insect pests and fungi attacks usually affect the ecosystems in the Alps at fine-scale; however, in the last decades, mountain areas are more subjected to broad-scale disturbances due to relevant changes of socio-economic, ecological and climatic factors, often acting simultaneously (Ammer, 1996; Schönenberger, 2001; Nagel and Diaci, 2006; Firm et al., 2009). In this context, the fire considered as a disturbance, is increasing in both frequency that on the surface affected per event. In the Alps, fires involving large areas, even if quite rare, are often developed in heterogeneous gradients due to high variability of fuel load, topographical and meteorological conditions as well (Fahnestock and Hare 1964). The degree of change caused by fire in the organic matter of soil and vegetation can be defined as *fire severity*, the impact of fire on the ecosystem (White et al., 1996; Keeley, 2009).

Monitoring fire severity over a forested mountain area could be quite complicated, due to the high spatial and temporal variation of the disturbance: on a broad-scale, remote sensing (RS) has proved to be a helpful tool for screening the effects of fire in many different ecosystems (Caetano et al., 1996; White et al., 1996; Hudak et al., 2007). Field measurements of severity can be combined with spectral information provided by RS, defining a map of fire severity (Key and Benson, 2006; Escuin et al., 2008). Multispectral images from the Landsat TM/ETM+ archives, allow the extraction of Vegetation Indices (VIs), which are indicators of the state of vegetation: several ecological studies used these indices for applications related with vegetation dynamics, and landscape transformations, such as those induced by fire (López-García and Caselles, 1991; Salvador et al., 2000; Isaev et al., 2002; Chafer et al., 2004; Key and Benson, 2005; Miller and Thode, 2007). At a broad-scale, RS imagery supports the estimation of fire-severity and the study of vegetation dynamics after disturbance, with low costs and reliable results (Diaz-Delgado and Pons, 2001; French et al., 2008; Veraverbeke et al., 2010). A clear comprehension of the spatial pattern of severity may facilitate the scheduling of restoration activities: *i.e*. steep slopes affected by high severity of fire require interventions aiming to promote vegetation recovery because of the high hydro-geological risk. An enhanced impact of rainfall on bare soil, often related with the lack of residual vegetation cover, following high severity fire, leads to runoff and erosion (Cocke et al., 2005). However, in the past restoration activities have been frequently planned without a proper evaluation of ecological and economic consequences: altering physico-chemical factors of the ecosystem, restoration activities can limit *de-facto* vegetation recovery (Johnstone and Kasischke, 2005; Johnstone and Chapin, 2006; Mendoza et al., 2009; Beghin et al., 2010). Furthermore, evaluating the economic value of wood, the degrees of hydro-geological risk and the pattern of fire severity, the range of post-fire interventions can be rather wide (Beschta et al., 2004; Spanos et al., 2005; Foster and Orwig, 2006; Lindenmayer and Noss, 2006).

This study investigates the vegetation recovery after a wildfire that affected a pine forest, in the North-Eastern Italian Alps. The dynamics of tree regeneration and the effects of restoration

activities are evaluated through the time, aiming to combine regeneration and environmental measures with RS data, at different scales of investigation. The main goals are:

- to assess fire severity and vegetation response after the fire by means of time-series data from remote sensing images and field data sampling;
- to investigate possible relationships between vegetation indices and ecological/environmental factors involved in the recovery processes;
- to evaluate the effects of restoration activities on forest regeneration dynamics and their environmental implications.

Methods

Study area

The study area is located in Cellina valley on Eastern part of the Italian Alps. In the early spring of 1997 a wildfire, driven by a strong wind blowing from East to West along the Southern slope above Barcis village, burnt around 2300 ha of pine forest (approximate center of study area is 46°11'58"N 12°34'28"E). The altitude of the fire-affected area ranges between 450-1300 m a.s.l. South-East limited by stream Cellina and North-West by rocky peaks of dolomites. Average annual temperature is 9-11 °C with minimum -5 °C (January) and maximum 27 °C (July); average annual precipitation is 2100 mm distributed throughout the year (more than 100 mm/month) with spring and autumn maximum.

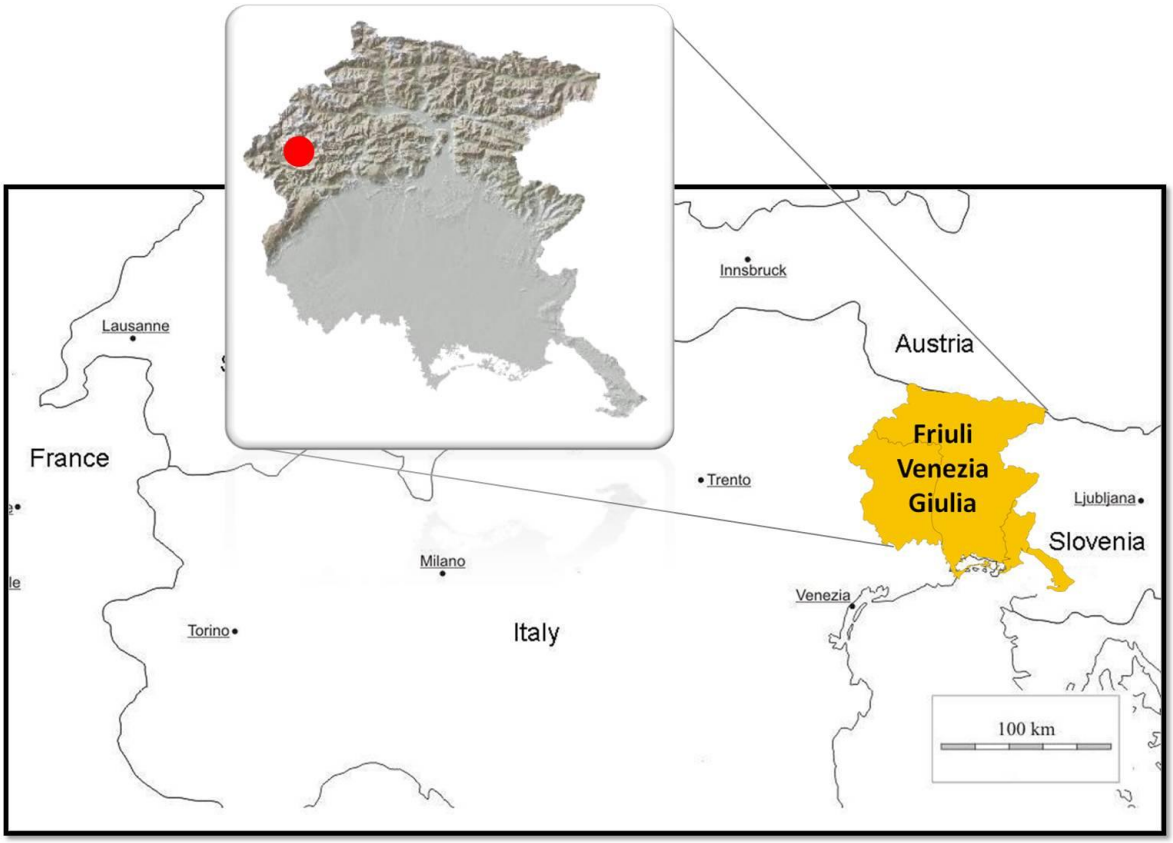

Figure 2.1 - Study area located in Cellina valley (Friuli Venezia-Giulia Region), included in the Eastern Italian Alps.

The most common mineral soil type is calcareous-dolomitic and the soil is permeable, nutrient-poor with shallow depth above the parent rock surface.

The burnt area was mainly a forest dominated by *Pinus nigra* Arnold mixed with *Pinus sylvestris* L. and limited presences of *Fagus sylvatica* L. - *Acer pseudoplatanus* L. (at higher elevation, Northern exposition), *Fraxinus ornus* L. - *Ostrya carpinifolia* Scop. (at lower elevation, Southern exposition).

The *P. nigra* forest colonized the former grazing abandoned in post world war II years, becoming a protection stand with a positive role about the reduction of the soil erosion on the steepest slopes.

After the fire, the local forest department defined the perimeter of burnt area, the ignition point, the daily chronological sequence of the area involved, the burnt and un-burnt forested areas within the perimeter (visually estimated).

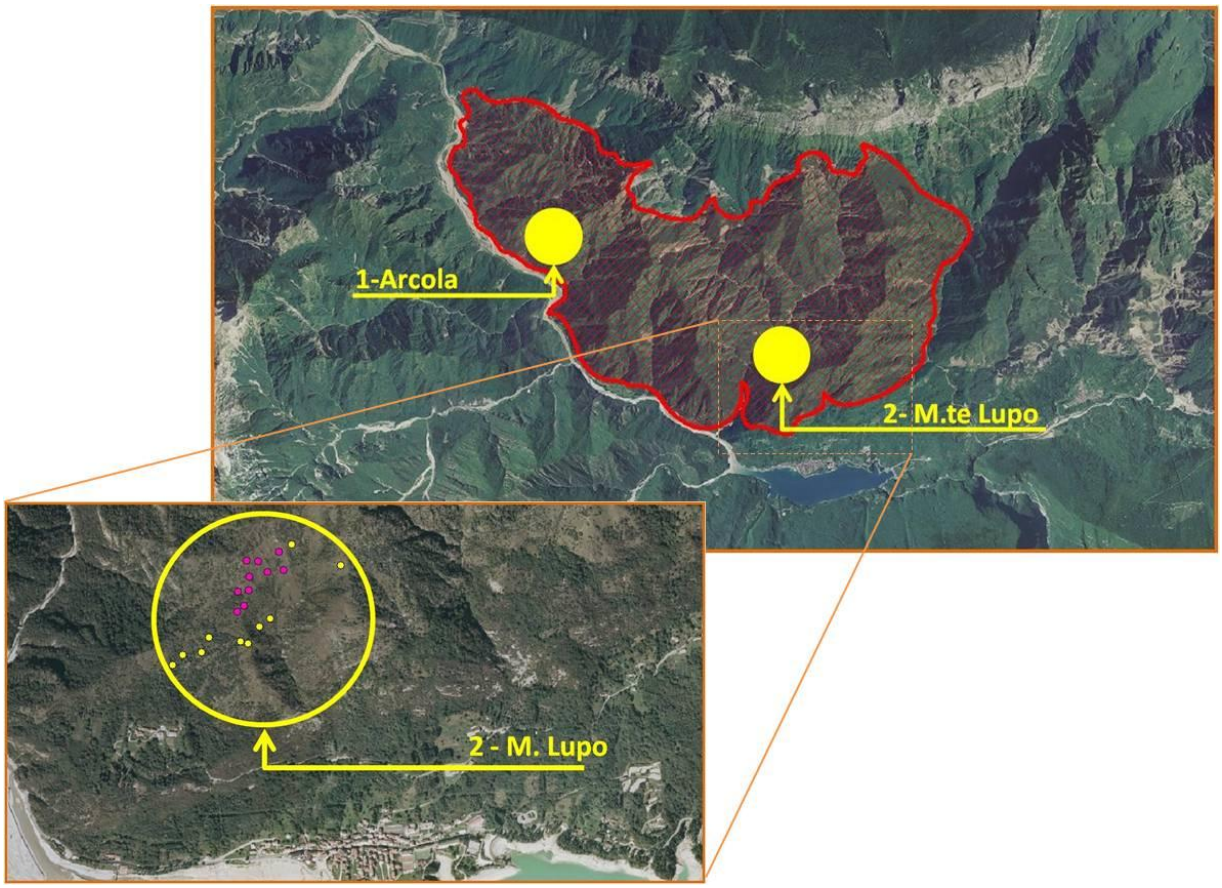

Figure 2.2 - Orthoimages of Cellina valley: perimeters of the burnt area (red line) and restored zones (area I: Arcola, area II: M. Lupo). The zoomed image reports the arrangement of sampling plots within Area II (M.Lupo): yellow - treated, red - control (un-treated).

Data collection

In 2000, two geographically different areas were subject to restoration (area I: Arcola; area II: M.Lupo); salvage logging and seedlings plantation of indigenous species were applied nearby the villages in the steepest slopes affected by high-severity fire.

In summer 2010, a total of forty sampling plots (circular shape, 6 meter radius) were randomly distributed in area I (Arcola) and area II (M. Lupo). Within each area, ten sampling plot were placed in salvaged zones contrasted by ten control plots where no restoration was applied (no-intervention) (Beghin et al., 2010; Jonásová et al., 2010).

Parameters collected at plot-level:

- GPS position of the plot center (sub metric resolution), mainly exposition and slope degrees;
- estimated (to the nearest 5%) ground cover of grasses, shrubs, bare soil and rock exposed, Coarse Wood Debris, Litter;
- dead stumps or snags;
- living trees diameter (DBH > 10 cm), species, height, crown length to the nearest meter, crown radius projection to the ground;
- regeneration characteristics of woody species, seed or sprout origin, height, root collar diameter (RCD) and estimated age; for the sprouting regeneration the number of shoots was counted and the height of tallest shoot per stump measured.

a) b)

c)

d)

Figure 2.3 - images taken in 2010:
a), b) restored areas (treated) with salvage logging and seedlings plantation; c), d) control areas (untreated), no interventions.

Climatic conditions, forest type and mineral soil exposure are factors influencing vegetation response to the disturbance; in addition to this, restoration activities and different levels of fire severity affect post-fire vegetation recovery (Johnstone and Kasischke, 2005; Johnstone and Chapin, 2006). In this context, considering the extension of the forest involved, the Landsat Thematic Mapper (TM) and Enhanced Thematic Mapper (ETM+) multi-spectral satellite scenes, allow a broad-scale investigation. A temporal series of ten multispectral images was acquired from Glovis USGS website (Table 2.1). The images selected ranges between the 1991 and 2010, each taken in the middle of vegetation season (to reduce phenotypic diversity) showing less than 20% cloud-cover, with specific awareness to ensure that the study area was totally cloud-free.

Landsat sensor	Acquisition date	Path/Row
TM	23-Jul-1991	191/028
TM	05-Aug-1993	191/028
TM	23-Jul-1994	191/028
ETM+	15-Sep-1999	191/028
ETM+	23-Aug-2000	192/028
ETM+	28-Jul-2002	192/028
TM	01-Sep-2006	192/028
TM	18-Jul-2007	192/028
TM	17-Aug-2009	191/028
TM	03-Jul-2010	191/028

Table 2.1 - Summary of multispectral image characteristics.

The entire dataset was converted from initial Digital Numbers to At-Surface Reflectance, according to - Chander et al., 2009. The Pseudo Invariant Features structures and methods were applied (Hall et al., 1991; Hill and Sturm, 1991), in order to compare the different images.
A comprehensive examination of the burnt area was conducted through the use of VIs extracted from the multispectral images, aiming to:

- define spatial pattern of fire severity;
- explore through the years the vegetation response to the fire, using a temporal series of multispectral images.

Three groups of VIs were used to assess different levels of fire severity and the relationships of spectral information with regeneration characteristics measured in the sampling plots:

I. Green-leaf indices: group of VIs chosen to evaluate the spectral differential responses of near-infrared (NIR), mid-infrared (SWIR) and photosynthetic active (RED) bands.

- *Normalized Burn Ratio* (NBR): calculated combining NIR and SWIR information (bands 4 and 7 of Landsat TM/ETM+), is used to detect burnt areas (Miller and Yool, 2002; Brewer et al., 2005; Epting et al., 2005; Key & Benson, 2005). NBR values spans between +1 and -1 (positive values in vegetated area, while negative values correspond to bare soil) and

presents a strong inverse correlation with fire severity. At this purpose, the subtraction (dNBR) of post-fire NBR values from pre-fire ones had wide applications for burnt area detection and fire severity investigation (Key and Benson, 2002; Howard and Lacasse, 2004).

$$NBR = \frac{NIR-SWIR}{NIR+SWIR}$$

- *Normalized Difference Vegetation Index* (NDVI): a measure of the photosynthetic 'greenness', was used to evaluate vegetation cover dynamics since the early 1980s (Asrar et al., 1984; Tucker and Sellers, 1986; Wiegand et al., 1991, Woodcock et al., 2001). NDVI has been useful for a long time to assess phenological condition, (Justice et al., 1985; Reed et al., 1994) and monitor vegetation changes in low to moderate density cover, like semi-arid areas (Kerr et al., 1989; Nicholson et al., 1990).

$$NDVI = \frac{NIR-RED}{NIR+RED}$$

- *Soil Adjusted Vegetation Index* (SAVI): the presence of low-density vegetation cover and background noises, like soil brightness and color, plays a relevant role influencing the spectral responses of a vegetated area. SAVI was introduced to mitigate this problem (Huete, 1988): using the same spectral information of NDVI, an adjusting factor in SAVI reduces soil noise throughout a broad range of vegetation density.

$$SAVI = (1 + L)\frac{NIR-RED}{NIR+RED+L}$$

(with L = 0.5)

II. Tasseled cap indices (TC): a combination of spectral information, derived from all Landsat TM/ETM+ bands; TC has been widely-used for temporal investigations of forest disturbances (Kauth and Thomas, 1976; Crist and Cicone, 1984). Taking advantage of sensitivity to the soil and vegetation moisture (Jin and Sader, 2005), TC indices enable to detect forest structure and land cover changes (Cohen and Spies, 1992; Cohen et al., 1995; Franklin et al., 2002;). Differential combinations of TC indices proved to be helpful for stand-replacing and complex patterns disturbances (Healey et al., 2005; Hais et al., 2009; He et al., 2011).

- *Brightness* (Br), *Greenness* (Gr), *Wetness* (Wet): principal components transformation of six Landsat TM and ETM+ bands (Crist and Cicone, 1984; Huang et al., 2002), these three components include most of the spectral information (directly related to the environmental parameters: Br-soil exposed presence, Gr-vegetation cover, Wet-water content).

- *Modified Disturbance Index* (mDI): calculated by subtraction of TC basic components, mDI is used to highlight the spectral differences between live forest and areas affected by high-severity fire (Healey et al., 2006), filtering the Greenness dynamics for mixed severity disturbance (Hais et al., 2009).

$$mDI = Wetness - Brightness$$

III. Forest z-score indices: in order to investigate the probability of a pixel being forested (Huang et al., 2008; Schroeder et al., 2011), an undisturbed forested area was set as training reference-forest (exposition, vegetation cover and density similar to the burnt area): two VIs were calculated in terms of pixel-distance of the burnt area from a reference forest (assuming the training forest as a sort of "normality" condition).

- *Integrated Forest Index* (IFI): a z-score measure of a pixels likelihood of being forested; it has given good results in detecting forest change without prior knowledge of forest type (Huang et al. 2008, 2009, 2010). Extracting IFI values of a disturbed area, allows to identify forest pixels using a procedure of image analysis (Huang et al., 2008; Chen et al., 2011; Schroeder et al., 2011).

$$IFI_p = \sqrt{(\frac{1}{3}\sum_{i=1}^{3} (\frac{b_{pi} - \bar{b}_i}{SD_i})^2}$$

  where: *p* pixel of an image, *i* band (Landsat TM/ETM+ bands: RED-band 3, MIR-band 5 and SWIR-band 7), b_{pi} spectral value for pixel *p*, $\bar{b}_i$ and SD_i mean and standard deviation of forest training pixels on band *i.*

- *Modified Composite Burn Index* (mCBI): we supposed that the use of all spectral information could provide a more detailed map of all vegetation layers involved in the changes (Meng and Meentemeyer, 2011); mCBI merged sensitivity related to vegetation dynamics with the idea of normalized distance from a reference-forest (Huang et al., 2008).

$$mCBI_p = \sqrt{(\frac{1}{5}\sum_{i=1}^{5} (\frac{b_{pi} - \bar{b}_i}{SD_i})^2}$$

  where band *i* and b_{pi} refer to five Landsat TM and ETM+ bands (band 2÷7).

Aiming at comparing multiple image dates, inter-annual noises factors as vegetation phenology and sensor-geometry displacements (sun-surface alignment) can be further reduced with a standardization of VIs (Rondeaux et al., 1996; Wulder et al., 2009); for every year taken into account, all indices were normalized with a rescaling technique to the mean and standard deviation values of a undisturbed pine stand in the same area (Healey et al., 2005; Masek, 2005; Hais et al., 2009):

$$I_r = \frac{I - I_\mu}{I_\sigma}$$

where Ir is a rescaled index value, Iμ, Iσ are the mean and standard deviation of the reference forest index.

Data analysis

An analysis of the fire severity affecting the burnt area was performed using the pre-fire 1994 and post-fire 1999 scenes. At this purpose we used two VIs: NBR, widely used in fire-severity mapping (Epting et al., 2005; Loboda et al., 2007; Escuin et al., 2008), and mCBI:

$$dNBR = NBR_{pre} - NBR_{post} \qquad dmCBI = mCBI_{pre} - mCBI_{post}$$

The mCBI index was introduced in comparing with dNBR performances because, in some study case, dNBR proved a diminished accuracy in discriminating between burnt pixels and un-burnt ones (Wulder et al., 2004; Chen et al., 2011). Subtraction and classification pixel by pixel of the VI values produced two fire severity maps (one for each index) according to three classes: high severity (greater than 1 S.D., but lower than 2 SD), low severity (greater than 0.5 SD, but lower than 1 SD) and no change class (lower than 0.5 SD); values of differential VIs greater than 2 SD were considered outliers.

The map of severity resulting from the dNBR index was compared with the one derived from dmCBI. Validation of indices performances was done by overlapping the severity maps over two different training areas, identified as burnt and un-burnt zones, whose perimeters were defined by ground measurements immediately after the fire.

Using a twenty-meter circular buffer for each sample plot (Figure 2.4), a corresponding VI value was extracted (mean of the neighboring pixels crossed by the buffer plot) and organized in a data matrix (VIs data matrix).

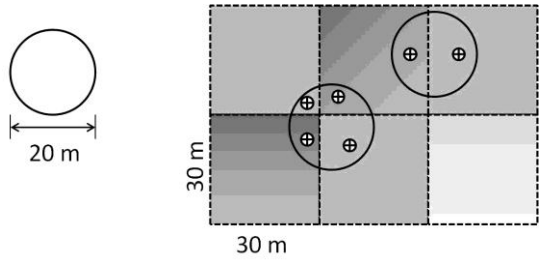

Figure 2.4 - A circular area, with a diameter of 20 meter, located around each sampled plot, was overlapped to VI layer: the VI value assigned to the sampled plot resulted from the average of the extracted values among crossing pixels (the small circles inside each pixel).

The Two-way cluster analysis using Ward's method and Euclidean distance (McCune and Grace, 2002) was applied to this indices matrix to identify possible patterns of similar plots; Spearman rank correlation coefficients were calculated between VIs. Two-way cluster analysis performs two separate cluster analysis: a) looking for similarities of VI values at plot level, b) looking for groups within the VIs (correlations between VIs).

In order to evaluate the vegetation recovery patterns and effects of interventions towards natural regeneration, all forty sampled data plots were analyzed: twenty were grouped as *treated* and twenty as *un-treated*. A second matrix of data included all regeneration variables (seedlings density, number of living sprouts and shoots, age of seedlings, RCD and height). Furthermore, species diversity using Shannon index (Magurran, 2004) and the following structural parameters of

natural regeneration seedlings were considered: height diversity by THD index (Kuuluvainen et al., 1996) with 10-cm horizontal layers, and TDD diameter diversity index (Rouvinen and Kuuluvainen, 2005) applied to 1-cm RCD classes.
A third matrix reported the environmental parameters related to:

- living adult trees: - basal area, trees density and canopy cover - calculated according to USDA-SVS tools (McGaughey, 2002);

- taking into account the particular soil permeability and the prevalent Southern exposition of the burnt area, a *North-ness* index (N_{ness}) was calculated, assuming the north-exposition as the more suitable in terms of water availability for the forest growth (Beers et al., 1966; Elson et al., 2006). Higher values of N_{ness} indicate north-facing slopes, while lower values correspond to Southern exposition.

$$N_{ness} = \cos(aspect) \cdot \tan(slope)$$

- the total amount of incoming solar radiation (direct + diffuse) calculated by GIS tool raster analysis as a direct clear-sky short-wave radiation measurement based on latitude, season, time interval and a DEM (Kumar et al., 1997); the value of seasonal solar radiation was extracted for each sampling plot.

Cluster analysis and Spearman rank correlation were performed to highlight the possible relationships within regeneration and environmental matrix.
VIs, regeneration and environmental matrices were normalized by standard deviation and outliers removed (> ± 2σ).
Assuming the spectral clustering as underlying patterns, a PCA analysis technique was used to explore the relationships between VIs and:

- regeneration variables (PCA-1);
- environmental parameters (PCA-2).

In both analysis, VIs were used as dependent variables, while the regeneration descriptors (in PCA-1) and the environmental variables (in PCA-2) as explanatory variables; VI cluster was used as passive categorical indicator variable.
In order to verify the separation between the groups of VIs-clustered plots, a multi-response permutation procedure - MRPP (Biondini et al., 1988) was performed separately for VIs, regeneration variables and environmental parameters matrices; MRPP is a non-parametric procedure which verifies the hypothesis there shall be any difference between two or more a-priori groups (VIs clusters in our study), while test statistics describe the separation between the groups (McCune and Grace, 2002). Furthermore, overlaying data rank correlations were explored among regeneration, environmental and VIs data.
A Discriminant Analysis classification - DA (Legendre and Legendre, 1998) was performed on the VIs-clustered plots, allowing to classify the entire burnt area into associated pixel groups.

The field-data collected was divided into two groups: treated and untreated plots; a MRPP was applied to assess separation between groups, using a Euclidean distance measure.
VI values, regeneration and environmental variables of plots belonging to different treatments were compared, according to the non-parametric Mann-Whitney W-test (95% confidence level).
The differences between regeneration variables among different treatments were examined using a permutational multivariate analysis of variance (PerMANOVA), with Euclidean distance measures and one fixed factor (Anderson, 2001; McArdle and Anderson, 2001). PerMANOVA allows to apply a nonparametric F-test for differences in mean within-group distances among groups (Peck, 2010).
To evaluate the post-fire dynamics of vegetation recovery, we used the temporal series of VIs between 1991 and 2010 (discontinuous) for each treatment (treated, no intervention).
The ANOVA comparisons with Tukey HSD post hoc test were performed on VIs:

- among contiguous years within each treatment;
- between treatments in the same year.

Processing and editing RS data were supported by ENVI version 4.7 (ITT VIS, 2009). All multivariate analysis (PCA, MRPP, Two-way cluster, PERMANOVA) were conducted using PC-ORD version 6.0 (McCune and Mefford, 2011). Comparison and DA were performed by means of Statgraphics (Statgraphics Centurion XVI, 2010).

Results

Severity map

The ability of VIs in detectingt changes of fire severity, enabled to describe zones associated to different severity levels within the burnt area (Figure 2.5).

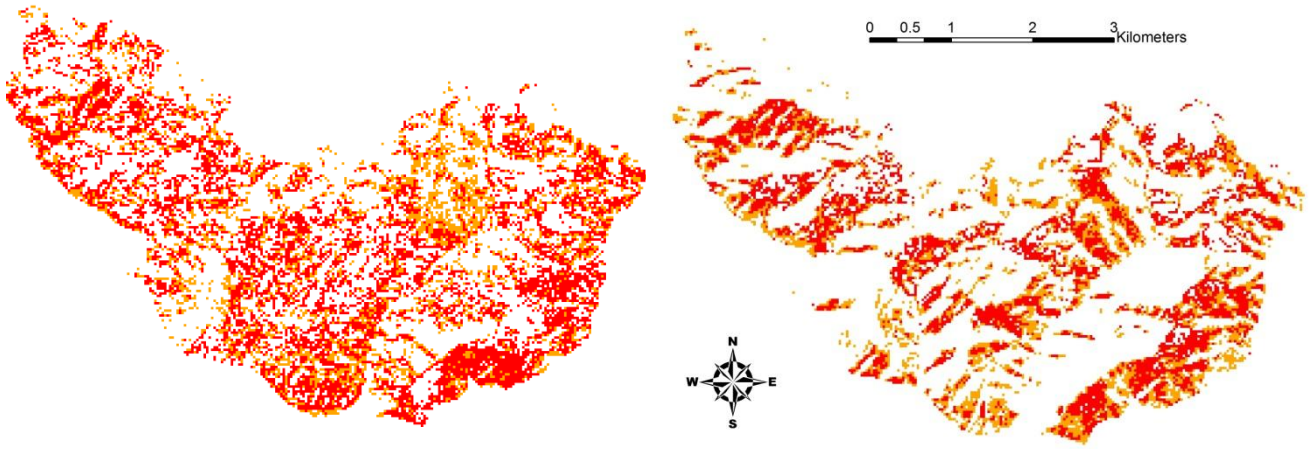

a) b)

Figure 2.5 - Maps of fire severity classified according to 3 levels: no change (white), low severity (orange), high severity (red);
a) dNBR derived, b) dmCBI derived .

The dNBR index classified as burnt pixels 46% of the area delimited by the perimeter, 31% at high severity level; dmCBI allocated as burnt the 34% of total pixels inside the perimeter, 18% at high severity (Table 2.2).

	High severity		Low Severity		No change		tot. surface	
	Greater than 1 SD		Greater than 0.5 SD		Lower 0.5 SD			
	(ha)	(%)	(ha)	(%)	(ha)	(%)	(ha)	(%)
dmCBI	333.0	18.3	285.8	15.7	1204.6	66.1	1823	100.0
dNBR	557.7	30.6	276	15.1	989.6	54.3		

Table 2.2 - Definition of fire severity classes referred to the severity maps built by dNBR and dmCBI.

In the overall statistical, a comparison between the two indices leads to highlight the tendency of dNBR to overestimate the number of pixels classified as burned (Table 2.3). Therefore, within the burnt pixels group, the pixels classified by dNBR as high severity are clearly higher than dmCBI.

		High severity		Low Severity		No change		Total	Correctly classified
		(ha)	(%)	(ha)	(%)	(ha)	(%)	(ha)	(%)
Burnt	dmCBI	7.29	30.6	10.17	42.6	6.39	26.8	23.85	73.2
	dNBR	12.87	54.0	4.41	18.5	6.57	27.5	23.85	72.5
Unburnt	dmCBI	0.63	1.4	0.54	1.2	43.83	97.4	45	97.4
	dNBR	5.13	11.4	6.75	15.0	33.12	73.6	45	73.6

Table 2.3 - Comparison between the ability of fire severity indices to detect burnt and un-burnt pixels over the training areas.

Using the two training areas as ground truth, it was possible to test the ability of discriminating burnt/un-burnt pixels for both severity indices; dNBR showed a higher percentage of commission error in areas unaffected by fire (pixels classified them as burnt areas despite being un-burnt). As previously noticed within the burnt classes, dNBR confirms its tendency to identify as high severity a greater percent of pixels than dmCBI.

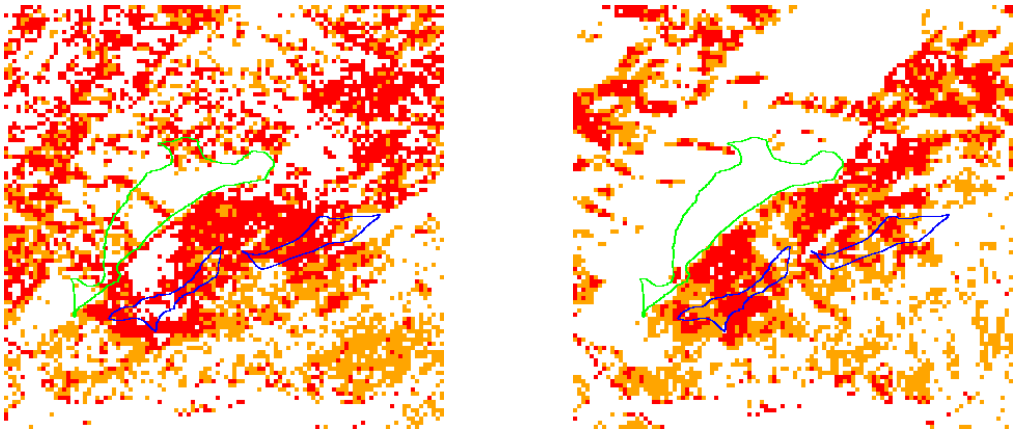

a) b)

Figure 2.6 - Detailed view of the training areas overlapped to the correspondent maps of fire severity: a) dNBR), b) dmCBI. Burnt training area (blue), un-burnt training area (green).

The burnt area diagrams highlighted the range of elevation classes involved by fire, from 500 m (the ignition point) to 1300 m a.s.l. (Figure 2.7, 2.8). Slopes with south, south-west exposure were mostly affected by fire, with high severity spots located mainly around south-facing slopes, while north-facing areas were minimally involved. Both fire-severity maps showed the macro-differences in fire behavior according to the morphology of the slopes (facing exposition), the climatic factors (mainly wind direction) and topographic influence (rock slopes, crossing streams) as spatial constraints as well.

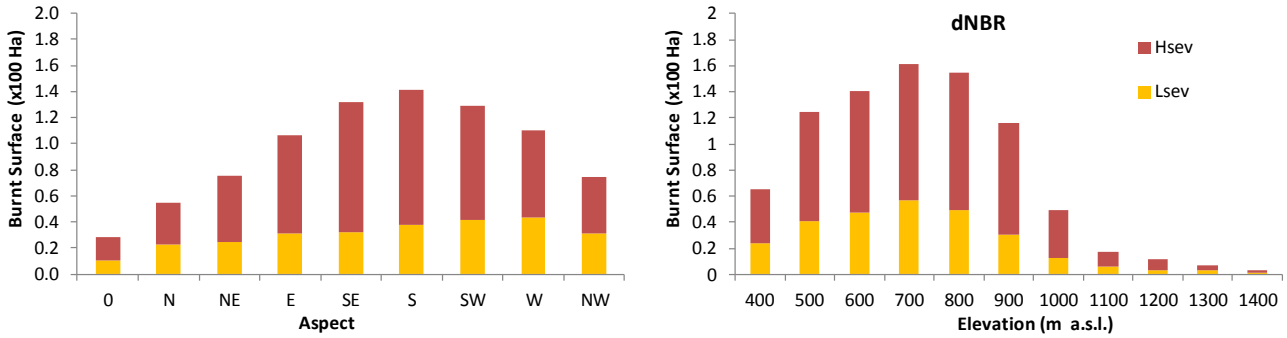

a) b)

Figure 2.7 - Fire severity and extension of burnt area as detected by dNBR index, according to: a) slope exposition, b) altitude classes.

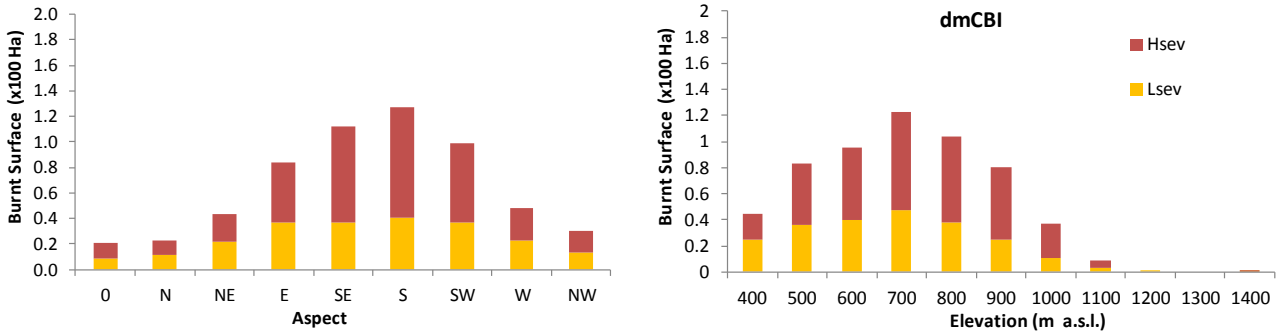

a) b)

Figure 2.8 - Fire severity and extension of burnt area as detected by dmCBI index, according to: a) slope exposition, b) altitude classes.

Vegetation recovery

The cluster dendrogram described as VIs values are arranged according to three spectral clusters Sp1, Sp2, Sp3 (Figure 2.9). A residual information greater than 80% highlights strong similarities among VIs that allow to select five indices as representative for unique spectral information (see VIs similarities in Figure 2.9):

- NDVI, SAVI, Brightness, Grenness: rank correlation $r = 0.88 \div 0.95$, $p < 0.001$;
- mDI, Wetness: rank correlation $r = 0.84$, $p < 0.001$;
- IFI;
- NBR.

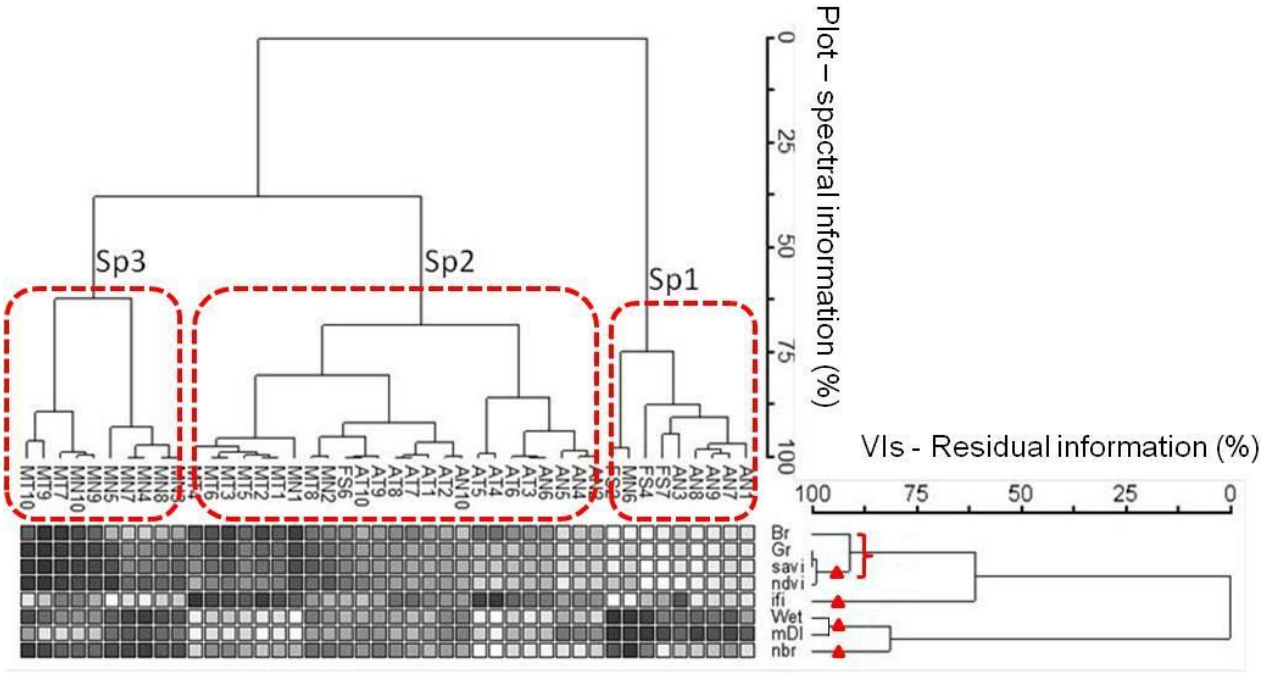

Figure 2.9 - Two-way cluster dendrogram showing the three clusters of plots (Sp1, Sp2, Sp3) as results of common arrangement of the VIs values among the sampled plots. VIs similarities (to the right) allows to restrict the subsequent analysis to five VIs (red triangles), for a acceptable description of the spectral variability: IFI, NBR, mDI, NDVI and SAVI (keeping NDVI and SAVI because of the wide applications in other previous studies).

MRPP procedure with the selected VIs among the three spectral groups (Sp1, Sp2, Sp3), shows a strong and significant separation between groups ($T = -22.0$; $p < 0.0001$) with high within-group homogeneity ($A = 0.42$). In the clustered arrangement of the sampled plots about half of the plots were assigned to Sp2, while the remaining plots were equally divided into Sp1 and Sp3.
Regeneration data referring to each group show:

i. in Sp1, the highest conifer (pine) seedlings density and the lowest values of growth and structural parameters (age, average RCD, TDD, THD);

ii. in Sp2, the highest values of growth (age, average RCD, TDD, THD) and growth variability parameters;

iii. in Sp3, the highest broadleaf seedlings density and the greatest density of shoots and sprouts.

Environmental variables among spectral groups exhibit a greater severity associated with higher burnt wood presence (snags and CWD) in Sp2 and lower tree density and canopy cover; plots assigned to Sp1 manifest the greatest tree density and cover, while a lower value of tree density was associated to the highest incoming radiation values and the lowest radiation variability in Sp3.

Spectral group	Plot (n)	Agemax (years)	NRCfO50 (n/ha)	NRCfU50 (n/ha)	NRBlO50 (n/ha)	NRBlU50 (n/ha)	NSprout (n/ha)	NShoot (n/ha)	Nsp (n)	H' (-)
Sp1	10	7.6[b] (0.5)	3061.9[a] (945.5)	2922.0[a] (924.5)	503.6[b] (133.0)	385.6[b] (212.0)	2391.7[b] (311.4)	9293.1[c] (1432.7)	7.4[a] (0.6)	1.12[b] (0.09)
Sp2	20	9.1[a] (0.3)	1188.6[b] (234.9)	938.5[b] (286.1)	606.7[b] (130.6)	283.0[b] (71.6)	3043.3[b] (293.9)	14371.0[b] (1484.2)	7.7[a] (0.4)	1.54[a] (0.05)
Sp3	10	7.9[b] (0.5)	901.1[b] (160.4)	536.6[b] (141.3)	1843.9[a] (384.6)	553.3[a] (104.2)	3756.9[a] (343.3)	21184.5[a] (1620.2)	7.2[a] (0.4)	1.48[a] (0.05)

Spectral group	Plot (n)	avgDR (cm)	StdDR (cm)	avgHR (cm)	StdHR (cm)	DmCf (cm)	DmBl (cm)	TDD (-)	THD (-)
Sp1	10	1.1[c] (0.1)	0.7[c] (0.1)	61.7[b] (5.9)	34.3[b] (4.9)	1.2[b] (0.1)	1.1[b] (0.2)	0.90[b] (0.09)	1.57[c] (0.10)
Sp2	20	2.3[a] (0.3)	1.7[a] (0.2)	109.2[a] (11.3)	78.3[a] (8.7)	2.9[a] (0.5)	1.5[a] (0.2)	1.29[a] (0.06)	1.72[b] (0.05)
Sp3	10	1.6[b] (0.2)	1.2[b] (0.2)	106.7[a] (7.3)	76.9[a] (5.8)	2.2[a] (0.5)	1.4[a] (0.1)	1.28[a] (0.07)	2.21[a] (0.07)

Table 2.4 - Regeneration characteristics related to each group (mean ± SE): the upper table reports maximum of estimated age (Agemax), density of conifer (NRCf) and broadleaf (NRBl) seedlings, sprouting density (NSprout, NShoot), number of woody species (Nsp), Shannon index (H'). The -O50 and -U50 suffix refer respectively to seedlings taller and shorter than 50cm. In the bottom table avgDR, avgHR are the average of Root collar diametesr RCD and height of seedlings, StdDR and StdHR represent the standard deviation of RCD and height of seedlings, DmCf, DmBl the mean diameter of conifers and broadleaf regeneration, TDD, THD the diversity indices of diameter and height of seedlings. The Plot column reports the total plot score per group. Different letters highlight differences between groups (Mann-Whitney non-parametric comparison, p<0.05).

Spectral group	Plot (n)	Snags (n/ha)	Shrubs (%)	Herbs (%)	CWD (%)	Litter (%)	Soil (%)	BATree (m²/ha)	NTree (n/ha)	TCC (%)
Sp1	10	609.9[b] (195.6)	20.0[a] (2.9)	55.5[a] (4.4)	7.5[b] (0.8)	10.0[a] (1.7)	7.0[b] (1.10)	18.4[a] (4.7)	458.8[a] (135.2)	50.3[a] (11.8)
Sp2	20	1117.5[a] (162.8)	20.0[a] (2.2)	45.6[b] (3.4)	13.1[a] (1.4)	8.3[a] (1.0)	12.9[a] (1.8)	6.8[b] (2.0)	209.7[b] (66.1)	18.6[b] (5.7)
Sp3	10	365.5[c] (156.9)	25.0[a] (2.1)	45.0[b] (3.5)	8.5[b] (1.7)	9.0[a] (1.2)	12.5[a] (2.0)	8.4[b] (3.1)	189.9[b] (85.1)	17.5[b] (5.5)

Spectral group	Plot (n)	Nness (-)	Rad (KWh/m²)	StRad (KWh/m²)	Severity (dNBR)
Sp1	10	-0.37[b] (0.12)	599.6[c] (36.3)	65.19[a] (15.62)	2.41[b] (0.31)
Sp2	20	-0.58[a] (0.04)	661.0[b] (23.7)	60.23[a] (9.26)	3.04[a] (0.13)
Sp3	10	-0.45[b] (0.11)	778.0[a] (9.9)	16.77[b] (3.84)	2.18[b] (0.13)

Table 2.5 - Environmental parameters extracted from the spectral groups (mean ± SE): the upper table includes density of snags, estimated soil cover (Shrubs, Herbs, CWD, Litter, Soil); BAtree, Ntree, TCC represent the basal area, the density and the canopy cover estimate of living trees (DBH > 10 cm). The bottom table reports values of Nness (north-ness exposition index), Rad and StRad (average and standard deviation of incoming solar radiation), Severity (average fire severity according to dNBR map). The Plot column reports the total plot score per group. Different letters highlight differences between groups (Mann-Whitney non-parametric comparison, p<0.05).

All pixels classified as burnt were divided into three groups according to DA procedure, that uses spectral groups (Sp1-3) as classification factors and VIs as variables discriminating among the groups. DA allows to assign the burnt pixels to the spectral groups by means of Classification Function (Table 2.6).

Discriminant Function	Wilks Lambda	P-Value	Classification rate
1	0.108	0.0000	97.8%
2	0.437	0.0000	

Classif. Function / VIs	FC1	FC2	FC3
IFI	-24.57	-24.94	-23.69
SAVI	-4575.8	-4553.5	-4297.4
mDI	-6107.4	-6232.7	-5969.3
NBR	2969.7	2999.9	2924.4
constant	-901.56	-965.45	-944.13

Table 2.6 - (To the left): results from Discriminant Analysis (DA) of VIs amongst three spectral groups (Sp1, Sp2, Sp3). Classification rate shows the percent of pixels exactly classified according to the Classification Functions FC1, FC2, FC3. (To the right): classification functions as resulting from DA. The classification functions are used to determine which Sp-group any individual pixel is most likely to belong to.

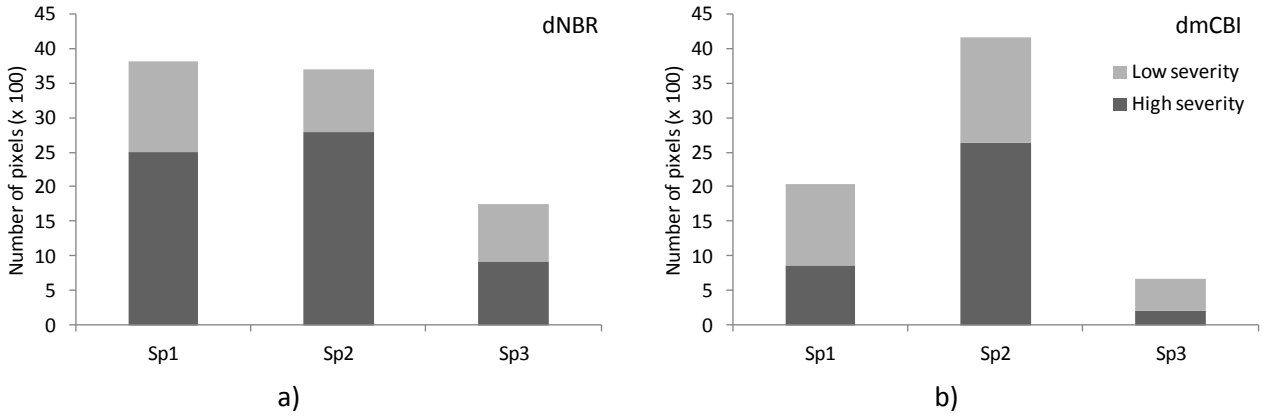

Figure 2.10 - Severity classification of the burnt pixels assigned by DA procedure to the three spectral groups, according to: a) dNBR, b) dmCBI maps .

The burnt pixels assigned to every spectral group were classified into different severity levels overlapping the map of fire severity (Figure 2.10). The results highlight group two (Sp2) as the largest in terms of number of burnt pixels and severity level as well. Sp3 appears minimally involved in the burnt area. Different performances of severity indices (dNBR, dmCBI) were connected to sensitivity: the discrimination previously noticed in burnt/un-burnt validation (Table 2.2), linked to dNBR tendency of identifying a higher number of burnt pixel, as in Sp1 and Sp3 cases.

Relationships between VIs and regeneration data has been explored with PCA tool (PCA1): the first two components showed significant correlations of mDI (r = 0.83), IFI (r = - 0.93) and NBR (r=

0.79) with the secondary axis, while, NDVI (r=-0.98), SAVI (r=-0.99) were negative correlated with the first axis. The first two axes explain the 95% of total variation. PCA1 biplot suggests strong positive correlations between NDVI and SAVI indices, while a negative correlation was noticed for IFI and mDI. The first component was related to the density of pine seedlings (NCf), number of shoots (Nshoot - sprouting regeneration) whereas the second resumed the variations of broadleaf seedlings (NBl).

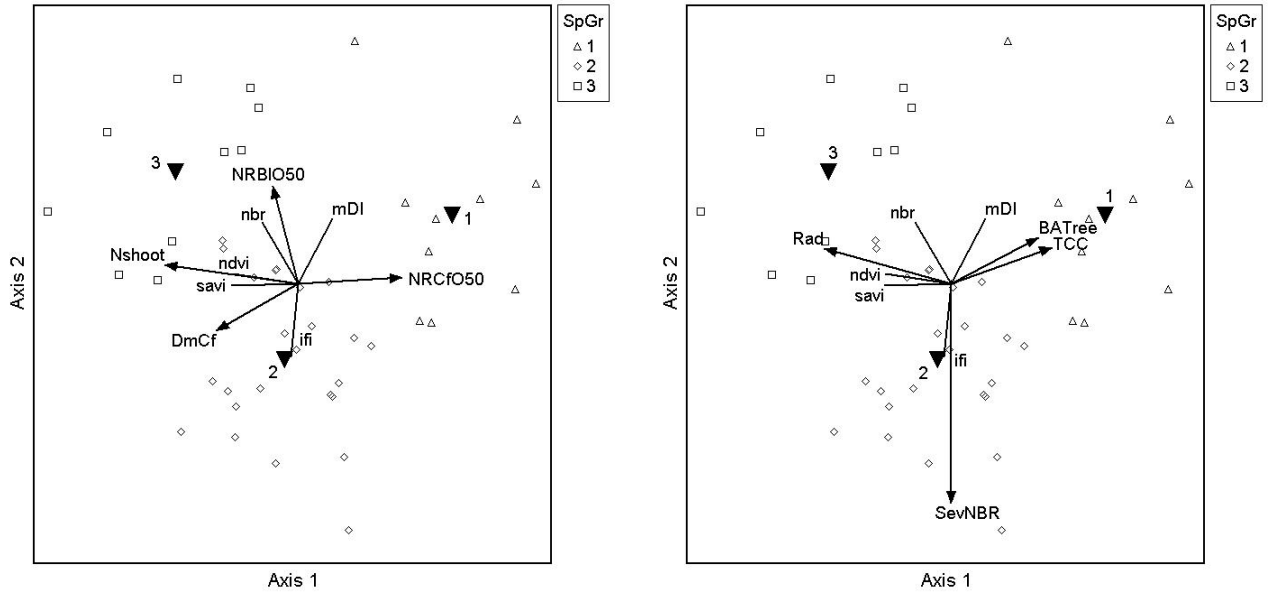

Figure 2.11 - a) PCA1: VIs and regeneration variables, NRCfO50, NRBlO50 represent the density of conifer and broadleaf seedlings taller than 50 cm; Nshoot is the density of shoots from sprouting regeneration, DmCf represents the average diameter of conifer seedlings.
b) PCA2: VIs and environmental parameters, Rad is the incoming solar radiation, BATree, TCC represent the basal area and the fractional canopy cover of the living trees (1, 2, 3 represent the centroids of spectral groups Sp1, Sp2, Sp3).

The biplot PCA2 shows the associations linking VIs and environmental variables: the first 2 axes explained a total variance of approximately 93%. The first factor showed high loadings on Incoming solar radiation (Rad), Tree Canopy Cover (TCC), basal area of living trees (BATree), whereas the second axis pursued the variations of fire-severity (SevNBR).
The first two components maintained the same correlation coefficients with the VIs, as described for PCA1.
For both PCA bi-plots, three centroids represented the average position in the ordination space of each spectral group of plots. Clear separation between centroids was noted along the ordination axis, by relating group1 with the high values of tree cover, basal area (PCA2) and conifer (pine) regeneration (PCA1); group 2 with the high values of severity (PCA2), diameter of pine seedlings (PCA1) and group 3 with higher incoming solar radiation (PCA2), density of shoots and broadleaf seedlings.

VIs show sensitivity to the different layers of vegetation recovery (Table 2.7): NDVI, SAVI are most positively correlated with re-sprouting regeneration and bare soil, negatively to tree canopy cover and density. NBR resulted correlated with broadleaf seedling, re-sprouting regeneration and bare soil. IFI and mDI show inverse relationships: mDI is positively correlated with litter, density of seedlings and tree canopy cover; relationships of opposite sign come from IFI which shows a positive correlation with CWD.

	PineU50	PineO50	BleafU50	BleafO50	Sprouts	Shoots
ndvi	-0.58	-0.39			0.37	0.65
ifi				-0.38		
savi	-0.63	-0.42				0.63
mDI	0.48			0.38		
nbr			0.50	0.51	0.44	0.55

	CWD	Litter	Soil	TCC
ndvi			**0.43**	**-0.39**
ifi	0.35	-0.36		-0.30
savi			**0.45**	**-0.47**
mDI	-0.32	0.37		**0.56**
nbr			0.35	

Table 2.7 - Spearman rank correlations ($p < 0.01$; $p < 0.05$) among VIs, regeneration variables (above) and ground cover type (bottom); PineU50, PineO50 represent respectively the density of pine regeneration shorter and taller than 50cm, BleafU50 is the density of broadleaf seedlings shorter than 50 cm, Sprouts, Shoots are the density of sprouting regeneration, CWD (coarse wood debris), Litter, Soil represent the correspondent fractional ground cover, TCC the canopy cover of living trees.

The definition of the three spectral groups (Sp1, Sp2, Sp3), each well related to the different regeneration and environmental variables, allows to built a map resuming the spatial distribution of vegetation responses in the burnt area detected in year 2010; this map (Figure 2.12) allows to discriminate areas covered by vegetation from those where the recovery dynamics seem to have a slower rate.

The effects of restoration activities on field-data and the extracted VIs were evaluated by means of a MRPP, to assess any differences between treated and un-treated plots: regeneration variables showed no separation among groups ($T=-1.7$, $p>0.05$, $A=0.3$). PerMANOVA highlighted a minimal difference ($F = 3.27$; $P < 0.01$) and low variability explained by the treatments (10%). MRPP performed on environmental parameters ($T=-9.3$, $p<0.001$, $A=0.14$) and VIs ($T=-6.3$, $p<0.001$, $A=0.10$) showed a significant separation between treated and un-treated groups, with a low homogeneity-within group arrangement.

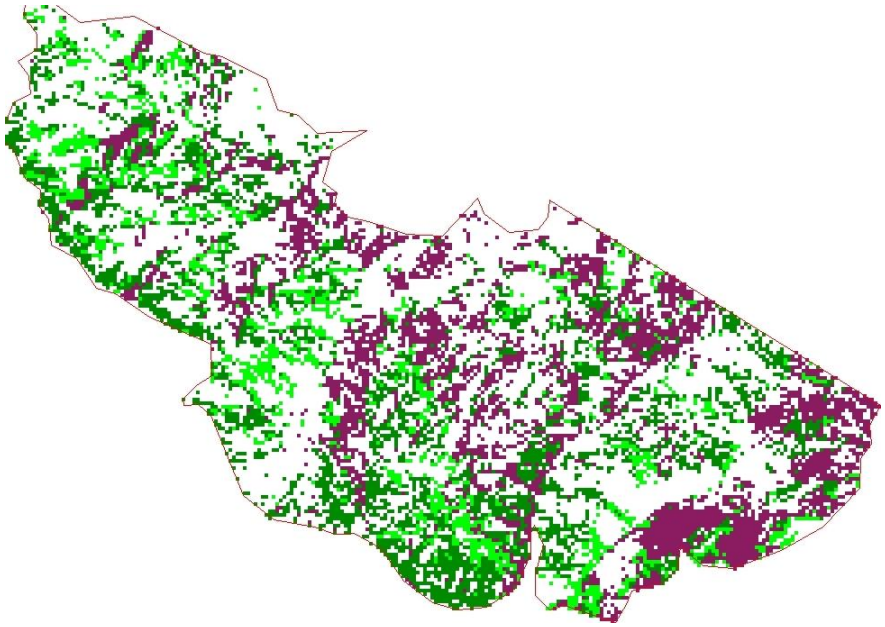

Figure 2.12 - Map of vegetation recovery detected in 2010, according to the spectral groups arrangement: the residual living trees and pine regeneration (Sp1 - dark green), the re-sprouting and broadleaf species regeneration (Sp3 - light green), the highest severity zones with lowest regeneration density (Sp2 - brown).

Treatment	**Plot** (n)	**Agemax** (years)	**NRCfO50** (n/ha)	**NRCfU50** (n/ha)	**NRBlO50** (n/ha)	**NRBlU50** (n/ha)	**NSprout** (n/ha)	**NShoot** (n/ha)	**Nsp** (n)	**H'** (-)
Treated	20	9.2[a] (0.3)	920[b] (147.9)	530.1[b] (168.7)	661.7[b] (160.4)	284.6[b] (58.2)	3474.5[a] (320.9)	16692.5[a] (1453.2)	7.5[a] (0.4)	1.55[a] (0.05)
Un-treated	20	7.9[b] (0.4)	1501.6[a] (336.4)	2028.1[a] (572.4)	1096.3[a] (256.2)	405.8[a] (117.0))	2749.0[b] (267.5)	12650.3[b] (1450.8)	7.0[a] (0.3)	1.29[b] (0.06)

Treatment	**Plot** (n)	**avgDR** (cm)	**StdDR** (cm)	**avgHR** (cm)	**StdHR** (cm)	**DmCf** (cm)	**DmBl** (cm)	**TDD** (-)	**THD** (-)
Treated	20	2.3[a] (0.3)	1.7[a] (0.3)	110.5[a] (11.4)	77.6[a] (8.9)	3.2[a] (0.5)	1.4[a] (0.2)	1.33[a] (0.07)	1.78[a] (0.06)
Un-treated	20	1.6[b] (0.2)	1.1[b] (0.2)	89.0[b] (10.2)	62.5[b] (8.4)	1.7[b] (0.4)	1.4[a] (0.1)	1.09[b] (0.07)	1.79[a] (0.10)

Table 2.8 - Regeneration characteristics in the treated and un-treated plots (mean ± SE): the upper table reports maximum of estimated age (Agemax), density of conifer (NRCf) and broadleaf (NRBl) seedlings, sprouting density (NSprout, NShoot), number of woody species (Nsp), Shannon index (H'). The -O50 and -U50 suffix refer respectively to seedlings taller and shorter than 50cm. The bottom table reports the average and standard deviation of seedling diameter (avgDR, StdDR), the average and standard deviation of seedling height (avgHR, StdHR), the mean diameter of conifer and broadleaf seedlings (DmCf, DmBl), the diversity indices of diameter and height of seedlings (TDD, THD). The Plot column reports the total plot score per group. Different letters highlight differences between groups (Mann-Whitney non-parametric comparison, p<0.05).

The Mann-Whitney test applied on the regeneration dataset showed significant differences between management ($p<0.05$) in seedling densities (higher in un-treated plots), seedling diameter and age, TDD and Shannon index values (greater in treated plots).

Treatment	Plot (n)	Snags (n/ha)	Shrubs (%)	Herbs (%)	CWD (%)	Litter (%)	Soil (%)	BATree (m^2/ha)	NTree (n/ha)	TCC (%)
Treated	20	1369.7^a (210.9)	22.7^a (2.2)	40.0^b (3.4)	14.0^a (1.5)	7.3^a (0.7)	16.0^a (1.8)	3.8^b (1.6)	110.1^b (49.8)	9.4^b (4.1)
Un-treated	20	642.9^b (123.7)	19.0^a (2.2)	55.7^a (2.9)	8.0^b (1.0)	9.3^a (1.0)	8.0^b (1.1)	12.9^a (2.8)	334.7^a (84.8)	36.5^a (7.5)

Treatment	Plot (n)	Nness (-)	Rad (KWh/m^2)	StRad (KWh/m^2)	Severity (dNBR)
Treated	20	-0.65^b (0.04)	700.8^a (17.1)	54.1^a (9.0)	3.06^a (0.12)
Un-treated	20	-0.34^a (0.12)	658.7^a (34.4)	51.7^a (11.6)	2.55^b (0.18)

Table 2.9 - Environmental parameters in the treated and un-treated plots (mean ± SE): the upper table includes density of snags, estimated ground cover (Shrubs, Herbs, CWD, Litter, Soil); BAtree, Ntree, TCC represent the basal area, the density and the fractional canopy cover of living trees (DBH > 10 cm). The bottom table reports values of Nness (north-ness exposition index), Rad and StRad (average and standard deviation of incoming solar radiation), Severity (average fire severity according to dNBR map). Different letters highlight differences between groups (Mann-Whitney non-parametric comparison, p<0.05).

The comparison on environmental data highlights higher values of severity, CWD, snags and bare soil in the treated plots, while tree density and cover, grass cover resulted greater in the un-treated group (Table 2.9). The comparison of VIs between treated and un-treated groups, showed the higher IFI values for treated plots and mDI values un-treated plots (Table 2.10).

Treatment	Plot (n)	NDVI	SAVI	NBR	mDI	IFI
Treated	20	-0.26^a (0.12)	0.15^a (0.13)	-0.88^a (0.16)	-2.24^b (0.17)	8.33^a (0.38)
Un-treated	20	-0.48^a (0.14)	-0.29^a (0.16)	-0.62^a (0.18)	-0.71^a (0.29)	6.01^b (0.40)

Table 2.10 - Standardized values of VIs in the treated and un-treated plots (mean ± SE). Different letters highlight differences between groups (Mann-Whitney non-parametric comparison, p<0.05).

Multitemporal sequences of VIs

The diagrams in Figure 2.13 show the evolution of NDVI and SAVI (mean and CI 95% according to Tukey HSD) in the treated and un-treated plots The indices exhibit a similar behavior before the fire and a strong difference between the pre-fire period, with stationary values, and the post-fire one, where the temporal series, after the common-in-time lowest value, tend to increase their values. The upper bars (non-significant differences between years) show three homogeneous groups of the index values between a year and the subsequent, identifying three different periods:

I) pre-fire, II) early post-fire (the lowest index values), III) late post-fire. The plots belonging to the treated group didn't show any statistically significant difference neither in NDVI nor in SAVI, except for 2002, the year in which the treated plots assumed quite high values of SAVI when compared with the un-treated group. Both indices retrieve pre-fire values around 2002, with a shift forward to 2006 for NDVI values of un-treated plots. NDVI and SAVI show different performances after recovering to pre-fire values: SAVI tends to increase, stabilizing at a higher level, in comparison with the values of the index before the fire; NDVI stops its increase around pre-fire values. The scenes in Figure 2.14 show NDVI maps in four different years, before (1993) and after the fire, proving a full recovery of the index values to the pre-fire ones. Therefore NDVI shows a higher range of variation than SAVI on early post-fire period.

The spectral trajectory of NBR (Figure 2.15) in treated and un-treated plots exhibits relevant differences of the index values before and after the fire: three different periods of NBR values are highlighted by the upper bars: the pre-fire, the early and the late post-fire arrangements. Temporal paths of treated and un-treated groups are quite similar and significantly differ only in 2006. After the fire, NBR values decrease to a minimum value in year 2000 for both groups; afterwards the trend sees an increase in NBR values, though not reaching the pre-fire ones. The maps (Figure 2.16) visually confirmed the temporal trajectory of NBR, stopping after an initial period of increase. The NBR trend didn't present any particular divergence after the restoration treatments realized in 2000.

The diagram of mDI (Figure 2.17) shows the temporal paths of a low-severity zone, treated and un-treated plots. In the restored zones mDI manifests evident changes between pre-fire and post-fire values, while the low severity zone maintain a constant level in time. Upper bars highlight three different blocks of mDI values: I) a first before the fire, II) a second period of concordance between a year and the subsequent after the fire; III) since 2000, mDI values decrease in treated plots, whereas un-treated plots keep their values around a constant level. After the fire, both treated and un-treated plots decrease their mDI values reaching a minimum level: this latter is maintained in the un-treated plots whereas, after 2000, the spread with the treated plots become more conspicuous.

IFI diagram (Figure 2.18) describes the variation of the values between pre-fire and post-fire period. Since small index values indicate a similarity with the spectral center of the forest training, the graphic area was divided into: a dense forest area, a low-density forest mixed with shrubs, a shrub-land area and a grassland. Before the fire, all the plots exhibited similar spectral values, in proximity of the border between dense and rare forest cover. After the fire, IFI rises to higher values: treated plots move into the grassland area and un-treated ones into the shrub-land zone. The comparison of IFI values through the time, according to the upper bars, displays three separate periods: a first pre-fire period, a second one immediately after the fire (up to the year 2000 in treated plots, till the end of sequence within un-treated group); finally, a third period where the treated plots partially recover to the low-density forest. After the fire, a significant difference between treated and un-treated plots highlights the different levels of fire-severity among treatments. A series of thematic maps of IFI values (Figure 2.19), exhibits the differences in vegetation structure between pre- and post-fire, confirming a slower recovery rate in comparison to NDVI and SAVI path (Figure 2.13).

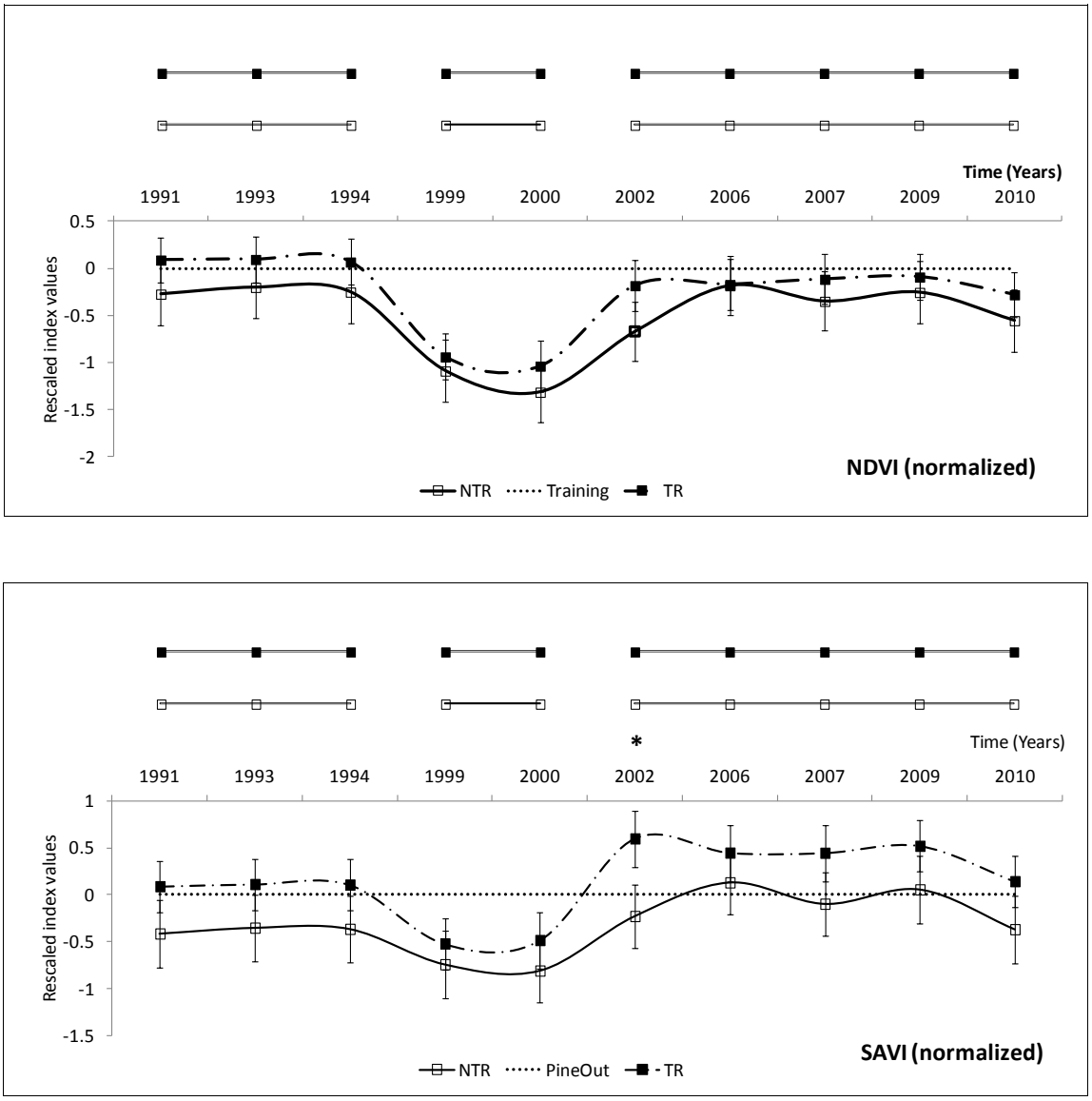

Figure 2.13 - Comparison of NDVI and SAVI temporal trajectories between Treated (TR) and un-treated (NTR) plots. In the upper part, the horizontal lines suggest non-significant differences between the years (Tukey HSD post hoc test; p<0.05). The marked year highlights a significant difference between TR and NTR groups.

Figure 2.14 - NDVI maps resuming four years through the temporal trajectory: index values ranging from the highest values (dark green) to the lowest (white), before (1993) and after the fire.

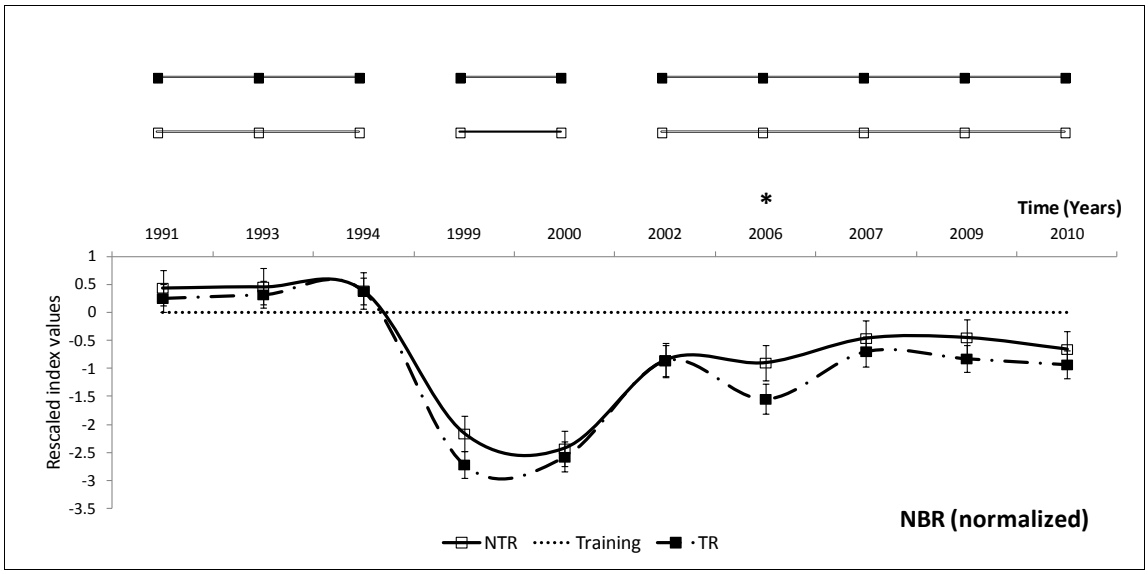

Figure 2.15 - Comparison of NBR temporal trajectories between Treated (TR) and Un-treated (NTR) plots. In the upper part, the horizontal lines suggest non-significant differences between the years (Tukey HSD post hoc test; p<0.05). The marked year highlights a significant difference between TR and NTR groups.

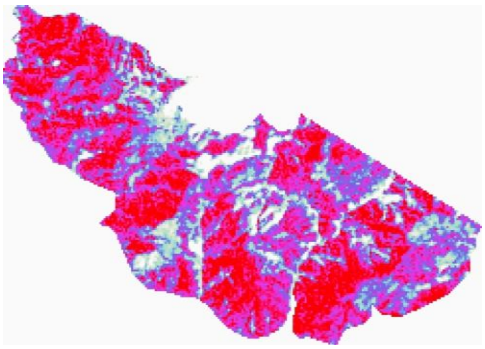

1993

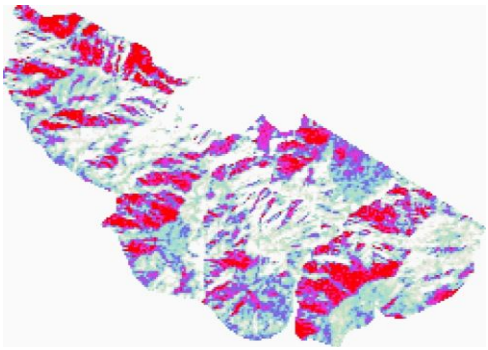

1999

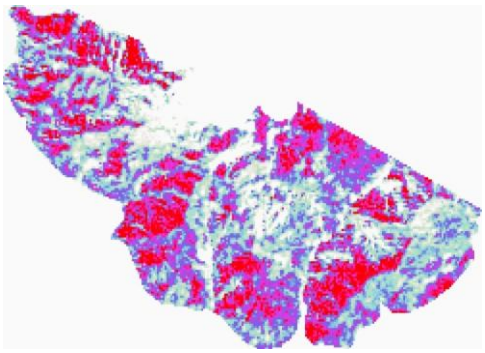

2006

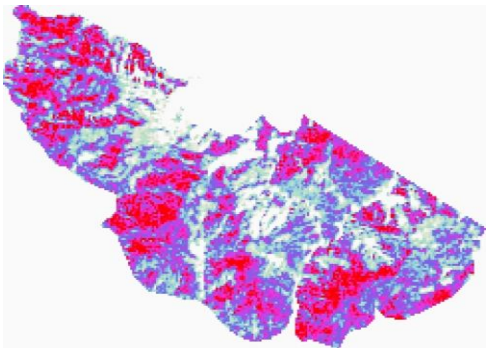

2009

Figure 2.16 - NBR maps resuming four years through the temporal trajectory: index values ranging from higher value (red) to lower (downward to light blue and white), before (1993) and after the fire.

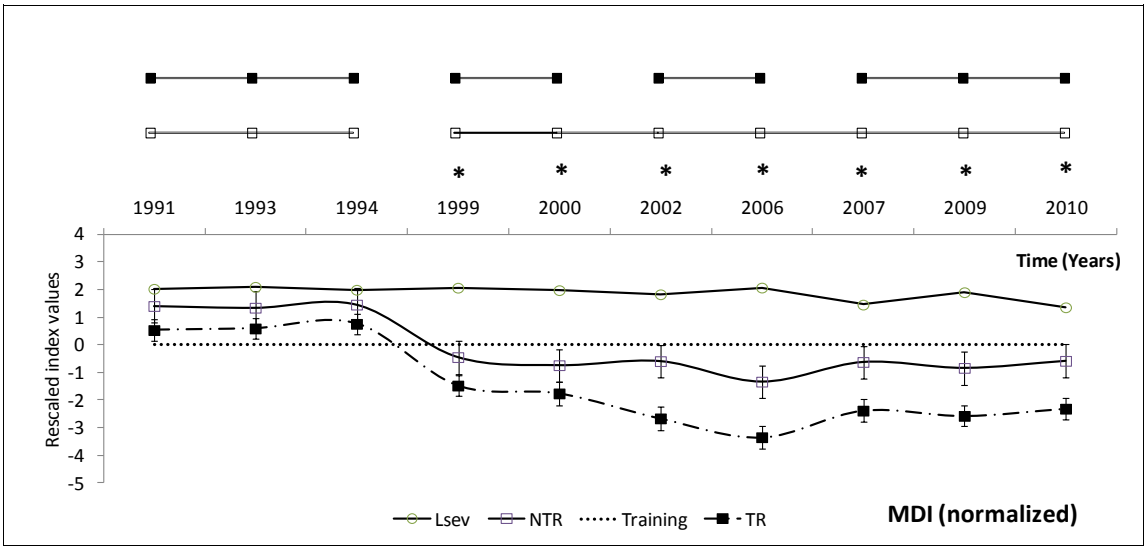

Figure 2.17 - Comparison of mDI temporal trajectories among Treated (TR), Un-treated (NTR) plots and a zone characterized by low-severity fire (Lsev). In the upper part, the horizontal lines suggest non-significant differences between the years (Tukey HSD post hoc test; p<0.05). The marked years highlight a significant difference between TR and NTR groups.

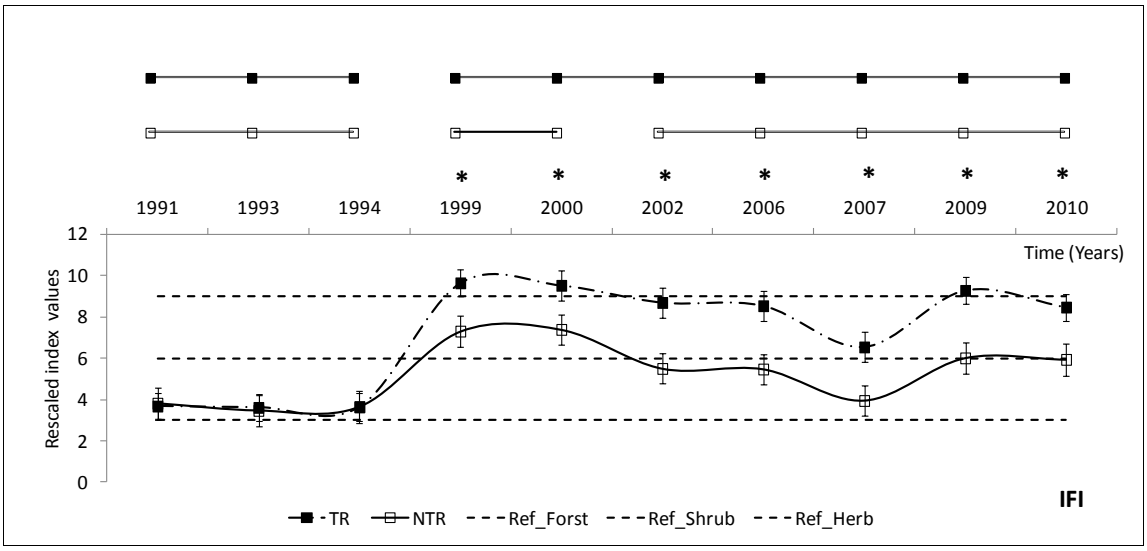

Figure 2.18 - Comparison of IFI temporal trajectories between Treated (TR) and Un-treated (NTR) plots. In the upper part, the horizontal lines suggest non-significant differences between the years (Tukey HSD post hoc test; p<0.05). The marked years highlight a significant difference between TR and NTR groups. Ref_Forst, _Shrub, _Herb represent upper thresholds delimitating areas of dense forest, low-density forest and shrubland respectively. IFI values greater than Ref_Herb are included in grassland zone

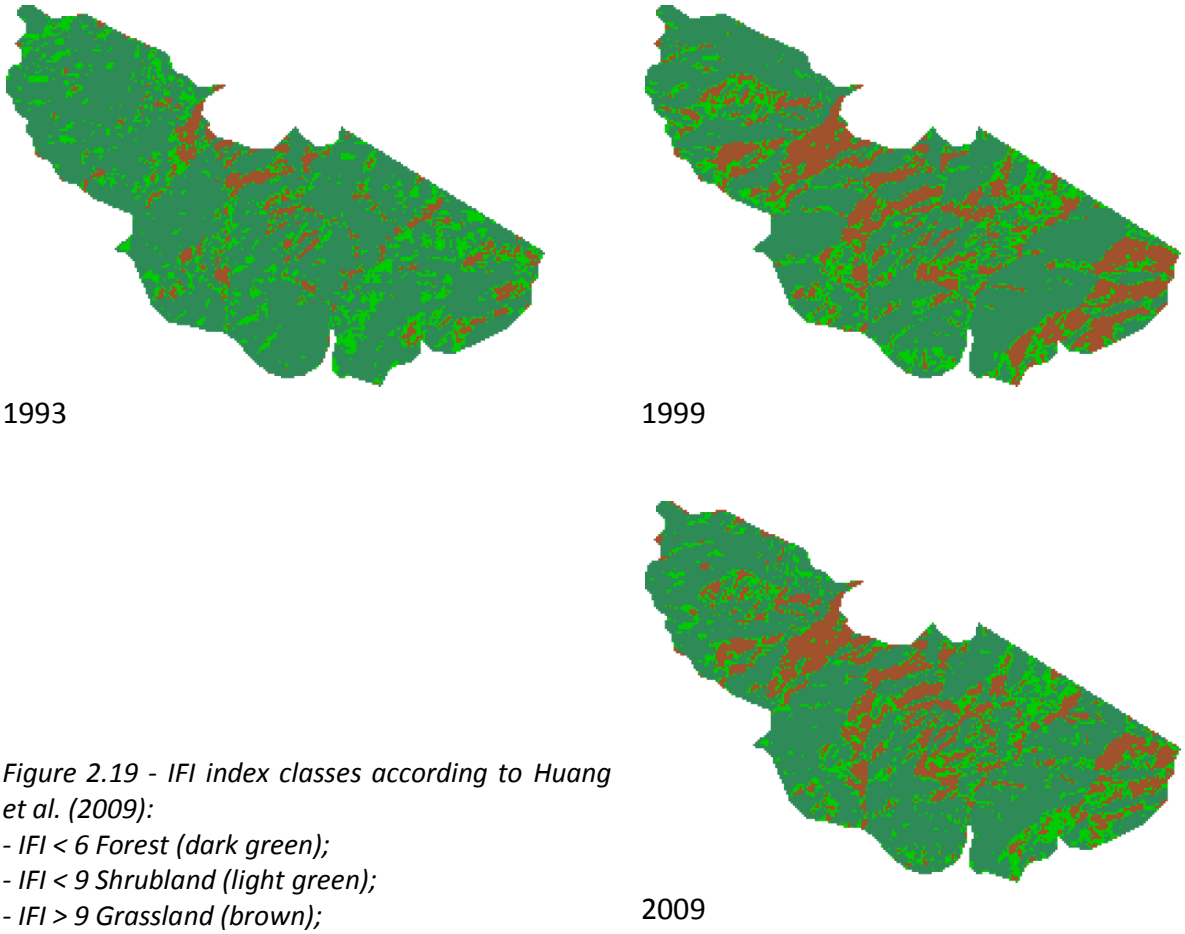

Figure 2.19 - IFI index classes according to Huang et al. (2009):
- IFI < 6 Forest (dark green);
- IFI < 9 Shrubland (light green);
- IFI > 9 Grassland (brown);

Discussion

The first target of this study was to analyze the relationships between fire-severity and mid-term response of vegetation in a pine forest, identified as one of the widest burnt areas of the Italian Alps in the last decades. After a fire, an ecosystem is affected by two types of consequences: the first occurs immediately after the event as a result of the combustion, ash, gas, production of exhaust fumes, loss of vegetation, heating of soil which causes chemical and physical modification and loss of microorganism communities. The other consequences arise over time, such as soil erosion, microclimate modifications, habitat changes and vegetation succession with species substitution (Brown et al., 2004; Eidenshink et al., 2007). Fire-severity plays a relevant role since the highest values of severity are often associated with higher rates of soil loss, lower rates of vegetation recovery caused by the destruction of the forest floor, loss of the seed bank and sensible reduction of the canopy (DeBano et al., 1998).

Remote Sensing (RS) imagery analysis allows to survey the changes in progress as a cause of relevant modifications on surface reflectance characteristics. A relevant number of studies prove the ability of the Normalized Burn Ratio (NBR) index to recognize post-fire effects (Key and Benson, 2005; Smith et al., 2007; Escuin et al.,2008). Aiming to define the map of fire-severity, better performances are linked to dNBR (first year post-fire subtraction from pre-fire NBR values), because of its higher range of disturbance detection; dNBR also exhibits a good correlation with Composite Burn Index (CBI), an index of fire severity built by means of field measurements and ground-truth (van Wagtendonk et al., 2004; Key and Benson, 2006; French et al., 2008; Chen et al., 2011). However, previous studies reported some cases where dNBR failed in detecting fire-severity, showing poorly relationships with CBI (Epting et al., 2005; Allen and Sorbel, 2008; Hoy et al., 2008; Murphy et al., 2008).

Considering the discontinuous vegetation cover due to changes in soil morphology, the detection of fire severity could be more suitable using the whole spectral information provided by the Landsat TM/ETM+ dataset (Meng and Meentemeyer, 2011); at this purpose, mCBI index has been introduced. However, in this study the first multispectral image available after the fire comes two years after the event; it is known that the ability to distinguish among the severity levels decreases with the arise of the regeneration layers (Wulder et al., 2004).

The comparison between dNBR and mCBI in this site leads to a greater ability for mCBI index to distinguish between burnt and un-burnt pixels, showing a very low commission error. This result confirms other previous studies where NBR and dNBR indices have been considered not optimal for severity detection in forest with sparse tree cover, since their performance is strongly related with the pre-fire green biomass (Epting et al. 2005; Roy et al., 2006; Miller and Thode, 2007).

The evaluation of the relationships between regeneration variables and environmental parameters, mediated by VIs from RS data, highlighted preferential patterns of vegetation recovery. Three spectral groups, clearly defined by the arrangement of VI values, identified three different scenarios: the first one associates high mDI and TCC (tree canopy cover) values, with low-severity of the fire and the greatest density of seedlings; the regeneration is characterized by a

recent establishment, as suggested by the low values of height, age and mean diameter of the seedlings. The second scene is characterized likewise by low-severity conditions, but higher values of NDVI and differs from the previous one by a scarce presence of adult trees and higher presence of bare soil and rocks. Due to this constrains, the vegetation tends towards recovery mainly by means of re-sprouting species, even though the seedlings density of broadleaf species seems to follow a positive gradient of incoming solar radiation and low competition with others vegetation layers. Differences in vegetation recovery seem determined by environmental conditions: regeneration of *P. nigra* seems to take advantage from moderate levels of fire severity, perhaps due to the reduction in competitive pressure by herbaceous and shrub species, the exposure of bare mineral soil and better light availability, as highlited by previous studies (Ordonez et al., 2004; Zlatanov et al., 2010). Furthermore, the presence of broadleaf regeneration, within un-disturbed *P. nigra* stands, out-competes with pine seedlings (Amorini, 1983). In presence of high severity disturbance, the establishment of tree seedlings tends to be limited if compared with shrubs and a sensible reduction of adult trees caused by fire can be a relevant restriction, in terms of seed availability (Mendoza et al., 2009). *P. nigra* and *P. sylvestris* don't produce serotinous cones and the diffusion of the seeds occurs in late winter or spring (Gracia et al., 2002). When a high severity wild-fire affects a pine forest after this period, seeds are more likely to come from un-burnt marginal areas. However, in ordinary conditions, the diffusion of *P. nigra* and *P. sylvestris* seeds is usually short, no more than 50 m from dispersal trees; consequently, a gradient of decreasing seed availability is inversely coupled with the adult tree density (Retana et al., 2002). Furthermore, after the passage of fire, severity may influence the residual living pines inducing low percentages of germination in seeds produced (Clark et al., 1998). As a consequence of the limited presence of adult pines, vegetation recovery is expected according to the re-sprouting strategy and seedling establishment of heliophilous species, especially from shrub layer (Mendoza et al., 2009).

All this leads to the third scenario where the analysis of regeneration and environmental data is strictly associated with the consequences of high-severity fire: the absence of adult trees and the highest values of IFI index. In these conditions seedling density is lower when compared with the others two scenes previously described. However, the structural parameters of regeneration, such as seedling height, age, average diameter and TDD, reveal that an early regeneration establishment (especially of pine seedlings) occurred under such environmental conditions. This could be due to different concurrent factors*, i.e.* the removal of relevant amounts of litter by high severity fire and the exposure *de-facto* of the mineral soil (Smith et al., 2007). Therefore, a greater presence of snags, CWD and burnt wood downed to the ground, probably induced these facilitative effects towards the regeneration establishment (Beghin et al., 2010; Castro et al., 2011). The low presence of recently affirmed regeneration seems related with high-severity conditions, whereas slow recovery time is tied to the lack of seed availability, as reported also by Thomas and Wein (1985), Chen et al. (2011).

The second target of this study was to provide an ecological significance to the elaborated VIs in order to use them to monitor the processes of recovery and vegetation post-fire dynamics, including an evaluation of the efficiency of restoration activities. The use of RS technique as a valuable tool for broad scale investigation on post-disturbance areas is proved by many studies,

even if the ecological meanings of VIs and the connections between spectral recovery and forest regeneration has not been focused yet (Meng and Meentemeyer, 2010; Solans-Vila and Barbosa, 2010; Schroeder et al., 2011). The images from Landsat TM/ETM+ free-series data provide a large amount of spectral information on a given area. VIs, indirectly related with many physical and biological parameters (*i.e.* LAI, amount of biomass, vegetation cover), enable to monitor the recovery of different vegetation layers (Carlson and Ripley, 1997). The multi-temporal analysis, by means of different *green-leaf* indices (so-called because NDVI, SAVI, NBR are indices commonly used to detect photo-synthetically active surfaces), displays a similar behavior in the areas affected by fire. After an abrupt drop of VI values, they can still be decreasing 2-3 years after the event, thus giving evidence of delayed mortality and reduction in canopy cover (Thies et al., 2006). Recovery of NDVI and SAVI values to the pre-fire ones is achieved in a few years (around 5 years). The short recovery time, the low specific sensitivity towards LAI (Leprieur et al., 1994) and the high correlation with the fractional vegetation cover of these VIs (Verstraete and Pinty, 1991), led to the conclusion that the re-sprouting of vegetation saturates the green-ness sensitivity of this group of VIs (Volcani et al., 2005). This conclusion confirms the previously detected correlations between NDVI and SAVI with the re-sprouting regeneration density. The recovery of SAVI to higher values than the pre-fire ones, is probably due to a better sensitivity of the index on sparse vegetation conditions (Gilabert et al., 2002). The spectral trajectories of NBR differs from NDVI and SAVI for a slower rate of recovery which does not reach pre-fire values. Differences between the recovery of NDVI and NBR are probably due to the limits of this latter in detecting the dynamics of grass regeneration, thus making NBR unsuitable to correctly evaluate post-fire effects in grasslands and shrub-lands (Lentile et al., 2006; Chen et al., 2011). However, the remarkable relationship with broadleaf regeneration allows using NBR to monitor forest dynamics connected with tree regeneration of deciduous species. This multi-temporal analysis agrees with recent studies which proved that NBR provides good estimates of severity in burnt forest, because of its wider range of sensitivity with respect to NDVI (Epting et al., 2005; Loboda et al., 2007; Escuin et al., 2008). Wider information about changes in forest structure come from IFI and mDI long-term survey of post-fire vegetation recovery; mDI index, derived from *Tasseled cap* indices (TC), exhibits a significant correlation with canopy cover of trees, and has proved to give good results in other forest type as well (Healey et al., 2005). mDI facilitates the assessment of the post-fire dynamics of tree canopy cover trough time (Hais et al., 2009). A global information of changes in forest-structure comes from the temporal projection of IFI values. Differences on increasing rates and stabilizing levels of IFI values after the fire, imply some divergences in fire severity and forest structure among the examined zones: this behavior highlights, a greater efficiency of IFI index when compared to the *green-leaf* indices for long term monitoring of post-fire recovery (Chen et al., 2011). Coupling IFI values with field-data enabled to verify the index feasibility in detecting the severity magnitude, that is the cause of the transformations in the forest structure. Changes of forest structure trough time can be tracked by IFI spectral paths (Huang et al., 2009). As previously highlighted, the VIs of the *green-leaf* group showed some decreasing values since year 2000, meaning that the loss of vegetation and a reduction in canopy may continue for years after the fire. The second group of VIs, including mDI and IFI, exhibits a stable low level of values immediately after the fire. The relationships between the regeneration variables and the VIs, in

addition to the high separation between regeneration and environmental parameters among the spectral groups, provide a useful description of the state of vegetation recovery. This map of vegetation recovery within the burnt area could be helpful to evaluate the spatial dynamics of vegetation.

The effects of restoration activities towards the vegetation recovery were evaluated by means of a temporal analysis of VIs combined with the field-data measurements. The analysis in the two restoration groups did not detect any appreciable consequence in regeneration density and cover due to the restoration treatments. Differences between treated and un-treated groups seem more likely due to the different severity of fire. Exploring the relationships between environmental and regeneration variables highlighted the role of fire severity in determining the differences of vegetation recovery after the fire. The treated areas, affected by a general greater fire severity, exhibit a lower density of regeneration than un-treated ones. Furthermore, in high severity areas the tendency of seedlings to an early establishment is highlighted where CWD and density of snags were greater. The presence of adult living trees, which act as seed dispersers, is a determining condition for the species of pine involved: most of seedlings were detected into the un-treated group, associated to the high rate of surviving trees. Differences between treated and un-treated groups have been investigated after the treatment interventions, by means of VIs: IFI and mDI significantly distinguish the differences of fire severity among the groups, immediately after the fire. Furthermore, modifications of the tree canopy cover and structure of the forest were observed in the years after the interventions as well. Previous studies proved mDI sensitivity to the seedlings plantation (Jonášová and Prach, 2004); in our case, the comparison of mDI values among treated and un-treated areas seems to confirm that the activities of reforestation in the salvage areas have not brought any appreciable result towards the vegetation recovery.

Conclusions

The main goal of this paper was to arrange, at different scales of investigation, a general-purpose procedure to evaluate the role of fire severity and the effects of post-fire restoration in a burnt forest of the Alps; the study was conducted combining field ecological measurements with remote sensing data. The synergy between the field-data measurements and the analysis of the vegetation recovery through the years, has allowed to reach the following three objectives:

I) mapping the fire severity to detect the influence of severity on vegetation recovery, over a wide burnt area;

II) assessing the vegetation response to the fire over time.

III) evaluating the effects of restoration activities on regeneration establishment.

I) The change-detecting is a consolidated procedure to define maps of fire severity subtracting pixel by pixel the post-fire values from pre-fire ones. The forest is characterized by a complex of spectral signatures related to the multistrata set of trees, shrubs, grass and intermediate combinations; each layer exhibits a specific response detected by Landsat TM/ETM+ sensors. A map of fire severity defined by means of change-detection of NBR index, is limited to the spectral information exclusively provided by the Landsat bands associated with NBR. A new VI was introduced (mCBI), based on the sum of all the contributions of those spectral bands proved to be sensitive to the different vegetation-strata. A change-detection technique applied to mCBI allowed an enhanced discrimination of severity classes. However, the evaluation of this procedure to define severity maps requires a future validations and feedback, through field-severity indices and ground-measures (*i.e* CBI index validation).

II) Disturbance history and vegetation response through the years can be evaluated according to the temporal availability and resolution of the Landsat multispectral archive (Huang et al., 2009). Recovery processes are strongly influenced by severity. Regeneration establishment of *P. Nigra* and *P. sylvestris* in mid-term observations is clearly greater in areas where low levels of severity allow the survival of seed-trees. This fact appears to be related more to species-specifics characteristics of seed dispersion than to environmental constrains (Donato et al., 2006; Pausas et al., 2003). In order to schedule proper restoration treatments aiming at the recovery of the vegetation cover, a powerful tool may consist in combining the information provided by the maps of fire severity with hydro-geological hazard (Chen et al., 2011). Therefore, fire severity mapping and surveying of post-fire dynamics of vegetation allow to identify areas in which vegetation recovery may have difficulty to evolve from the earlier stages of succession.

Despite the past widespread use of NDVI to investigate post-disturbance vegetation dynamics, in this particular situation it appears specifically related with the re-sprouting recovery, resulting unsuitable to detect the complexity of interactions between the different layers of

vegetation. NDVI seems more correlated with the fractional vegetation cover: in this case, sprouting and deciduous regeneration provide the faster vegetation response. An assessment of the dynamics of vegetation covering the soil appears possible by analyzing the performance of other indices through time (IFI, mDI): these VIs have proved to be more related to vegetation structure and tree canopy cover, appearing a feasible way to explore the different responses of vegetation to the disturbance.

III) In this study, the effects of restoration activities appear negligible regarding the re-planting of saplings for vegetation cover improvements. However, in areas affected by higher severity levels, an early regeneration establishment has been noticed where the presence of burnt wood on the soil was greater. At this purpose, planning of restoration activities in *P.nigra* and *P.sylvestris* forests should consider the presence of living trees as seed dispersers, and the positive effect induced by the release of burnt wood *in situ*, with regard to the establishment of natural regeneration.

References

Allen JL, Sorbel B, 2008. Assessing the differenced Normalized Burn Ratio's ability to map burn severity in the boreal forest and tundra ecosystems of Alaska's national parks. International Journal of Wildland Fire 17, 463–475.

Ammer, C., 1996. Impact of ungulates on structure and dynamics of natural regeneration of mixed mountain forests in the Bavarian Alps. Forest Ecology and Management 88, 43–53.

Amorini E, 1983. Thinning trials in the black pine stand of Monte della Modina in the Tuscan Apennines. Ann Ist Sper Selvic 14:47–99.

Anderson, M. J., 2001. A new method for non-parametric multivariate analysis of variance. Austral Ecology, 26, 32–46.

Asrar, G., Fuchs, M., Kanemasu, E. T., and Hatfield, J. L., 1984. Estimating absorbed photosynthetic radiation and leaf area index from spectral reflectance in wheat, Agron. J. 76:300-306.

Beers, R.W., Dress, P.E. and Wensel, L.C., 1966. Aspect transformation in site productivity research. J. For. 64:691-692.

Beghin, R., Lingua, E., Garbarino, M., Lonati, M., Bovio, G., Motta, R., Marzano, R., 2010. *Pinus sylvestris* forest regeneration under different post-fire restoration practices in the northwestern Italian Alps. Ecological Engineering 36, 1365-1372.

Beschta, R. L., J. J. Rhodes, B. Kauffman, R. E. Gresswell, W. Minshall, J. R. Karr, D. A. Perry, F. R. Hauer, Frissell C. A., 2004. Post-fire management on forested public lands of the Western United States. Conservation Biology 18:957–967.

Biondini, M.E., Mielke Jr., P.W., Berry, K.J., 1988. Data-dependent permutation techniques for the analysis of ecological data. Vegetation 75, 161–168.

Brewer K, Winne C, Redmond R, Opitz D, Mangrich M, 2005. Classifying and mapping wildfire severity: a comparison of methods. Photogrammetric Engineering and Remote Sensing 71, 1311–1320.

Brown, R.T., Agee, J.K., Franklin, J.F., 2004. Forest restoration and fire: principles in the context of place. Conservation Biology 18, 903–912.

Caetano, M., Mertes, L., Cadete, L., and Pereira, J. M. C., 1996. Assessment of AVHRR data for characterizing burned areas and post-fire vegetation recovery. EARSeL Advances in Remote Sensing, 4, 124–134.

Carlson T., Ripley D., 1997. On the relation between NDVI, fractional vegetation cover, and leaf area index. Remote Sensing of Environment, 62: 241–252.

Castro, J., Allen, C.D., Molina-Morales, M., Marañón-Jiménez, S., Sánchez-Miranda, Á., Zamora, R., 2011. Salvage Logging Versus the Use of Burnt Wood as a Nurse Object to Promote Post-Fire Tree Seedling Establishment. Restoration Ecology 19, 537–544.

Chafer CJ, Noonan M, Macnaught E.,2004. The post-fire measurement of fire severity and intensity in the Christmas 2001 Sydney wildfires. International Journal of Wildland Fire 13, 227–240. doi:10.1071/WF03041.

Chander, G., Markham, B.L., Helder, D.L., 2009. Summary of current radiometric calibration coefficients for Landsat MSS, TM, ETM+, and EO-1 ALI sensors. Remote Sensing of Environment 113, 893–903.

Chen, X., Vogelmann, J., Rollins, M., 2011. Detecting post-fire burn severity and vegetation recovery using multitemporal remote sensing spectral indices and field-collected composite burn index data in a ponderosa pine. International Journal of Remote Sensing 32, 7905-7927.

Clark, J. S., Macklin E., Wood. L., 1998. Stages and spatial scales of recruitment limitation in southern Appalachian forests. Ecological Monographs 68:213-235.

Cocke, A., Fule, P., Crouse, J., 2005. Comparison of burn severity assessments using differenced Normalized Burn Ratio and ground data. International Journal of Wildland Fire 14, 189–198.

Cohen, W. B., Spies, T. A., 1992. Estimating structural attributes of Douglas-Fir/Western Hemlock forest stands from Landsat and Spot Imagery. Remote Sensing of Environment, 41,1–17.

Cohen, W. B., Spies, T. A., Fiorella, M., 1995, Estimating the age and structure of forests in a multi-ownership landscape of western Oregon, U.S.A., International Journal of Remote Sensing, 16: 721-746.

Crist, E.P., Cicone, R.C., 1984. A Physically-Based Transformation of Thematic Mapper Data-The TM Tasseled Cap. IEEE Transactions on Geoscience and Remote Sensing GE-22, 256-263.

DeBano, L. F., Savage, S. M., Hamilton, D. M., 1977, The transfer of heat and hydrophobic substances during burning. Journal of the Soil Science Society of America, 40, 779–782.

DeBano, L. F., Neary, D. G., Ffolliott, P. F.,1998. Fire's effects on ecosystems. New York: John Wiley and Sons, Inc. 333 pp.

Díaz-Delgado, R., Salvador, R., Pons, X., 1998, Monitoring of plant regeneration after fire by remote sensing. In Fire Management and Landscape Ecology, edited by L. Trabaud (Fairfield: International Association of Wildland Fire), pp. 315–326.

Díaz-Delgado, R., Pons, X., 2001, Spatial patterns of forest fires in Catalonia (NE Spain) along the period 1975–1995. Analysis of vegetation recovery after fire. Forest Ecology and Management, 147, 67–74.

Díaz-Delgado, R., Lloret, F., Pons, X., 2003. Influence of fire severity on plant regeneration by means of remote sensing imagery. International Journal of Remote Sensing 24, 1751-1763.

Donato, D.C., Fontaine, J.B., Campbell, J.L., Robinson, W.D., Kauffman, J.B., Law, B.E., 2006. Post-wildfire logging hinders regeneration and increases fire risk. Science 311, 352.

Eidenshink, J., Schwind, B., Brewer, K., Zhu, Z., Quayle, B.,Howard, S., 2007. A project for monitoring trends in burn severity. Fire Ecology 3, 3–21.

Elson, L.T., Simon, N.P.P., 2006. Plant Abundances Following Clearcutting and Stripcutting in Central Labrador. North J Appl For 1-19.

Epting, J., Verbyla, D., Sorbel, B., 2005. Evaluation of remotely sensed indices for assessing burn severity in interior Alaska using Landsat TM and ETM+ . Remote Sensing of Environment, 96, pp. 328–339.

Escuin, S., Navarro, R., Fernández, P., 2008. Fire severity assessment by using NBR (Normalized Burn Ratio) and NDVI (Normalized Difference Vegetation Index) derived from LANDSAT TM/ETM images. International Journal of Remote Sensing 29, 1053-1073.

Fahnestock, G. R., Hare, R. C., 1964. Heating of tree trunks in surface fires. Journal of Forestry, 62, 779–805.

Firm, D., Nagel, T.A., Diaci, J., 2009. Disturbance history and dynamics of an old- growth mixed species mountain forest in the Slovenian Alps. For. Ecol. Manage. 257, 1893–1901.

Foster, D.R., Orwig, D.A., 2006. Preemptive and salvage harvesting of New England forests: when doing nothing is a viable alternative. Conserv. Biol. 20, 959–970.

Franklin, S. E., Lavigne, M. B., Wulder, M. A., McCaffrey, T.M., 2002. Large-area forest structure change detection: An example. Canadian Journal of Remote Sensing, 28(4), 588–592.

French, N.H.F., Kasischke, E.S., Hall, R.J., Murphy, K. a., Verbyla, D.L., Hoy, E.E., Allen, J.L., 2008. Using Landsat data to assess fire and burn severity in the North American boreal forest region: an overview and summary of results. International Journal of Wildland Fire 17, 443.

Gilabert, M., González-Piqueras, J., Garćia-Haro, F., Meliá, J., 2002. A generalized soil-adjusted vegetation index. Remote Sensing of Environment 82, 303-310.

Gómez-Aparicio, L., Zamora, R., Gómez, J.M., Hódar, J. a., Castro, J., Baraza, E., 2004. Applying Plant Facilitation To Forest Restoration: a Meta-Analysis of the Use of Shrubs As Nurse Plants. Ecological Applications 14, 1128–1138.

Gracia, M., 2002. Mid-term successional patterns after fire of mixed pine–oak forests in NE Spain. Acta Oecologica 23, 405-411.

Hais, M., Jonášová, M., Langhammer, J., Kučera, T., 2009. Comparison of two types of forest disturbance using multitemporal Landsat TM/ETM+ imagery and field vegetation data. Remote Sensing of Environment 113, 835-845.

Hall, Forrest G., D.E. Strebel, J.E. Nickeson, S.J. Goetz, 1991. Radiometric Rectification: Toward a Common Radiometric Response among Multidate, Multisensor Images, Remote Sensing of Environment, 35:ll-27.

He, L., Chen, J.M., Zhang, S., Gomez, G., Pan, Y., McCullough, K., Birdsey, R., Masek, J.G., 2011. Normalized algorithm for mapping and dating forest disturbances and regrowth for the United States. International Journal of Applied Earth Observation and Geoinformation 13, 236–245.

Healey S. P., Cohen W.B., Yang Z., Krankina O. N., 2005. Comparison of tasseled cap-based Landsat data structures for use in forest disturbance detection. Remote Sensing of Environment, 97,301−310.

Healey, S. P., Yang, Z., Cohen,W. B., & Pierce, D. J., 2006. Application of two regression- based methods to estimate the effects of partial harvest on forest structure using Landsat data. Remote Sensing of Environment, 101,115−126.

Hill J. e Sturm B., 1991. Radiometric correction of multitemporal Thematic Mapper data for use in agricultural land-cover classification and vegetation monitoring. International Journal of Remote Sensing. 12 (7): 1471-1491.

Howard, S.M., Lacasse, M.L., 2004, An evaluation of Gap-Filled Landsat SLC-Off imagery for wildland fire burn severity mapping. Photogrammetric Engineering and Remote Sensing, 70, pp. 877–879.

Hoy EE, French NHF, Turetsky MR, Trigg SN, Kasischke ES, 2008.Evaluating the potential of Landsat TM/ETM+ imagery for assessing fire severity in Alaskan black spruce forests. International Journal of Wildland Fire 17, 500–514.

Huang, C., Wylie, B., Yang, L., Homer, C., Zylstra, G., 2002. Derivation of a tasselled cap transformation based on Landsat 7 at-satellite reflectance. International Journal of Remote Sensing 23, 1741-1748.

Huang, C., Song, K., Kim, S., Townshend, J.R.G., Davis, P., Masek, J.G., Goward, S.N., 2008. Use of a dark object concept and support vector machines to automate forest cover change analysis. Remote Sensing of Environment 112, 970-985.

Huang, C., Goward, S.N., Schleeweis, K., Thomas, N., Masek, J.G., Zhu, Z., 2009. Dynamics of national forests assessed using the Landsat record: Case studies in eastern United States. Remote Sensing of Environment 113, 1430-1442.

Huang, C., Goward, S.N., Masek, J.G., Thomas, N., Zhu, Z., Vogelmann, J.E., 2010. An automated approach for reconstructing recent forest disturbance history using dense Landsat time series stacks. Remote Sensing of Environment 114, 183–198.

Hudak, A., Morgan, P., Bobbitt, M., Smith, A., Lewis, S., Lentile, L., Robichad, P., Clark, J., McKinley, R., 2007. The relationship of multispectral satellite imagery to immediate fire effects. Journal of Fire Ecology 3, 64–90.

Huete, A.R., 1988. A soil-adjusted vegetation index (SAVI). Rem. Sens. Environ. 25, 295–309.

Isaev A, Korovin G, Bartalev S, ErshovD, Janetos A, Kasischke E, Shugart H, French N, Orlick B, Murphy T, 2002. Using remote sensing to assess Russian forest fire carbon emissions. Climatic Change 55, 235–249.

ITT VIS., (2009). ENVI 4.7-The Environment for Visualizing Images. Boulder, Colorado, USA: ITT Visual Information Solutions.

Jin, S., Sader, S., 2005. Comparison of time series tasseled cap wetness and the normalized difference moisture index in detecting forest disturbances. Remote Sensing of Environment 94, 364-372.

Johnstone, J.F., Kasischke, E.S., 2005. Stand-level effects of burn severity on post- fire regeneration in a recently burned black spruce forest. Can. J. For. Res. 35, 2151–2163.

Johnstone, J.F., Chapin, F.S. 2006. Effects of soil burn severity on post-fire tree recruitment in the boreal forest. Ecosystems, 9: 14–31.

Jonášová, M., Prach, K., 2004. Central-European mountain spruce (Picea abies (L.) Karst.) forests: regeneration of tree species after a bark beetle outbreak. Ecological Engineering 23, 15-27.

Jonásová, M., Vávrová, E., Cudlin, P., 2010. Western Carpathian mountain spruce forest after a windthrow: Natural regeneration in cleared and uncleared areas. Forest Ecology and Management 259, 1127–1134.

Justice, C.O., Townshend, J.R.G., Holben, B.N., Tucker, C.J., 1985. Analysis of the phenology of global vegetation using meteorological satellite data. Int. J. Remote Sens. 6, 1271–1318.

Kauth, R. J., Thomas, C. S., 1976. The Tasseled Cap-a graphic description of the spectral-temporal development of agricultural crops as seen by Landsat, Proceedings of the Symposium on Machine Processing of Remotely Sensed Data, Purdue University, West Lafayette, IN, pp. 4B41-4B51.

Keeley, J.E., 2009. Fire intensity, fire severity and burn severity: a brief review and suggested usage. International Journal of Wildland Fire 18, 116.

Kerr, Y.H., Imbernon, J., Dedieu, G., Hautecoeur, O., Lagouarde, J.P., Seguin, B., 1989. NOAA AVHRR and its uses for rainfall and evapotranspiration monitoring. Int. J. Remote Sens. 10, 847–854.

Key CH, Benson NC, 2002. Measuring and remote sensing of burn severity. In 'US Geological Survey Wildland Fire Workshop Report', Los Alamos, NM 31 October– 3 November 2000, USGS Open-File Report 02–11:55-56.

Key CH, Benson NC, 2005. Landscape assessment: ground measure of severity; the Composite Burn Index, and remote sensing of severity, the Normalized Burn Index. In 'FIREMON: Fire Effects Monitoring and Inventory System'. (Eds D Lutes, R Keane, J Caratti, C Key, N Benson, S Sutherland, L Grangi) USDA Forest Service, Rocky Mountain Research Station, General Technical Report RMRS-GTR-164-CD LA, pp. 1–51. (Fort Collins, CO).

Key CH, Benson NC, 2006. Landscape Assessment (LA). In 'FIREMON: Fire Effects Monitoring and Inventory System'. (Eds DC Lutes, RE Keane, JF Caratti, CH Key, NC Benson, S Sutherland, LJ Gangli) USDA Forest Service, Rocky Mountain Research Station, General Technical Report RMRS-GTR-164-CD. (Fort Collins, CO).

Kumar, L., Skidmore, A.K., Knowles, E., 1997. Modelling topographic variation in solar radiation in a GIS environment. International Journal for Geographical Information Science 11, 475–497.

Kuuluvainen, T., Penttinen, A., Leinonen, K., Nygren, M., 1996. Statistical Opportunities for Comparing Stand Structural Heterogeneity in Managed and Primeval Forests: An Example from boreal Spruce forest in southern Finland. Silva Fennica 30, 315-328.

Legendre, P., and L. Legendre. 1998. Numerical ecology, 2nd English Ed. Developments in environmental modeling, Vol. 20. Elsevier, Amsterdam, The Netherlands. 853 p.

Lentile LB, Holden ZA, Smith AM, Falkowski MJ, Hudak AT, Morgan P, Lewis S, Gessler PE, Benson NC, 2006. Remote sensing techniques to assess active fire characteristics and post-fire effects. International Journal of Wildland Fire 15, 319–345.

Leprieur, C., Verstraete,M.M., Pinty, B., 1994. Evaluation of the performance of var- ious vegetation indices to retrieve vegetation cover from AVHRR data. Remote Sensing Reviews 10, 265–284.

Lindenmayer, D. B., Noss R. F., 2006. Salvage logging, ecosystem processes, and biodiversity conservation. Conservation Biology 20: 949–958.

Loboda, T., O'Neal, K., Csiszar, I., 2007. Regionally adaptable dNBR-based algorithm for burned area mapping from MODIS data. Remote Sensing of Environment, 109, 429–442.

López García M, Caselles V, 1991. Mapping burns and natural reforestation using Thematic Mapper data. Geocarto International 6, 31–37.

Magurran A.E., 2004. Measuring Biological Diversity. Blackwell Publishing, pp.256.

Masek, G. J., 2005. LEDAPS disturbance products: User's guide and algorithm description v.2. NASA GSFC, Greenbelt MD. http://ledaps.nascom.nasa.gov.

McArdle BH, Anderson MJ, 2001. Fitting multivariate models to community data: a comment on distance-based redundancy analysis. Ecology 82:290–297.

McCune, B., Grace, J.B., 2002. Analysis of Ecological Communities. MjM Software, Gleneden Beach, Oregon, U.S.A.

McCune, B., Mefford, M.J., 2011. PC-ORD. Multivariate Analysis of Ecological Data. MjM Software Design, Gleneden Beach, Oregon, USA.

McGaughey, RJ, 2002. SVS – Stand Visualization System. A product of the USDA Forest Service, Pacific Northwest Research Station [online] http://faculty.washington.edu/mcgoy/svs.html

Mendoza, I., Gómez-Aparicio, L., Zamora, R., Matías, L., 2009. Recruitment limitation of forest communities in a degraded Mediterranean landscape. Journal of Vegetation Science 20, 367-376.

Meng, Q., Meentemeyer, R.K., 2011. Modeling of multi-strata forest fire severity using Landsat TM Data. International Journal of Applied Earth Observation and Geoinformation 13, 120-126.

Miller JD, Yool SR, 2002. Mapping forest post-fire canopy consumption in several overstory types using multi-temporal Landsat TM and ETM data. Remote Sensing of Environment 82, 481–496.

Miller J, Thode A, 2007. Quantifying burn severity in a heterogeneous landscape with a relative version of the delta Normalized Burn Ratio (dNBR). Remote Sensing of Environment 109, 66–80.

Murphy KA, Reynolds JH, Koltun JM, 2008. Evaluating the ability of the differenced Normalized Burn Ratio (dNBR) to predict ecologically significant burn severity in Alaskan boreal forests. International Journal of Wildland Fire 17, 490–499.

Nagel, T.A., Diaci, J., 2006. Intermediate wind disturbance in an old-growth beech–fir forest in southeastern Slovenia. Can. J. For. Res. 36, 629–638.

Nicholson, S.E., Davenport, M.L., Malo, A.R., 1990. A comparison of the vegetation response to rainfall in the Sahel and East-Africa, using normalized difference vegetation index from NOAA AVHRR. Clim. Change 17, 209–241.

Ordonez, J.L., Franco, S., Retana, J., 2004. Limitation of the recruitment of *Pinus nigra* in a gradient of post-fire environmental conditions. Ecoscience 11, 296–304.

Parr, C.L., Andersen, A.N., 2006. Patch mosaic burning for biodiversity conservation: a critique of the pyrodiversity paradigm. Conserv. Biol. 20, 1610–1619.

Pausas, J.G., Ouadah, N., Ferrán, A., Gimeno, T., Vallejo, R., 2003. Fire severity and seedling establishment in *Pinus halepensis* woodlands, eastern Iberian Peninsula. Plant Ecol. 2, 205–213.

Peck, J., 2010. Multivariate Analysis for Community Ecologists - step by step using PD-ORD, MJM Software.

Reed, B.C., Brown, J.F., Vanderzee, D., Loveland, T.R., Merchant, J.W., Ohlen, D.O., 1994. Measuring phenological variability from satellite imagery. J. Veg. Sci. 5, 703–714.

Retana, J., Espelta, J.M., Habrouk, A., Ordonez, J.L., de Sola-Morales, F., 2002. Regeneration patterns of three Mediterranean pines and forest changes after a large wildfire in northeastern Spain. Ecoscience 9, 89–97.

Rondeaux, G., Steven, M., 1996. Optimization of soil-adjusted vegetation indices. Remote Sensing of Environment 55, 95-107.

Rouvinen, S., Kuuluvainen, T., 2005. Tree diameter distributions in natural and managed old -dominated forests. Forest Ecology and Management 208, 45-61.

Roy, D.P., Boschetti, L., Trigg, S.N., 2006. Remote Sensing of Fire Severity: Assessing the Performance of the Normalized Burn Ratio. IEEE Geoscience and Remote Sensing Letters 3, 112-116.

Salvador, R., Valeriano, J., Pons, X., Dı´az-Delgado, R., 2000. A semi-automatic methodology to detect fire scars in shrubs and evergreen forests with Landsat MSS time series. Int. J. Remote Sens. 4, 655–671.

Schönenberger, W., 2001. Trends in mountain forest management in Switzerland. Schweizerische Zeitschrift für Forstwesen 152, 152–156.

Schroeder, T., Wulder, M., Healey, S.P., Moisen, G.G., 2011. Mapping wildfire and clearcut harvest disturbances in boreal forests with Landsat time series data. Remote Sensing of Environment 115, 1421-1433.

Smith, M.S., Lentile, L.B., Hudak, T., Morgan, P., 2007. Evaluation of linear spectral unmixing and ΔNBR for predicting post-fire recovery in a North American ponderosa pine forest. International Journal of Remote Sensing 28, 5159-5166.

Solans Vila, J.P., Barbosa, P., 2010. Post-fire vegetation regrowth detection in the Deiva Marina region (Liguria-Italy) using Landsat TM and ETM+ data. Ecological Modelling 221, 75-84.

Spanos, I., Y Raftoyannis, G. Goudelis, E. Xanthopoulou, T. Samara, and A. Tsiontsis., 2005. Effects of postfire logging on soil and vegetation recovery in a *Pinus halepensi*s Mill. forest of Greece. Plant and Soil 278:171–179.

Statgraphics Centurion XVI, 2010. StatPoint technologies, Inc., Virginia, USA.

Thies, W.G., Westlind, D.J., Loewen, M., Brennerm, G., 2006. Prediction of delayed mortality of fire damaged ponderosa pine following prescribed fires in eastern Oregon, USA. International Journal of Wildland Fire, 15, pp. 19–29.

Thomas, P.A., Wein, R.W., 1985. The influence of shelter and the hypothetical effect of fire severity on the postfire establishment of conifers from seed. Can. J. For. Res. 15, 148–155.

Tucker, C. J., Sellers, P. J., 1986. Satellite remote sensing of primary production. International Journal of Remote Sensing, 7, 1395−1416.

van Wagtendonk JW, Root RR, Key CH, 2004. Comparison of AVIRIS and Landsat ETM+ detection capabilities for burn severity. Remote Sensing of Environment 92, 397–408.

Veraverbeke, S., Verstraeten, W.W., Lhermitte, S., Goossens, R., 2010. Evaluating Landsat Thematic Mapper spectral indices for estimating burn severity of the 2007 Peloponnese wildfires in Greece. International Journal of Wildland Fire 19, 558–569.

Verstraete,M.M., Pinty, B., 1991. The potential contribution of satellite remote sensing to the understanding of arid lands processes. Plant Ecology 91: 1-2, 59–72.

Volcani, A, Karnieli, A, Svoray, T., 2005. The use of remote sensing and GIS for spatio-temporal analysis of the physiological state of a semi-arid forest with respect to drought years. Forest Ecology and Management 215, 239-250.

White, J. D., Ryan, K. C., Key, C., Running, S. W., 1996. Remote sensing of forest fire severity and vegetation recovery. International Journal of Wildland Fire, 6, 125–136.

Wiegand, C. L., Richardson, A. J., Escobar, D. E., and Gerber- mann, A. H. (1991), Vegetation indices in crop assessments, Remote Sens. Environ. 35:105-119.

Woodcock, C. E., Macomber S. A., Pax-Lenney M., Cohen W. B., 2001. Monitoring large areas for forest change using Landsat: Generalization across space, time and Landsat sensors, Remote Sens. Environ., 78, 194–203.

Wulder, M., White, J.C., Alvarez, F., Han, T., Rogan, J., Hawkes, B., 2009. Characterizing boreal forest wildfire with multi-temporal Landsat and LIDAR data. Remote Sensing of Environment 113, 1540-1555.

Wulder, M.A., Hall, R.J., Coops, N.C., Franklin, S.E., 2004. High spatial resolution remotely sensed data for ecosystem characterization. Bioscience 54, 511–521.

Zlatanov, T., Velichkov, I., Lexer, M.J., Dubravac, T., 2010. Regeneration dynamics in aging black pine (*Pinus nigra* Arn.) plantations on the south slopes of the Middle Balkan Range in Bulgaria. New Forests 40, 289-303.

Chapter 3

Deadwood facilitation on seedling establishment after a stand-replacing wildfire in Aosta Valley.

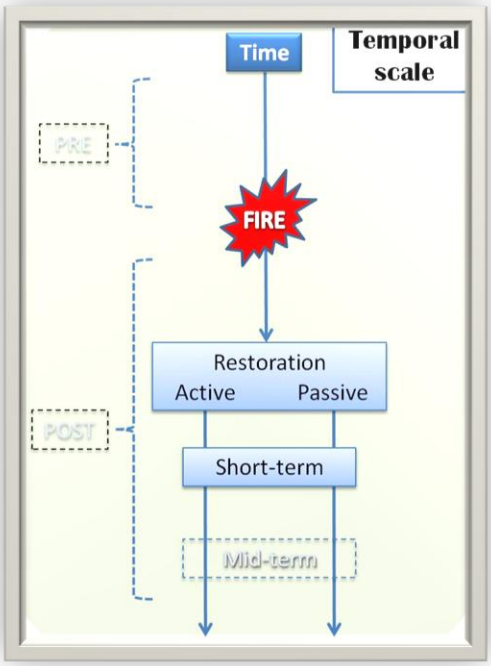

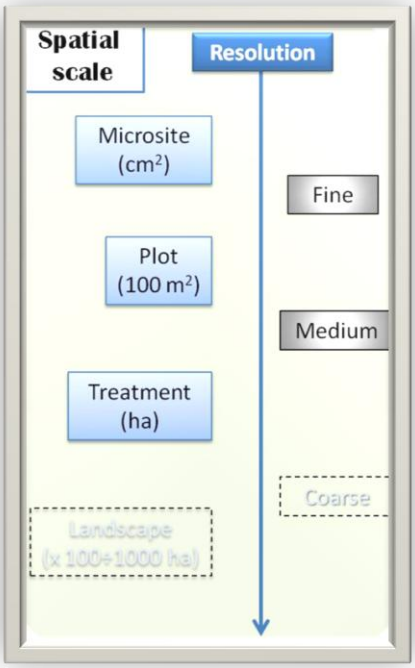

Introduction

After a major disturbance, natural regeneration of forest ecosystems results from the complex interactions between propagules and site factors (Kozlowski, 2002). Numerous scales related biotic and abiotic factors (Clark et al. 1998, 1999) influence current recruitment patterns, playing a role in determining future forest structure and composition (Barbeito et al., 2009) by affecting the initially established tree cohort. The type of regeneration (seed or sprouting) directly influences the spatial pattern of plants (Pardos et al., 2008).

The successful establishment of a seedling depends on several processes, such as seed viability, dispersal, germination, the presence of symbiotic organisms (e.g., mycorrhizae), mortality factors due to seedling predation, competition, and abiotic stress (Nathan and Muller-Landau, 2000; Castro et al., 2004; Kipfer et al., 2009), whose impact is usually local and species-specific (Pardos et al., 2008).

Mechanisms operating at small scales may in particular limit the abundance and performance of seedlings (Collins and Good, 1987).

Seedling establishment is a key component in plant distribution patterns (Harper, 1977).

After germination, seedling mortality rates are usually high and the probability of long-term survival is strictly related to the physical habitat surrounding a seedling (Collins and Good, 1987). Preferential recruitment is associated with the availability of 'safe sites' for germination and is linked to the regeneration niche concept (Grubb, 1977). This is particularly evident in climatically stressed sites, where seedlings establishment is strongly limited by harsh conditions. Mature plants, shrubs, deadwood or rocks can play a positive role in ameliorating microsites along with surface microtopography (Castro et al., 2002; Resler et al., 2005; Franzese et al., 2009; Beghin et al., 2010; Legras et al., 2010). Especially in water stressed/limited environment these elements can reduce soil temperature (shading effect) and wind (less transpiration), and increase relative humidity (Flores and Jurado, 2003; Castro et al., 2011). Intra- or interspecific facilitation mechanisms and sheltering effects of abiotic elements proved to be determinant in tree seedling establishment and survivorship in arid environments (Callaway, 2007).

In drought-stressed Mediterranean mountain ecosystems, already established vegetation has been often identified as one of the main factors favouring tree regeneration survival through a direct protection against high radiation, high temperatures, and high transpiration rates (e.g. Callaway, 1995, 2007). After a stand-replacing fire, with no mature plants or shrubs remaining to facilitate seedling performance after germination, deadwood, rocks as well as surface microtopography may be critical to restoration patterns.

An accurate description of early successional dynamics and the role that microhabitat plays in tree seedling establishment following a major disturbance may be of great importance to clarify restoration patterns aiding in defining ecologically adequate management strategies and silvicultural practices (Pardos et al., 2008; Legras et al., 2010). Post-fire management may greatly affect the resilience of the ecosystem to restore, influencing recruitment both directly and indirectly recruitment (Beghin et al., 2010; Moreira et al., 2012).

In this context we implemented two different post-fire management treatments within a large wildfire in the Western Italian Alps (Aosta Valley). Our objectives were: (1) to analyse natural regeneration dynamics in a post-fire environment characterized by harsh conditions in terms of solar radiation and water availability; (2) to verify the impact of post-fire management (namely salvage logging) on seedling establishment and survival. We hypothesized that post-fire burnt wood management would greatly influence the availability of sites for seedling survival. To address these issues we conducted an experimental study contrasting two common post-fire management practices, no intervention and conventional salvage logging (Beghin et al., 2010), to identify the main environmental variables affecting naturally established seedlings and to quantify the effect of shelter elements, particularly lying and standing deadwood on tree recruitment.

Methods

Study site

The study site is located in the Aosta Valley Region (NW Italy), within the municipality of Verrayes, in an area named Bourra (45°46'14''N, 7°29'58''E), that was severely affected by a stand replacing fire in March 2005. The wildfire, which is one of the biggest and more severe fire events ever experienced in the region, burned 257 ha, completely destroying 160 ha of an almost pure *Pinus sylvestris* stand.

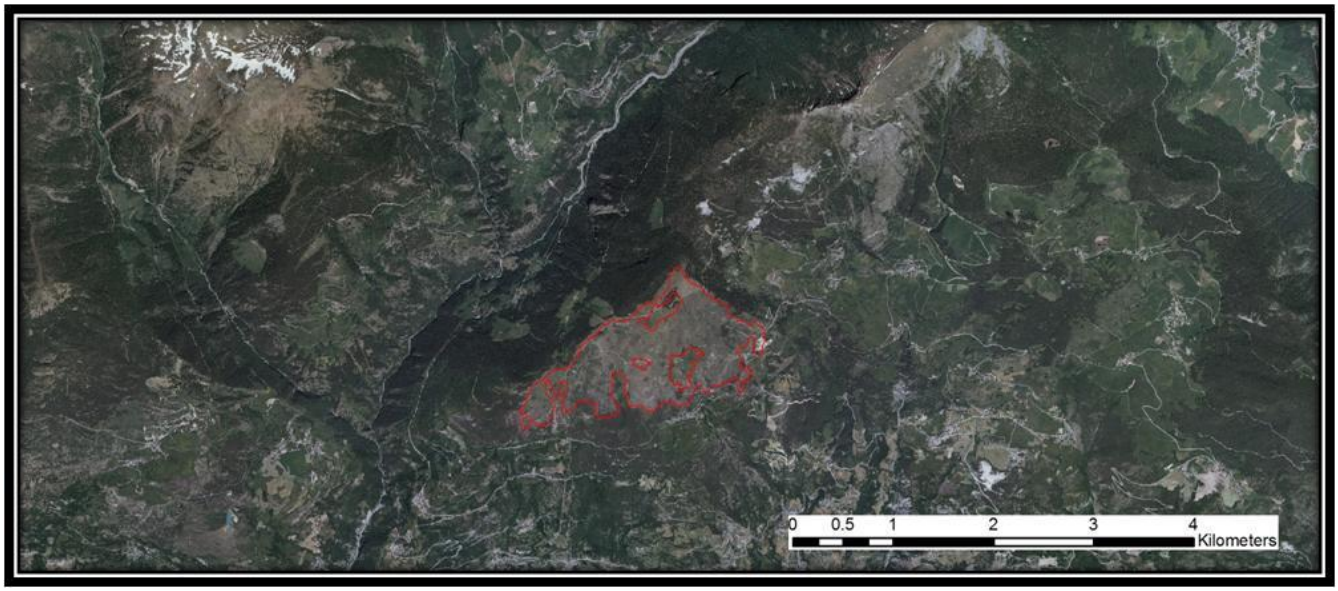

Figure 3.1 - Ortho-image of the study area located in Bourra - Verrayes (Aosta valley): red boundaries mark the perimeter of the burnt area (overlapped to the image).

A post-fire salvage-logging project was approved in December 2005; salvage logging operations started during autumn 2007. Approximately 8 ha within the burned surface were destined in

agreement with the Regional Administration to natural regeneration monitoring studies, establishing two adjoining areas, both characterized by total mortality of the previous stand. To contrast active management and non-intervention (Figure 3.2), one area was salvaged (salvage logging - SL) according to the conventional post-fire management activities in the Region (Beghin et al., 2010) was compared to another one left untouched (passive management - PM). Both areas have a surface of 5 ha; they are adjoining and were characterized by similar pre-fire conditions and total mortality of the previous stand. The altitude of the area ranges between 1650 m and 1800 m a.s.l. and the slope is facing south with an average inclination of 25°. The bedrock is formed by ophiolite and schist and the soils are classified as entisols (Soil Taxonomy USDA). The mean annual temperature is 5.6 °C and the mean annual precipitation is approximately 751 mm, the driest month being February, coinciding with the main peak of the fire season.
The tree vegetation consisted almost solely of dense even-aged *P. sylvestris* stands, with a sporadic presence of *Larix decidua* Miller, *Picea abies* L. Karst, *Quercus pubescens* Will., *Populus tremula* L., *Betula pendula* Roth.

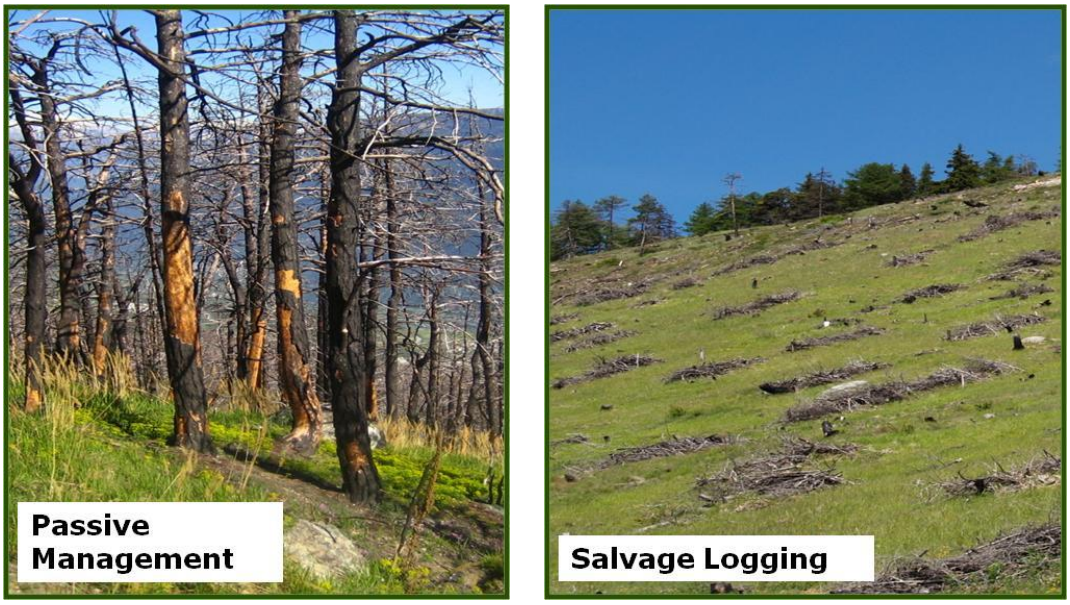

Figure 3.2 - Images of treatments applied to the experimental area.

Experimental design and field data collection

Field surveys were conducted in summer 2010 following two different approaches in order to capture regeneration patterns at different spatial scales (site and microsite) (Kuuluvainen and Juntunen, 1998; Beghin et al., 2010; Jonásová et al., 2010). At site-scale we adopted a complete random design, locating on the ground 60 circular sample plots with a 6 m radius (about 113 m^2). Twenty plots were established within the salvaged area, the remaining in the unsalvaged area. Given the relative environmental homogeneity of the salvaged area, a lower number of plots (20) were considered sufficient (Figure 3.3).

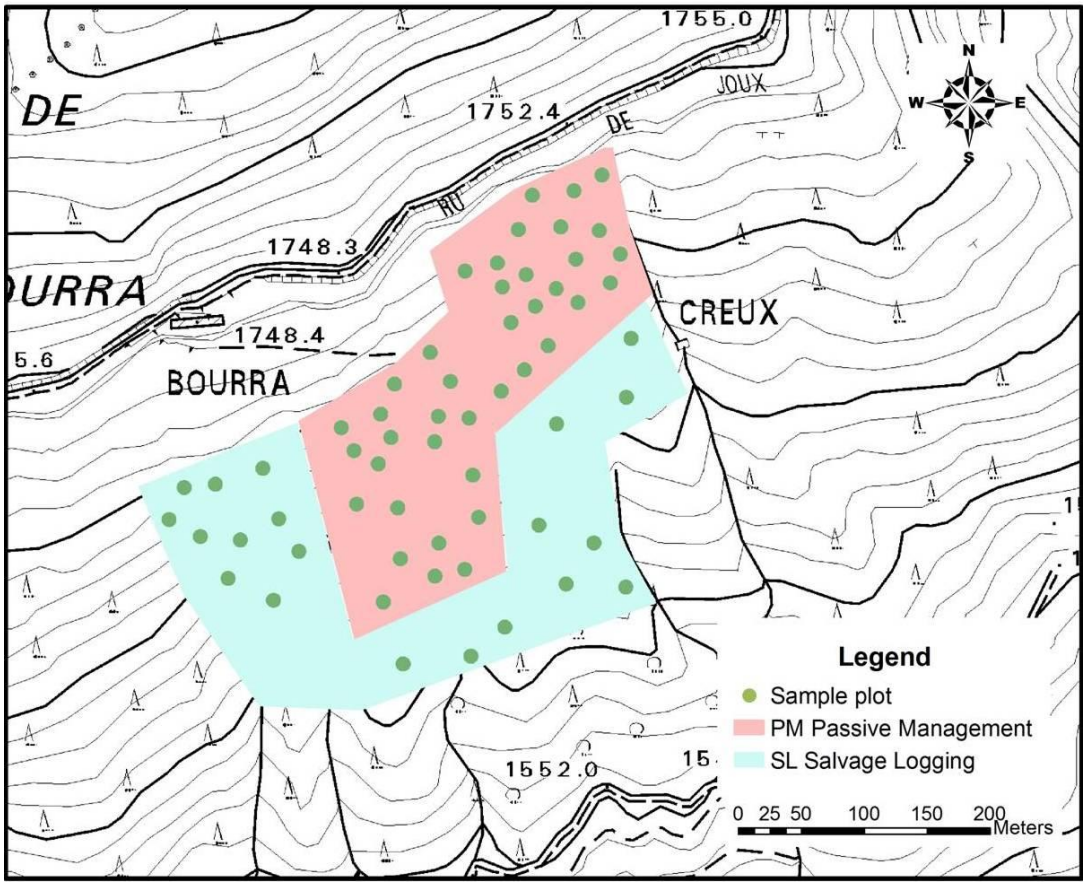

Figure 3.3 - Layout of the experimental design (SL and PM treatments) and distribution of 60 sampling plots (20 plots in SL, 40 plots in PM).

Site-scale collected parameters (Table 3.1a-b) included UTM coordinates (submetric GPS device - Figure 3.4), regeneration characteristics (species, seed or sprout origin, root collar diameter - RCD, height, age), and ground cover. This latter was estimated to the nearest 5% and comprised litter, lying deadwood, bare soil, grasses, forbs, shrubs, and gravel. Game damaged was assessed by counting regeneration presenting signs of browsing. The number of standing dead trees was also recorded in the unsalvaged area. Regeneration age was estimated in the field by counting the terminal bud scars (internodes) along the main stem. Topographic variables (slope, aspect, elevation) were computed from a DTM (1-m resolution) derived from LiDAR data acquired in June 2011.

At microsite-scale we adopted a matched case-control design, where seedlings were actively located and 20cm x 20cm quadratic plots (microsites) were centred on them. Microsites with seedlings (cases) were then matched with microsites without seedlings (controls) for comparison. Controls were always positioned one meter east from their case (Figure 3.5). Sprout-origin regeneration was excluded from this analysis. Microsite-scale parameters were recorded in 720 microsites, representing 360 matched pairs of cases and controls. Besides collecting the seedling (if present) characteristics, as described above, the parameters used to characterize microsites were: (1) seedbed type, classified as litter, rotten wood, bare soil, grasses, forbs, shrubs, and gravel; (2) presence and relative position (distance, azimuth) of standing or lying deadwood

elements within one meter from the microsite centre; (3) presence and relative position of rock elements (minimum height 10 cm) within 1 m from the microsite centre. Microsites position was recorded with a submetric GPS to allow further monitoring.

Figure 3.4 -Left: setting up of a sampling plot (circular shape, 6 m radius) within a salvaged area. Right: detailed view of a GPS antenna placed to the plot center.

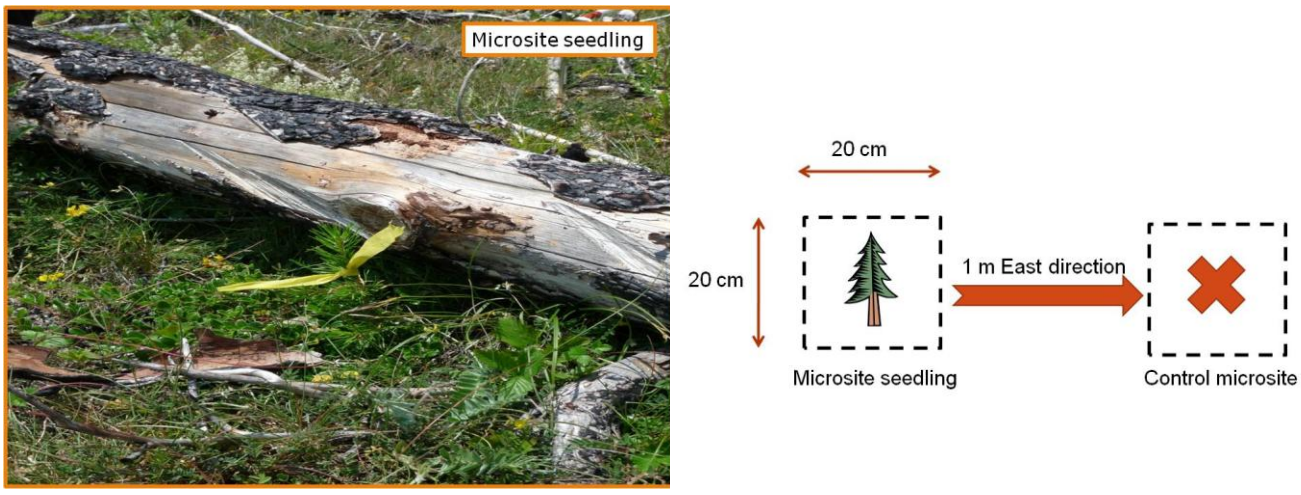

Figure 3.5 - Design of investigation for microsite characteristics: the selected seedling (image to the left) was the centre of the 20 centimeters square-shaped microsite (case). Conventionally, at a distance of 1 meter in an easterly direction, an equal shaped microsite was fixed (control). The investigations at microsite level were conducted according to this matched case-control approach.

Data analysis

Multivariate statistical analyses (ordination, grouping, and regression methods) were combined to assess the impact of environmental variables and post-disturbance management on tree regeneration and composition. A nonparametric group comparison procedure (MRPP) was used to test the effects produced by different post-disturbance management options on tree species composition. The variability in natural regeneration structure at site-scale (6 variables x 60 plots) (Table 3.1a) in relation to management type and environmental factors (13 variables x 60 plots) (Table 3.1b) was analyzed through redundancy analysis (RDA) (Rao, 1964; ter Braak and Prentice, 1988). Redundancy analysis is an extension of principal component analysis and was used to investigate the variability explained by the explanatory variables and their correlation with regeneration structure variation. Redundancy analysis was performed using Canoco® (ter Braak and Smilauer, 1998), while MRPP test was performed using PC-ORD statistical package (McCune and Mefford, 1999). The statistical significance of all ordination analyses was tested by Monte Carlo permutation method based on 10,000 runs with randomized data.

Conditional logistic regression analysis for matched-pairs data (Breslow, 1982) was used to relate the occurrence (case) and absence (control) of seedlings with microsite variables. The within-pair differences in all variables were calculated, resulting in a constant value of 1 for the response variable "seedling occurrence" and a set of new potential explanatory variables that are the differences between the case and the control for each matched pair (Gibbons et al., 2008). The probability of occurrence of a seedling as related to differences in the variables characterizing matching microsites pair is expressed by odd ratio values (OR). Odds ratios (OR = p/(1-p), with p = proportion of an event, i.e., a seedling present) were calculated by comparing proportions of microsites with and without seedlings. The conditional logistic regression was performed using the SPSS 17 statistical package.

Table 3.1a - Regeneration variables included in the ordinations for plot-level analyses

Variable category	Code	Description	Unit	Data source
Regeneration structure	PT	*Populus tremula* regeneration density	$\#ha^{-1}$	Field
	Other trees	Regeneration density of all tree species except *P. tremula*	$\#ha^{-1}$	Field
	RCD-Mean	Mean root collar diameter	cm	Field
	RCD-Std.Dev	Standard deviation of root collar diameter	cm	Field
	Age-Max	Age of the oldest seedling	years	Field
	Diversity	Tree species diversity (Shannon index applied to tree species)	-	Field

Table 3.1b - Site variables included in the ordinations for plot-level analyses

Variable category	Code	Description	Unit	Data source
Environmental	Slope	Slope	°	DTM (LiDAR)
	HLI	Heat load index (McCune and Grace 2002)	-	DTM (LiDAR)
	Cover-div	Ground cover diversity (Shannon index applied to ground cover types)	-	Field
	Shrubs	Shrub cover	%	Field (visually estimated)
	Forbs	Forb cover	%	Field (visually estimated)
	Grasses	Grass cover	%	Field (visually estimated)
	Soil	Bare soil cover	%	Field (visually estimated)
	Gravel	Gravel cover	%	Field (visually estimated)
	Litter	Litter cover	%	Field (visually estimated)
	Ly.deadwood	Coarse woody debris cover	%	Field (visually estimated)
	St.deadwood	Snag density	$\#ha^{-1}$	Field
	Salvage logging	Post fire logging treatment	-	Nominal variable
	No intervention	Absence of post fire treatment	-	Nominal variable

Results

Regeneration structure and composition at site-scale

Tree regeneration ranged between 0 and 8319 seedlings ha^{-1}, averaging 558 ha^{-1} (± 242) in passive management plots, 702 ha^{-1} (± 355) in salvaged plots. Sprouts accounted for 77% and 82 % of the total regeneration in PM and SL respectively.

The estimated age of the regeneration ranged from 1 to 5 years. Mean diameter and height of sprout-origin regeneration were respectively 0.74 (±0.04) cm and 49.06 (±2.10) cm. Seedling mean diameter was 0.73 (±0.05) and mean height was 35.51 (±3.09). Damage from wild ungulate browsing was observed on 44% of regeneration individuals, thus affecting height values. No statistically significant differences were found (χ^2 test; $p < 0.05$) among management types and species. The management type emerged as an influential factor only for seedling species composition (MRPP: T = -2.128, p < 0.05). Considering each species separately, *P. sylvestris* and *L. decidua* relative abundances were higher in passive management sites (Figure 3.6; Table3.2). Most sprouter species, particularly *P. tremula*, *Q. pubescens* and *Sorbus aria* were more abundant in salvaged plots (Figure 3.6; Table3.2).

Figure 3.6 - Seedling of Pinus sylvestris in the passive management area (left); Quercus pubescens in a salvaged plot (right).

Table 3.2 - Mean density (seedlings/ha) and standard error (in parentheses) of regeneration, divided by species and management type.

Species	Passive Management	Salvage logging	Tot.
Pinus sylvestris	14.50 (±12.28)	-	9.66 (±8.20)
Larix decidua	14.72 (±7.53)	5.06 (±5.06)	11.50 (±5.30)
Populus tremula	387.90 (±238.92)	504.61 (±325.02)	426.80 (±191.17)
Quercus pubescens	7.65 (±5.64)	54.91 (±30.36)	23.40 (±11.02)
Fraxinus excelsior	10.02 (±7.82)	10.32 (±7.11)	10.12 (±5.69)
Betula pendula	7.21 (±4.06)	-	4.81 (±2.73)
Salix caprea	66.27 (±14.10)	72.64 (±48.28)	68.39 (±18.38)
Sorbus aria	-	25.00 (±16.15)	8.33 (±5.51)
Sorbus aucuparia	17.63 (±8.05)	-	11.75 (±5.45)
Juniperus communis	27.04 (±9.28)	9.77 (±6.73)	21.28 (±6.63)
Tot.	558 (±242)	702 (±355)	606 (±198)

The role of environmental and management factors on the structure of regeneration of tree species was analyzed through direct gradient analysis. Redundancy analysis of regeneration structure related to the examined management options and environmental variables is shown in Figure 3.7. The first and second axes accounted for 19.9 and 3.1% of the total variation, respectively. Density, diversity, and maximum age of tree seedlings were positively associated to lying and standing deadwood. Regeneration density of 'other trees' (all tree species except *P. tremula*) was weakly and negatively associated to sites with abundant bare soil, gravel, litter, and shrub cover at the ground. *P. tremula* density was uncorrelated with 'other trees' density and seemed not influenced by the presence of deadwood.

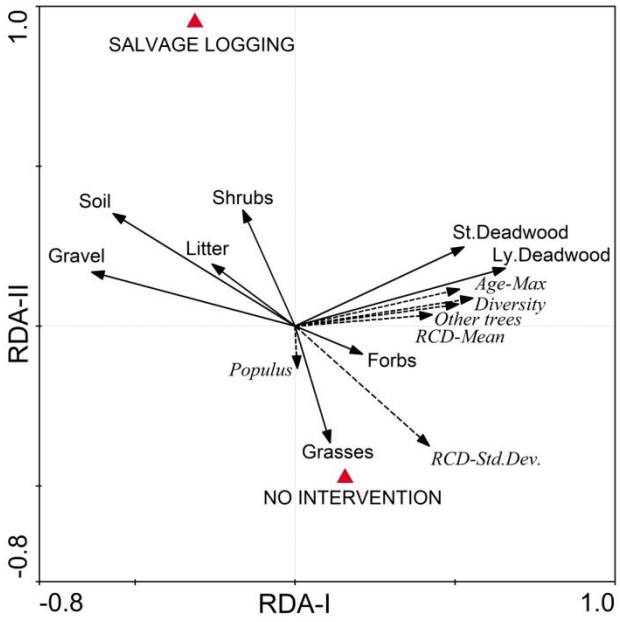

Figure 3.7 - Redundancy analysis (RDA of 60 plots) of regeneration structure in relation to environmental characteristics and management options at site-scale. Dashed arrows are the regeneration structure variables (RCD-Mean: average Root Collar Diameter ; RCD-Std.Dev: standard deviation of Root Collar Diameter; Diversity: Shannon diversity index; Populus: density of Populus tremula; Other trees: density of all tree species except P. tremula; Age-Max: maximum seedling age). Full line arrows represent the "biplot scores of site variables" (St.Deadwood: standing deadwood or snags; Ly.Deadwood: lying deadwood; Shrubs: shrubs cover; Litter: litter cover; Soil: bare soil cover; Gravel: gravel cover; Grasses: graminoids cover; Forbs: non-graminoid herb cover). Triangular dots are management options (No intervention: absence of post-fire treatment; Salvage logging: post-fire logging treatment) categorical variables. The species-environment correlation for the first RDA axis was 63.0.

Microsite influence on seedling occurrence

Three hundred and sixty matched pairs of microsites with and without seedlings were measured in the salvage logging and the untreated area. The root collar diameter of measured seedlings ranged from 0.1 to 3.2 cm with a mean of 0.84 cm (±0.02). Seedling height ranged from 6 to 134 cm with a mean of 38.57 cm (±1.09). The most abundant species measured were *P. sylvestris* (15%), *Salix caprea* (15%), *Q. pubescens* (14%), *L. decidua* (13%), and *P. tremula* (11%). The other species measured accounting for 31% of the total amount of seedlings were *B. pendula*, *Sorbus aucuparia*, *S. aria*, *Prunus avium*, *Populus alba*, *Fraxinus excelsior*, *Juniperus communis*, and *Corylus avellana*.
The conditional logistic regression analysis for matched-pairs on presence-absence of tree seedlings demonstrated the importance of deadwood as a facilitative element (Table 3.3).

Table 3.3 - Results of conditional logistic regression analysis for 360 matched pair's data (seedlings and controls). The significant explanatory variables used in the conditional logistic regression model are expressed in bold. Only variables having an odds ratio above 1 (i.e. indicating a higher occurrence of saplings on a given microsite than would be expected by chance) are shown.

Explanatory variable	*Beta*	S.E.	*p*-Value	Odds ratio	95% Confidence interval for odds ratio
Proximity to					
Deadwood_W	1.281	0.279	0.000	3.600	2.084-6.221
Deadwood_S	0.957	0.260	0.000	2.605	1.566-4.334
Deadwood_E	0.937	0.236	0.000	2.553	1.607-4.057
Deadwood_N	0.612	0.254	0.016	1.844	1.122-3.033
Rocks_N	0.608	0.603	0.313	1.837	0.563-5.99
Rocks_W	0.390	0.846	0.645	1.477	0.281-7.753
Rocks_S	0.387	0.800	0.628	1.473	0.307-7.064

Recruitment was highly associated with specific locations of surrounding deadwood.

The proximity of at least one element of deadwood (stump, log or snag) within 1 m radius increased the probability of a successful establishment and survival of tree seedlings.

Azimuth locations of seedlings with respect to deadwood were highly non-uniform (χ^2 test; $p < 0.05$). Seedling regeneration pattern thus evidenced a marked anisotropy. In particular seedlings occurred significantly more often than by chance when deadwood elements were located on west (odds ratio [OR] = 3.6), south (OR = 2.6), east (OR = 2.5), and north (OR = 1.9) azimuth quadrants (Table 3.3). All other explanatory variables (Table 3.4) used in the model emerged as not significantly ($p > 0.05$) affecting the occurrence or absence of tree seedlings. A further stratification involving separately the matched-pair data of seedling species did not produce any significant model. Analysing seedling species data and pooled deadwood presence/absence data nevertheless revealed a significant and positive ($\chi^2 = 4.58$; $p < 0.05$) influence of deadwood elements on *P.sylvestris* seedlings.

Table 3.4 - Mean and standard error (in parentheses) of explanatory variables used in the conditional logistic regression model of microsite plots with vs. without seedlings.

Explanatory variable	Seedling (n = 360)	No seedling (n = 360)
Seedbed (%)		
Grasses	29.25 (±1.49)	26.99 (±1.51)
Bare soil	24.95 (±1.21)	21.55 (±1.32)
Rotten wood	14.98 (±0.86)	15.99 (±1.16)
Forbs	14.38 (±0.80)	18.09 (±1.06)
Shrubs	14.37 (±1.13)	15.81 (±1.22)
Proximity to (n)		
Deadwood_S	0.27 (±0.03)	0.15 (±0.02)
Deadwood _N	0.25 (±0.03)	0.16 (±0.03)
Deadwood_E	0.19 (±0.03)	0.11 (±0.02)
Deadwood_W	0.19 (±0.03)	0.14 (±0.02)
Rocks_N	0.04 (±0.01)	0.02 (±0.01)
Rocks_E	0.04 (±0.01)	0.01 (±0.01)
Rocks_S	0.02 (±0.01)	0.02 (±0.01)
Rocks_W	0.02 (±0.01)	0.02 (±0.01)

Discussion

Regeneration density five years after the fire was still low even though tree species recruitment started immediately after the fire. Resprouts dominated the regeneration layer and higher densities of regenerating stems were observed in particular for *P. tremula*. *Populus tremula* is able to produce both stump sprouts and root suckers, and this reproductive strategy is very efficient in maintaining the population under severe disturbance or stressful condition (Hamberg et al., 2011). Root suckers are specialized in efficiently and quickly encroaching a wide underground space after a high severity disturbance (Homma et al., 2003). The high production of juveniles from suckering, producing dense clonal thickets could balance the high browsing pressure since aspen is a preferred species by ungulates (Hamberg et al., 2011; de Chantal and Granström, 2007; Myking et al., 2011). Browsing of regeneration was actually rather high, affecting the height of sprout-origin individuals (data not shown).

Despite the short time since post-fire interventions, management strategies proved to produce an immediate influence on regeneration species composition. Facultative sprouters (e.g. *P. Tremula* and *Q. Pubescens*), showing a preference for salvage logged areas, confirmed the high resilience of these species in harsher post-fire conditions due to their main regeneration strategy. On the contrary obligate seeders, namely those conifer species (*P. Sylvestris* and *L. Decidua*) that were present in the pre-fire stand, although less abundant in absolute numbers, were favoured by leaving deadwood on site.

Regeneration was in fact positively associated with deadwood. Its density and species diversity were higher when lying and/or standing deadwood were present. This positive effect proved to be essential from the first post-fire growing season, as demonstrated by a stronger association evidenced for older seedlings (i.e. seedlings established in the harsher early post-fire environment).

The removal of dead or damaged trees produced by salvage logging strongly reduces the availability of biological legacies (Lindenmayer, 2006). Furthermore salvage harvesting can produce ground disturbance affecting vegetation development (Macdonald, 2007). The presence of patches of standing dead trees could moreover favor tree recruitment by providing perching sites for frugivore birds, potentially improving species richness in the regeneration layer (McClanahan and Wolfe, 1993; Rost et al., 2009; Castro et al., 2009).

Ground cover conditions contributed to patterns of seedling occurrence. Regeneration was most successful in sites where the amount of bare soil, litter, gravel or shrub species was reduced. In our dry site with a water stress condition, even pioneer conifer species (*P. sylvestris* and *L. decidua*) did not thrive on exposed mineral soil in open sites available in salvaged area, preferring safe sites close to deadwood. The facilitative effect of shrubs on tree seedling establishment and survival commonly seen in dry sites (see Callaway, 2007) is not evident in our site probably because in this short post-fire period they are both competing for colonizing the burnt area. We might expect future evidence of this facilitative role when shrubs cover will be higher as found in

other studies (Castro et al., 2004; Gómez-Aparicio et al., 2004) and in an older burned area having similar site conditions in the same region (Beghin et al., 2010).
An exception was represented by *P. tremula*, the most abundant species in the regeneration layer, whose behaviour differed from the other regenerating tree species, being uncorrelated with the presence of deadwood. *P. tremula* proved to successfully encroach grass cover dominated sites (Figure 3.8). The fast growth of *Populus* root suckers undoubtedly provided a competitive advantage for light with the grass layer (Homma et al., 2003; Myking et al., 2011). Similar results were found by Beghin et al. (2010) with the sprouting ability of this broadleaved species providing an explanation for its widespread presence in areas characterized by a dominance of grasses, where reduced germination limited establishment of tree species dependent on sexual reproduction.

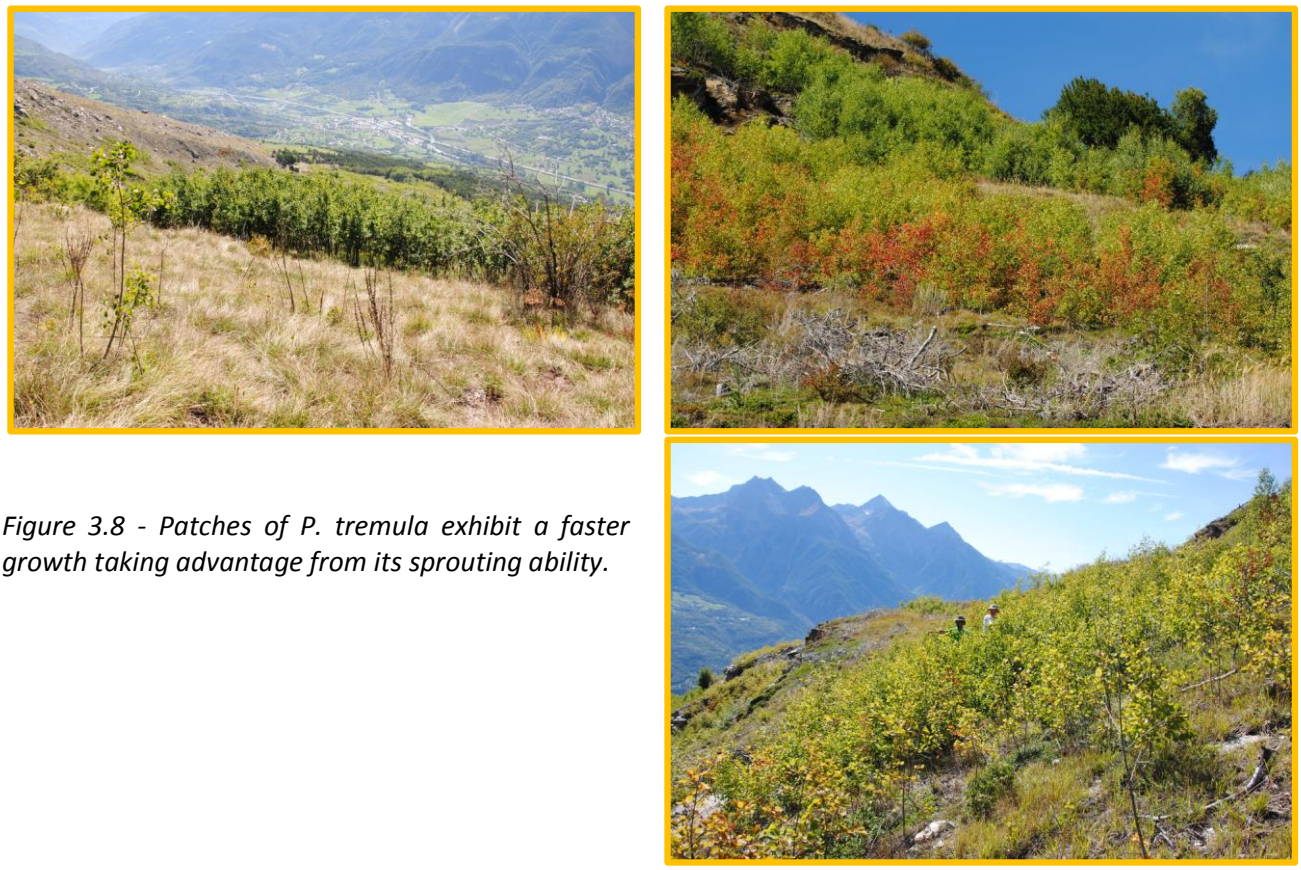

Figure 3.8 - Patches of P. tremula exhibit a faster growth taking advantage from its sprouting ability.

Analysing regeneration presence at the microsite level, the probability of a seedling was always higher when a deadwood element was present.
The strong spatial association of tree seedlings with deadwood suggests that deadwood produces microsites that enhance the establishment of seedlings.
The presence of abiotic shelter elements can potentially provide safe microsite conditions for recruitment, without producing competition dynamics with the seedlings.
Nurse objects can enhance both seedling establishment and survival (Coop and Schoettle, 2009; Resler et al., 2005; Castro et al., 2011). They can efficiently act as seed traps for wind-dispersed

seed, and provide shading, resulting in reduced evaporation and higher soil moisture (Flores and Jurado, 2003; Carlucci et al., 2011).

With water being a critical resource in xeric environments, microsites where microclimatic conditions help in conserving water can play a key role for tree seedling growth and development (Legras et al., 2010). Several studies have reported reduced growth and survival of tree species associated with low soil moisture content was present (e.g. Conard and Radosevich, 1982; Germaine and McPherson, 1999).

In our study area, characterized by low winter temperatures, the beneficial effect of deadwood material could also result in holding higher soil temperatures during night, thus affecting winter seedling survival, as found by Castro et al. (2011).

The positive anisotropic relationship that we found between seedlings and deadwood was also evidenced in other harsh environments where shield effects were produced by shrubs or live trees (Kitzberger et al., 2000; Haase, 2001; Lingua et al., 2008).

In xeric woodlands direct protection from radiation and the effects of shade on soil water availability are among the main factors facilitating the establishment of regeneration, with seedlings preferentially occurring on shady sides of the shelter elements (Kitzberger et al., 2000; Callaway, 2007; Beghin et al., 2010; Castro et al., 2011), in microsites protected in the sunniest hours.

On average, seedlings occurred four times more often than would be expected under the assumption of a random distribution if a deadwood element were present Westward. Besides the shadow effect, in this case the positive anisotropic relationship is probably also related with seed trapping. The main wind direction in our study site is East-west, and the live edge of untouched forest is bordering East, thus Westward deadwood elements are obstacles that can trap wind-dispersed seed (Pounden et al., 2008).

In our site only deadwood showed a positive effect on tree regeneration probably because rocks were generally small and single, not providing enough shadow.

Seedbed characteristics did not prove to have a significant influence on seedling establishment/survival at microsite level.

P. sylvestris was the species whose presence was more correlated with deadwood. Its seedling are known to be dependent on a sufficient water supply (Hille and den Ouden, 2004), consequently a stable soil moisture regime in the initial stages of recruitment is essential for their survival. *P. sylvestris* regeneration is therefore more likely to have taken advantage of the shelter effect provided by deadwood elements.

Despite the facilitative effect produced by deadwood, *P. sylvestris* regeneration 5 years after the fire was still very scarce. The species has no cone serotiny (Tapias et al., 2004). Its winged seeds are typically dispersed by wind in a period of about 2 or 3 weeks after cone opening in early spring (Debain et al., 2007), thus benefitting from spring rains (Debain et al., 2005). Good seed production usually occurs every 4-6 years (Lanner, 1998). Variation in seed production and quality between years is higher in harsh environments (Karlsson and Örlander, 2000). Cones and seeds of *P. sylvestris* show a very limited resistance to fire (Habrouk et al., 1999), thus after a stand-replacing fire the only potential sources for regeneration being unburned edges or green islands.

Despite its pioneer attributes, a difficulty of *P. sylvestris* to germinate after fire has been observed (Retana et al., 2002), together with a limited capacity of recolonization from unburned edge due to limited dispersal distances (Vilà-Cabrera et al., 2012).

Foreseen changes in fire regimes worldwide (Dale et al., 2001; Cary, 2002; Flannigan et al., 2005; Westerling et al., 2006) and specifically in the Mediterranean Basin (Pausas and Fernández-Munõz, 2012) will probably increase the vulnerability of pine stands to fire. The forthcoming scenario calls for a full understanding of post-disturbance tree recruitment processes; in particular, knowledge on severe crown fires' effects needs to be further explored (Marzano et al., 2012). A recent rise in crown fire occurrence in *P. sylvestris* forests at the southwestern distribution limit of the species has already been reported (Pausas et al., 2008; Beghin et al., 2010). *P. sylvestris* stands in dry sites will more likely be affected, with possible vegetation shifts towards shrublands or mixed resprouter forests (Rodrigo et al., 2004; Vilà-Cabrera et al., 2012). Post-fire rehabilitation and restoration treatments of these ecosystems should thus be implemented in the light of this scenario, acknowledging their potential to alter microsites variety and diversity, with possible implications on the species composition of restored forests.

References

Barbeito, I., Fortin, M.J., Montes, F., Cañellas, I., 2009. Response of pine natural regeneration to small-scale spatial variation in a managed Mediterranean mountain forest. Appl. Veg. Sci. 12, 488–503.

Beghin, R., Lingua, E., Garbarino, M., Lonati, M., Bovio, G., Motta, R., Marzano, R., 2010. *Pinus sylvestris* forest regeneration under different post-fire restoration practices in the northwestern Italian Alps. Ecol. Eng. 36, 1365-1372.

Breslow, N., 1982. Covariance adjustment of relative-risk estimates in matched studies. Biometrics 38, 661-672.

Callaway, R.M., 1995. Positive interactions among plants. Bot. Rev. 61, 306-349.

Callaway, R.M., 2007. Positive interactions and interdependence in Plant Communities. Springer, Dordrecht, The Netherlands.

Carlucci, M.B., da, S., Duarte, L., Pillar, V.D., 2011. Nurse rocks influence forest expansion over native grassland in southern Brazil. J. Veg. Sci. 22, 111-119.

Cary, G.C., 2002. Importance of a changing climate for fire regimes in Australia. In: Bradstock, R.A., Williams, J.E., Gill, A.M. (Eds.), Flammable Australia: The Fire Regimes and Biodiversity of a Continent. Cambridge University Press, Melbourne, Australia, pp. 26–48.

Castro, J., Zamora, R., Hódar, J. A., Gómez, J. M., 2002. The use of shrubs as nurse plants: a new technique for reforestation in Mediterranean mountains. Restor. Ecol. 10, 297-305.

Castro, J., Zamora, R., Hódar, J. A., Gómez, J. M., 2004. Seedling establishment of a boreal tree species (*Pinus sylvestris*) at its southernmost distribution limit: consequences of being in a marginal Mediterranean habitat. J. Ecol. 92, 266-277.

Castro, J., Moreno-Rueda, G., Hódar, J.A., 2009. Experimental test of postfire management in pine forests: impact of salvage logging versus partial cutting and nonintervention on bird-species assemblages. Conserv. Biol. 24, 810-819.

Castro, J., Allen, C.D., Molina-Morales, M., Marañón-Jiménez, S., Sánchez-Miranda, Á., Zamora, R., 2011. Salvage logging versus the use of burnt wood as a nurse object to promote post-fire tree seedling establishment. Restor. Ecol. 19, 537-544.

Clark, J.S., Macklin, E., Wood, L., 1998. Stages and spatial scales of recruitment limitation in southern Appalachian forests. Ecol. Monogr. 68, 213-235.

Clark, J.S., Beckage, B., Camilla, P., Cleveland, B., HilleRisLambers, J., Lichter, J., McLachlan, J., Mohan, J., Wyckoff, P., 1999. Interpreting recruitment limitation in forests. Am. J. Bot. 86, 1-16.

Collins, S.L., Good, R.E., 1987. The seedling regeneration niche: habitat structure of tree seedlings in an oak-pine forest. Oikos 48, 89-98.

Conard, S.G., Radosevich, S.R., 1982. Growth responses of white fir to decreased shading and root competition by montane chaparral shrubs. Forest Sci. 28, 309–320.

Coop, J.D., Schoettle, A.W., 2009. Regeneration of Rocky Mountain bristlecone pine (*Pinus aristata*) and limber pine (*Pinus flexilis*) three decades after stand-replacing fires. Forest Ecol. Manag. 257, 893-903.

Dale, V.H., Joyce, L.A., McNulty, S., Neilson, R.P., Ayres, M.P., Flannigan, M.D., Hanson, P.J., Irland, L.C., Lugo, A.E., Peterson, C.J., Simberloff, D., Swanson, F.J., Stocks, B.J., Wotton, B.M., 2001. Climate change and forest disturbances. Bioscience 51, 723–734.

Debain, S., Curt, T., Lepart, J., 2005. Indirect effect of grazing on the establishment of *Pinus sylvestris* and *Pinus nigra* seedlings in calcareous grasslands in relation to resource levels. Ecoscience 12, 192–201.

Debain, S., Chadoeuf, J., Curt, T., Kunstler, G., Lepart, J., 2007. Comparing effective dispersal in expanding population of *Pinus sylvestris* and *Pinus nigra* in calcareous grasslands. Can. J. Res. 37, 705-718.

de Chantal, M., Granström, A., 2007. Aggregations of dead wood after wildfire act as browsing refugia for seedlings of *Populus tremula* and *Salix caprea*. Forest Ecol. Manag. 250, 3-8.

Flannigan, M.D., Logan, K.A., Amiro, B.D., Skinner, W.R., Stocks, B.J., 2005. Future area burned in Canada. Clim. Change 72, 1-16.

Flores, J., Jurado, E., 2003. Are nurse-protégé interaction more common among plants from arid environments? J. Veg. Sci. 14, 911-916.

Franzese, J., Ghermandi, L., Bran, D., 2009. Post-fire shrub recruitment in a semi-arid grassland: the role of microsites. J. Veg. Sci. 20, 251-259.

Germaine, H.L., McPherson, G.R., 1999. Effects of biotic factors on emergence and survival of *Quercus emoryi* at lower tree line, Arizona U.S.A. Ecoscience 6, 92–99.

Gibbons, P., Cunningham, R.B., Lindenmayer, D.B., 2008. What factors influence the collapse of trees retained on logged sites? A case-control study. Forest Ecol. Manag. 255, 62-67.

Gómez -Aparicio, L., Zamora, R., Gómez, J. M., Hódar, J. A, Castro, J., Baraza, E., 2004. Applying plant positive interactions to reforestation in Mediterranean mountains: a meta-analysis of the use of shrubs as nurse plants. Ecol. Appl. 14,1128–1138.

Grubb, P.J., 1977. The maintenance of species-richness in plant communities: the importance of the regeneration niche. Biol. Rev. Camb. Philos. Soc. 52, 107-145.

Haase, P., 2001. Can isotropy *vs*. anisotropy in the spatial association of plant species reveal physical *vs*. biotic facilitation? J. Veg. Sci. 12, 127-136.

Habrouk, A., Retana, J., Espelta, J.M., 1999. Role of heat tolerance and cone protection of seeds in the response of three pine species to wildfires. Plant Ecol. 145, 91-99.

Hamberg, L., Malmivaara-Lämsä, M., Löfström, I., Vartiamäki, H., Valkonen, S., Hantula, J., 2011. Sprouting of *Populus tremula* L. in spruce regeneration areas following alternative treatments. Eur. J. Forest Res. 130, 99-106.

Harper, J.L., 1977. Population Biology of Plants. Academic Press, London, U.K.

Hille, M., den Ouden, J., 2004. Improved recruitment and early growth of Scots pine (*Pinus sylvestris* L.) seedlings after fire and soil scarification. Eur. J. Forest Res. 123, 213–218.

Homma, K., Takahashi, K., Hara, T., Vetrova, V.P., Vyatkina, M.P., Florenzev, S., 2003. Regeneration processes of a boreal forest in Kamchatka with special reference to the contribution of sprouting to population maintenance. Plant Ecol. 166, 25–35.

Karlsson, C., Örlander, G., 2000. Soil scarification shortly before a rich seed-fall improves seedling establishment in seed tree stands of *Pinus sylvestris*. Scand. J. Forest Res. 15, 256–266.

Kipfer, T., Egli, S., Ghazoul, J., Moser, B., Wohlgemuth, T., 2009. Susceptibility of ectomycorrhizal fungi to soil heating. Fungal Biol. 114, 467–472.

Kitzberger, T., Steinaker, D.F., Veblen, T.T., 2000. Effects of climatic variability on facilitation of tree establishment in Northern Patagonia. Ecology 81, 1914-1924.

Kozlowski, T.T., 2002. Physiological ecology of natural regeneration of harvested and disturbed forest stands: implications for forest management. Forest Ecol. Manag. 158, 195-221.

Kuuluvainen, T., Juntunen, P., 1998. Seedling establishment in relation to microhabitat variation in a windthrow gap in a boreal Pinus sylvestris forest. Journal of Vegetation Science 9, 551–562.

Jonásová, M., Vávrová, E., Cudlin, P., 2010. Western Carpathian mountain spruce forest after a windthrow: Natural regeneration in cleared and uncleared areas. Forest Ecology and Management 259, 1127–1134.

Lanner, R.M., 1998. Seed dispersal in *Pinus*. In: Richardson D.M. (ed) Ecology and Biogeography of Pinus. Cambridge University Press, Cambridge, pp 281–295.

Legras, E.C., Vander Wall, S.B., Board, D.I., 2010. The role of germination microsite in the establishment of sugar pine and Jeffrey pine seedlings. Forest Ecol. Manag. 260, 806-813.

Lindenmayer, D., 2006. Salvage harvesting – past lessons and future issues. Forest. Chron. 82, 48-53.

Lingua, E., Cherubini, P., Motta, R., Nola, P., 2008. Spatial structure along an altitudinal gradient in the Italian central Alps suggests competition and facilitation among coniferous species. J. Veg. Sci. 19, 425–436.

Macdonald, S.E., 2007. Effects of partial post-fire salvage harvesting on vegetation communities in the boreal mixedwood forest region of northeastern Alberta Canada. Forest Ecol. Manag. 239, 21-31.

Marzano, R., Lingua, E., Garbarino, M., 2012. Post-fire effects and short-term regeneration dynamics following high severity crown fires in a Mediterranean forest. iForest 5, 93-100.

McClanahan, T.R., Wolfe, R.W., 1993. Accelerating forest succession in a fragmented landscape: the role of birds and perches. Conserv. Biol. 7, 279-288.

McCune, B., Grace, J.B., 2002. Analysis of Ecological Communities. MjM Software Design. Gleneden Beach.

McCune, B., Mefford, M.J., 1999. PC-ORD. MjM Software Design. Gleneden Beach.

Moreira, F., Arianoutsou, M., Corona, P., De las Heras, J. (Eds.), 2012. In: Managing Forest Ecosystems, vol. 24. Springer, Dordrecht.

Myking, T., Bøhler, F., Austrheim, G., Solberg, E.J., 2011. Life history strategies of aspen (*Populus tremula* L.) and browsing effects: a literature review. Forestry 84, 61-72.

Nathan, R., Muller-Landau, H.C., 2000. Spatial patterns of seed dispersal, their determinants and consequences for recruitment. Trends Ecol. Evol. 15, 278–285.

Pardos, M., Montes, F., Cañellas, I., 2008. Spatial dynamics of natural regeneration in two differently managed *Pinus sylvestris* stands before and after silvicultural intervention using replicated spatial point patterns. Forest Sci. 54, 260-272.

Pausas, J.G., Fernández-Muñoz, S., 2012. Fire regime changes in the Western Mediterranean Basin: from fuel-limited to drought-driven fire regime. Clim. Change 110, 215-226.

Pausas, J.G., Llovet, J., Rodrigo, A., Vallejo, R., 2008. Are wildfires a disaster in the Mediterranean basin? – A review. Int. J. Wildland Fire 17, 713–723.

Pounden, E., Greene, D.F., Quesada, M., Contreras Sánchez, J.M., 2008. The effect of collisions with vegetation elements on the dispersal of winged and plumed seeds. J. Ecol. 96, 591-598.

Rao, C.R., 1964. The use and interpretation of principal components analysis in applied research. Sankhya 26, 329-358.

Resler, L.M., Butler, D.R., Malanson, G.P., 2005. Topographic shelter and conifer establishment and mortality in an alpine environment, Glacier National Park, Montana. Phys. Geogr. 26, 112-125.

Retana, J., Espelta, J.M., Habrouk, A., Ordóñez, J.L., Solà-Morales, F., 2002. Regeneration patterns of three Mediterranean pines and forest changes after a large wildfire in northeastern Spain. Écoscience 9, 89-97.

Rodrigo, A., Retana, J., Picó, F.X., 2004. Direct regeneration is not the only response of Mediterranean forests to large fires. Ecology 85, 716–729.

Rost, J., Pons, P., Bas, J.M., 2009. Can salvage logging affect seed dispersal by birds into burned forests? Acta Oecol. 35, 763-768.

Tapias, R., Climent, J., Pardos, J., Gil, L., 2004. Life histories of Mediterranean pines. Plant Ecol. 171, 53-68.

ter Braak, C.J.F., Prentice, I.C., 1988. A theory of gradient analysis. Adv. Ecol. Res.Explor. 18, 271–317.

ter Braak, C.J.F., Smilauer, P., 1998. Reference Manual and User's Guide to Canoco for Windows: Software for Canonical Community Ordination (version 4). Microcomputer Power, Ithaca, NY, USA.

Vilà-Cabrera, A., Rodrigo, A., Martínez-Vilalta J., Retana J., 2012. Lack of regeneration and climatic vulnerability to fire of Scots pine may induce vegetation shifts at the southern edge of its distribution. J. Biogeogr. 39, 488-496.

Westerling, A.L., Hidalgo, H.G., Cayan, D.R., Swetnam, T.W., 2006. Warming and earlier spring increase western US forest wildfire activity. Science 313, 940-943.

Chapter 4

A broad scale analysis of concurrent post-fire restoration practices.

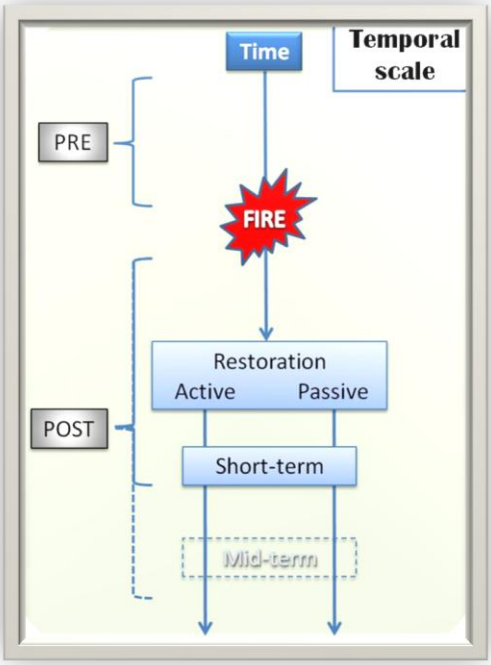

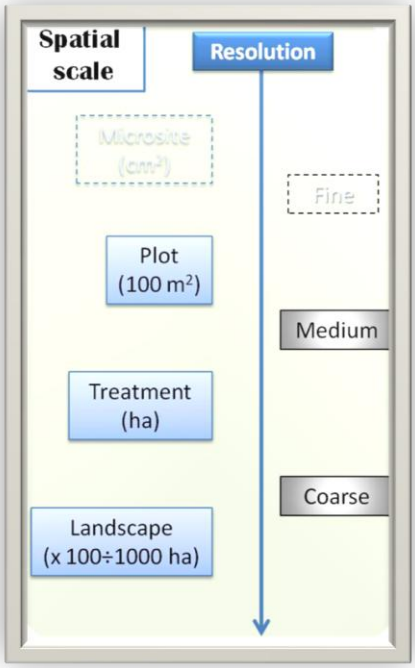

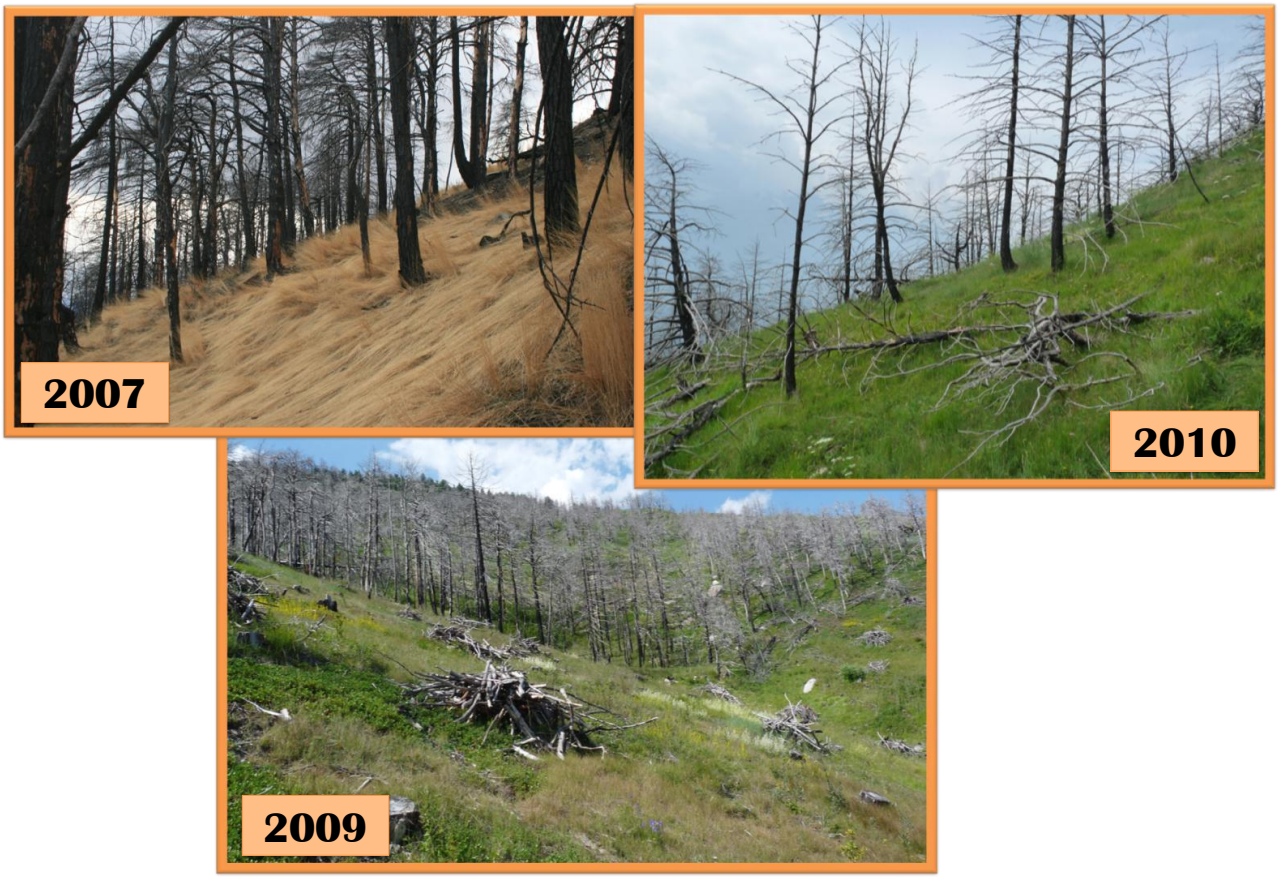

Introduction

A wildfire involving a large surface in alpine environment may present complex patterns of severity due to the high spatial variability in both vegetation and climatic conditions. Extended periods without significant precipitation, strong permeability of soils, abrupt changes of climatic conditions and availability of burnable material are some of the factors triggering the fire. Remote Sensing (RS) techniques at broad-scale, provide tools to estimate fire-severity and vegetation recovery, with low costs and reliable results (Dìaz-Delgado and Pons, 2001; Mitri and Gitas, 2004; Hudak et al., 2007; Veraverbeke et al., 2010). Validation and improvement in detecting fire severity by RS require suitable field-data collections and measurements (Key and Benson, 2006; Escuin et al., 2008). Monitoring fire frequency and severity, by means of satellite sensors over large forested areas, allows to evaluate the possible reduction of ecosystem ability to recover pre-fire conditions (Díaz-Delgado et al., 2002). Detecting fire severity by means of change-detection tools led to classify different zones showing a homogeneous impact of fire on soil and vegetation. Classes of fire severity are typically broad damage groups (low, moderate, high) defined by appropriate thresholds in the spectral changes due to fire (Patterson and Yool, 1998; Robichaud, 2000; Dìaz-Delgado and Pons, 2001). Classes amplitude could have significant variations depending on vegetation types and eco-regions (Lentile et al., 2006). Multispectral images from Landsat TM/ETM+ archives, allow the extraction of Vegetation Indices (VIs), which are indicators of vegetation state and have been used in several studies on vegetation dynamics and landscape transformations, such as those induced by fire (García and Caselles, 1991; Isaev et al., 2002; Miller and Thode, 2007).

The topography of burnt area significantly contributes in influencing post-fire vegetation dynamics (Jain and Graham, 2007). Detailed spatial information about the morphology of the slopes and vegetation structure across landscapes, can be derived from Light Detecting and Ranging (LiDAR) data. High resolution DTM, derived from LiDAR, allows a detailed description of terrain surface useful to assess microsite variables affecting the regeneration establishment, such as surface roughness, aspect, slope (De Chantal et al., 2009; Legras et al., 2010). LiDAR data can provide also reliable measures on vertical structure of vegetation, distinguishing tree characteristics (height, canopy extension and length) from lower background vegetation (Wulder et al., 2009; Wing et al., 2010).

The aim of this study was to describe at broad scale the impact of a wildfire affecting a *Pinus sylvestris* stand in the Western Italian Alps. Using a RS multispectral dataset in connection with field-data collection on regeneration characteristics, environmental parameters and topographical descriptors, within the study area we assessed:

- the fire severity over the burnt area;
- the role of fire severity, topography and environmental constraints on natural regeneration establishment;

- the effects of restoration activities on environmental parameters which affect regeneration dynamics.

Methods

The analysis was performed in the Bourra site (45°46'14''N, 7°29'58''E, Aosta valley - Italy). In order to explore the opportunities provided from the Remote Sensing (RS) techniques, investigations of the major environmental factors were performed linking field-data sampling of regeneration and site characteristics with a RS dataset available for the area.

The *P. sylvestris* forest of Bourra was affected by a 257 ha wildfire during spring 2005 that completely destroyed 160 ha (Figure 4.1 - image comparison). The extension of the burnt area after the fire was defined by means of ground surveys: an area showing vegetation scorch was bounded discriminating, within this latter, the crown-fire conditions from those of surface-fire (Figure 4.2).

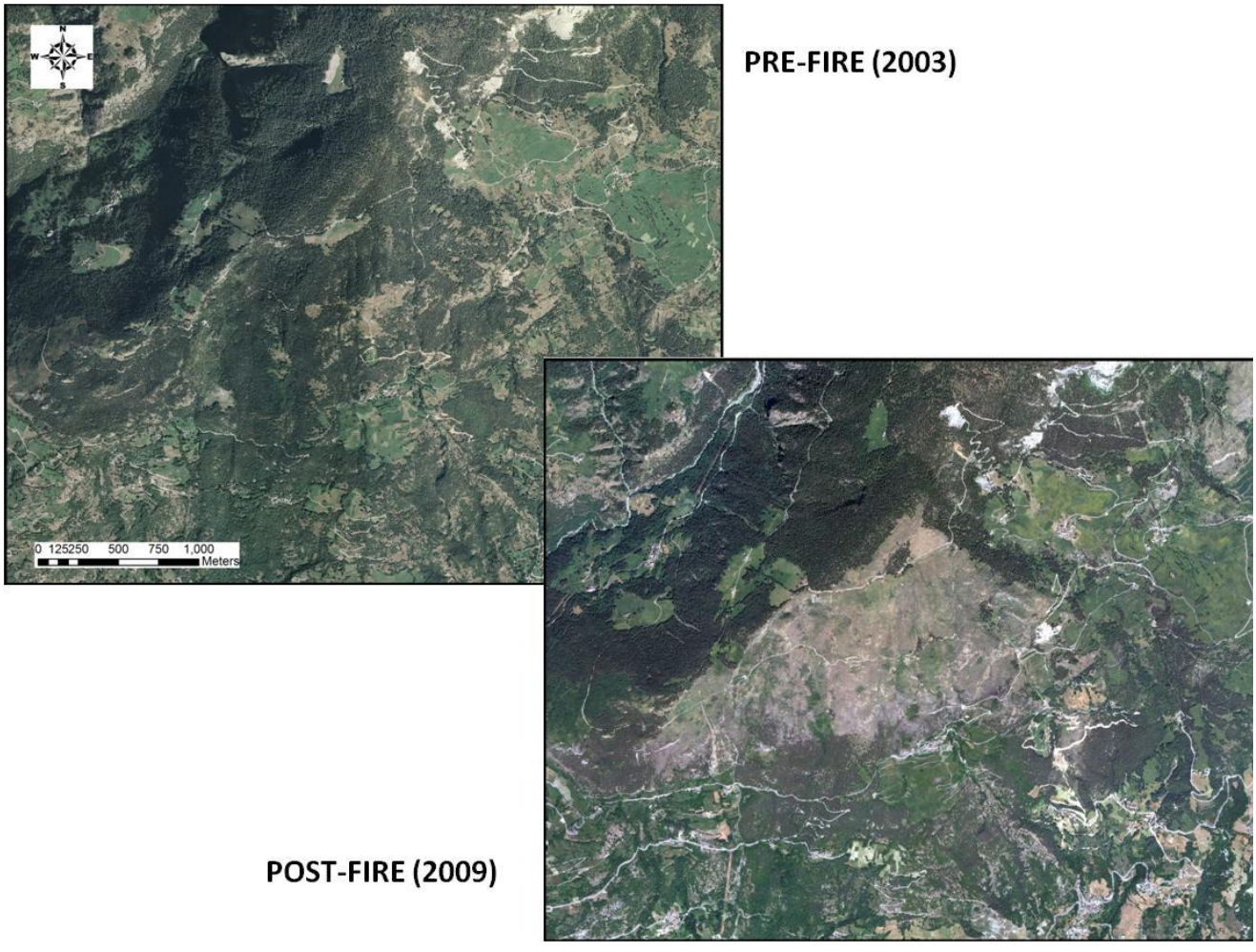

Figure 4.1 - A landscape view of the study area: orthophotos taken before the fire in 2003 (left-above) and after the fire in 2009 (bottom).

From 2007 to 2009 the area was subjected to salvage logging interventions, consisting in felling the burnt trees and removing the wood. An experimental area (surface extension around 4 ha)

was set within the crown-fire perimeter and no intervention was applied. A similar extension of salvage area (SL) was used as control aiming to contrast the "No intervention" (Passive management - PM).

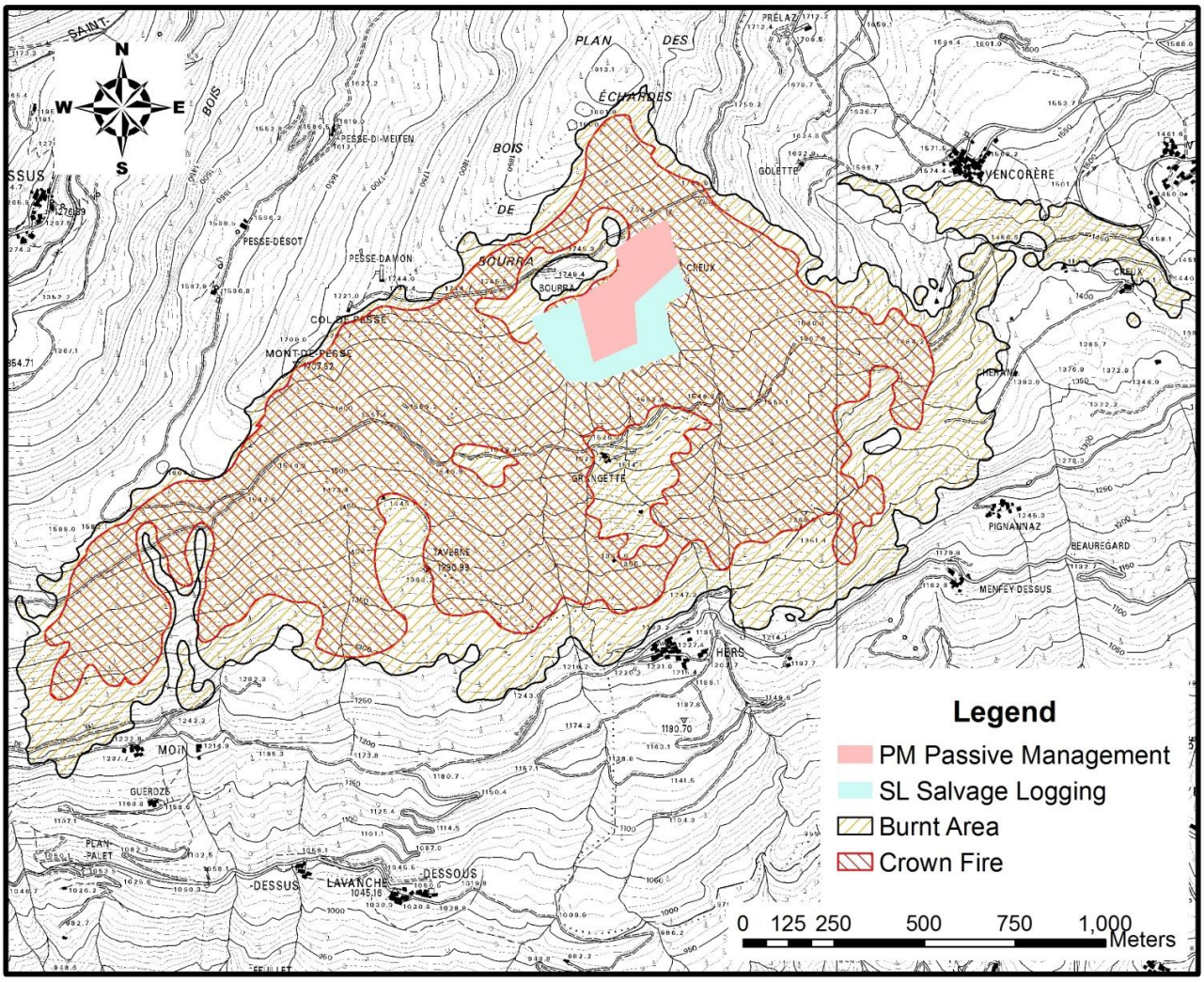

Figure 4.2 - Perimeter of the burnt area with the crown-fire area (map by G.Cesti). The experimental zones are completely included within the crown-fire area.

Data collection

During summer 2010 a field campaign was carried out in 60 sampling plot randomly distributed (for details on sampling design and field protocol see Chapter 3 - section Methods). Within these plots regeneration variables and environmental parameters were recorded. Considering the low density and the differentiated dynamics of seedlings (Chapter 3 - section Discussions), the regeneration variables collected at-plot level (density of seedlings, estimated maximum age, Root Collar Diameter) were splitted into 2 groups: *Populus tremula* seedlings and *other-species* seedlings. The environmental parameters collected at-plot level were: ground cover (percentage estimate of litter, lying deadwood, bare soil, grasses, forbs, shrubs and gravel), standing dead trees (within the unsalvaged area), stumps (within the salvaged area).

The RS dataset consists of Landsat TM/ETM+ multispectral-information provided by USGS through GLOVIS support (Global Visualization Viewer at http://www.glovis.usgs.gov, last access November, 15th). Two data-images temporally related with the fire were downloaded (in 2003 to acquire the spectral signature of the area before and, in 2006, after the fire). The scenes selected (Table 4.1) were taken approximately in the middle of growing season (to reduce phenotypic diversity), cloudless and according to the Landsat format at level 1T. The images were already radiometric, geometric, precision-corrected and a Digital Elevation Model was used to correct parallax error due to local topographic relief – (see Landsat Data Format Control Book-DFCB- at USGS website).

Landsat sensor	Acquisition date	Path/Row
TM	13-Aug-2003	195/028
TM	20-Jul-2006	195/028
TM	01-Sep-2010	195/028

Table 4.1 - Acquisition dates of the Landsat TM images used in this study.

In June 2011 an Airborne Laser Scanning data on the overall area were acquired. A Digital Terrain Model (DTM) and a Digital Surface Model (DSM) were extracted from the LiDAR dataset, both with 1-m resolution. Topographic variables (slope, aspect, elevation, referred to GPS position of each sampling plot), were extracted from the DTM and inserted into a data matrix of site-descriptors. Furthermore, a set of orthophotos referred to years 2003, 2009, and 2011 was acquired. Subtracting DTM values from DSM ones provided the normalized DSM (nDSM), which is the height of detected objects with respect to the ground. Aiming at describing the surface roughness associated with the experimental area, a Roughness Index (RI) was elaborated as the standard deviation of nDSM within a given moving window (3 x 3 pixels) after the removal of negative values and those greater than 1 m (conservative threshold for filtering out standing dead trees). Considering the trees taller than 4 m as potential disperser seeder, a data-layer of minimum distance and associated direction from potential seed tree was built, filtering nDSM to the lower threshold of 4m. Annual potential solar radiation was estimated for the study area and extracted for each plot using DTM layer at 1m resolution in a Geographical Information System (GIS) (Rich et al., 1994; Fu and Rich, 2002).

RS dataset was arranged and combined with ground-measures by means of multivariate tools, aiming at investigating the sensitivity of LandsatTM/ETM+ multispectral sensors to detect the environmental patterns affecting the study area. The multispectral dataset was pre-processed converting the initial Digital Numbers to At-Surface Reflectance (Chander et al., 2009); afterwards, Pseudo Invariant Features (PIF) structures and methods were applied to the images enabling the temporal comparison between the different Landsat data (Hall et al., 1991; Hill and Sturm, 1991). The extraction of Vegetation Indices (VIs) from multispectral images, enabled to build a map of fire severity. According to the methods introduced in Chapter 2, the NBR and the mCBI were elaborated in relation to the pre-(2003) and post-(2006) fire conditions.

Normalized Burn Ratio (NBR) : $NBR = \frac{NIR-SWIR}{NIR+SWIR}$

where near-infrared (NIR) and mid-infrared (SWIR) correspond to Landsat TM bands 4 and 7 respectively.

For mCBI definition, an undisturbed forested area had been set as training reference-forest (exposition and vegetation cover similar to the pre-fire condition of the burnt area): mCBI was calculated in terms of pixel-distance of the burnt area from the reference forest, assuming this latter as a sort of training area for "normality" condition:

modified Composite Burn Index (mCBI): $mCBI_p = \sqrt{(\frac{1}{5}\sum_{i=1}^{5}(\frac{b_{pi}-\bar{b}_i}{SD_i})^2}$

where, *p* pixel image, *i* band (five Landsat TM bands *b2÷b7*):), b_{pi} spectral value for pixel *p,* $\bar{b}_i$ and SD_i mean and standard deviation of training pixels on band *i.*

An additional set of VIs was extracted from 2010 data-images:

I. Green-leaf indices: highlight the spectral differential responses of near-infrared (NIR), photosynthetic active (RED) and (BLUE) bands.

- *Fractional vegetation cover* (F_c): the proportion of vegetation cover detected by Normalized Difference Vegetation Index (NDVI), which is defined as a ratio of red (RED) and near-infrared (NIR) reflectance, Landsat TM/ETM+ bands 3 and 4 respectively (Tucker and Sellers, 1986; Wiegand et al., 1991; Nishida et al., 2003).

$$NDVI = \frac{NIR-RED}{NIR+RED} \qquad Fc = \frac{NDVI - NDVI_{min}}{NDVI_{max} - NDVI_{min}}$$

where $NDVI_{max}$ and $NDVI_{min}$ correspond to full vegetation (Fc = 1) and bare soil (Fc = 0) conditions.

- *Soil Adjusted Vegetation Index* (SAVI): a VI exploiting the same spectral information of NDVI, corrected by an adjusting factor to reduce soil noise throughout a broad range of vegetation density (Huete, 1988).

$$SAVI = (1+L)\frac{NIR-RED}{NIR+RED+L}$$

(with L = 0.5).

- *Enhanced Vegetation Index* (EVI): derived from NDVI-method, should correct some distortions caused by the particles in the air as well as soil background noises (Huete et al., 2002).

$$EVI = 2.5\frac{NIR-RED}{NIR+6\cdot RED-7.5\cdot BLUE+1}$$

where BLUE corresponds to Landsat TM/ETM+ band 1.

II. Tasseled cap indices (TC): a combination of spectral information, derived from all Landsat TM/ETM+ bands (Crist and Cicone, 1984; Jin and Sader, 2005).

- *Brightness* (Br), *Greenness* (Gr), *Wetness* (Wet): principal components transformation of six Landsat TM and ETM+ bands (Huang et al., 2002).
- *Modified Disturbance Index* (mDI): derived from difference between TC basic components, mDI is sensitive to the contrast between the spectral signature of live forest and the area affected by high-severity fire (Healey et al., 2006); the uncertainties of mixed severity conditions are avoided filtering the Greenness component (Hais et al., 2009).

$$mDI = Wetness - Brightness$$

III. Forest z-score indices: VIs calculated in terms of pixel-distance of the burnt area from a reference forest (*i.e*. the previously introduced mCBI).

- *Integrated Forest Index* (IFI): considering as a reference the same training area chosen for mCBI definition, IFI exhibits a z-score measure of a pixels likelihood of being forested (Huang et al., 2008, 2010). Classifying the pixels of a burnt area according to some empirical IFI thresholds, allows to identify the zones covered by different vegetation layers (Chen et al., 2011; Schroeder et al., 2011).

$$IFI_p = \sqrt{\left(\frac{1}{3}\sum_{i=1}^{3}\left(\frac{b_{pi} - \bar{b}_i}{SD_i}\right)^2\right)}$$

where: *p* pixel of an image, *i* band (Landsat TM/ETM+ bands: RED-band 3, MIR-band 5 and SWIR-band 7), b_{pi} spectral value for pixel *p*, $\bar{b}_i$ and SD_i mean and standard deviation of forest training pixels on band *i.*

Data analysis

A change-detection procedure was applied to test the ability of dNBR in detecting the different levels of fire severity (Key and Benson, 2006; Loboda et al., 2007; Escuin et al., 2008). Likewise, the dmCBI was obtained subtracting post-fire mCBI values from the pre-fire ones. This latter was used, together with dNBR, to evaluate the performances of both VIs on severity-detection. At this purpose, ground-measures were used as references. As a consequence of dNBR and dmCBI definition, two correspondent maps of severity were built classifying pixels into three classes: a high severity (greater than 2 standard deviation δ), a low severity (greater than 1δ, but lower than 2δ) and no changes (lower than 1δ). Thresholds of the classes were calibrated according to the ground-measured perimeters of crown-fire and surface-fire areas.

The VIs values corresponding to the sixty plots were extracted by averaging the VI-value of pixels included within a circular area (20 m diameter) centered on each plot (Figure 4.3). These values were used to fill a first matrix (VIs matrix). A second matrix was created with the parameters collected at-plot level (regeneration, topographic and environmental variables).

A two-way cluster analysis was performed on VIs matrix to find similarities of VI values at-plot level and correlations between VIs (McCune and Grace, 2002).

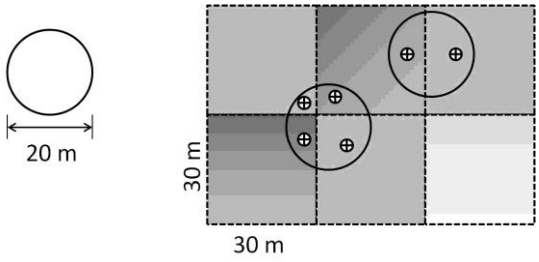

Figure 4.3 - A circular area, with a diameter of 20 meters, located around each sampled plot, was overlapped to VI layer: the VI value assigned to the sampled plot resulted from the average of the extracted values among crossing pixels (the small circles inside each pixel).

VIs data associated with the 60 plots were subjected to Non-metric Multidimensional Scaling (NMS) ordination to display the variations and to verify the grouping of VIs data-plots highlighted by cluster-analysis. The relationships among this groups and the environmental parameters were explored setting the environmental parameters as 2nd data matrix. NMS was used to explore possible patterns among VIs groups and environmental data providing a biologically meaningful view of multispectral data. The NMS was chosen because of the high number of zeros for the regeneration occurrences and the relaxed assumptions in terms of normality (Legendre and Legendre, 1998; Zuur et al., 2010). We used Euclidean distance measures for NMS ordination, specifying 2 dimensions and 250 iterations (data relativized respect to standard deviation). The significance of dimensional solutions was assessed using Monte Carlo permutation procedures (250 interactions) and the evaluation of stress reduction (McCune and Grace, 2002).
In order to test the multivariate differences among VIs groups, a nonparametric Multi-Response Permutation Procedure (MRPP) was used with a Euclidean distance measure (Biondini et al., 1988). The MRPP procedure was also used to perform pairwise comparisons among groups.
A Discriminant Analysis classification - DA (Legendre and Legendre, 1998) was performed on VIs-matrix, using the spectral groups as classification variable in order to derive functions which allowed to extend DA classification to the entire experimental area.

Assuming the significant sensitivity of Landsat TM/ETM+ sensors to the environmental patterns (Jakubauskas, 1996), the relationships between VIs and field-data were further explored by means of Spearman correlations coefficients (p-value < 0.01).
The impacts of environmental constraints on regeneration density were evaluated through General Linear Models (GLMs) procedure (McCulloch, 2000) using environmental data matrix as quantitative predictor, while “Management-type” (Salvage, Unsalvage) and “direction of the nearest seed tree” as categorical variables.

All variables were assessed for normality, prior to statistical analyses. Data were log- or angular-transformed when required to improve normality and homoscedasticity (Zar, 2009). For all statistical tests, $p = 0.05$ was considered significant where no other indication was given.
All multivariate procedures were performed using PC–ORD 6.0 software (McCune and Mefford, 2011). Comparison and DA were performed by means of Statgraphics Centurion version XVI (StatPoint Technologies Inc, Virginia, USA). Processing and editing of RS data were supported by ENVI version 4.7 (ITT Visual Information Solutions, Boulder, Colorado, USA).

Results

Detection of fire severity

Change-detection of NBR and mCBI indices before and after the fire, enabled to define two maps describing the levels of fire severity detected (Figure 4.4).

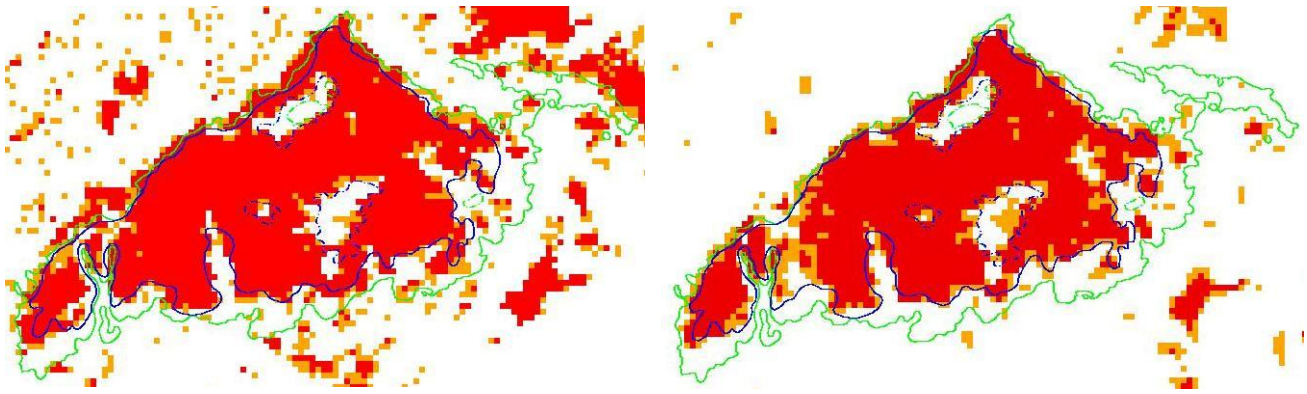

a) b)

Figure 4.4 - Maps of fire severity classified according to 3 classes: no change (white), low severity (orange), high severity (red); continue lines delimit the total burnt area (green) and the crow-fire area (blue). The zones beyond the perimeter, eastwards, were involved in earthmoving and excavation over the years after the fire; a) dNBR map, b) dmCBI map.

The field survey carried right after the fire allowed to evaluate the performances of the two VIs (dNBR , dmCBI) with respect to the boundaries of the burnt area (Table 4.2).

	High severity		Low severity		Nochange		Tot. surface	
	(ha)	(%)	(ha)	(%)	(ha)	(%)	(ha)	(%)
dmCBI	140.9	55	36.1	14	79.8	31	256.9	100
dNBR	159.8	62	25.6	10	71.6	28		

Table 4.2 - Definition of fire severity classes referred to the severity maps built by dNBR and dmCBI: the surface involved was computed referring to the perimeter of the burnt area resulting by ground measurements after the fire. Amplitude of severity classes is calibrated by means of the crown-fire perimeter achieved by ground-measurements: the low severity class includes changes greater than 1 standard deviation, while, the high severity one over 2 standard deviation units.

A comparison between the two indices performances shows a quite similar result in classifying burnt pixels within the perimeter delimiting the burnt area (identifying around 70% pixels within the area affected by fire). A slight tendency of dNBR to classify a higher number of pixels as burned and with higher severity than dmCBI was found (Table 4.2). Considering the zones named "crown-fire" and "surface-fire" within the burnt area, a similar behaviour of the two indices seems to occur (Table 4.3). As expected, the "crown-fire" area includes mostly high severity pixels (80-86% of total), while "surface-fire" area takes in mainly no-change pixels (61-70%) with equal amount of pixels classified as low severity ones (both to 16%).

	High severity		Low severity		Nochange		Tot. surface		
	(ha)	(%)	(ha)	(%)	(ha)	(%)	(ha)	(%)	
dmCBI	128	80	20	13	12	7	160	100	Crown-fire area
dNBR	138	86	10	6	13	8	160	100	
dmCBI	13	14	16	16	68	70	97	100	Surface-fire area
dNBR	22	23	15	16	59	61	97	100	

Table 4.3 - Comparison between the ability of fire severity indices to discriminate pixels with different levels of severity within the crown-fire area and the surface-fire one.

Figures 4.5 and 4.6 show that wildfire affected greatly south and south-east facing slopes located between 1300 and 1900 m a.s.l.

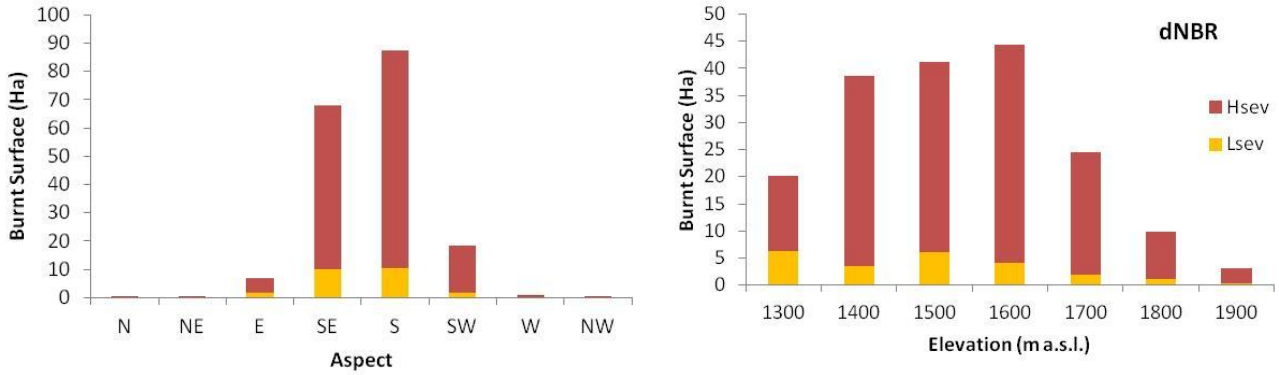

a) b)

Figure 4.5 - Fire severity and extension of the burnt area as detected by dNBR index, according to: a) slope exposition, b) altitude classes.

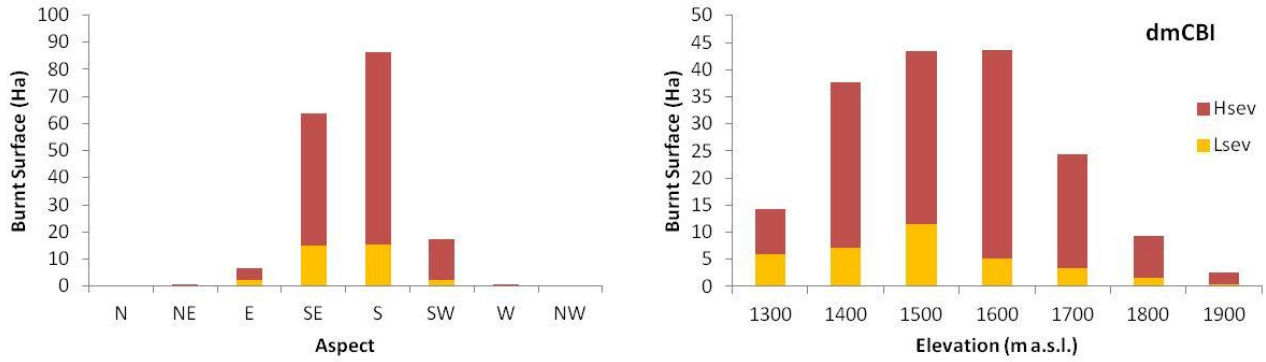

a) b)

Figure 4.6 - Fire severity and extension of the burnt area as detected by dmCBI index, according to: a) slope exposition, b) altitude classes.

Spectral and environmental patterns

Cluster analysis highlights grouping of VIs values among the sixty plots into four distinct groups, keeping a residual information around 70% (Figure 4.7). According to the management-type, a notable differentiation of the plots assigns the SL plots to groups Sp3, Sp4 and the unsalvaged plots to groups Sp1, Sp2.

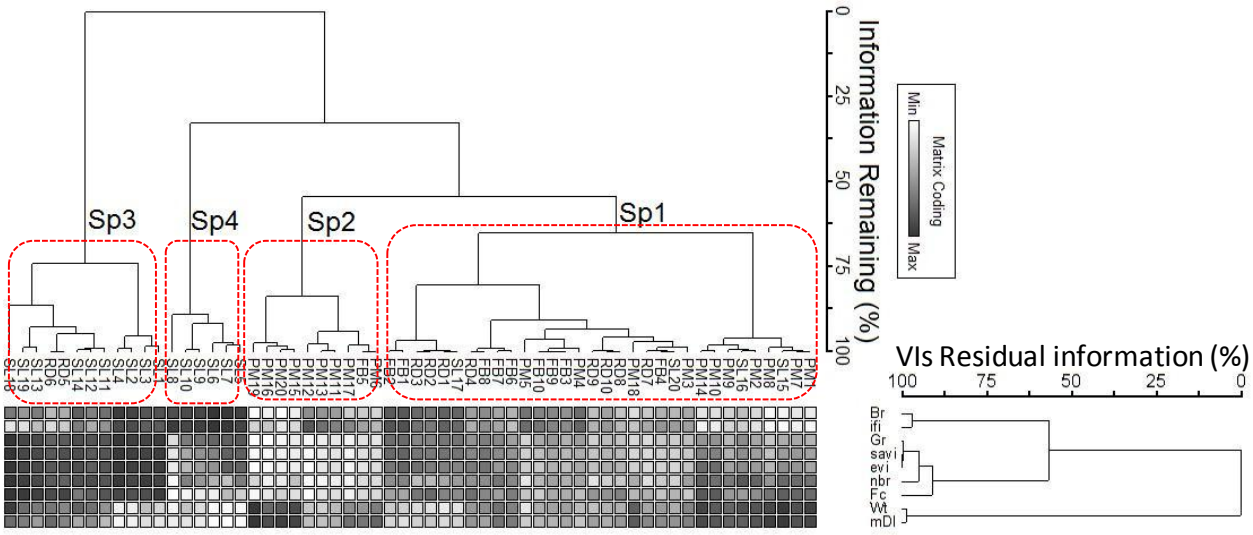

Figure 4.7 - Two-way cluster dendrogram showing the four clusters of plots (Sp1-Sp4) as results of common arrangement of the VIs values among the sampled plots. VIs similarities (to the right) allows to restrict the subsequent analysis to five VIs, for a acceptable description of the spectral variability: IFI, SAVI, NBR, Fc and mDI.

The results from MRPP analysis show a significant differentiation of VIs among the spectral groups (Table 4.4). The four groups were well separated by a very low test statistics (T = -25.4) and a relatively high chance-corrected within-group agreement (A = 0.44). The average within-group distance was lower in group Sp2 and higher in Sp3, respectively indicating greater homogeneity of VIs values within group Sp2 and greater dispersion among the plots of group Sp3.

	Sp1	Sp2	Sp3	Sp4
Size (n)	32	10	12	6
Avg. distance within-group	0.25	0.22	0.39	0.28
Sp1		T=-13.7 A=0.22 P<0.001	T=-16.5 A=0.22 P<0.001	T=-12.6 A=0.21 P<0.001
Sp2			T=-13.3 A=0.46 P<0.001	T=-8.8 A=0.41 P<0.001
Sp3				T=-9.7 A=0.39 P<0.001
Global	T=-25.4, A=0.44, P<0.001			

Table 4.4 - MRPP statistics testing the overall differences among VIs groups: global and pairwise comparisons.

NMS biplot displays the plot arrangement among the four different groups (Sp1-Sp4). Shift from groups Sp1 to Sp3 follows a gradient along axis 1, while along axis 2 group Sp4 is separated from the others (Figure 4.8). Changes along axis 2 follow variations in fire severity (both indices dNBR and dmCBI). VIs characterized by sensitivity to the greenness component of the vegetation (SAVI, EVI, TCap-Greenness) exhibit the strongest positive correlations with axis 1 ($r > 0.9$). Indices mDI and TCap-Wetness have the greatest positive correlations with the axis 2 ($r > 0.7$), conversely, IFI shows a strong negative correlation with axis 2 ($r = -0.85$) (Table 4.5).

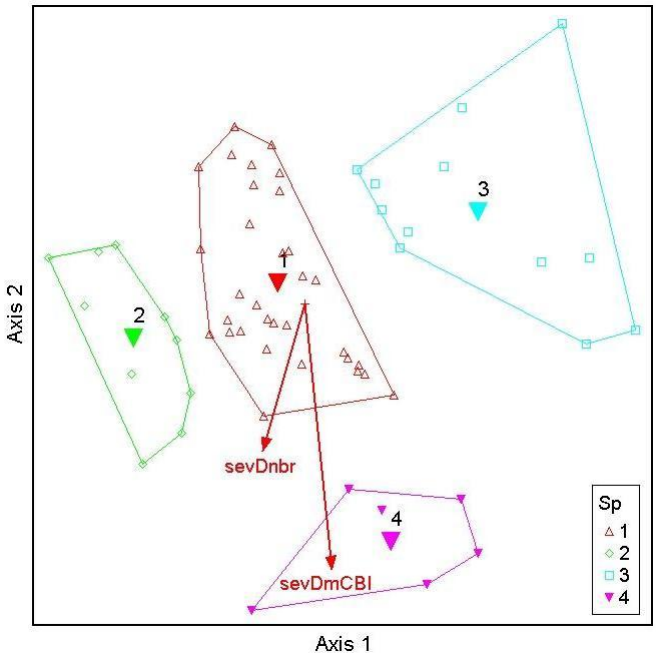

Figure 4.8 - Non-metric multidimensional scaling ordination of VIs data matrix. Each symbol represents a plot (N = 60 plots). Free polygons contain data-plots included in the same group: each group has a centroid labelled from 1 to 4 corresponding to Sp1-Sp4 groups previously identified by cluster analysis. Vector lengths are proportional to the correlations with ordination axes. The final solution had two dimensions, stress = 2.87 and P = 0.004.

	VIs	Correlation coeff.
Axis 1	Greenness	0.974
	SAVI	0.945
	EVI	0.933
	NBR	0.770
	Brightness	0.765
	Fc	0.648
	mDI	-0.663
Axis 2	Wetness	0.844
	mDI	0.747
	Fc	0.699
	NBR	0.589
	IFI	-0.885
	Brightness	-0.630

Table 4.5 - Pearson's r correlation coefficients ($p < 0.05$) from main data-matrix of VIs.

VIs reporting information of fire severity are both included in ordination (2nd matrix of environmental data) showing significant correlations with axis 2 (Table 4.6).

	Environmental variable	Correlation coefficient
Axis 2	SeveritydmCBI	-0.600
	SeveritydNBR	-0.448
	Solar radiation	-0.427
	Slope	-0.338

Table 4.6 - Pearson's r correlation coefficients ($p < 0.05$) from the second data-matrix of environmental parameters.

All pixels included in the burnt area were divided into four groups according to DA procedure, that uses spectral groups (Sp1-4) as classification factor and VIs as variables discriminating among the groups. Considering the similarities among VIs in the 2-way diagram (Figure 4.7) and the correlations between them showed in NMS ordination, the three TCap-components and EVI index were not taken into consideration for DA analysis. DA allows to assign each pixel to the correspondent spectral group by means of the Classification Function (Table 4.7). The map in Figure 4.9 reports the burnt area classified according to the four spectral groups.

Discriminant Function	*Wilk Lambda*	*P-Value*	Classification rate
1	0.017	<0.001	96.1 %
2	0.12	<0.001	
3	0.56	<0.001	

	FC1	*FC2*	*FC3*	*FC4*
SAVI	-349780	-341660	-347817	-358833
NBR	87181.6	85236.6	86892.1	89260.1
mDI	67947.9	65021.5	67751.5	72669.2
IFI	1528.9	1481.4	1523.3	1595.6
Fc	80340.1	78159.7	80023.6	82781.6
Const.	-14704.5	-14115.4	-14668.1	-15082.6

Table 4.7 - (Left): results from Discriminant Analysis (DA) of VIs amongst the four spectral groups (Sp1-4). Classification rate shows the percentage of pixels classified according to the Classification Functions FC1-4. (Right): coefficients of Classification Functions used to determine which of the Sp-groups every single pixel is most likely to belong to.

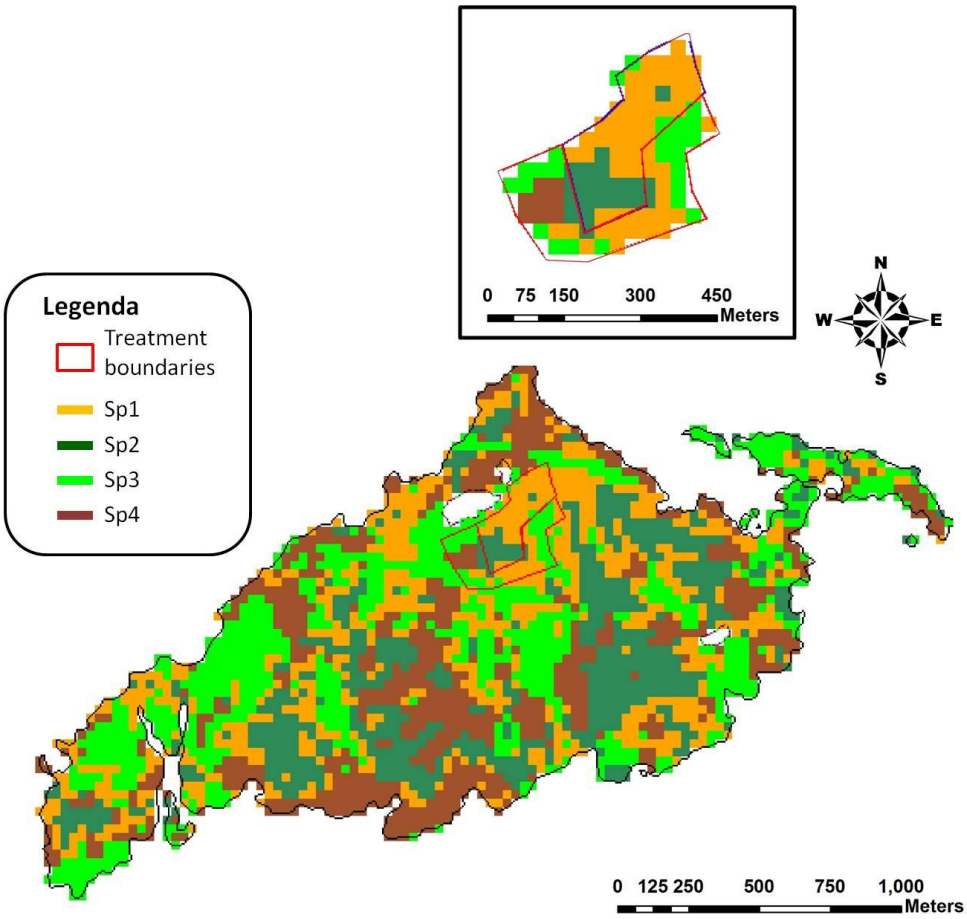

Figure 4.9 - Map of Spectral groups as defined by DA-classification functions. In the top box, a detailed view of the experimental area: groups Sp1-2 mostly include unsalvage plots, Sp3-4 salvage ones. Pixel resolution displayed is the standard-Landsat TM/ETM+ resolution (30m).

The DA classification of pixels in the experimental area shows, within Salvage Logging, similar percentages of surface assigned to Sp1 and Sp3; unsalvaged area is mostly covered by Sp1 (Table 4.8). High numbers of zero-frequencies for seedlings, heterogeneous and small size groups (low number of plots), do not allow a statistic comparison of the regeneration density among the Spectral groups; anyway, the extremes values of regeneration density are denoted in Sp3 (higher density) and Sp4 (absence of regeneration).

Amount of surface (%)	SpGr1	SpGr2	SpGr3	SpGr4	Total
No Intervention	65.5	29.0	5.5	-	100
Salvage Logging	35.9	7.5	41.5	15.1	100

Table 4.8 - A summarized list of cumulated area loading each Spectral group with respect to the treatments.

Group 4 exhibits higher distances from the seed trees, loads of annual solar radiation, and slope degrees (Table 4.9). Maximum roughness is associated with group 1 which shows lower distance from seeders. Despite the fact that the experimental areas have been entirely placed in zones affected by high severity fire, group 3 exhibits a mean value of severity index slightly lower than the other groups and lower values of solar radiation.

Site variables	SpGr1		SpGr2		SpGr3		SpGr4	
	mean (±δ)	n	mean (±δ)	n	mean (±δ)	n	mean (±δ)	n
Seeder-distance (m)	108^{a} (±46)	49500	167^{c} (±33)	18000	140^{b} (±49)	22500	189^{d} (±21)	7200
Radiation ($kW \cdot h/m^2 \cdot y^{-1}$)	1473^{b} (±76)	49500	1487^{c} (±51)	18000	1464^{a} (±67)	22500	1506^{d} (±53)	7200
Severity (-)	18.7^{a} (±2.8)	55	18.2^{a} (±2.0)	20	16.8^{a} (±4.6)	22	23.0^{b} (±1.4)	11
Roughness (-)	0.17^{a} (±0.08)	49500	0.16^{a} (±0.08)	18000	0.15^{b} (±0.07)	22500	0.15^{b} (±0.06)	7200
Slope (°)	26^{a} (±6)	49500	28^{ab} (±5)	18000	26^{a} (±7)	22500	32^{b} (±4)	7200

Table 4.9 - Environmental parameters characterizing the experimental area: the columns report mean values ± standard deviation for each group, n the number of pixels included in the statistics (1m pixel resolution, except for Severity, 30m pixel resolution). Different letters highlight differences between Spectral groups (ANOVA comparison using post-hoc Tukey HSD, p-value < 0.05). Seeder-distance is the minimum distance from a potential seeder tree, Radiation is the annual potential solar radiation (diffuse + direct), Severity is dmCBI-data layer, Roughness is Roughness Index (RI)-data layer, Slope is Slope degrees.

Correlations between VIs and the field vegetation data indicate weak relationships (Table 4.10). Fc (fractional vegetation cover) is positively correlated with regeneration presence and inversely with Gravel ground cover. Grass layer seems to be positively related with mDI index.

	Herbs	Litter	Gravel	Snags (density)	Seedlings (density)	Age-max seedlings
Fc			-0.49		0.36	0.39
mDI	0.35					
NBR				-0.43		
SAVI		0.37		-0.40		

Table 4.10 - Spearman's correlations between spectral indices and field vegetation data in year 2010. Herbs, Litter and Gravel are referred to the estimated ground cover. Snags is the density of standing dead trees, Seedling and Age-max are referred to the density of seedlings and the maximum estimated age of these seedlings per plot. All the correlation coefficients reported are considered as significant with p-value < 0.01.

Site variables (Figure 4.10, 4.11, 4.12) show significant relationships with Wetness component of TCap indices and IFI (Table 4.11a). Annual loads of solar radiation, level of fire severity and slope degrees are negatively correlated with Wetness component. Conversely, IFI is positively related with surface roughness (RI), annual solar radiation, fire severity and slope degrees. Site variables are significantly related with regeneration and ground cover parameters as well (Table 4.11b). Seeder distance is negatively related with the density of seedlings and seedlings-species diversity. Surface roughness is positively related with CWD (Coarse Wood Debris) and regeneration. Fire severity shows positive relationships with IFI index (Table 4.11a), CWD and standing dead trees (Snags).

a)	Seeder distance	Roughness	Solar radiation	Severity	Slope
Wetness (TCap-component)			-0.38	-0.37	-0.35
IFI		0.35	0.35	0.41	0.35

b)	Seeder distance	Roughness	Solar radiation	Severity
Seedlings (density)	-0.55	0.32		
Age-max seedlings				
RCD-variability	-0.53	0.35		
Snags (density)	-0.53			0.38
CWD	-0.60	0.53		0.43
Bare soil	0.41			
Gravel			0.43	
Species-diversity (Shannon)	-0.44			

Table 4.11 - Spearman's correlation coefficients between Site-variables and :
a) VIs extracted for each plot, b) regeneration variables and ground cover (RCD variability is referred to standard deviation of Root Collar Diameter of the seedlings measured for each plot; CWD is Coarse Wood Debris estimated; Snags is density of standing dead trees and Species diversity is the Shannon index calculated for the seedling species within each plot). All the correlation coefficients reported are significant with p-value < 0.01.

Density of seedlings is influenced by the seeder distance (GLM - Seeder distance factor, p-value < 0.001) (Table 4.12). Spearman correlation (-0.55) highlights the relationship between regeneration and Seeder distance (Table 4.11b). GLM reports weak but significant influence of solar radiation and management-type predictors with respect to the regeneration establishment (Table 4.12). Solar radiation doesn't show particular connections with regeneration density, but the inverse correlation (-0.38) to Wetness (TCap-component) may indicate an indirect effect in seedlings presence caused by the reduction in soil moisture (Table 4.11a).

Response	General Linear statistical Model			Predictor	D.f.	F-ratio	p-value
Seedlings (density)	R^2	F-ratio	p-value	Seeder distance	1	17.4	**<0.001**
	0.47	4.24	**<0.001**	Solar radiation	1	5.2	0.02
				Management-type	1	4.1	0.04

Table 4.12 - Fitting models relating response variable "density of seedlings" to the predictors "Seeder distance", "annual potential solar radiation", "management-type" (salvage, unsalvage treatments as categorical predictor). P-value < 0.01 meaning a statistical relationship between response and predictors at 99% confidence.

The variable "Direction from the nearest seed source" (eight cardinal directions) used as categorical predictor did not show significant effect with regard to regeneration density (D.f. = 7, F-ratio = 1.88, p = 0.09). Including ground-cover and site-variables to the predictors listed in Table 4.12, GLM fitted significantly to the same response variable (seedling density), increasing R^2 to 0.61, F =2.9, p < 0.01 (model explained by the same significant predictors).

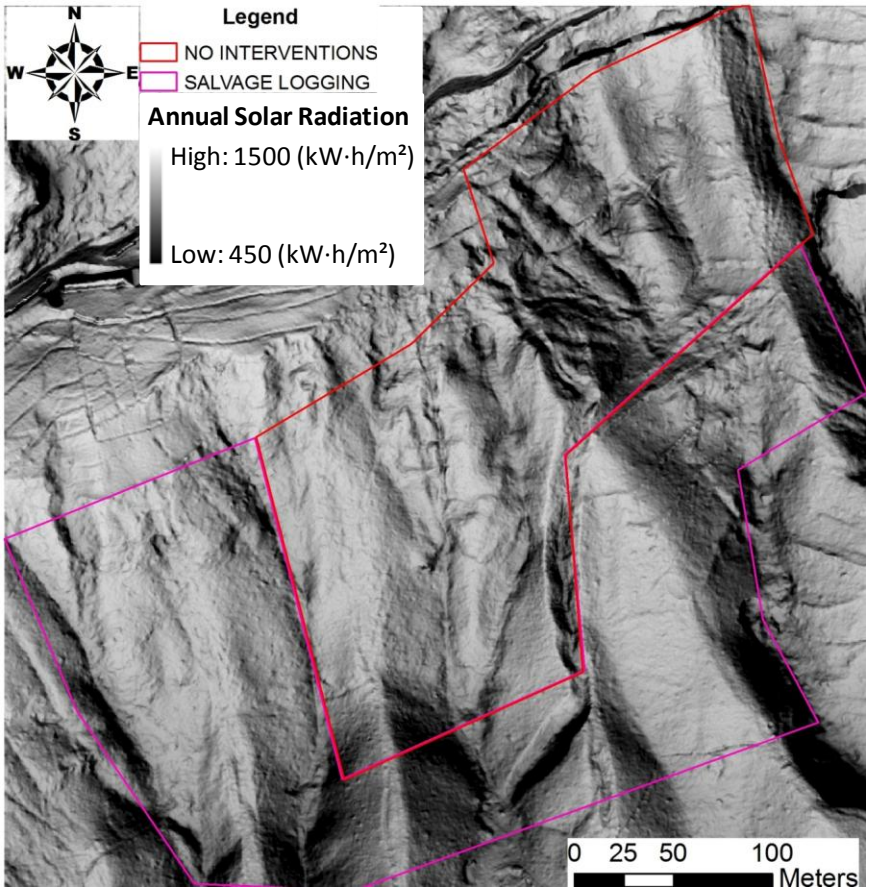

Figure 4.10 - Map of the potential solar radiation in the experimental area: annual cumulated values ranging from low levels (dark) to the highest (light grey). Values of solar radiation were estimated by GIS tools on the basis of DTM (1-m resolution) derived from LiDAR data acquired in June 2011.

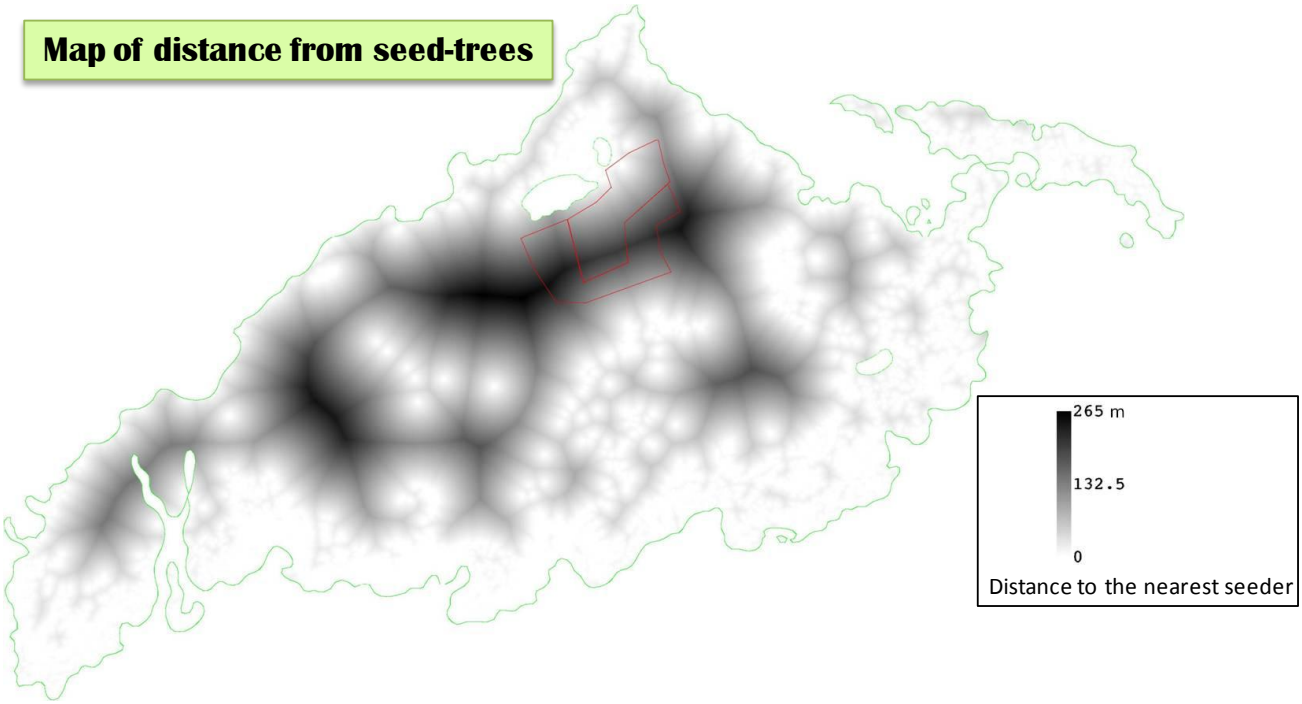

Figure 4.11 - Map of the entire burnt area showing the minimum distance of each pixel from a potential seed-tree. Distance information was achieved from nDSM data-layer (1m resolution) ranging from low (white) to high distances (black). The maximum distance from potential seeders within the experimental area (red perimeter) is equal to 253 m.

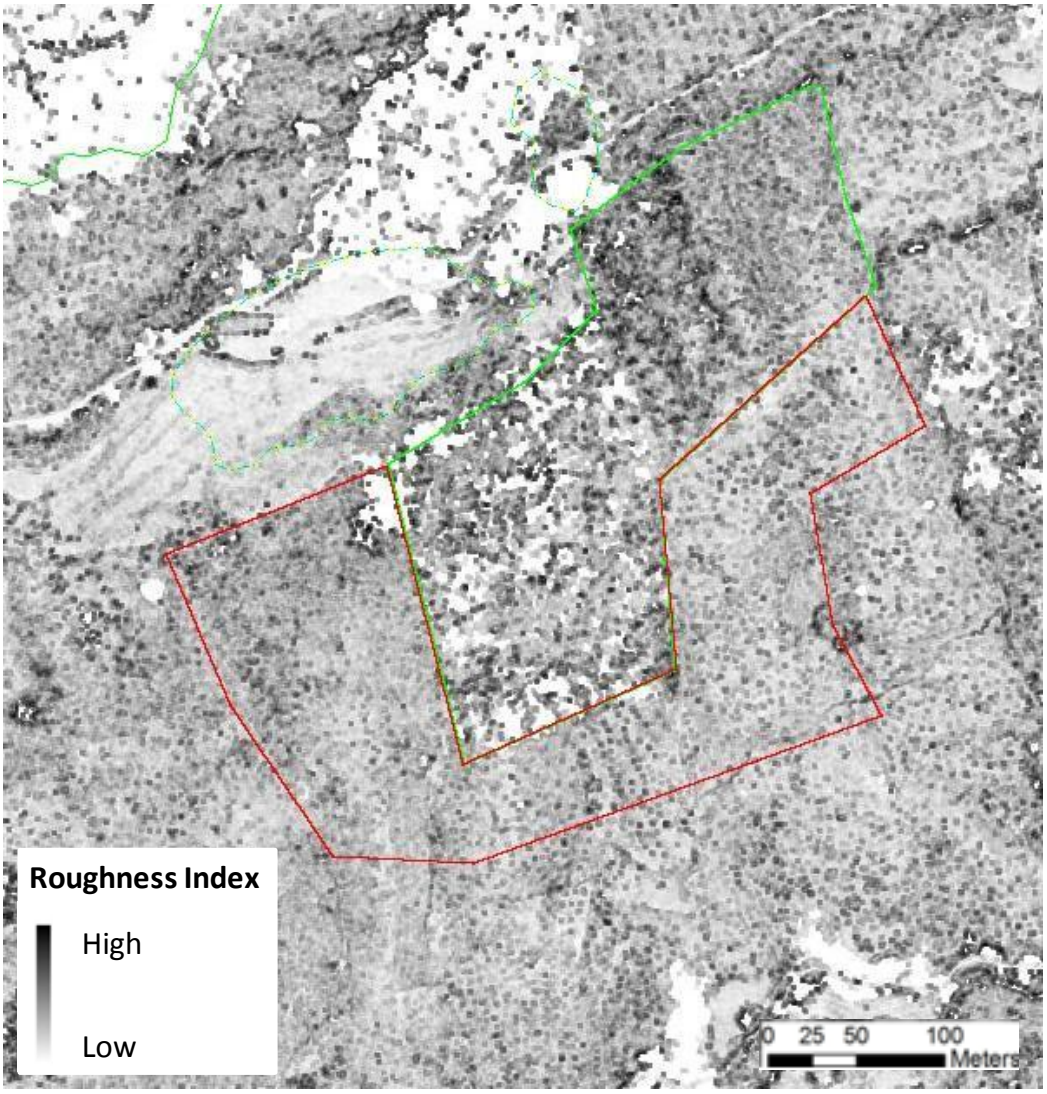

Figure 4.12 - Detailed view of the RI-data layer (used as indirect measure of surface roughness) in the experimental area. SL treatment (within red boundaries) exhibits a homogeneous surface with low level of RI (light grey). More variations are notable within the unsalvage area (green-line delimited) where the values of RI are greater (dark grey-black).

Discussions

Fire severity detection

The wildfire in Bourra site has had a strong impact on the *P. sylvestris* forest, causing the loss of woody plants in the burnt area. Destruction of the forest floor, dramatic decrease of seed availability and sensible reduction of the canopy are associated with a wide extension of the surface affected by high levels of fire severity. These conditions often led to high rates of soil loss making the site hostile to natural regeneration establishment (DeBano et al., 1998; Díaz-Delgado et al., 2003). A coarse detection of fire severity has proven to be reliable on a broad scale, by mean of Landsat TM multispectral data calibrated by ground truth (86% of crown-fire area was detected as high severity). The efficiency of dNBR in severity detection has been compared with dmCBI index, in order to use a wider spectral information with respect to dNBR (Huang et al., 2008; Meng and Meentemeyer, 2011). The ability of both indices in defining maps of fire severity resulted similar, though confirming the tendency for dNBR to classify a higher number of pixels as burned and identifying, within these latter, more high severity pixels than dmCBI (a trend also mentioned in the study reported in chapter 2). The choice of appropriate thresholds to set the amplitude of severity classes, has to receive the necessary feedback from field-data surveys. However, the evaluation of dmCBI performances requires future detailed tests, especially linked to the opportunity of a specific protocol for ground-severity validation (e.g. design protocols in: Van Wagtendonk et al., 2004; Key and Benson, 2006; Chen et al., 2011). Both severity indices indicate, with equal clarity, the distribution of fire severity among classes of altitude and exposition.

Spectral patterns and evaluation of environmental constraints

Landsat TM/ETM+ multispectral data allow to schedule a wide range of VIs with proven sensitivity to the different strata of vegetation (Meng and Meentemeyer, 2011). Exploiting the ability of VIs to explore the burnt area at landscape level, field-data sampling plots have been assigned and splitted into four different spectral groups. The association of VIs with the environmental parameters and the site descriptors enables an analysis of the arising patterns. Spectral groups Sp1, Sp2 mostly include unsalvage plots, while Sp3, Sp4 salvage ones. All the groups are well separated and both the restoration treatments include groups of pixels corresponding to plots with scarce or absence of regeneration (pixels belonging to Sp4 in SL and to Sp2 in PM treatment). Within the salvage logging area (SL), Sp4 includes plots located in zones with higher values of IFI, fire severity and lower values of Wetness, mDI, Fc with respect to the other spectral groups; this combination of VIs values is associated with those areas with higher slope degrees, solar radiation loadings, in which the seeder distance is maximum. Spectral group Sp2, within the unsalvaged area (PM), includes plots showing low values of those VIs associated with the green component of vegetation (SAVI, EVI, Greenness-TCap, Fc). In addition to this, Sp2 involves zones showing greater solar radiation loadings, slope degrees and seeder distance (similar to the group Sp4). The other two groups (Sp3 in SL and Sp1 in PM) show higher values of those VIs usually linked to regeneration layers (Fc, SAVI) and those indicating positive environmental conditions for

regeneration establishment (mDI, Wetness-TCap). At this purpose, the significant negative correlations between Wetness TCap-component and solar radiation, slope and severity variables confirm the sensitivity of this VI towards soil moisture conditions (Patterson and Yool, 1998) (which are presumably the worst in the areas displaying, at the same time, greater solar radiation loadings, slope degrees and high levels of fire severity). Overall statistics within the experimental area, in terms of amount of surface assigned to each group, show a percentage of surface approximately equal to 70% presenting favorable factors for the regeneration establishment (areas included in groups Sp1 and Sp3). Despite the experimental areas being located in comparable high severity conditions (detected by ground measures and visual estimates), a gradient of increasing severity is associated with zones presenting scarcity of regeneration (areas included in group Sp4). However, the distance from the seed trees acquires a significant importance (as confirmed by GLMs): in spite of other positive environmental factors that promote regeneration recovery, seeds availability is a necessary requirement. The four groups include areas in which the distance from the seeders, seems a critical factor for the re-colonization process of the burnt slopes, especially for *P. sylvestris* regeneration (Retana et al., 2002; Vilà-Cabrera et al., 2012). In addition to this, seeder distance exhibits a negative relationship with species diversity of regeneration (Shannon index); this may be a consequence of the reduced "edge effect", due to the increasing distances from the forest borders, affecting not only the processes directly connected with regeneration dynamics but also in relation to the changes in ecosystem communities (Yahner, 1988; Desrochers and Fortin, 2000; Harper et al., 2005).

This study supports the reliability of RS techniques, in this case of multispectral Landsat TM/ETM+ images, in detecting and surveying the process of vegetation recovery at-broad scale in an alpine environment. The combination of field-data sampling and spectral information allows to describe the severity of the event and the environmental patterns, extending the analysis to the landscape. In spite of the poorly establishment of seedlings from natural regeneration (see Chapter 3 - Results), VIs with different sensitivities to vegetation, site and environmental variables allowed to highlight those factors having a decisive role in the regeneration establishment. Distance from seeders becomes a relevant constraint in the recovery process of *P. sylvestris* and has to be considered for planning the restoration activities in conjunction with a detailed information on fire severity affecting the area. Under these specific constraints, salvage logging treatment may counteract the seedling establishment (see Chapter 3 - Discussion).

References

Biondini, M., Mielke, P., Berry, K., 1988. Data-dependent permutation techniques for the analysis of ecological data. Vegetation 75, 161–168.

Chander, G., Markham, B.L., Helder, D.L., 2009. Summary of current radiometric calibration coefficients for Landsat MSS, TM, ETM+, and EO-1 ALI sensors. Remote Sensing of Environment 113, 893–903.

De Chantal, M., Lilja-Rothsten, S., Peterson, C., Kuuluvainen, T., Vanha-Majamaa, I., Puttonen, P., 2009. Tree regeneration before and after restoration treatments in managed boreal Picea abies stands. Applied Vegetation Science 12, 131–143.

Chen, X., Vogelmann, J., Rollins, M., 2011. Detecting post-fire burn severity and vegetation recovery using multitemporal remote sensing spectral indices and field-collected composite burn index data in a ponderosa pine. International Journal of Remote Sensing 32, 7905–7927.

Cocke, A.E., Fulé, P.Z., Crouse, J.E., 2005. Comparison of burn severity assessments using Differenced Normalized Burn Ratio and ground data. International Journal of Wildland Fire 14, 189.

Crist, E.P., Cicone, R.C., 1984. A Physically-Based Transformation of Thematic Mapper Data---The TM Tasseled Cap. IEEE Transactions on Geoscience and Remote Sensing GE-22, 256–263.

DeBano, L., Neary, D., Ffolliott, P., 1998. Fire Effects on Ecosystems. Wiley.

Desrochers, A., Fortin, M.-J., 2000. Understanding avian responses to forest boundaries: a case study with chickadee winter flocks. Oikos 91, 376–384.

Dìaz-Delgado, R., Pons, X., 2001. Spatial patterns of forest fires in Catalonia (NE of Spain) along the period 1975–1995: Analysis of vegetation recovery after fire. Forest Ecology and Management 147, 67–74.

Díaz-Delgado, R., Lloret, F., Pons, X., 2003. Influence of fire severity on plant regeneration by means of remote sensing imagery. International Journal of Remote Sensing 24, 1751–1763.

Díaz-Delgado, R., Lloret, F., Pons, X., Terradas, J., 2002. Satellite evidence of decreasing resilience in Mediterranean plant communities after recurrent wildfires. Ecology 83, 2293–2303.

Escuin, S., Navarro, R., Fernández, P., 2008. Fire severity assessment by using NBR (Normalized Burn Ratio) and NDVI (Normalized Difference Vegetation Index) derived from LANDSAT TM/ETM images. International Journal of Remote Sensing 29, 1053–1073.

Fu, P., Rich, P.M., 2002. A geometric solar radiation model with applications in agriculture and forestry. Computers and Electronics in Agriculture 37, 25–35.

García, M.J.L., Caselles, V., 1991. Mapping burns and natural reforestation using thematic Mapper data. Geocarto International 6, 31–37.

Hais, M., Jonášová, M., Langhammer, J., Kučera, T., 2009. Comparison of two types of forest disturbance using multitemporal Landsat TM/ETM+ imagery and field vegetation data. Remote Sensing of Environment 113, 835–845.

Hall, F.G., Strebel, D.E., Nickeson, J.E., Goetz, S.J., 1991. Radiometric rectification: Toward a common radiometric response among multidate, multisensor images. Remote Sensing of Environment 35, 11–27.

Harper, K.A., MacDonald, S.E., Burton, P.J., Chen, J., Brosofske, K.D., SAUNDERS, S.C., EUSKIRCHEN, E.S., Roberts, D., Jaiteh, M.S., Esseen, P.-A., 2005. Edge Influence on Forest Structure and Composition in Fragmented Landscapes. Conservation Biology 19, 768–782.

Healey, S.P., Yang, Z., Cohen, W.B., Pierce, D.J., 2006. Application of two regression-based methods to estimate the effects of partial harvest on forest structure using Landsat data. Remote Sensing of Environment 101, 115–126.

Hill, J., Sturm, B., 1991. Radiometric correction of multitemporal Thematic Mapper data for use in agricultural land-cover classification and vegetation monitoring. International Journal of Remote Sensing 12, 1471–1491.

Huang, C., Goward, S.N., Masek, J.G., Thomas, N., Zhu, Z., Vogelmann, J.E., 2010. An automated approach for reconstructing recent forest disturbance history using dense Landsat time series stacks. Remote Sensing of Environment 114, 183–198.

Huang, C., Song, K., Kim, S., Townshend, J.R.G., Davis, P., Masek, J.G., Goward, S.N., 2008. Use of a dark object concept and support vector machines to automate forest cover change analysis. Remote Sensing of Environment 112, 970–985.

Huang, C., Wylie, B., Yang, L., Homer, C., Zylstra, G., 2002. Derivation of a tasselled cap transformation based on Landsat 7 at-satellite reflectance. International Journal of Remote Sensing 23, 1741–1748.

Hudak, A.T., Morgan, P., Bobbitt, M.J., Smith, A.M.S., Lewis, S.A., Lentile, L.B., Robichaud, P.R., Clark, J.T., Mckinley, R.A., 2007. The relationship of multispectral sattellite imagery to immediate fire effects. Fire Ecology 3, 64–90.

Huete, a, Didan, K., Miura, T., Rodriguez, E.., Gao, X., Ferreira, L.., 2002. Overview of the radiometric and biophysical performance of the MODIS vegetation indices. Remote Sensing of Environment 83, 195–213.

Huete, A.., 1988. A soil-adjusted vegetation index (SAVI). Remote Sensing of Environment 25, 295–309.

Isaev, A., Korovin, G., Bartalev, S., 2002. Using remote sensing to assess Russian forest fire carbon emissions. Climatic Change 55, 235–249.

Jain, T., Graham, R., 2007. The relation between tree burn severity and forest structure in the Rocky Mountains. USDA Forest Service Gen. Tech. Rep. PSW-GTR-203. 2007.

Jakubauskas, M., 1996. Thematic Mapper characterization of lodgepole pine seral stages in Yellowstone National Park, USA. Remote Sensing of Environment 132, 118–132.

Jin, S., Sader, S. a., 2005. Comparison of time series tasseled cap wetness and the normalized difference moisture index in detecting forest disturbances. Remote Sensing of Environment 94, 364–372.

Key, C.H., Benson, N.C., 2002. Measuring and remote sensing of burn severity. In "US Geological Survey Wildland Fire Workshop Report", Los Alamos, NM 31 October– 3 November 2000, USGS Open-File Report 02–11:55-56.

Key, C.H., Benson, N.C., 2006. Landscape Assessment (LA) Sampling and Analysis Methods.

Legendre, P., Legendre, L., 1998. Numerical Ecology. Elsevier.

Legras, E.C., Vander Wall, S.B., Board, D.I., 2010. The role of germination microsite in the establishment of sugar pine and Jeffrey pine seedlings. Forest Ecology and Management 260, 806–813.

Lentile, L.B., Holden, Z. a., Smith, A.M.S., Falkowski, M.J., Hudak, A.T., Morgan, P., Lewis, S. a., Gessler, P.E., Benson, N.C., 2006. Remote sensing techniques to assess active fire characteristics and post-fire effects. International Journal of Wildland Fire 15, 319.

Loboda, T., O'Neal, K.J., Csiszar, I., 2007. Regionally adaptable dNBR-based algorithm for burned area mapping from MODIS data. Remote Sensing of Environment 109, 429–442.

McCulloch, C.E., 2000. Generalized Linear Models. Journal of the American Statistical Association 95, 1320–1324.

McCune, B., Grace, J., 2002. Analysis of Ecological Communities. MjM Software Design.

McCune, B., Mefford, M., 2011. PC-ORD 6.0. Multivariate Analysis of Ecological Data. MjM Software, Gleneden Beach, Oregon, USA.

Meng, Q., Meentemeyer, R.K., 2011. Modeling of multi-strata forest fire severity using Landsat TM Data. International Journal of Applied Earth Observation and Geoinformation 13, 120–126.

Miller, J.D., Thode, A.E., 2007. Quantifying burn severity in a heterogeneous landscape with a relative version of the delta Normalized Burn Ratio (dNBR). Remote Sensing of Environment 109, 66–80.

Mitri, G.H., Gitas, I.Z., 2004. A semi-automated object-oriented model for burned area mapping in the Mediterranean region using Landsat-TM imagery. International Journal of Wildland Fire 13, 367–376.

Nishida, K., Nemani, R., Running, S., Glassy, J., 2003. An operational remote sensing algorithm of land surface evaporation. Journal of Geophysical Research 108.

Patterson, M., Yool, S., 1998. Mapping fire-induced vegetation mortality using Landsat Thematic Mapper data: A comparison of linear transformation techniques. Remote Sensing of Environment 4257.

Retana, J., Espelta, J.M., Habrouk, A., Ordonez, J.L., De Sola-Morales, F., 2002. Regeneration patterns of three Mediterranean pines and forest changes after a large wildfire in northeastern Spain. Ecoscience 9, 89–97.

Rich, P.M., Dubayah, R., Hetrick, W.A.., Saving, S.C., 1994. Using Viewshed Models to Calculate Intercepted Solar Radiation: Applications in Ecology. American Society for Photogrammetry and Remote Sensing Technical Papers 524–529.

Robichaud, P.., 2000. Fire effects on infiltration rates after prescribed fire in Northern Rocky Mountain forests, USA. Journal of Hydrology 231-232, 220–229.

Schroeder, T. a., Wulder, M. a., Healey, S.P., Moisen, G.G., 2011. Mapping wildfire and clearcut harvest disturbances in boreal forests with Landsat time series data. Remote Sensing of Environment 115, 1421–1433.

Tucker, C.J., Sellers, P.J., 1986. Satellite remote sensing of primary production. International Journal of Remote Sensing 7, 1395–1416.

Veraverbeke, S., Verstraeten, W.W., Lhermitte, S., Goossens, R., 2010. Evaluating Landsat Thematic Mapper spectral indices for estimating burn severity of the 2007 Peloponnese wildfires in Greece. International Journal of Wildland Fire 19, 558–569.

Vilà-Cabrera, A., Rodrigo, A., Martínez-Vilalta, J., Retana, J., 2012. Lack of regeneration and climatic vulnerability to fire of Scots pine may induce vegetation shifts at the southern edge of its distribution. Journal of Biogeography 39, 488–496.

Van Wagtendonk, J.W., Root, R.R., Key, C.H., 2004. Comparison of AVIRIS and Landsat ETM+ detection capabilities for burn severity. Remote Sensing of Environment 92, 397–408.

Wiegand, C.L., Richardson, A.J., Escobar, D.E., Gerbermann, A.H., 1991. Vegetation indices in crop assessments. Remote Sensing of Environment 35, 105–119.

Wing, M.G., Eklund, A., Sessions, J., 2010. Applying LiDAR technology for tree measurements in burned landscapes. International Journal of Wildland Fire 19, 104.

Wulder, M. a., White, J.C., Alvarez, F., Han, T., Rogan, J., Hawkes, B., 2009. Characterizing boreal forest wildfire with multi-temporal Landsat and LIDAR data. Remote Sensing of Environment 113, 1540–1555.

Yahner, R.H., 1988. Changes in Wildlife Communities Near Edges. Conservation Biology 2, 333–339.

Zuur, A.F., Ieno, E.N., Elphick, C.S., 2010. A protocol for data exploration to avoid common statistical problems. Methods in Ecology and Evolution 1, 3–14.

Chapter 5

Microclimate implications of different post-fire management.

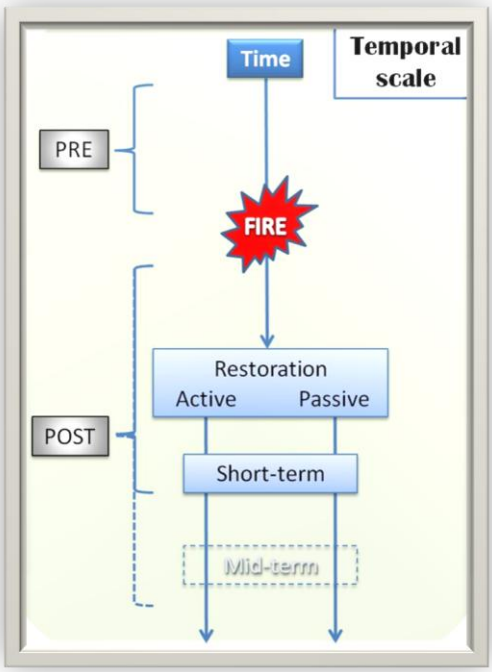

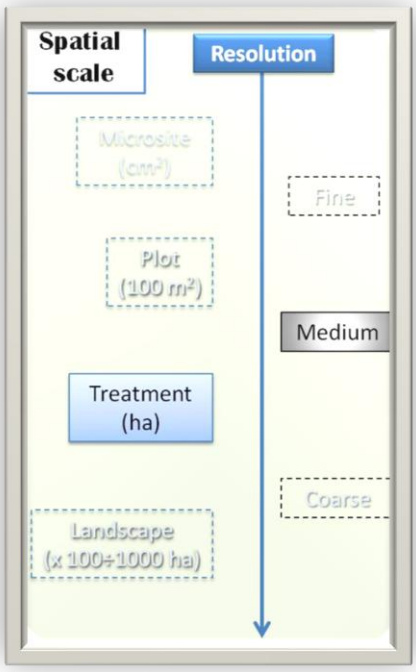

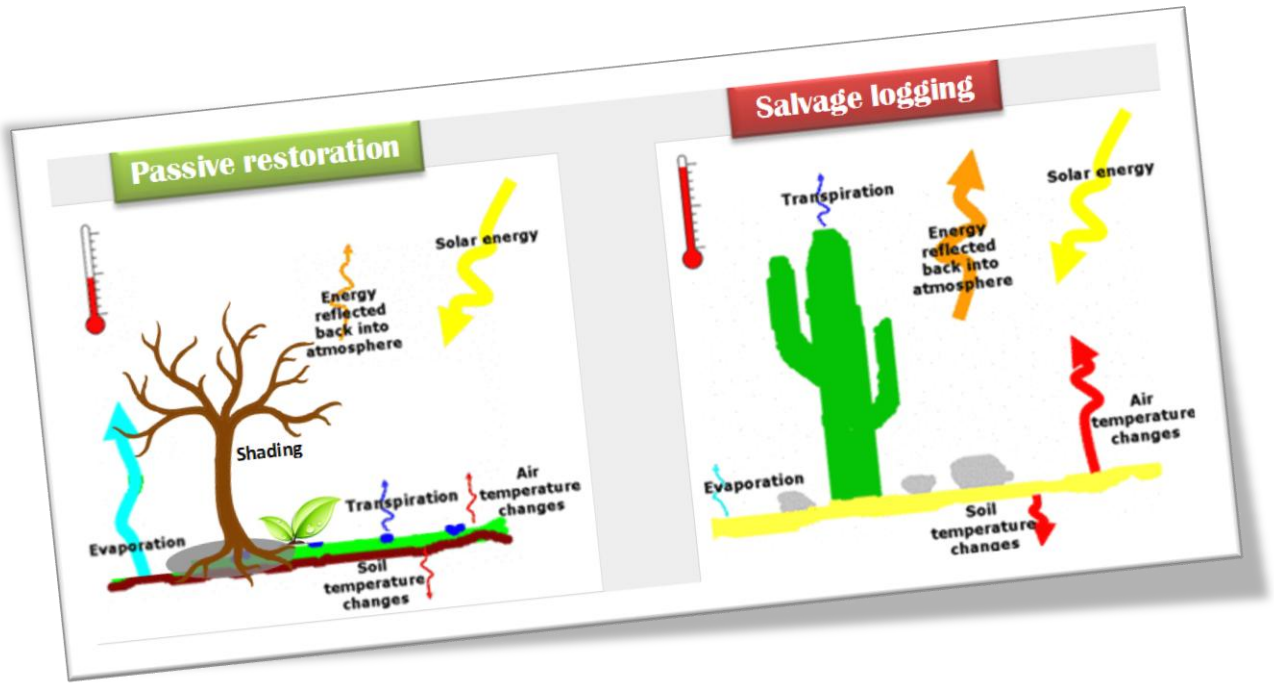

Introduction

Close to the southern limits of their natural geographic distribution, the forests of Scots pine (*Pinus sylvestris* L.) are quite common in the Italian Alps, from East to West and along a broad altitudinal gradient. *Pinus sylvestris* is the most widespread conifer in Europe, showing an early-seral character and a great sensitivity to land use (Caplat et al., 2006): in the inner valleys of the Alps, the continental climate and dry conditions promote the dominance of pine in the coniferous forests, especially on southern slopes. In these conditions fire is one of the most common natural disturbances, often with an active role in shaping pine forest dynamics (Pezzatti et al., 2009; Kloss et al., 2012). The impact of fire on alpine ecosystem depends on many factors: the amount and spatial pattern of burnt surface, the magnitude of the event, the edaphic and topographic characteristics. The high variability of the alpine environment (slopes morphology, fuel availability) combined with abrupt climatic variations, contrast *de facto* wildfires from spreading to extensive areas (Wastl et al., 2013). Average size of surface affected by fire in the Alps ranges from decades to few hundreds of hectares (Valese et al., 2011). The magnitude of fire-impact on the ecosystem is linked to the loss of vegetation cover, transformations of physical and chemical soil properties with remarkable changes in soil organic matter (SOM) and nutrient availability (Whelan, 1995; DeBano et al., 1998; DeBano, 2000). The different degrees of fire severity act providing contrasted micro-site conditions. High severity causes extreme changes in soil texture, bulk density and soil water properties (Ulery and Graham, 1993; Bodí et al., 2011; Gabet and Bookter, 2011). Uneven fire severity prompts variability in structure and vegetation composition, but also in soil respiration since fire acts removing plants and affecting soil microbes community: as a consequence, soil respiration often declines following the fire (Bergner et al., 2004; Hamman et al., 2008). When high severity affects large extensions, as in a wildfire, the balances of energy and water at-ground level can be heavily altered (Santos et al., 2003; Amiro et al., 2006).

Reductions in canopy cover caused by wildfires bring to an enhanced near-ground solar radiation, that is the input of energy for several ecological processes (Royer et al., 2010). Solar radiation significantly affects water budget, changing the ratio of soil evaporation, thus providing relevant patterns of soil temperature and soil respiration (Breshears et al., 1998; Klopatek et al., 1998; Davidson et al., 2000; Zhang et al., 2010). A high level of solar radiation after a wildfire causes huge evaporative losses from the soil surface. Soil moisture content (SM) is one of the most influencing parameters in relation with eco-hydrology and land surface climatology (Verstraeten et al., 2008). High levels of direct solar radiation associated with low SM levels and high temperature typically make the site hostile to tree regeneration, since the germination process is sensitive to SM and seedlings need more time to develop root depth (Gray and Spies, 1997; Gray et al., 2005; Gutiérrez-Jurado et al., 2006). Germination and survival of herbaceous and woody species can be affected by little differences in SM, mostly in the Alps, where steep slopes typically present shallow soil depths, with marked variation of SM because of great exposure to solar radiation (Lauenroth et al., 1994).

Soil temperature is strictly linked with the amount of solar radiation reaching the ground, slope exposition and the season of the year: south-facing slopes could considerably differ in daily soil temperature from north-facing ones (Haskell et al., 2012). The increase in soil temperature leads to a great soil drying rate with high differences in daily temperature: as a consequence, natural and planted regeneration shows high mortality, especially due to desiccation during the first growing season (Russel, 1988; Gray et al., 2005).

Soil temperature and SM are directly related to soil-nutrient concentration: water evaporation process promotes the upward movement of nutrients increasing the soil-nutrient availability. Slopes presenting high temperature and drier soils, as following a wildfire, cannot be easily exploited by regeneration, because of the lack of water available for transpiration and nutrient-solution. At the mid-term, the perspective of nutrient loss due to runoff, leaching or erosion leads to soil impoverishment (Matías et al., 2011). Fire severity influences soil respiration rates: higher respiration rates in soils affected by low-severity fire without strong SM limitations (Castro et al., 2011; Marañón-Jiménez et al., 2011). Furthermore, soil respiration is an index of fungi and microbes activities, directly connected with pedological processes (Bergner et al., 2004).

The transfer of soil water to the atmosphere is a process involving a complex range of sources such as evaporation from water bodies, land surfaces, surface snow-packs, vegetation canopy interception and plant transpiration. Evapotranspiration (ET, evaporation from the soil + plant transpiration) could be considered in terms of mass and energy transfer as well (Verstraeten et al., 2008). SM is a limiting factor for soil evaporation and plant transpiration processes (ET), linking soil water dynamics with the energy balance at ground level (Priestley and Taylor, 1972; Churkina et al., 1999). Energy partition at ground level between Evapotranspiration (ET) and sensible heat flux (H) is strongly dependent on soil temperature, SM, vapour pressure deficit and surface roughness (Allen et al., 1998; Shuttleworth, 2007). The input of energy to the biosphere-system by means of solar radiation, is partially conditioned by the reflected component at surface level (albedo); immediately after the fire, the burned surfaces show a dramatic change in albedo, related to fire severity (Field et al., 2007).

Post-fire regeneration depends on fire severity since intensity of Soil Organic Matter (SOM) consumption, mineral soil exposure and seedbed preservation drive variability in natural regeneration patterns (Greene et al., 2005). However, seedling establishment and survival heavily depend on environmental constrains as well, such as availability of light, water, nutrients and seeds. The most common post-fire management practice is salvage logging (felling and removal of burnt trees), sometimes coupled with seedlings plantations (McIver and Starr, 2001; Beschta et al., 2004). The Alps slope morphology often counseled land-managers to apply salvage logging (SL) in order to keep safety slopes (*i.e.* against rainfall and aeolian soil erosion or tree-fall accidents), for the extraction of valuable wood products (Beghin et al., 2010). In the last decade, the scientific debate about the opportunity to apply salvage logging as main post-fire intervention led to investigate alternative management practices. An increasing number of studies focused on the critical evaluation of the ecological consequences of salvage interventions on regeneration establishment (Donato et al., 2006; Noss and Lindenmayer, 2006; Castro et al., 2011; Serrano-Ortiz et al., 2011). Post-fire restoration activities mostly aim at facilitating the establishment of herbaceous and tree regeneration. Post-fire site preparation and planting of saplings turned out to

be the most common restoration activities applied, with high costs and, sometimes little effects as a result of the interventions (Leverkus et al., 2012). Restoration activities alternative to salvage logging, usually manage the burnt wood in the site, using it to facilitate the vegetation recovery process. The role of microsites, at a scale of tens of centimeters, is enhanced since in these sites regeneration can find positive microclimate conditions (Purdy et al., 2002; Greene et al., 2007; de Chantal et al., 2009; Legras et al., 2010). There is an increasing trend of experimental applications where active restoration methods (burnt wood is managed) are contrasted by passive management (no intervention, burnt and living trees remain *in situ*) (Beschta et al., 2004; Noss et al., 2006; Beghin et al., 2010). In a forest affected by a wildfire, burnt wood may have a relevant role on post-fire recovery dynamics, providing favourable microsite features (*i.e.* in terms of soil temperature and moisture, nutrient storage - Gray and Spies, 1997; Haskell et al., 2012). Downed wood material (DWD) proved to improve seedlings recruitment (see chapter 3) especially in arid conditions, where drought season matched the maximum water demand of established regeneration.

Establishment of natural regeneration was investigated in burnt areas managed with salvage logging and other restoration practices, that kept burnt wood in site. The positive role of dead wood in facilitating the establishment and survival of seedlings, led us to hypothesize an association with microsite features. The effects of post-fire restoration activities on the microenvironment were investigated, analyzing the response to the different treatments of the major parameters linked to microclimate: (I) near-ground solar radiation, (II) soil moisture and temperature, (III) surface roughness and (IV) total shortwave albedo.

Methods

Site description

The study area is located at Bourra site (45°46'14"N, 7°29'58"E), in the Aosta Valley Region (approximately 20 km East to Aosta, Italy). In march 2005 a stand-replacing fire burned approximately 260 ha of alpine forest dominated by Scot pine (*Pinus sylvestris* L.). Wildfire affected southern slopes (average inclination 25°) at an altitude ranging from 1650 to 1800 m a.s.l.

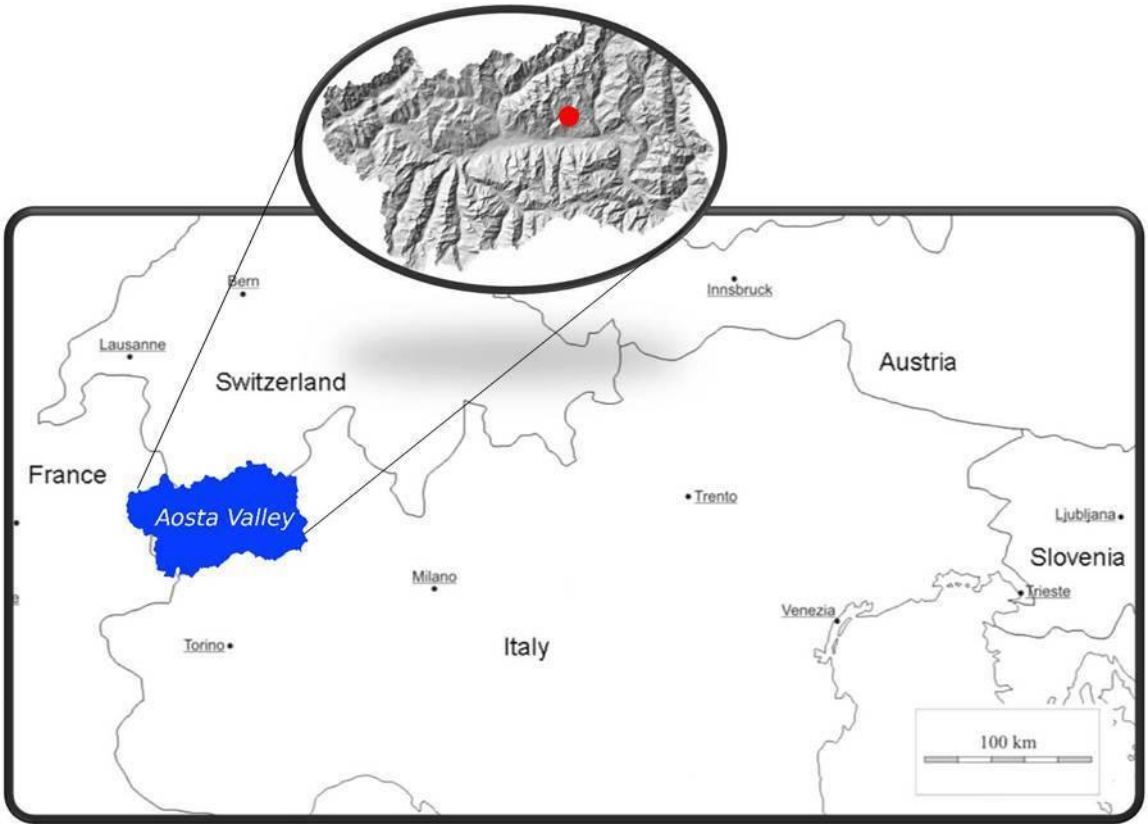

Figure 5.1 - National boundaries along the Alpine region and location of the study area.

In Aosta Valley the factors that mostly influence the climate are the significant differences in altitude and orientation of the slopes: the East-West orientation of the main valley determines a strong climate variability with respect to the small lateral valleys. The main valley is characterized by a mean annual temperature of approximately 5.6°C and annual precipitation is close to 750 mm (250 mm in the summer season); on average, there are less than 100 rainy days per year, February being the driest month (Cold Continental climate - Dfc according to Köppen climate classification, Kottek et al., 2006; Peel et al., 2007). Snow falls in the study area are usually distributed in November-December and March-April, reaching an average annual amount of 150 cm, with fast melting dynamics caused by the southern exposition (Mercalli and Cat Berro, 2003). The soils are well drained Entisols (Soil Taxonomy USDA) and the bedrock is formed by ophiolite and schist.

Experimental design

Given the quite homogeneous southern exposition of burned slopes, three adjacent areas of long-term monitoring have been established, each one characterized by a different management strategy. Starting from autumn 2007 the whole burnt area was subjected to a Salvage Logging (SL) intervention, excluding two zones, managed as Cut and Release (CR) and Passive Management (PM).

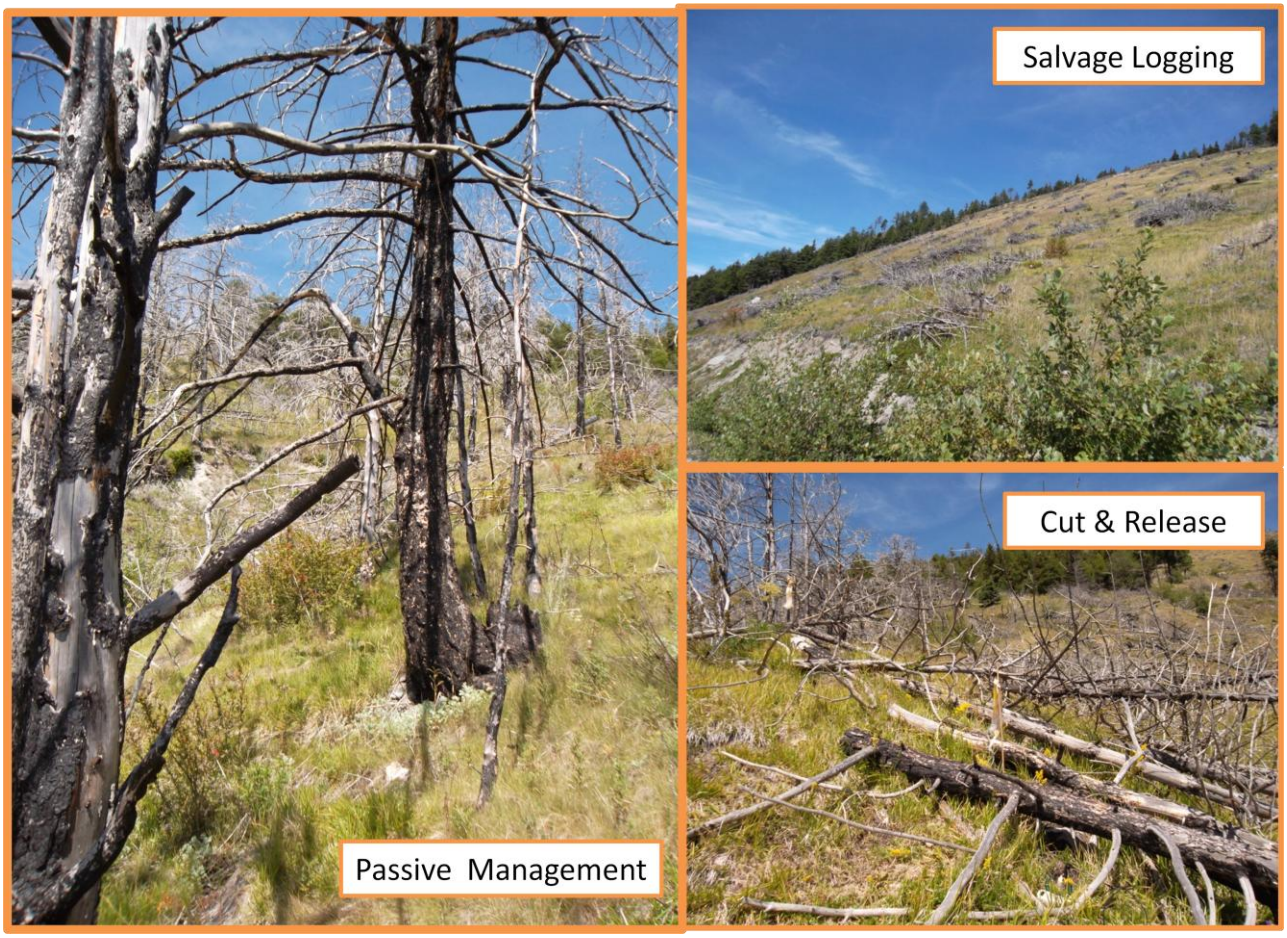

Figure 5.2 - Images taken in the experimental area: "Passive Management" and "Cut & Release" treatments keep burnt material in situ, showing the notable difference respect to "Salvage Logging".

In the salvage logging area, all the trees were felled, trunks and large branches removed, the residual wood stacked in piles (Beghin et al., 2010). A Passive Management (PM) area was delimited, where all trees were released and there wasn't any kind of intervention applied. An intermediate management treatment was the Cut and Release mode (CR), where all the trees were felled over the ground and the wood remained *in situ*. CR and PM treatments were applied to homogeneous areas of approximately 2 ha each one, while for our studies, SL area was considered restricted such all experimental design proves to a sequence of three adjacent zones

(Figure 5.3). Each treatment had a comparable size, presented similar pre-treatment conditions in terms of pre-fire stand characteristics, soil, slope, aspect and fire severity (stand-replacing fire).

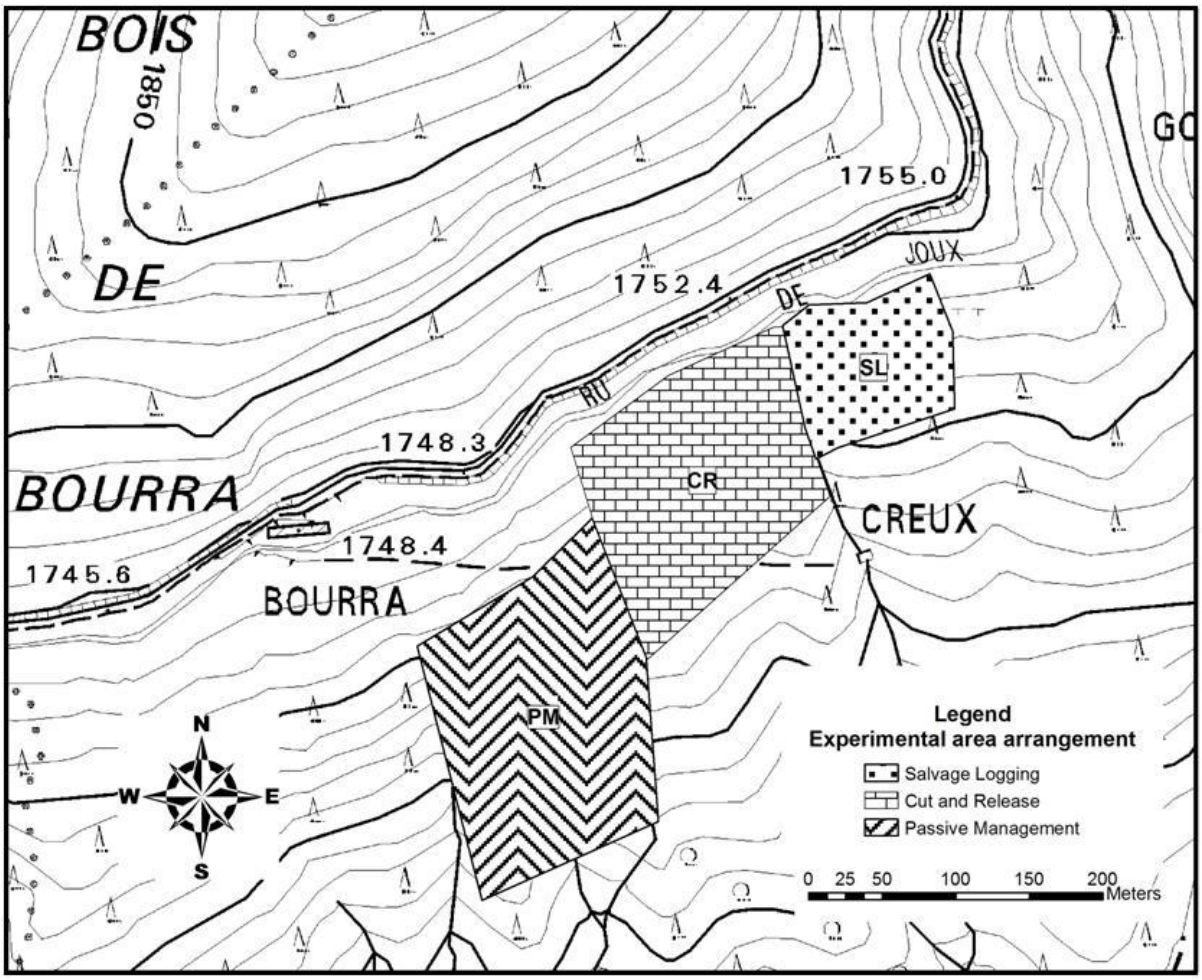

Figure 5.3 - Study site layout in Bourra Forest - Verrayes, Aosta valley, Italy: arrangement of the treatments applied in 2007-2008.

Survey of environmental factors

Considering the simplified energy balance at ground level, ET is a part of the total energy coming from solar radiation (Shuttleworth et al., 1989), assuming that:

$$R_n = ET + G + H \qquad (1)$$

where R_n is the surface net radiation, G the ground heat flux and H the sensible heat flux (at this level photosynthesis energy storage is negligible since it is estimated as a few percent of R_n - Meyers and Hollinger, 2004).

Soil Moisture (SM) is a limiting factor for soil evaporation and plant transpiration processes (ET), linking soil water dynamics with the energy balance at-ground level (Priestley and Taylor, 1972; Churkina et al., 1999). Combining the energy balance with the mass transfer it is possible to express ET referring to a standard vegetated surface (without any limit in soil water availability) according to the FAO Penman-Monteith equation (Allen et al., 1998):

$$ET = \frac{\Delta(R_n - G) + \rho_a \cdot c_p \cdot \frac{(e_s - e_a)}{r_a}}{\Delta + \gamma(1 + \frac{r_s}{r_a})} \qquad (2)$$

where R_n is the net radiation, G is the soil heat flux, (e_s - e_a) represents the vapour pressure deficit between the air and soil layers, ρ_a is the mean air density at constant pressure, c_p is the specific heat of the air, Δ represents the slope of the saturation vapour pressure-temperature relationship, γ is the psychrometric constant, r_s and r_a are the (bulk) surface and aerodynamic resistances.

In equation (1), the soil heat flux G is the energy to heat the soil (G > 0 = soil warming, G < 0 = soil cooling). Foe our aims, G may be negligible compared to R_n (Allen et al., 1998).
Surface heat flux H, as a component of the energy balance at-ground level, is usually determined following the equation (Monin and Obukhov, 1959; Drexler et al., 2004):

$$H = \frac{\rho \cdot C_p \cdot (T_o - T_a)}{r_a} \qquad (3)$$

where ρ is the density of air, C_p is the specific heat of air, T_o is the surface aerodynamic temperature, T_a is the near-surface air temperature, and r_a is the aerodynamic resistance to heat transfer (depending on surface wind speed and surface roughness); soil temperature (Ts) retrieval is often used instead of the surface aerodynamic temperature T_o (Kustas et al., 1989) .

The net surface radiation could also be presented as (Wang and Liang, 2008):

$$R_n = [R_d\downarrow - R_u\uparrow]_S + [L_d\downarrow - L_u\uparrow]_L + G \qquad (4)$$

meaning the short-wave radiation component within the *S*-brackets (R_d incoming, R_u reflected) and long-wave radiation the *L*-term (L_d incoming, L_u outgoing); arrows help to identify the path of the energy at-ground level.

The component R_u shows high variability after a wildfire since it is related with the marked changes in albedo, as a consequence of soil and vegetation cover differences before and after the fire. These changes result comparable in magnitude to those induced by other significant land-surface variations (Gash and Nobre, 1997; Field et al., 2007).
During summer 2011 a field campaign was launched, focusing on the investigation of basic environmental factors influencing the establishment and first survival of natural regeneration seedlings. Factors directly monitored were near-ground solar radiation, soil temperature, and soil moisture. Furthermore, by means of remote sensing techniques, we derived a dataset concerning other two significant environmental parameters involved in the energy balance at ground level: surface albedo and slope surface roughness. All investigated parameters influence the energy balance at-ground level, according to equations (1)÷(4).

Solar radiation

Near-ground solar radiation was estimated using hemispherical photographs collected on 16 points located within the treatments: 5 points in SL, 7 in CR and 4 in PM (Figure 5.5).

a) b)

Figure 5.4 - Hemispherical images taken from different treatments 30 cm above the ground level: a) CR - Cut and Release; b) PM - Passive Management.

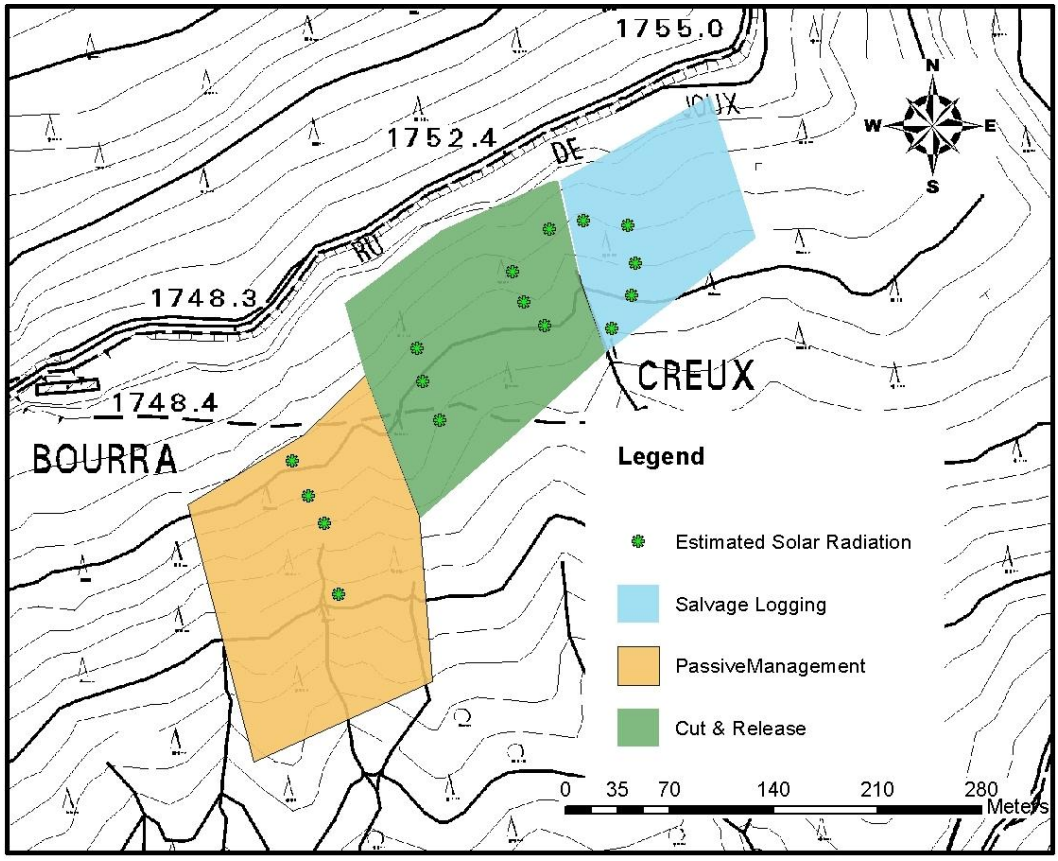

Figure 5.5 - Layout arrangement and 16 measurement points for estimated near-ground solar radiation, by means of hemispherical images.

Photographs were taken at 30 cm and 50 cm above the ground level, after the sunset or almost with uniform cloud cover, for homogenous light conditions. In each point a digital camera (Nikon CoolPix 5000) with a fish-eye lens of 180◦ field of view (Nikon FCE8) was mounted on a tripod, horizontally levelled and compass-oriented to the north. Hemispherical images allowed to estimate the characteristic near-ground solar radiation transmittance as affected by sky-view interferences surrounding a given point, the residual tree cover and the slope topography (Figure 5.4).

Each digital hemispherical image was processed by Gap Light Analyzer (GLA) tool Version 2.0 (Frazer, 1999; Hardy et al., 2004) to extract the near-ground potential solar radiation (expressed as gap light transmission) and the site openness (proportion of free visible sky [SKY%]). GLA computed canopy openness ratio as Total Site Factor (TSF) ranging from 0, in a completely covered location (light absence), to 1 in a completely open one (100% light availability).

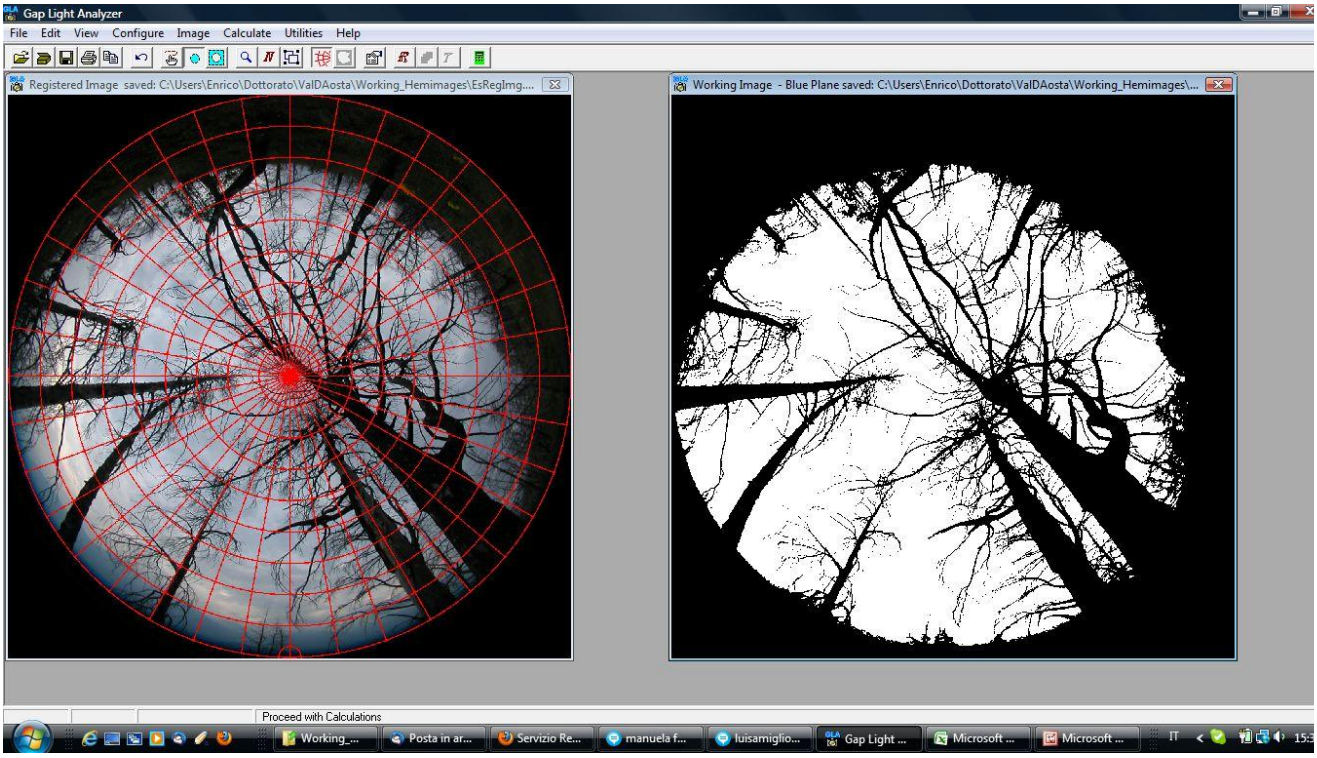

Figure 5.6 - Gap Light Analyzer screenshot: registration and editing of an hemispherical image.

TSF includes the estimated proportion of indirect and direct radiation compared with an open site at the same latitude, elevation and slope aspect. Site openness allowed to estimate the annual potential incoming near-ground solar radiation based on TSF and land position (geographic coordinates, elevation, slope inclination). TSF values were calculated at monthly intervals with GLA tools, considering the variation of sun inclination and the portion of visible sky. Total Site Factor was calculated as TSF = DSF + ISF, sum of Direct Site Factor (DSF) and Indirect Site Factor (ISF), which are respectively the estimated proportion of direct and indirect (diffuse) radiation at ground level, compared with an open site. Diffuse shortwave radiation (beam scattered by atmospheric gases and aerosols) ranges from approximately 10% of total shortwave radiation under clear-sky conditions to 100% under overcast conditions or under dense canopies (Hay, 1976). In order to

standardize solar radiation constraints (Rich, 1989, 1990; Frazer, 1999), all GLA processes considered the following parameter settings: solar constant value = 1367 W/m^2, Cloudiness index = 1 (no clouds), Spectral fraction = 1 (including the entire global solar radiation spectrum, from 0.25 μm to 25.0 μm), sky-region brightness adopting SOC model with a Clear-Sky Transmission Coefficient = 0.65 (Frazer, 1999; Jarčuška, 2008; Promis and Butler-Manning, 2011).

Soil temperature and moisture

In order to evaluate soil temperature during the growing season, 13 measurement points were chosen within the experimental area to characterize each treatment and distributed according to a regular scheme (Figure 5.8): 4 points within PM perimeter, each one in the neighbourhood of clustered standing burnt trees, 6 points close to downed wood elements in CR area and 3 points in SL area. All measurement points were located at similar elevation, following the layout in Appendix. Soil temperatures were recorded every minute for the whole growing seasons (from June to September 2011) using 13 EL-USB data-loggers (Lascar electronics Ltd., Salisbury, UK), equipped with temperature sensor, that were buried 5 cm beneath the soil surface (Figure 5.7a). All temperature sensors locations were also covered by hemispherical images.

Soil moisture was manually measured in the first 5 cm of the soil by means of Time Domain Reflectometry HH2 soil moisture meter and PM300 probe (Delta-T Devices Ltd, Cambridge, UK), calibrated for mineral soils (Figure 5.7b); in the same point, a measure of soil temperature was taken through a digital meter RX-4X8000 and K-thermocouple probe inserted at a 45◦ angle and at a depth of 10 cm under the ground (meter resolution 0.1 °C at 23 °C operations). The measurements were taken in 50 locations (20 for PM, 20 for CR, 10 in SL) including the 13 sites of soil temperature continuous monitoring (Figure 5.9). The measurement points were permanently flagged on terrain enabling us to come back each month from June to September. Blocks of measurements started at least 24 h after a significant precipitation event and the operations lasted a short period (1-2 days) to minimize variation due to time: each manual measure was recorded and performed at random order to prevent confounding interactions between time and treatment.

a) b)

Figure 5.7 - Equipment used for soil temperature and moisture measurement: a) EL-USB data-logger (Lascar electronics Ltd., Salisbury, UK) and b) TDR HH2 soil moisture meter and PM300 probe (Delta-T Devices Ltd, Cambridge, UK).

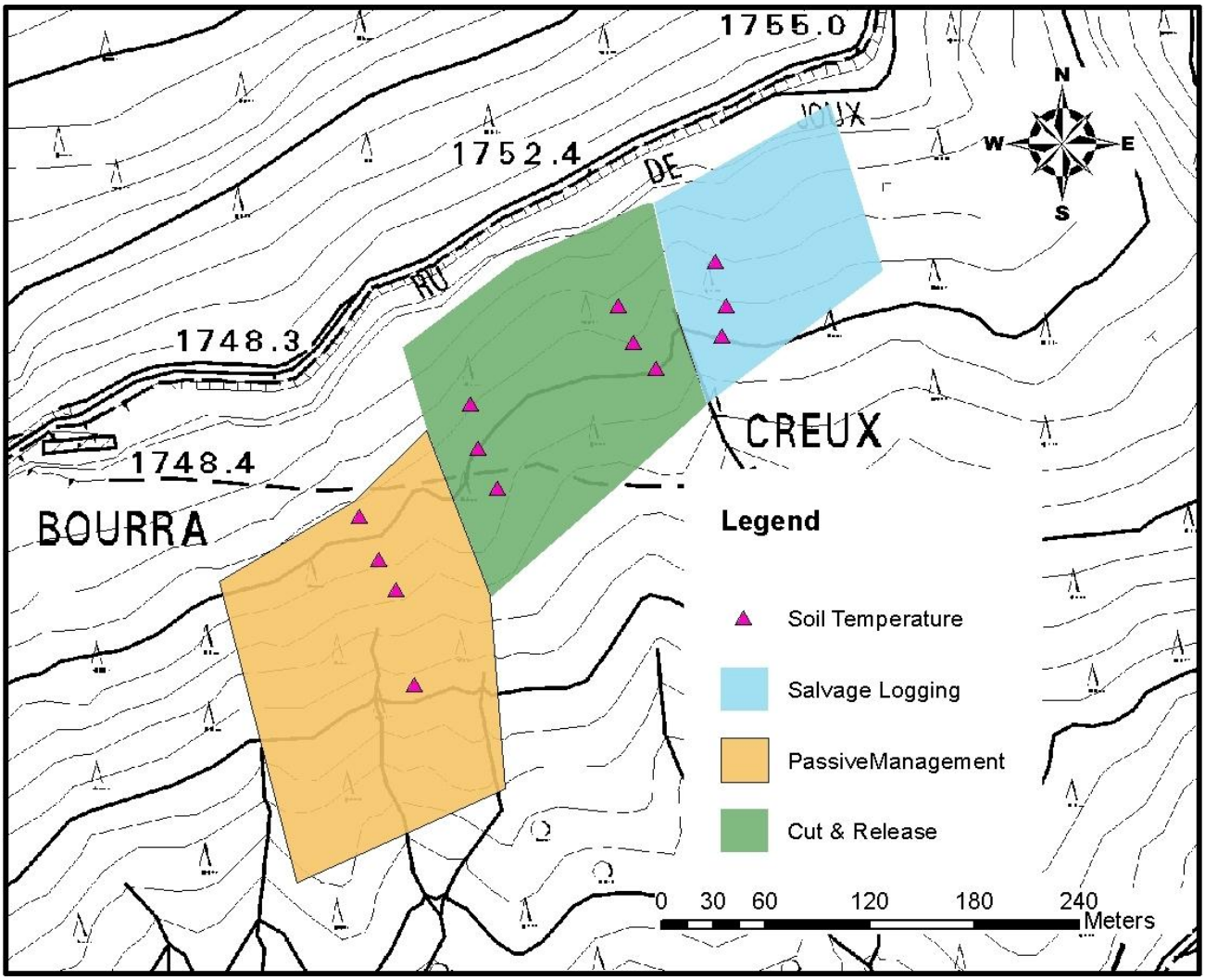

Figure 5.8 - Layout arrangement and 13 measurement points for soil temperature, by means of EL-Lascar datalogger equipped with temperature sensor.

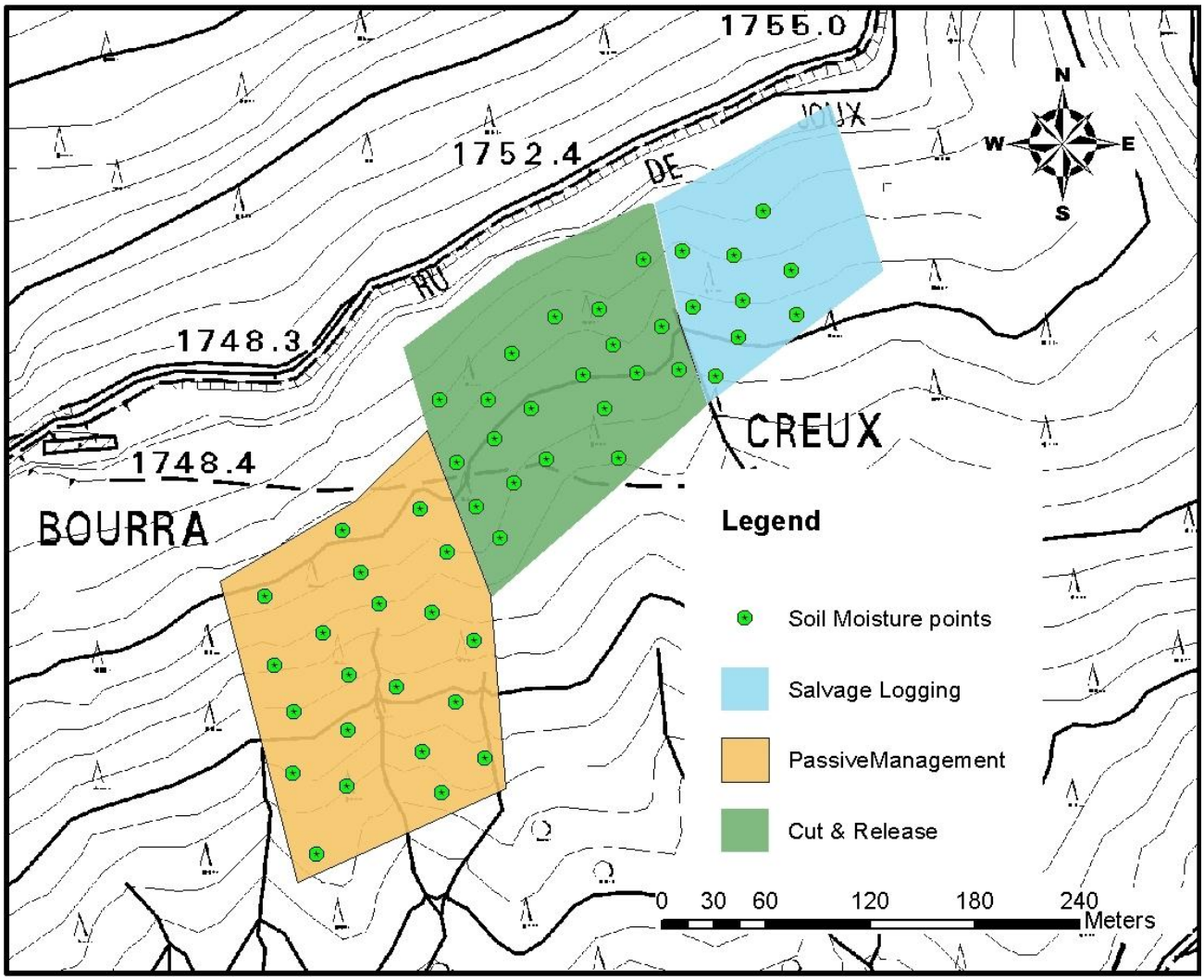

Figure 5.9 - Layout arrangement and 51 measurement points for soil moisture, by means of Delta TDR meter.

Surface short-wave albedo

Albedo is defined as the incident radiation diffusely reflected from a reference surface (Monteith and Unsworth, 2008). Table 5.1 shows a list of measured surfaces albedo: it may range from 0.95 for freshly fallen snow to 0.05 after a high-severity forest wildfire or for a wet bare soil. A green vegetation cover has an albedo of about 0.20-0.25, then the green grass reference crop is assumed to have a value of 0.23 (Figure 5.10). Albedo variation also depends on the radiation angle of incidence and the slope of the ground surface (Allen et al., 1998). The use of data from remote sensing earth observation, to estimate at regional scales biophysical parameters of land surface, such as albedo (Yao et al., 2011), is a viable tool for ecological investigations (Li and Islam, 1999; Verhoef and Bach, 2003; Wirth et al., 2009). A database of Landsat TM and Landsat ETM+ images, for the period 2003÷2011, was used to identify possible differences among treatments in inter-annual surface total short-wave albedo in mid-summer images (Liang, 2000; Tsouni et al., 2008).

Surface albedo typical values	
Conifer forest (Summer)	0.08 to 0.15
Deciduous forest	0.15 to 0.18
Bare soil	0.17
Green grass (Summer)	0.25
Fresh asphalt	0.04
Worn asphalt	0.12
Fresh snow	0.75 - 0.95
Old snow	0.40 - 0.70

Table 5.1 - Simplified list of total shortwave albedo values for a common range of surfaces (Campbell and Norman, 1998; Scharmer and Greif, 2000).

The database comprised nine cloudy-free images, acquired from Glovis USGS website, of which one in spring immediately after the fire (Table 5.2). The database was pre-processed using published post-launch gains and offsets (Chander et al., 2009) to convert Landsat TM and ETM+ data to exo-atmospheric reflectance (Top-Of-Atmosphere). Afterwards, an atmospheric correction (QUick Atmospheric Correction, see Bernstein et al., 2005) was applied to the images, in order to guarantee temporal homogeneity and spatial comparability of the dataset (Huang et al., 2002). Radiometric calibration and atmospheric correction were performed by mean of ENVI tools (ITT, Visual Information Solutions).

Landsat sensor	Acquisition date	Path/Row
TM	13-Aug-2003	195/028
ETM+	22-Jul-2004	195/028
ETM+	19-Mar-2005	195/028
ETM+	10-Aug-2005	195/028
ETM+	10-Jun-2006	195/028
ETM+	15-Jul-2007	195/028
ETM+	10-Jul-2008	195/028
TM	28-Jul-2009	195/028
ETM+	11-Aug-2011	195/028

Table 5.2 - Acquisition dates of the Landsat5 Thematic Mapper (TM) and Landsat7 Enhanced Thematic Mapper Plus (ETM+) images used in this study.

Measures of remote total shortwave albedo were retrieved from the Landsat TM, ETM+ satellite images (Liang, 2000):

$$ALBEDO = 0.356\rho 1 \ + \ 0.130\rho 3 \ + 0.373\rho 4 \ + 0.085\rho 7 \ + \ 0.072\rho 7 \ - \ 0.0018 \quad (5)$$

where $\rho_{1\div7}$ represent the top of atmosphere (TOA) reflectance bands at Landsat TM/ETM+ sensors, after the pre-processing procedure.

LANDSAT TM/ETM+ Bands	Spectral wavelength	Resolution
Band 1 (BLUE)	450-520 nm	30-meter
Band 2 (GREEN)	520-600 nm	30-meter
Band 3 (RED)	630-690 nm	30-meter
Band 4 (NIR)	770-900 nm	30-meter
Band 5 (Mid IR)	1550-1750 nm	30-meter
Band 7 (Mid IR)	2080-2350 nm	30-meter

Table 5.3 - Summary spectral description of Landsat TM/ETM+ sensors.

Surface roughness

In equations (2) and (3), the transfer of heat and water vapour, from the evaporating surface into the air above the canopy, is determined by the resistance terms (Figure 5.10), which are directly related with surface roughness (Allen et al., 1998). In order to explore variations in microclimate

factors caused by different dead wood management, the surface roughness plays a significant role from the ecological point of view (*i.e.* microsites diversity favourable to seed germination, especially along steep slopes) influencing the local processes of evapotranspiration and sensible heat transfer (Kuuluvainen and Juntunen, 1998; Wang et al., 2007; de Chantal et al., 2009; Burles and Boon, 2011). Despite the abundance of methods to extract an index of surface roughness from topographic datasets, used especially at hydrological purposes (Cavalli and Tarolli, 2010 and references therein), a simple descriptive approach was chosen. A surface Roughness Index (RI) was introduced using a Digital Surface Model (DSM) and a Digital Terrain Model (DTM), both derived from LiDAR data, acquired in June 2011 and rasterized at 1m resolution. RI is calculated as the standard deviation of differences (DSM-DTM) within a given moving window (3 x 3 pixels) after the removal of negative values and those greater than 1m (conservative threshold for filtering out standing dead trees).

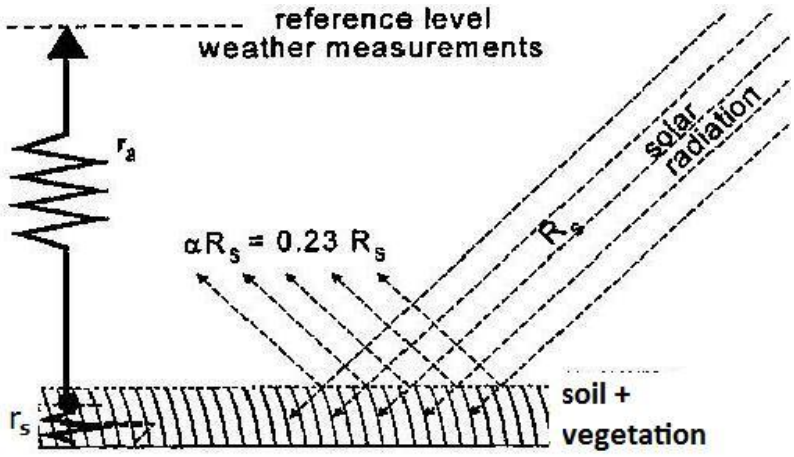

Figure 5.10 - Scheme of resistances to transfer sensible heat and evapotranspiration according to the worldwide adopted FAO Penman-Monteith method: hypothetical reference crop assumed an albedo of 0.23, ra (aerodynamic resistance), rs (surface resistance), closely resembling the evaporation of an extension surface of green grass of uniform height, actively growing and adequately watered (Allen et al., 1998).

Climate records

Metereological data were acquired from a station located at Nus-Saint Barthélemy (AO- Italy), relatively close to the study area and at similar elevation (1650 m a.s.l.; 45°47'24"N, 7°28'41"E). This station belong to a regional network of automated weather stations managed by the Meteorological Service of the Aosta Valley Region. The station collected data on rainfall, air temperature, incoming solar radiation at hourly resolution since 2002.

Statistical analysis

The effects of management and time of the year (month) on the variations of potential near-ground radiation, were tested by repeated measures ANOVA, which was performed using the general linear models (GLM) procedure. The GLM procedure is designed to build a statistical model describing the impact of one or more factors (post-fire treatment) on one or more

dependent variables (potential near-ground radiation). In order to highlight any difference among treatments in terms of solar radiation reaching the soil, TSF relating to the entire growing season (from the end of March to October) was compared. TSF differences among treatments were tested applying a multi comparison procedure (ANOVA test and Bonferroni's multiple comparison procedure). Difference was considered to be significant if p-value was < 0.01 (99.0% confidence level). Furthermore, since the openness portion of sky (SKY%) and DSF are important factors for the snow-melting processes (ranging from March to May), a similar multi comparison analysis was performed among treatments, focused on SKY% and DSF variables.

The soil temperature measurements for each sensor were hourly averaged and extracted from the entire growing season, and grouped by treatment-level. In order to avoid the variability caused by cloudy days and rainfall events, all data were summarized by calculating monthly mean temperature and mean diurnal curves for each month. The difference between soil and air temperature (To-Ta = ΔTsoil-air, equation (3)) is an important factor driving the partition of soil energy balance between evapotranspiration and sensible heat. It was thus calculated as the daily difference between maximum soil and air temperature. Furthermore, the rate of variation ΔTsoil-air was calculated for the day in correspondence to significant rainfall events, to evaluate the inertia-influences through time induced by the management type. Differences in soil temperature among treatments were analyzed with a General Linear Models (GLM) procedure, in which soil temperature was defined as the response-variable, while treatment and time (hour, month) as predictor variables. Statistically significant relationships between response and predictor variables were accepted for p-value < 0.01. Differences among treatments, about ΔTsoil-air and the variation rate of (ΔTsoil-air), were investigated with the paired t-test among mean daily values, while, sign and signed ranked test with the medians.

The Walter Index (Walter and Breckle, 2002) was calculated using the biweekly sum of daily precipitation and the average daily temperature collected:

$$WI = \left(\frac{Precipitation}{2}\right) - Temperature \qquad (6)$$

where *Precipitation* is the sum of daily data collected over 2 weeks, and *Temperature* the average of mean daily temperature of the same 2 weeks.

The WI has usually been applied to annual series of monthly data, but we used it to relate soil moisture with precipitation and temperature, thereby supplying an eco-hydrological point of view in a short time series (Kempes et al., 2008). In order to analyze any difference between treatments about SM measurements, a multiple comparison procedure was performed among treatments to determine significant differences between SM mean values. The method currently used to discriminate among means was Bonferroni's procedure at 99.0% confidence level.

Values of total shortwave albedo concerning each treated area were extracted from the correspondent raster data layer related to the temporal range 2003-2011 (considering an internal 10m buffer-distance from the boundaries of each treatment, in order to avoid overlapping). Albedo data referring to the same year were analyzed by means of a multiple comparison

procedure. Mean values were discriminated among treatments using Bonferroni's procedure at 99.0% confidence level.

Roughness index (RI) is a parameter derived from a Lidar data collection, rasterized at 1m resolution. Since the difference in surface extension among treatments and the non-normality of RI data, a Mann-Whitney (Wilcoxon) test was applied to compare RI medians among treatments. Furthermore, a Kolmogorov-Smirnov test allowed us to compare the distribution of the RI values between treatments; this test was performed by computing the maximum distance between the cumulative distributions of two RI dataset at a time (each dataset including RI values extracted from the area delimited by treatment perimeter).

All variables were assessed for normality prior to statistical analyses. Data were log or angular-transformed when required to improve normality and homoscedasticity (Zar, 2009).

Results

Near-ground solar radiation

The values of openness sky (SKY%) and transmitted radiation within each area were averaged to characterize the incoming near-ground energy and an annual projection was applied (Figure 5.11) considering the topographic and geographic variables of the study area (slope inclination, aspect, elevation, latitude). The ratio of direct to total spectral radiation, reaching the ground over a specified period, is largely a function of cloud cover, but for most regions of boreal hemisphere the beam ratio is approximately 0.5, when computed for the entire year.

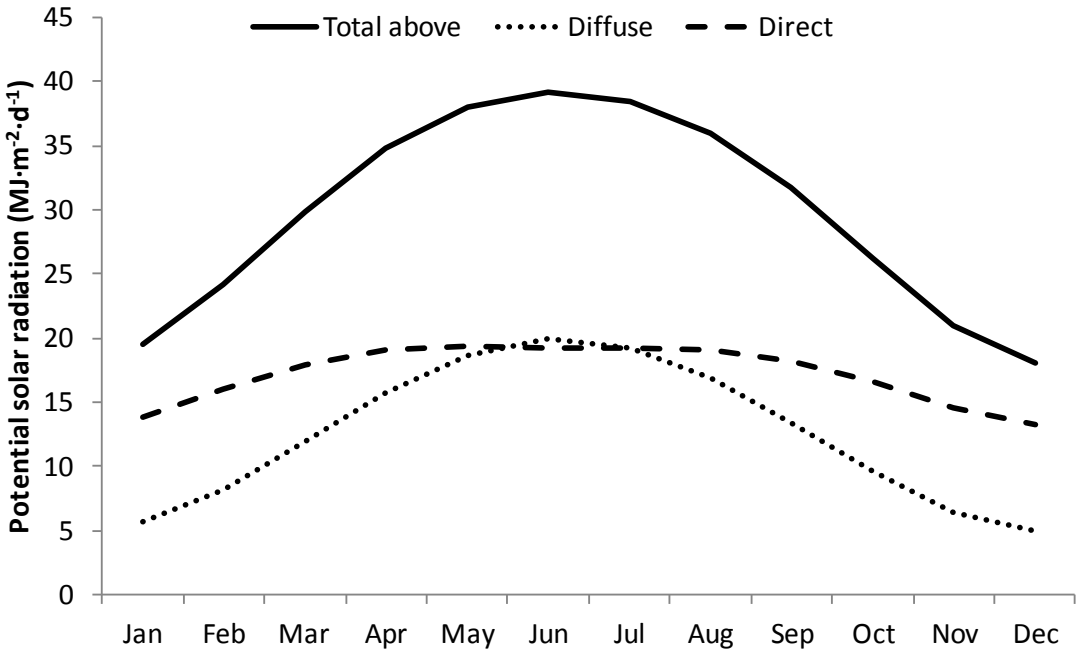

Figure 5.11 - Annual potential shortwave radiation ($MJ \cdot m^{-2} \cdot d^{-1}$) at ground-level: partition between diffuse and direct radiation considering a ratio around 0.5 in the middle of the growing season, Latitude 45°46'14''N, Longitude 7°29'58"E, 25° of slope inclination and southern exposition (Gap Light Analyzer processing). Total above radiation is the sum of Diffuse + Direct radiation.

A dynamic estimation of the potential incoming shortwave radiation reaching the ground, was modeled plotting the values of transmitted radiation for each treatment during the year (Figure 5.12). SL can be approximated to a no-cover site, whereas CR revealed light differences, mostly from October to February. Passive Management exhibits great differences from February to October, until 10 $MJ/m^2 \cdot d$ from May to July, that is around the total transmitted radiation of a winter day (10 $MJ/m^2 \cdot d$ correspond to the energy required to vaporize 4 mm/d of free water, according to FAO Penman-Monteith standard conditions).

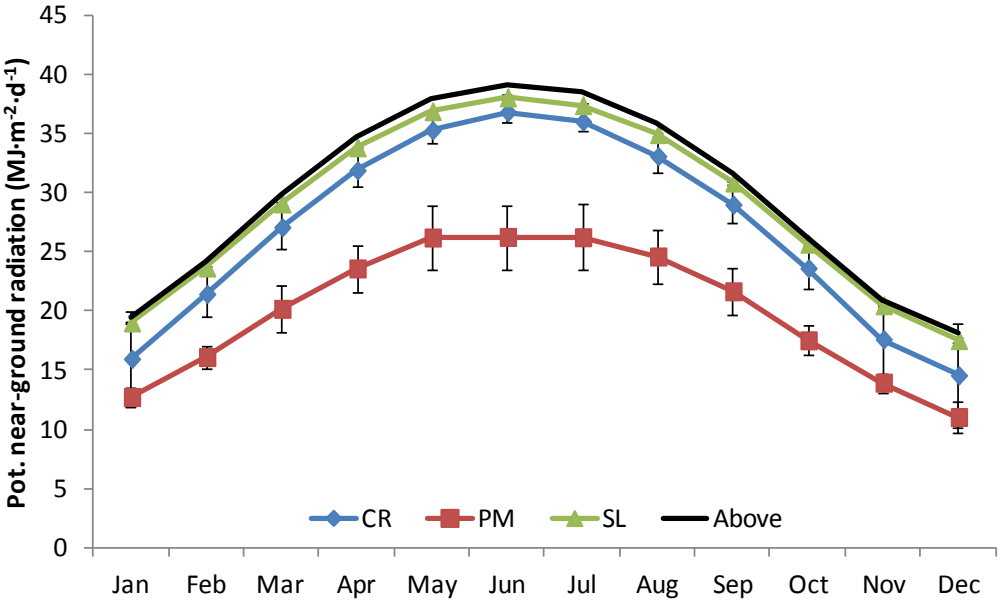

Figure 5.12 - Annual potential near-ground solar radiation (± 1 δ) estimated for each area: Cut and release (CR), Salvage logging (SL), Passive management (PM), (Above) without sky obstructions (Gap Light Analyzer processing).

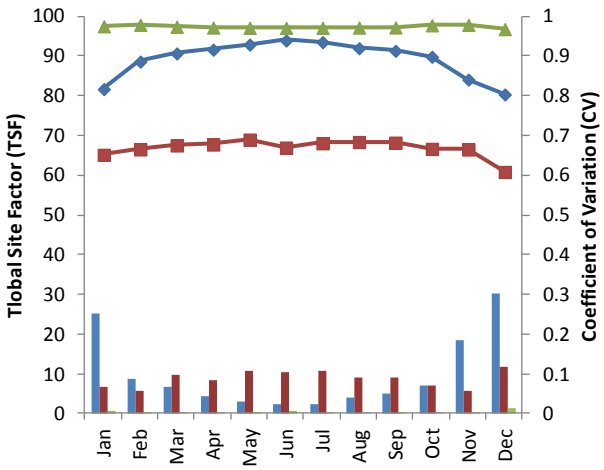

a)

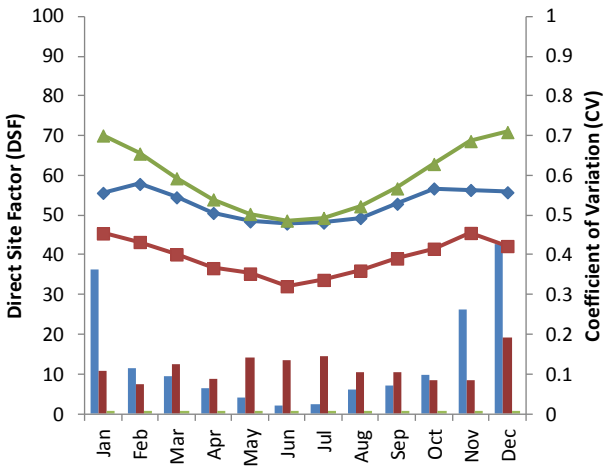

b)

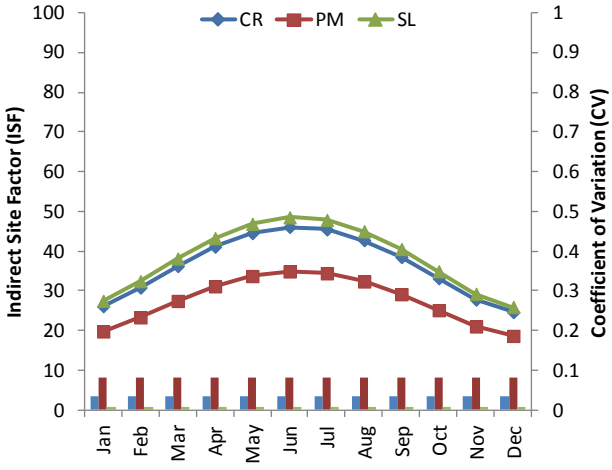

c)

Figure 5.13 - Yearly estimated solar radiation among different managed area: c) indirect site factor (ISF), b) direct site factor (DSF) and a) total site factor (TSF = DSF + ISF), are the estimated proportion of indirect, direct, and total radiation, respectively, compared with an open site. Variability of the indices are represented by means of the coefficient of variation (CV - bars).

The monthly DSF - Direct Site Factor (and consequently TSF - Total Site Factor) resulted remarkably influenced by the treatment effects, according to the GLM at $p < 0.01$ (Table 5.4). The annual plotted values show a relevant variability, revealed by CV values during winter months (December, January and February) for CR treatment (Figure 5.13).
Negligible variability during the year was found in SL, while, approximately constant CV values in PM treatment, in spite of the large annual variation of sun zenith angle and total solar radiation (Figure 5.14).

Response	General Linear statistical Model			Predictor	D.f.	F-ratio	p-value
TSF	R^2	F-ratio	p-value	Management type	2	204.2	**<0.001**
	0.737	12.5	**<0.001**	Time (month)	11	1.12	0.3510
				Management * Time	22	0.55	0.9496
DSF	R^2	F-ratio	p-value	Management type	2	95.36	**<0.001**
	0.653	8.39	**<0.001**	Time (month)	11	7.94	**<0.001**
				Management * Time	22	0.74	0.7871

Table 5.4 - The left half shows the fitting models relating response TSF and DSF to the predictors Management type (treatments SL, CR and PM); p-value < 0.01 implying a statistical relationship between response and predictors at 99% confidence level. The right part summarizes the statistical significance of each factor considered in the model: the p-values in bold indicate significant predictors at 99% confidence level. The R^2 means how the model fitted explains variability in the response variable.

TSF within each treatment was evaluated considering the growing season from April to September (Table 5.5). As expected, significant differences of TSF values were observed ($F_{2,93} = 481.4$, $p < 0.001$). SL exhibits the highest radiation charge (97%), PM treatment presents the lowest TSF (68%) and CR treatment shows (92%) a little lower than SL. The comparison of DSF and SKY%, among treatments (relating to the snow-melting period, from February to April) evidenced a clear distinction between SL (the greatest) and PM treatment (the lowest), with intermediate values for CR (Table 5.5).

Variable	Evaluation period	ANOVA statistics	Management type		
TSF	April ÷ September	$F_{2,93} = 481.4$ pvalue < 0.001	SL = 97.2 ± 0.4 [a]	CR = 92.6 ± 3.3 [b]	PM = 68.1 ±5.8[c]
SKY%	-	$F_{2,50} = 13.7$ pvalue < 0.001	SL = 74.5 ± 2.6 [a]	CR = 69.4 ± 3.2 [b]	PM = 68.2 ±5.9[b]
DSF	February ÷ April	$F_{2,50} = 13.7$ pvalue < 0.001	SL = 54.0 ± 3.4 [a]	CR = 51.2 ± 4.3 [a]	PM = 37.4 ±4.6[b]

Table 5.5 - Results from multi-comparison ANOVA using Bonferroni's procedure at 99% confidence level: Total Site Factor TSF, portion of openness sky (SKY%) and (DSF) Direct Site Factor (± S.D.) between different management type (Salvage Logging, Cut and Release, Passive Management). Reference range of evaluation for TSF spans from April to September, while SKY% and DSF variable ranged from March to May. The letters next the values highlight differences between treatment at α = 0.01 .

April

June

September

December

Figure 5.14 - The sun-path plotted for different months: notable differences in zenith values between June (summer solstice) and December (winter solstice). Thickness of the sun track shows zenith changes during each month displayed (Frazer, 1999; Muneer, 2004).

Soil temperature

Daily ΔTsoil-air series for each treatment were plotted taking into consideration the amount of daily rainfall (Figure 5.15). A large variability through the time is evident, especially in correspondence to the significant precipitation events, where the ΔTsoil-air in each treatment drops down. The evaluation of ΔTsoil-air trends over the entire period, highlights a clear difference between SL and the other management type, where SL treatment presents ΔTsoil-air values twice (in average around 10 °C) the others treatments (Table 5.6, $p < 0.01$). Within a relative drought period (from 16 July to 30 August - characterized by the absence of notable precipitation), ΔTsoil-air presents the greatest differences; however, in the days immediately around the only significant rainfall event, PM and CR treatments exhibit ΔTsoil-air values more similar to SL. Lack of precipitation lead to rising trend of (ΔTsoil-air), conversely, decreases of ΔTsoil-air trend matches the rainy periods.

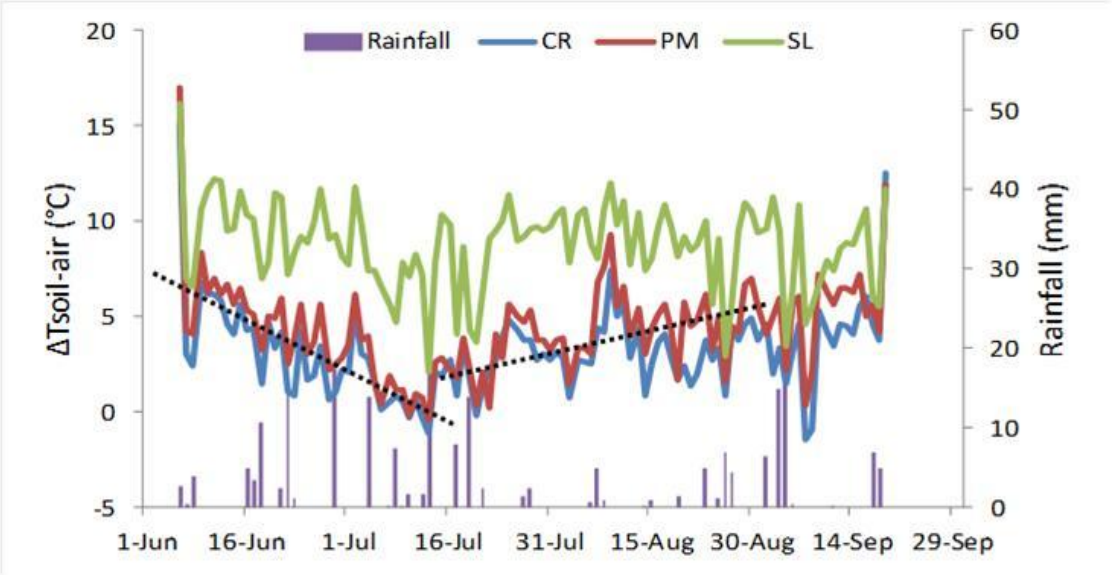

Figure 5.15 - Distribution of ΔTsoil-air over the entire growing season for each management type (CR: Cut and release; PM: Passive management; SL: salvage logging) and daily precipitation. To be considered the 45 days without relevant rainfall (16 July - 30 August) and the contrasting trends (dashed lines) linked to lack or abundance of precipitation.

ΔTsoil-air Treatment series	Paired test	Statistic value	Comparison difference
SL vs. CR	t-test	T = 30.8 p < 0.001	SL > CR
	Sign test	S = 10.0 p < 0.001	Avg difference = 5.5 °C
	Signed rank test	SR = 8.93 p < 0.001	Median diff. = 5.9 °C
PM vs. CR	t-test	T = 12.7 p < 0.001	PM > CR
	Sign test	S = 8.9 p < 0.001	Avg difference = 1.2 °C
	Signed rank test	SR = 8.1 p < 0.001	Median diff. = 1.1 °C
SL vs. PM	t-test	T = 22.9 p < 0.001	SL > PM
	Sign test	S = 9.6 p < 0.001	Avg difference = 4.4 °C
	Signed rank test	SR = 8.9 p < 0.001	Median diff. = 4.4 °C

Table 5.6 - Summary of paired tests between treated areas about ΔTsoil-air over the period June-September. The t-test verifies the null hypothesis that the difference between treatments of mean daily value ΔTsoil-air is equal to 0; p-value < 0.01 rejects the null hypothesis. The sign test verifies the null hypothesis for the paired medians daily values. The signed rank test is based on comparing the average ranks of values above and below the hypothesized median. The sign and signed rank tests are less sensitive to the presence of outliers but are somewhat less powerful than the t-test.

Daily rate of ΔTsoil-air Treatment series	Paired test	Statistic value	Comparison difference
SL vs. CR	t-test	T = 4.2 p < 0.001	SL > CR Avg difference = 1.5 °C/d Median diff. = 1.0 °C/d
	Sign test	S = 2.5 p < 0.01	
	Signed rank test	SR = 3.3 p < 0.001	
PM vs. CR	t-test	T = 0.03 p = 0.97	no statistical differences
	Sign test	S = 0 p = 1.0	
	Signed rank test	SR = 0.14 p = 0.89	
SL vs. PM	t-test	T = 3.4 p = 0.002	SL > PM Avg difference = 1.4 °C Median diff. = 0.8 °C
	Sign test	S = 3.2 p = 0.001	
	Signed rank test	SR = 3.05 p = 0.002	

Table 5.7 - Summary of paired tests between treated areas concerning the rate of daily changes in gradient soil-air temperature ΔTsoil-air over the June-September period. The t-test verifies the null hypothesis that the difference between treatment of mean daily value (daily variation of ΔTsoil-air) is equal to 0; p-value < 0.01 rejects the null hypothesis.

During the period June-September, 23 significant rainfall events (daily precipitation value was > 3mm) were identified. Daily variation rate of ΔTsoil-air, in proximity to a significant rainfall event, was compared among treatments, to assess in which way the different management type influences the rate of ΔTsoil-air daily changes (rate = $[\Delta\text{Tsoil-air}]_t$ - $[\Delta\text{Tsoil-air}]_{t-1}$). Paired comparison shows that SL treatment presents lightly greater daily variation rates of ΔTsoil-air than the others (Table 5.7), highlighting the lower inertia of SL to the temperature variation. The monthly arrangement of the hourly values of soil temperature highlights the predominant effect of the Management type (GLM Management factor, p-value < 0.001, Table 5.8). The comparison of hourly values between treatments shows that SL soil temperatures are always the greatest, with marked differences from June to August (Figure 5.16).

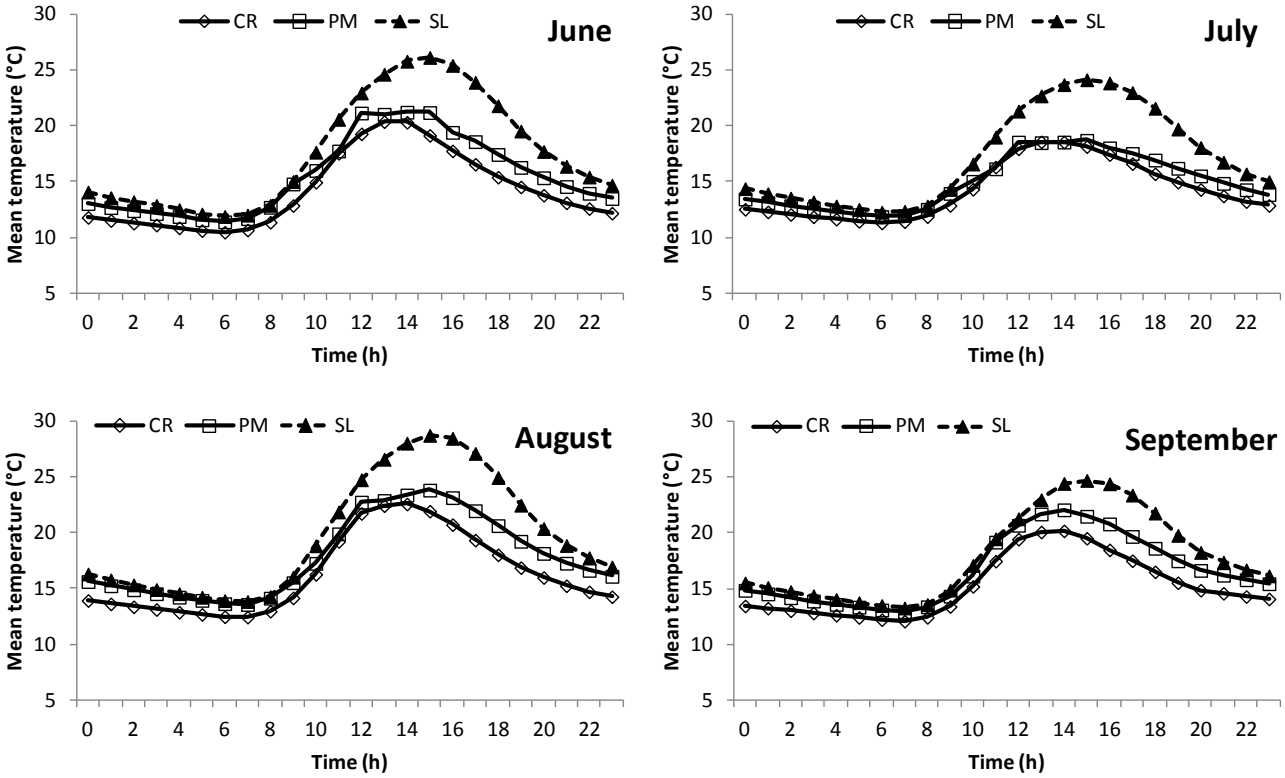

Figure 5.16 - Average diurnal soil temperature measured for each treated area during the period June - September.

The CR hourly values remain the lowest for the entire period, while the PM series exhibits an intermediate behavior: the temperature is similar to CR values during the first half of the day, but differs in the hottest hours (from 14 to 19 - Figure 5.16). However, SL treatment sets the highest values, especially from 14 to 19 in the afternoon, for all the summer months (GLM interaction for Management * Time (hour), p-value < 0.001, Table 5.8).

Response	General Linear statistical Model			Predictor	D.f.	F-ratio	p-value
Soil temperature (°C)	R^2	F-ratio	p-value	Management type	2	2519.0	**<0.001**
	0.737	616.4	**<0.001**	Management * hour	46	44.9	**<0.001**
				Management * month	6	19.0	**<0.001**

Table 5.8 - Fitting models relating response Soil Temperature to the predictors Management type (treatments SL, CR and PM), and interactions with Time (hour, month); p-value < 0.01 meaning a statistical relationship between response and predictors at 99% confidence level.

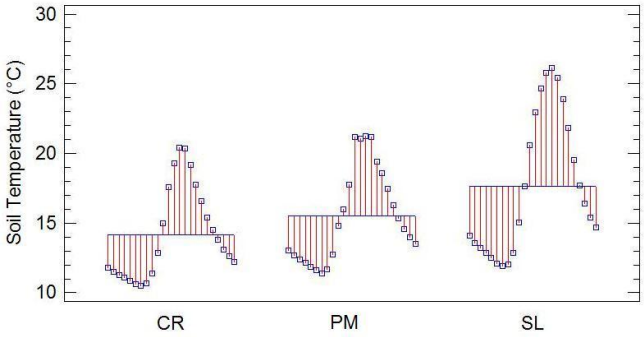

June

Factor	*Df*	Variance explained (%)
Management type	2	12.69
Time (hour)	69	87.31

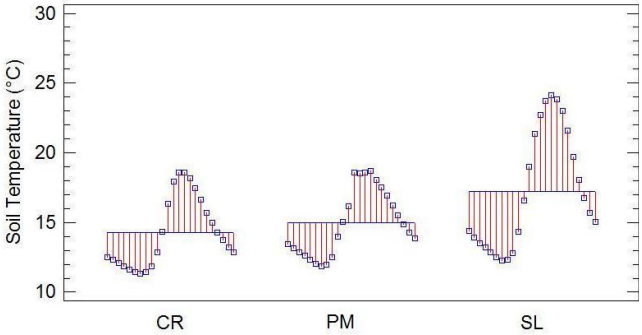

July

Factor	*Df*	Variance explained (%)
Management type	2	16.3
Time (hour)	69	83.7

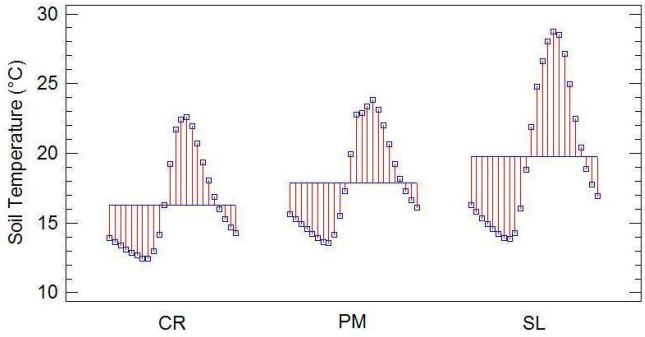

August

Factor	*Df*	Variance explained (%)
Management type	2	11.57
Time (hour)	69	88.43

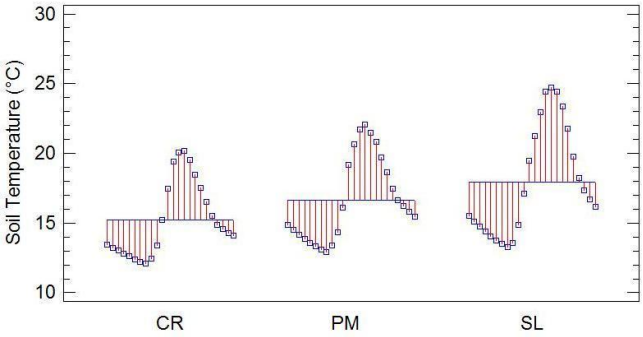

September

Factor	*Df*	Variance explained (%)
Management type	2	11.27
Time (hour)	69	88.23

Figure 5.17 - Diagrams showing the analysis of variance components of GLM applied: the variance of the output model splitted into 2 components, one for each factor of the model, to estimate the amount of variability contributed by each factor (variance component). Red bars shows the hourly (0 ÷ 23h) variance around the mean.

Results of variance component analysis extracted from GLM procedure (Figure 5.17) highlight the effects of different Management type related with the soil temperature variability (SL shows the greatest diurnal variation of hourly soil temperature for all four months).

Soil moisture

SM values were averaged for each treatment, plotted through the time (Figure 5.18) and WI index overlapped to SM series (negative values of WI reported relative drought periods).

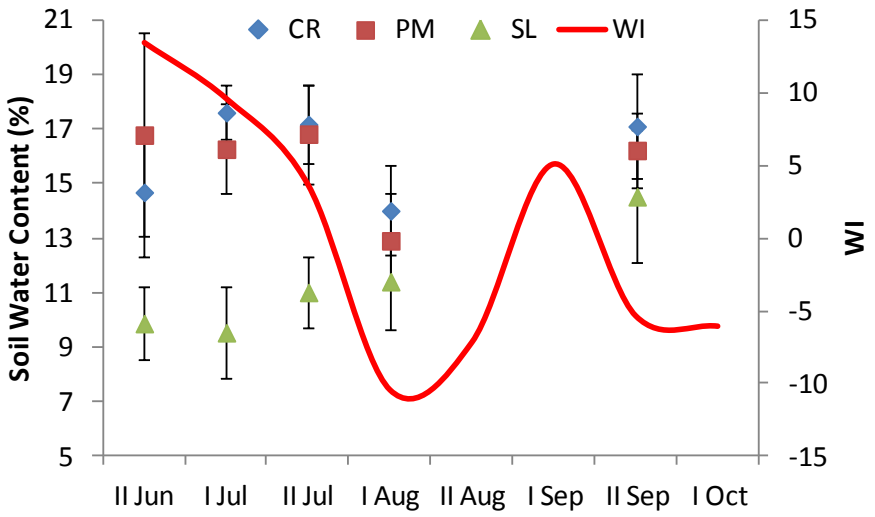

Figure 5.18 - Average Soil Water content in different treated areas (CR-cut and release, PM-passive management, SL-salvage logging) and Walter climate index (WI). Biweekly temperature and precipitation (I = the first half, II = the second half of the month) are concurrently evaluated to highlight periods of relative water deficit (WI negative values). Overlapped bars represent standard deviation of the measures.

Throughout summer 2011, mean values of SM (Table 5.9) measured in PM and CR (from 14.0 % to 17.6%) were significantly greater than those measured in SL area (from 9.6% to 14.5%), except for August session, when quite similar values of SM were measured among the treatments, matching the drought period highlighted by WI index (Figure 5.18) and seasonal rainfall diagram (Figure 5.15). Variability affecting measurements is similar for all experimental sessions and treatments, proving that the random measurement scheme applied over day time, overpasses time-dependence interactions.

Month	Management type			F-ratio	p-value
	CR	PM	SL		
Jun	14.7 ± 2.4^{a}	16.8 ± 3.7^{a}	9.9 ± 1.3^{b}	18.65	<0.001
Jul-I	17.6 ± 1.0^{a}	16.3 ± 1.6^{a}	9.6 ± 1.7^{b}	87.23	<0.001
Jul-II	17.1 ± 1.4^{a}	16.8 ± 1.8^{a}	11.0 ± 1.3^{b}	57.8	<0.001
Aug	14.0 ± 1.6^{a}	12.9 ± 1.7^{ab}	11.4 ± 1.8^{b}	7.21	0.002
Sep-II	17.1 ± 1.9^{a}	16.2 ± 1.3^{ab}	14.5 ± 2.4^{b}	8.16	<0.001

Table 5.9 - Summary of multiple sample-comparison between soil moisture (%) data (±SD) collected during summer 2011 and grouped according to management type (Cut and Release, Passive Management and Salvage Logging). ANOVA F-ratio in the table tests any significant difference amongst the means of the groups. Multiple range Tests output suggest which means are significantly different according to Bonferroni's procedure at 99.0% confidence interval. Different letters highlight differences between Management type (n = 25 measures/treatment per Month).

Surface roughness

The Roughness Index (RI) values extracted from the study area ranging in (0 ÷ 0.5) span: there are marked differences among treatments (Table 5.10).

Management type	n	RI Average ± SD	RI Median
PM	17686	0.17 ± 0.08	0.16
CR	13898	0.18 ± 0.07	0.17
SL	7877	0.11 ± 0.06	0.10

Table 5.10 - Summary statistics for the RI index data extracted from each Management-type (Passive Management, Cut and Release, Salvage Logging). Average column includes ± Standard Deviation.

Therefore, RI distribution shows significant differences among treatments: SL presents lower RI values than the others management type, as supported by frequency distribution diagrams (Figure 5.19), K-S results (Table 5.11; DN = 0.30 ÷ 0.39; K-S = 22.3 ÷27.7; p-value < 0.001) and medians comparison (Table 5.11).

Management type comparison	Kolmogorov-Smirnov Test	Mann-Whitney (Wilcoxon) Test
SL vs. PM	Estimated overall statistic DN = 0.30 K-S statistic = 22.3 p-value < 0.001	W = 3.9E7 p-value < 0.001
SL vs. CR	Estimated overall statistic DN = 0.39 K-S statistic = 27.7 p-value < 0.001	W = 2.7E7 p-value < 0.001
CR vs. PM	Estimated overall statistic DN = 0.09 K-S statistic = 8.2 p-value < 0.001	W = 1.1E8 p-value < 0.001

Table 5.11 - Results from multiple-sample comparison applying a Kolmogorov-Smirnov test to compare the Roughness Index distributions: this test is performed computing the maximum distance (DN) between the cumulative distributions of the two samples. Non-parametric Mann-Whitney W-test to compare the medians of the RI values among the treatments: the test is constructed by combining the two samples, sorting the data from the smallest to the largest, and comparing the average ranks of the two samples in the combined data. Both Kolgomorov-Smirnov and Mann-Whitney test are applied at 99.0% confidence level (significant differences between the distributions and between the medians of RI values respectively).

Significant but small differences between PM and CR treatments, with the latter presenting the greatest RI values (0.18 ± 0.07). In both CR and PM a quite homogeneous frequency distribution was found, meaning that surface roughness is spatially uniform within these areas (Figure 5.19).

These results were expected since in SL the increase in the surface roughness was due to the small piles of residual branches randomly distributed after the interventions. The loads of proportional cumulated area in RI was plotted in a quantile plot diagram to standardize and compare the trend among the treatments (Figure 5.20): a clear difference between SL and the other treatments indicates marked differences of surface roughness.

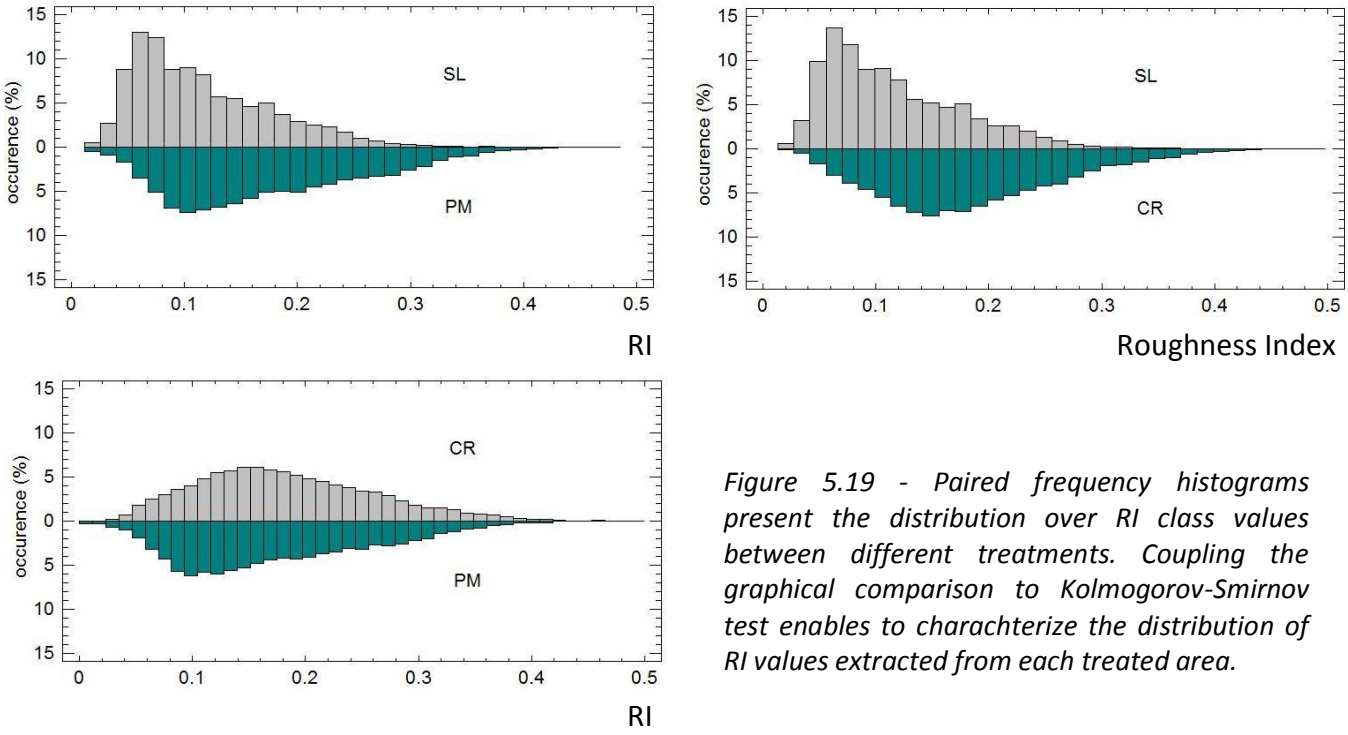

Figure 5.19 - Paired frequency histograms present the distribution over RI class values between different treatments. Coupling the graphical comparison to Kolmogorov-Smirnov test enables to charachterize the distribution of RI values extracted from each treated area.

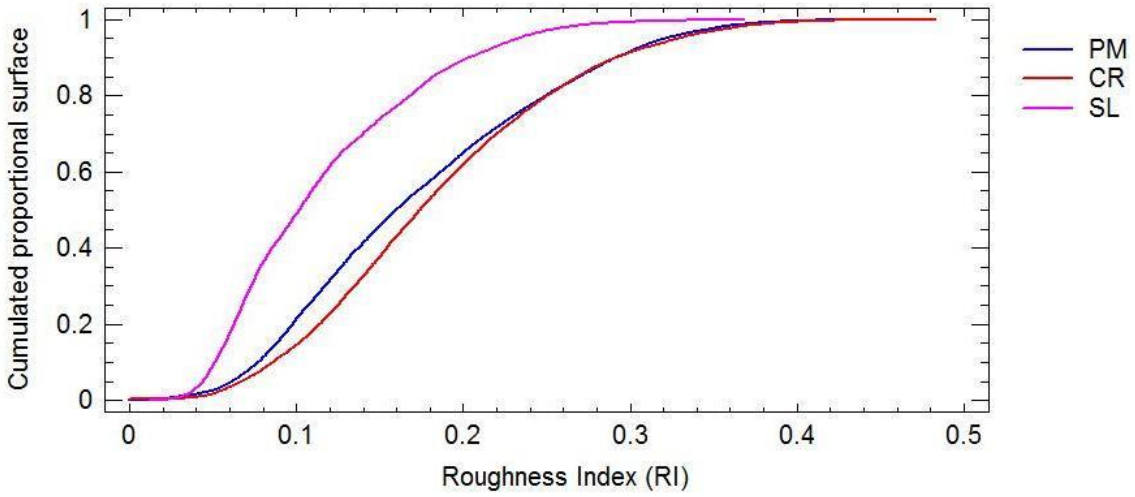

Figure 5.20 - Quantile plot-diagram illustrating the proportion of data in each Management type that is below a given value of Roughness Index (RI), as a function of RI. Closed plots reveal that the values extracted come from the same statistic population. The distance between the plot lines indicates a difference in RI distributions among the treatments (see frequency histogram and Kolmogorov-Smirnov test). Differences in the slope of the curves indicate a difference between the standard deviations.

Total short-wave albedo

Mean summer values and standard deviation bars of surface albedo were plotted through the time (Figure 5.21) for the period analyzed (2003÷2011), including albedo values immediately after the fire (end of March 2005). Temporal projection highlights 2005 disturbance and albedo dynamics related to the study area, focusing on the treatments (before and after the interventions). Albedo values before the fire were similar in all treated areas (Table 5.12; $p > 0.01$).

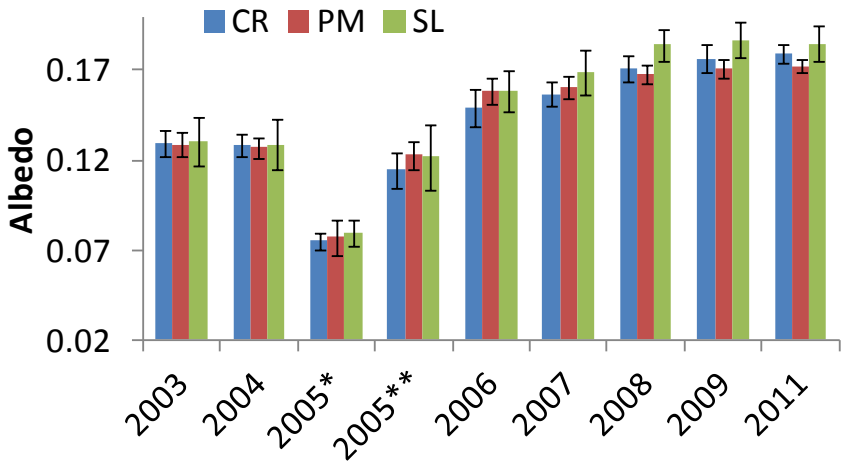

Figure 5.21 - Temporal diagram of albedo values (histograms shows means ± standard deviation) related to (I) the treated areas before the fire (march 2005), (II) after the fire and before the interventions (autumn 2007) , (III) after the interventions (: March right after the fire; **: August).*

The drop in 2005 presents uniformly low albedo values among the treatments (around 0.07, approximately a black surface, see Table 5.1 and Figure 5.22); after the fire, the mean summer albedo progressively increased until 2007 (without differences among the areas before interventions).

Year	Management type			F-ratio	p-value
	CR (n=30)	PM (n=30)	SL (n=40)		
2003	0.129 ± 0.007	0.129 ± 0.007	0.130 ± 0.014	0.27	0.93
2004	0.128 ± 0.06	0.127 ± 0.05	0.129 ± 0.014	0.31	0.86
2005*	0.075 ± 0.005	0.077 ± 0.01	0.079 ± 0.007	1.51	0.23
2005**	0.115 ± 0.01	0.122 ± 0.008	0.122 ± 0.018	1.69	0.19
2006	0.149 ± 0.011	0.159 ± 0.007	0.159 ± 0.011	2.64	0.08
2007	0.157 ± 0.007[a]	0.161 ± 0.006[ab]	0.168 ± 0.013[b]	9.67	**<0.01**
2008	0.171 ± 0.007[ab]	0.168 ± 0.005[a]	0.184 ± 0.009[b]	29.3	**<0.001**
2009	0.176 ± 0.008[ab]	0.172 ± 0.005[a]	0.187 ± 0.010[b]	25.0	**<0.001**
2011	0.179 ± 0.004[ab]	0.172 ± 0.004[a]	0.185 ± 0.008[b]	24.8	**<0.001**

Table 5.12 - Summary of multiple sample-comparison between albedo data (±SD) Landsat TM/ETM - derived and grouped according to management type (Cut and Release, Passive Management and Salvage Logging). ANOVA F-ratio in the table tests any significant difference amongst the means of the groups. Multiple range Tests output suggest which means are significantly different according to the Bonferroni's procedure at 99.0% confidence interval. Different letters highlight differences between Management type (n = number of samples per year).

After the interventions (starting in autumn 2007), the mean values of summer albedo differ among the treatments: SL shows mean albedo values (0.184 ÷ 0.187) greater than PM (0.168 ÷ 0.172) and CR (0.171 ÷ 0.179). All differences in albedo values among treatments are significant with p-values < 0.001 and marked F statistics (24.8 ÷ 29.3).

Figure 5.22 - Landscape view of the area some months after the fire.

Discussion

Restoration activities following the Bourra wildfire, enabled us to further investigate some relationships in alpine environment between burnt wood management, natural regeneration recovery and microclimate variations, previously studied in other sites as well (Gray et al., 2005; Beghin et al., 2010; Castro et al., 2011; Marañón-Jiménez et al., 2011).

Relevant differences of soil temperature and ΔTsoil-air values were evaluated among treated areas for the entire period investigated. SL treatment exhibits the highest soil temperature values during the hottest hours of the day, likewise, daily ΔTsoil-air values resulted clearly greater than those related to the other treatments. Furthermore, SL area presents clearly greater TSF values than the others but, at the same time, the lowest values of Soil Moisture (SM). Since we assume that our study site has homogeneous soil properties, slope inclination and aspect, the differences in soil temperature and SM seem to be a consequence of the differences in near-ground solar radiation (Russel, 1988; Breshears and Ludwig, 2010). Although, the differences in TSF (or near-ground solar radiation), ΔTsoil-air and SM among the treatments, prompt to consider different energy partitions between sensible and latent heat fluxes as well. Salvage area (SL) shows the lowest SM, highest ΔTsoil-air and TSF values, identifying a limited evapotranspiration (Oudin et al., 2005; Wang et al., 2007). Furthermore, as highlighted by equation (3), the sensible heat flux is a function of ΔTsoil-air and surface roughness (Senay et al., 2007): PM and CR areas show similar distributions of roughness index (RI) but quite higher values than SL. The energy balance at ground level (increasing sensible heat fluxes and less evapotranspiration), associated with the highest soil temperatures during all monitored months, allows the supposition that low soil-water availability is a common feature presented by SL treatment (Sadler et al., 2000). Generally speaking, salvage treatment causes an increase in sensible heat flux since less incoming energy could be used to evaporate water, as scarcity in soil water becomes the limiting factor.

After the fire, soil moisture (SM) become a limiting factor also for soil respiration and decomposition processes, which are strongly dependent on soil temperature (Davidson et al., 2000; Allison and Treseder, 2008; Zhang et al., 2010). In turn, mineralization rate and soil nutrients availability are conditioned by a combination of SM and soil temperature (Jonasson et al., 1999, 2006; Mlambo et al., 2007). During summer, evapotranspiration processes, inducing soil water movement, take an active role on the nutrient dynamics in the soil (Nye and Tinker, 1977). As a consequence, within the salvage area, lower SM levels with respect to the other treatments drive to a minor nutrients availability for the regeneration and to the concrete risk of soil degradation and erosion (Carroll et al., 2007; Matías et al., 2011). On the contrary, CR and PM areas exhibit greater SM than SL treatment, keeping burnt trees and DWD on site as a source of nutrients (Boulanger and Sirois, 2006; Boulanger et al., 2011), improving soil fertility and promoting microbial activity and soil respiration (Marañón-Jiménez et al., 2011; Ginzburg and Steinberger, 2012).

SL area shows a high thermal excursion and variability during the 24 hours. In addition to this, within the SL area the analysis of the rate of daily ΔTsoil-air variations confirms the wide

fluctuations of daily temperature values, despite a buffered diurnal trend with less variability for the other treatments. The different behaviour of soil temperature between SL and the other treatments, is comparable to the pattern highlighted in other studies between canopy and inter-canopy patches (Breshears et al., 1998). The effect provided by standing and fallen dead trees, branches and DWD shading the soil, allows to keep lower soil temperatures, and good availability of soil water for regeneration (Holmgren et al., 1997; Herr et al., 1999; Castro and Zamora, 2004; Legras et al., 2010). These results confirm the role of standing burnt trees and DWD (treatments PM and CR) as a positive trick to keep the difference between minimum and maximum daily soil temperature lower, and changes in SM lower as well, if compared with SL treatment (Harmon et al., 2004; Bhattacharjee et al., 2008; Haskell et al., 2012).

The treatment affects the summer albedo in the experimental area. Burnt wood, partially shading the soil in CR and PM treatments, adsorbs a part of short-wave radiation reducing the albedo in these areas. Within the SL area, that part of short-wave radiation is reflected, as proved by higher values of albedo. A summary of the interconnection processes involved is reported in flowchart (Figure 5.22-23).

Heating of burnt wood transforms this difference of radiation into long-wave emission contributing to keep the day-night temperature variability buffered (Pomeroy et al., 2009; Burles and Boon, 2011). The role of burnt material released (standing trees, trunks or branches on the soil) could become equally important also in the late winter in the Alps, when months are characterized by short days and a low solar elevation angle; the energy at ground level incoming by total broadband radiation is mostly provided by diffuse long-wave radiation, depending on sky openness, soil and burnt wood temperatures, and atmospheric emissivity (Lawler and Link, 2011). The presence of DWD and standing trees contribute to create warm, moist and protected microenvironment, suitable for regeneration establishment (Lampainen et al., 2004; de Chantal et al., 2009). Further investigations, extending the measurement campaign to the late winter months, could help to verify possible inversion in soil temperature trend (Breshears et al., 1998). During winter months, CR treatment shows a higher variability of DSF probably caused by the interaction between the increased DSF (low solar elevation angle) and the downed wood (DWD) material covering the area. Conversely, PM treatment exhibits an approximately constant variability among the year, implying that the standing dead trees provide the same homogeneous covering-effect all the year, in spite of the large annual variation of solar elevation angle and total solar radiation. A cross-evaluation among the treatments of TSF, DSF and ISF (Figure 5.13a-c) leads to note that during winter shortwave radiation is mostly coming from direct component.

Changes in albedo values, together with the variation of surface roughness, could drive to consistent variation of energy fluxes at ground level. After a wildfire, albedo variations strongly depend on spatial pattern of fire severity, and little changes can significantly affect the energy balance shifting between sensible heat and evapotranspiration fluxes (equation (4)). The processes connected with surface cooling or warming are strictly connected to this energy balance (Huxman et al., 2005).

High severity fire affected the study area quite uniformly, transforming the slope into a stressful environment where facilitative interventions may be crucial for vegetation recovery (Germino et al., 2002). The management applied, alternatively to SL, increases the surface roughness releasing

burnt material on site, providing microsite improvement for regeneration establishment and enhancing the surface aerodynamical resistance. Therefore, the burnt wood on the soil interferes with the surface boundary layer dynamics, thus influencing the turbulent flow (Monteith and Unsworth, 2008). The CR and PM areas are characterized from the greatest roughness index (RI) values, enabling a more efficient air mix, balancing both energy fluxes - evapotranspiration and sensible heat. At the same time, within the SL area the reduced land surface roughness implies higher wind speeds of the boundary surface layer. At the end, post-fire management forces environmental transformations in albedo, surface roughness, and ratio between evapotranspiration and sensible heat: these changes proved to be determinant to modify the surface fluxes, affecting the microclimate (Foley et al., 2003).

The design of post-fire restoration, targeting the recovery of pine regeneration in the area, should focus on the combination of temperature, moisture and also fire-severity effects on the soil. Germination of *Pinus* seed occurs at a fixed soil temperature and moisture regime, conditions often favoured by mineral soils (Winsa and Sahlén, 2001; Hille and den Ouden, 2004). At this purpose, the water availability during and after the disseminating period, could be a matter for future insights. *Pinus sylvestris* seed dispersal occurs in late winter or spring (Gracia, 2002), when the major contribution to the Soil Moisture (SM) derives from snowmelt processes. Evaluating the influence of post-fire management on water budgets in winter-snowmelt periods versus summer-drought periods (especially on Southern facing slopes), would be a future stretch of this investigation. During the winter months, SL area shows marked differences of incoming solar radiation with respect to CR and PM. Presence of standing and lying dead wood and the increasing weight of direct fraction in total solar radiation, influence the amount of energy reaching the snowpack. These differences of incoming energy between SL and the other treatments could cause a different spring runoff from burned slopes, a risk to be taken in consideration for the management planning (Winkler, 2011). Recent studies highlight significantly shortened snowmelt periods in the areas affected by wildfire, caused by the dramatic increase on solar radiation reaching the snow surface, respect to the pre-fire state (Burles and Boon, 2011; Winkler, 2011). SL area exhibits marked differences of incoming solar radiation, albedo and surface roughness with respect to the other areas. Overall these changes modify the ground energy balance, playing an important role in concerning to the snowmelt dynamics (Liston, 1995). A cross-evaluation among treatments of the sky openness (SKY%) and direct beam radiation (DSF) ranging in the months from February to April, allows a course assessment of post-fire management effects on snowmelt dynamics (Musselman et al., 2012). As expected, this comparison among treatments proves that SL area significantly differs from the others, probably reducing snow ablation timing (Lawler and Link, 2011) and influencing soil water availability for a spring establishment of regeneration.

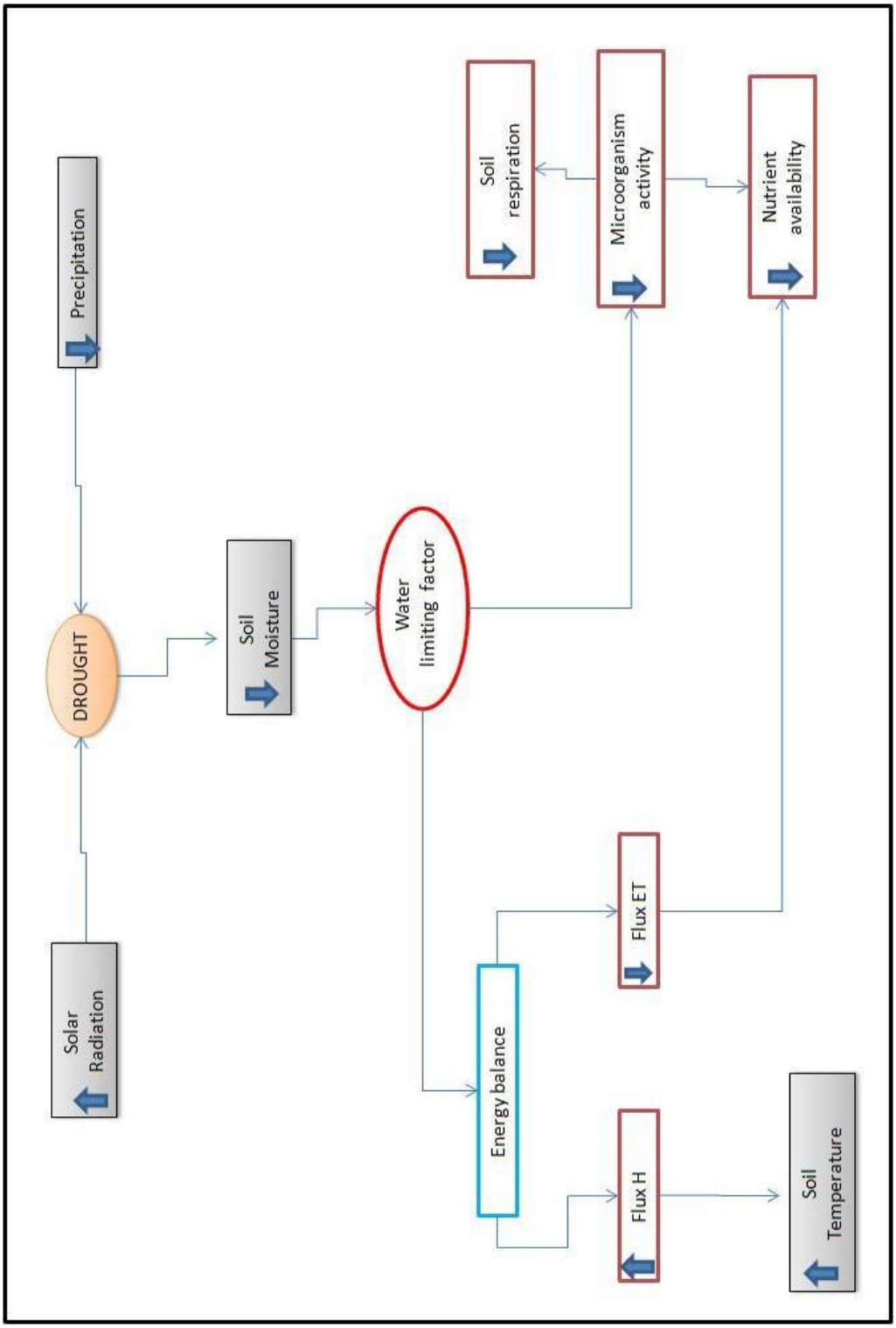

Figure 5.22 - Flowchart of interactions between components affected by reduced Soil Water availability. Increasing or decreasing trends are showed by up/down arrows.

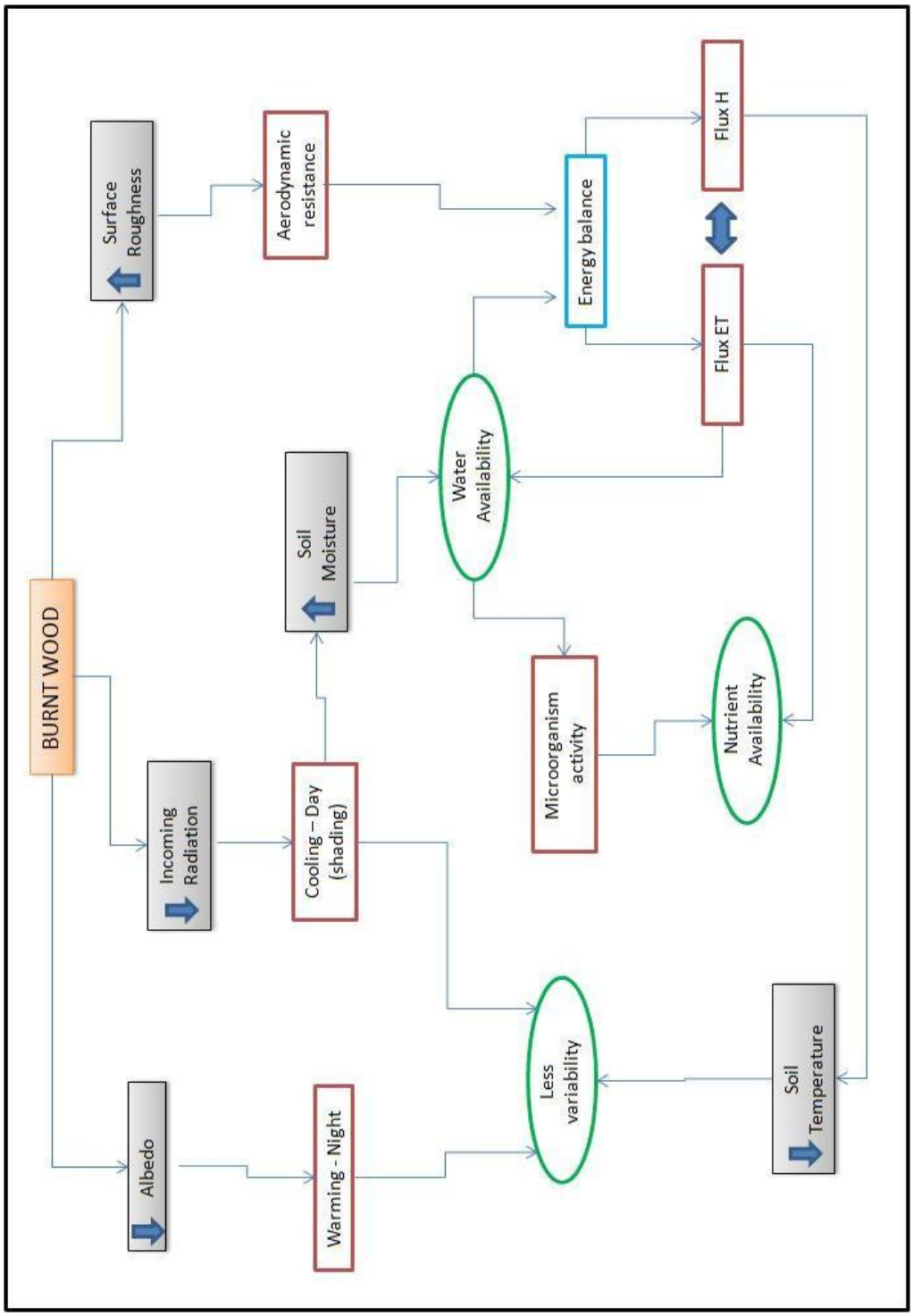

Figure 5.23 - Flowchart of interactions prompted by burnt wood presence resulting in improved Soil Water availability. Increasing or decreasing trends are showed by up/down arrows.

References

Allen, R.G., Pereira, L.S., Raes, D., Smith, M., Ab, W., 1998. Crop evapotranspiration - Guidelines for computing crop water requirements.

Allison, S.D., Treseder, K.K., 2008. Warming and drying suppress microbial activity and carbon cycling in boreal forest soils. Global Change Biology 14, 2898–2909.

Amiro, B., Barr, a, Black, T., Iwashita, H., Kljun, N., Mccaughey, J., Morgenstern, K., Murayama, S., Nesic, Z., Orchansky, a, 2006. Carbon, energy and water fluxes at mature and disturbed forest sites, Saskatchewan, Canada. Agricultural and Forest Meteorology 136, 237–251.

Beghin, R., Lingua, E., Garbarino, M., Lonati, M., Bovio, G., Motta, R., Marzano, R., 2010. *Pinus sylvestris* forest regeneration under different post-fire restoration practices in the northwestern Italian Alps. Ecological Engineering 36, 1365–1372.

Bergner, B., Johnstone, J., Treseder, K.K., 2004. Experimental warming and burn severity alter soil CO2 flux and soil functional groups in a recently burned boreal forest. Global Change Biology 10, 1996–2004.

Bernstein, L.S., Sundberg, R.L., Levine, R.Y., Perkins, T.C., Berk, A., 2005. A New Method for Atmospheric Correction and Aerosol Optical Property Retrieval for VIS-SWIR Multi- and Hyperspectral Imaging Sensors: QUAC (QUick Atmospheric Correction).

Beschta, R.L., Rhodes, J.J., Kauffman, J.B., Gresswell, R.E., Minshall, G.W., Karr, J.R., Perry, D. a., Hauer, F.R., Frissell, C. a., 2004. Postfire Management on Forested Public Lands of the Western United States. Conservation Biology 18, 957–967.

Bhattacharjee, J., Taylor, J.P., Smith, L.M., Spence, L.E., 2008. The Importance of Soil Characteristics in Determining Survival of First-Year Cottonwood Seedlings in Altered Riparian Habitats. Restoration Ecology 16, 563–571.

Bodí, M.B., Mataix-Solera, J., Doerr, S.H., Cerdà, A., 2011. The wettability of ash from burned vegetation and its relationship to Mediterranean plant species type, burn severity and total organic carbon content. Geoderma 160, 599–607.

Boulanger, Y., Sirois, L., 2006. Postfire dynamics of black spruce coarse woody debris in northern boreal forest of Quebec. Canadian Journal of Forest Research 36, 1770–1780.

Boulanger, Y., Sirois, L., Hébert, C., 2011. Fire severity as a determinant factor of the decomposition rate of fire-killed black spruce in the northern boreal forest. Canadian Journal of Forest Research 41, 370–379.

Breshears, D., Nyhan, J., Heil, C., Wilcox, B., 1998. Effects of woody plants on microclimate in a semiarid woodland: soil temperature and evaporation in canopy and intercanopy patches. International Journal of Plant Sciences 159, 1010–1017.

Breshears, D.D., Ludwig, J.A., 2010. Near-ground solar radiation along the grassland–forest continuum: Tall-tree canopy architecture imposes only muted trends and heterogeneity. Austral Ecology 35, 31–40.

Burles, K., Boon, S., 2011. Snowmelt energy balance in a burned forest plot, Crowsnest Pass, Alberta, Canada. Hydrological Processes 25, 3012–3029.

Campbell, G.S., Norman, J.M., 1998. Introduction to Environmental Biophysics. Springer.

Caplat, P., Lepart, J., Marty, P., 2006. Landscape patterns and agriculture: modelling the long-term effects of human practices on *Pinus sylvestris* spatial dynamics (Causse Mejean, France). Landscape Ecology 21, 657–670.

Carroll, E.M., Miller, W.W., Johnson, D.W., Saito, L., Qualls, R.G., Walker, R.F., 2007. Spatial analysis of a large magnitude erosion event following a Sierran wildfire. Journal of environmental quality 36, 1105–11.

Castro, J., Allen, C.D., Molina-Morales, M., Marañón-Jiménez, S., Sánchez-Miranda, Á., Zamora, R., 2011. Salvage Logging Versus the Use of Burnt Wood as a Nurse Object to Promote Post-Fire Tree Seedling Establishment. Restoration Ecology 19, 537–544.

Castro, J., Zamora, R., 2004. Seedling establishment of a boreal tree species (Pinus sylvestris) at its southernmost distribution limit: consequences of being in a marginal Mediterranean habitat. Journal of Ecology 92, 266–277.

Cavalli, M.A., Tarolli, P.A., 2010. Application of LiDAR technology for rivers analysis. Italian Journal of Engineering Geology and Environment 1, 5–16.

Chander, G., Markham, B.L., Helder, D.L., 2009. Summary of current radiometric calibration coefficients for Landsat MSS, TM, ETM+, and EO-1 ALI sensors. Remote Sensing of Environment 113, 893–903.

Churkina, G., Running, S.W., Schloss, A.L., Intercomparison, T.P.O.T.P., 1999. Comparing global models of terrestrial net primary productivity (NPP): the importance of water availability. Global Change Biology 5, 46–55.

Davidson, E.A., Verchot, L. V, Henrique, J., 2000. Effects of soil water content on soil respiration in forests and cattle pastures of eastern Amazonia 53–69.

DeBano, L., Neary, D., Ffolliott, P., 1998. Fire Effects on Ecosystems. Wiley.

DeBano, L.., 2000. The role of fire and soil heating on water repellency in wildland environments: a review. Journal of Hydrology 231-232, 195–206.

De Chantal, M., Lilja-Rothsten, S., Peterson, C., Kuuluvainen, T., Vanha-Majamaa, I., Puttonen, P., 2009. Tree regeneration before and after restoration treatments in managed boreal Picea abies stands. Applied Vegetation Science 12, 131–143.

Donato, D.C., Fontaine, J.B., Campbell, J.L., Robinson, W.D., Kauffman, J.B., Law, B.E., 2006. Post-wildfire logging hinders regeneration and increases fire risk. Science (New York, N.Y.) 311, 352.

Drexler, J.Z., Snyder, R.L., Spano, D., Paw U, K.T., 2004. A review of models and micrometeorological methods used to estimate wetland evapotranspiration. Hydrological Processes 18, 2071–2101.

Field, C.B., Lobell, D.B., Peters, H. a., Chiariello, N.R., 2007. Feedbacks of Terrestrial Ecosystems to Climate Change *. Annual Review of Environment and Resources 32, 1–29.

Foley, J.A., Costa, M.H., Delire, C., Ramankutty, N., Snyder, P., 2003. Green Surprise? How Terrestrial Ecosystems Could Affect Earth's Climate. Frontiers in Ecology and the Environment 1, 38.

Frazer, G.W., 1999. Gap Light Analyzer (GLA): Imaging software to extract canopy structure and gap light transmission indices from true-colour fisheye photographs.

Gabet, E.J., Bookter, A., 2011. Physical, chemical and hydrological properties of Ponderosa pine ash. International Journal of Wildland Fire 20, 443–452.

Gash, J.H.C., Nobre, C.A., 1997. Climatic effects of Amazonian deforestation: Some results from ABRACOS. Bulletin of the American Meteorological Society 78, 823–830.

Germino, M.J., Smith, W.K., Resor, A.C., 2002. Conifer seedling distribution and survival in an alpine-treeline ecotone. Plant Ecology 162, 157–168.

Ginzburg, O., Steinberger, Y., 2012. Salvage logging versus natural regeneration post-fire practices in a forest: Soil chemical and microbial aspects. Open Journal of Ecology 02, 29–37.

Gracia, M., 2002. Mid-term successional patterns after fire of mixed pine–oak forests in NE Spain. Acta Oecologica 23, 405–411.

Gray, A.N., Spies, T.A., 1997. Microsite controls on tree seedling establishment in conifer forest canopy gaps. Ecology 78, 2458–2473.

Gray, A.N., Zald, H.S.J., Kern, R.A., North, M., 2005. Stand conditions associated with tree regeneration in Sierran mixed-conifer forests. Forest science 51, 198–210.

Greene, D.F., Macdonald, S.E., Cumming, S., Swift, L., 2005. Seedbed variation from the interior through the edge of a large wildfire in Alberta. Canadian Journal of Forest Research 35, 1640–1647.

Greene, D.F., Macdonald, S.E., Haeussler, S., Domenicano, S., Noël, J., Jayen, K., Charron, I., Gauthier, S., Hunt, S., Gielau, E.T., Bergeron, Y., Swift, L., 2007. The reduction of organic-layer depth by wildfire in the North American boreal forest and its effect on tree recruitment by seed. Canadian Journal of Forest Research 37, 1012–1023.

Gutiérrez-Jurado, H., Vivoni, E.R., Harrison, J.B.J., Guan, H., 2006. Ecohydrology of root zone water fluxes and soil development in complex semiarid rangelands. Hydrological Processes 3316, 3289–3316.

Hamman, S.T., Burke, I.C., Knapp, E.E., 2008. Soil nutrients and microbial activity after early and late season prescribed burns in a Sierra Nevada mixed conifer forest. Forest Ecology and Management 256, 367–374.

Hardy, J.P., Melloh, R., Koenig, G., Marks, D., Winstral, a., Pomeroy, J.W., Link, T., 2004. Solar radiation transmission through conifer canopies. Agricultural and Forest Meteorology 126, 257–270.

Harmon, M.E., Franlklin, J.F., Swanson, F.J., Sollins, P., Gregory, S.V., Lattin, J.D., Anderson, N.H., Cline, S.P., Aumen, N.G., Sedell, J.R., Lienkaemper, G.W., Cromack Jr., K., Cummins, K.W., 2004. Ecology of course woody debris in temperate ecosystems. Advances in Ecological Research 34, 59–234.

Haskell, D.E., Flaspohler, D.J., Webster, C.R., Meyer, M.W., 2012. Variation in Soil Temperature, Moisture, and Plant Growth with the Addition of Downed Woody Material on Lakeshore Restoration Sites. Restoration Ecology 20, 113–121.

Hay, J.E., 1976. A revised method for determining the direct and diffuse components of the total short-wave radiation. Atmosphere 14, 278–287.

Herr, D.G., Duchesne, L.C., Reader, R.J., 1999. Effects of soil organic matter, moisture, shading and ash on white pine (*Pinus strobus* L.) seedling emergence. New Forests 18, 219–230.

Hille, M., Den Ouden, J., 2004. Improved recruitment and early growth of Scots pine (*Pinus sylvestris* L.) seedlings after fire and soil scarification. European Journal of Forest Research 123, 213–218.

Holmgren, M., Scheffer, M., Huston, M.A., 1997. The interplay of facilitation and competition in plant communities. Ecology 78, 1966–1975.

Huang, C., Wylie, B., Yang, L., Homer, C., Zylstra, G., 2002. Derivation of a tasselled cap transformation based on Landsat 7 at-satellite reflectance. International Journal of Remote Sensing 23, 1741–1748.

Huxman, T., Wilcox, B., Breshears, D., 2005. Ecohydrological implications of woody plant encroachment. Ecology 86, 308–319.

Jarčuška, B., 2008. Methodological overview to hemispherical photography, demonstrated on an example of the software GLA. Folia Oecologica 35, 1–4.

Jonasson, S., Castro, J., Michelsen, A., 2006. Interactions between plants, litter and microbes in cycling of nitrogen and phosphorus in the arctic. Soil Biology and Biochemistry 38, 526–532.

Jonasson, S., Michelsen, A., Schmidt, I.K., Nielsen, E. V., 1999. Responses in microbes and plants to changed temperature, nutrient, and light regimes in the arctic. Ecology 80, 1828–1843.

Kempes, C., Myers, O., Breshears, D., 2008. Comparing response of *Pinus edulis* tree-ring growth to five alternate moisture indices using historic meteorological data. Journal of Arid 72, 350–357.

Klopatek, J.M., Conant, R.T., Francis, J.M., Malin, R.A., Murphy, K.L., Klopatek, C.C., 1998. Implications of patterns of carbon pools and fluxes across a semiarid environmental gradient. Landscape and Urban Planning 39, 309–317.

Kloss, S., Sass, O., Geitner, C., Prietzel, J., 2012. Soil properties and charcoal dynamics of burnt soils in the Tyrolean Limestone Alps. CATENA 99, 75–82.

Kottek, M., Grieser, J., Beck, C., Rudolf, B., Rubel, F., 2006. World Map of the Köppen-Geiger climate classification updated. Meteorologische Zeitschrift 15, 259–263.

Kustas, W., Choudhury, B., Moran, M., Reginato, R., Jackson, R., Gay, L., Weaver, H., 1989. Determination of sensible heat flux over sparse canopy using thermal infrared data. Agricultural and Forest Meteorology 44, 197–216.

Kuuluvainen, T., Juntunen, P., 1998. Seedling establishment in relation to microhabitat variation in a windthrow gap in a boreal *Pinus sylvestris* forest. Journal of Vegetation Science 9, 551–562.

Lampainen, J., Kuuluvainen, T., Wallenius, T.H., Karjalainen, L., Vanha-Majamaa, I., 2004. Long-term forest structure and regeneration after wildfire in Russian Karelia. Journal of Vegetation Science 15, 245-256.

Lauenroth, W.K., Sala, O.E., Coffin, D.P., Kirchner, T., 1994. The Importance of Soil Water in the Recruitment of Bouteloua Gracilis in the Shortgrass Steppe. Ecological Applications 4, 741–749.

Lawler, R.R., Link, T.E., 2011. Quantification of incoming all-wave radiation in discontinuous forest canopies with application to snowmelt prediction. Hydrological Processes 25, 3322–3331.

Legras, E.C., Vander Wall, S.B., Board, D.I., 2010. The role of germination microsite in the establishment of sugar pine and Jeffrey pine seedlings. Forest Ecology and Management 260, 806–813.

Leverkus, A.B., Puerta-Piñero, C., Guzmán-Álvarez, J.R., Navarro, J., Castro, J., 2012. Post-fire salvage logging increases restoration costs in a Mediterranean mountain ecosystem. New Forests 43, 601–613.

Li, J., Islam, S., 1999. On the estimation of soil moisture profile and surface fluxes partitioning from sequential assimilation of surface layer soil moisture. Journal of Hydrology 220, 86–103.

Liang, S., 2000. Narrowband to broadband conversions of land surface albedo I Algorithms. Remote Sensing of Environment 76, 213-238.

Liston, G., 1995. Local advection of momentum, heat, and moisture during the melt of patchy snow covers. Journal of Applied Meteorology 34, 1705–1715.

Marañón-Jiménez, S., Castro, J., Kowalski, a. S., Serrano-Ortiz, P., Reverter, B.R., Sánchez-Cañete, E.P., Zamora, R., 2011. Post-fire soil respiration in relation to burnt wood management in a Mediterranean mountain ecosystem. Forest Ecology and Management 261, 1436–1447.

Matías, L., Castro, J., Zamora, R., 2011. Soil-nutrient availability under a global-change scenario in a Mediterranean mountain ecosystem. Global Change Biology 17, 1646–1657.

McIver, J.D., Starr, L., 2001. A Literature Review on the Environmental Effects of Postfire Logging. Western Journal of Applied Forestry 16, 159–168.

Mercalli, L., Cat Berro, D., 2003. Atlante climatico della Valle d'Aosta. SMS.

Meyers, T., Hollinger, S., 2004. An assessment of storage terms in the surface energy balance of maize and soybean. Agricultural and Forest Meteorology 125, 105–115.

Mlambo, D., Mwenje, E., Nyathi, P., 2007. Effects of tree cover and season on soil nitrogen dynamics and microbial biomass in an African savanna woodland dominated by *Colophospermum mopane*. Journal of Tropical Ecology 23, 437–448.

Monin, A.S., Obukhov, A.M., 1959. Basic laws of turbulent mixing in the surface layer of the atmosphere. Tr. Akad. Nauk SSSR Geophiz. Inst. 24, 163–187.

Monteith, J.L., Unsworth, M.H., 2008. Principles of Environmental Physics. Academic Press.

Muneer, T., 2004. Solar Radiation and Daylight Models. Elsevier.

Musselman, K.N., Molotch, N.P., Margulis, S.A., Kirchner, P.B., Bales, R.C., 2012. Influence of canopy structure and direct beam solar irradiance on snowmelt rates in a mixed conifer forest. Agricultural and Forest Meteorology 161, 46–56.

Noss, F., Lindenmayer, D.B., 2006. Special Section: The Ecological Effects of Salvage Logging after Natural Disturbance. Conservation Biology 20, 946–948.

Noss, R.F., Franklin, J.F., Baker, W.L., Schoennagel, T., Moyle, P.B., 2006. Managing fire-prone forests in the western United States. Frontiers in Ecology and the Environment 4, 481–487.

Nye, P.H., Tinker, P.B., 1977. Solute Movement in the Soil-Root System. University of California Press.

Oudin, L., Hervieu, F., Michel, C., Perrin, C., Andréassian, V., Anctil, F., Loumagne, C., 2005. Which potential evapotranspiration input for a lumped rainfall–runoff model? Journal of Hydrology 303, 290–306.

Peel, M., Finlayson, B., McMahon, T., 2007. Updated world map of the Köppen-Geiger climate classification. Hydrology and Earth System Sciences 11, 1633–1644.

Pezzatti, G.B., Bajocco, S., Torriani, D., Conedera, M., 2009. Selective burning of forest vegetation in Canton Ticino (southern Switzerland). Plant Biosystems 143, 609–620.

Pomeroy, J.W., Marks, D., Link, T., Ellis, C., Hardy, J., Rowlands, A., Granger, R., 2009. The impact of coniferous forest temperature on incoming longwave radiation to melting snow. Hydrological Processes 23, 2513–2525.

Priestley, C., Taylor, R., 1972. On the assessment of surface heat flux and evaporation using large-scale parameters. Monthly weather review 81–92.

Promis, A., Butler-Manning, D., 2011. Comparison of four different programs for the analysis of hemispherical photographs using parameters of canopy structure and solar radiation transmittance. Waldokologie, landschaftsforschung und naturschulz 11, 19–33.

Purdy, B.G., Macdonald, S.E., Dale, M.R.T., 2002. The regeneration niche of white spruce following fire in the mixedwood boreal forest. Silva Fennica 36, 289–306.

Rich, P.M., 1989. A Manual for Analysis of Hemispherical Canopy Photography. Los Alamos National Laboratory Report LA-11733-M., Science.

Rich, P.M., 1990. Characterizing plant canopies with hemispherical photographs. Remote Sensing Reviews 114, 95–29.

Royer, P.D., Breshears, D.D., Zou, C.B., Cobb, N.S., Kurc, S. a., 2010. Ecohydrological energy inputs in semiarid coniferous gradients: Responses to management- and drought-induced tree reductions. Forest Ecology and Management 260, 1646–1655.

Russel, E., 1988. Russell's Soil Conditions and Plant Growth. Longman Sc & Tech.

Sadler, E.J., Bauer, P.J., Busscher, W.J., Millen, J.A., 2000. Site-Specific Analysis of a Droughted Corn Crop : II. Water Use and Stress 92, 403–410.

Santos, a. J.B., Silva, G.T.D. a., Miranda, H.S., Miranda, a. C., Lloyd, J., 2003. Effects of fire on surface carbon, energy and water vapour fluxes over campo sujo savanna in central Brazil. Functional Ecology 17, 711–719.

Scharmer, K., Greif, J., 2000. The European Solar Radiation Atlas: Fundamentals and maps. Presses des MINES.

Senay, G.B., Budde, M., Verdin, J.P., Melesse, A.M., 2007. A Coupled Remote Sensing and Simplified Surface Energy Balance Approach to Estimate Actual Evapotranspiration from Irrigated Fields. Sensors 7, 979–1000.

Serrano-Ortiz, P., Marañón-Jiménez, S., Reverter, B.R., Sánchez-Cañete, E.P., Castro, J., Zamora, R., Kowalski, a. S., 2011. Post-fire salvage logging reduces carbon sequestration in Mediterranean coniferous forest. Forest Ecology and Management 262, 2287–2296.

Shuttleworth, W., 2007. Putting the'vap' into evaporation. Hydrology and Earth System Sciences 11, 210–244.

Shuttleworth, W., Gurney, R., Hsu, A., Ormsby, J., 1989. FIFE: the variation in energy partition at surface flux sites. IAHS Publication 186, 67–74.

Tsouni, A., Kontoes, C., Koutsoyiannis, D., Elias, P., Mamassis, N., 2008. Estimation of Actual Evapotranspiration by Remote Sensing: Application in Thessaly Plain, Greece. Sensors 8, 3586–3600.

Ulery, A.L., Graham, R.C., 1993. Forest Fire Effects on Soil Color and Texture. Soil Science Society of America Journal 57, 135.

Valese, E., Conedera, M., Vacik, H., Japelj, A., Beck, A., Cocca, G., Cvenkel, H., Di Narda, N., Ghiringhelli, A., Lemessi, A., Mangiavillano, A., Pelfini, F., 2011. Wildfires in the Alpine region : first results from the ALP FFIRS project, in: 5th International Wildland Fire Conference - South Africa. pp. 1–15.

Verhoef, W., Bach, H., 2003. Remote sensing data assimilation using coupled radiative transfer models. Physics and Chemistry of the Earth, Parts A/B/C 28, 3–13.

Verstraeten, W., Veroustraete, F., Feyen, J., 2008. Assessment of evapotranspiration and soil moisture content across different scales of observation. Sensors 8, 70–117.

Walter, H., Breckle, S.-W., 2002. Walter's Vegetation of the Earth: The Ecological Systems of the Geo-Biosphere. Springer.

Wang, K., Liang, S., 2008. Estimation of Surface Net Radiation from Solar Shortwave Radiation Measurements, in: IGARSS 2008 - 2008 IEEE International Geoscience and Remote Sensing Symposium. IEEE, pp. 483–486.

Wang, K., Wang, P., Li, Z., Cribb, M., Sparrow, M., 2007. A simple method to estimate actual evapotranspiration from a combination of net radiation, vegetation index, and temperature. Journal of Geophysical Research 112, 1–14.

Wastl, C., Schunk, C., Lüpke, M., Cocca, G., Conedera, M., Valese, E., Menzel, A., 2013. Large-scale weather types, forest fire danger, and wildfire occurrence in the Alps. Agricultural and Forest Meteorology 168, 15–25.

Whelan, R., 1995. The Ecology of Fire. Cambrige University Press.

Winkler, R., 2011. Changes in snow accumulation and ablation after a fire in south-central British Columbia. Streamline Watershed Management Bulletin 14, 1–6.

Winsa, H., Sahlén, K., 2001. Effects of Seed Invigoration and Microsite Preparation on Seedling Emergence and Establishment After Direct Sowing of *Pinus sylvestris* L. at Different Dates. Scandinavian Journal of Forest Research 16, 422–428.

Wirth, C., Gleixner, G., Heimann, M., 2009. Old-Growth Forests: Function, Fate and Value, Ecological. ed, Biological Invasions. Springer.

Yao, Y., Qin, Q., Ghulam, A., Liu, S., Zhao, S., Xu, Z., Dong, H., 2011. Simple method to determine the Priestley–Taylor parameter for evapotranspiration estimation using Albedo-VI triangular space from MODIS data. Journal of Applied Remote Sensing 5, 053505.

Zar, J., 2009. Biostatistical analysis, 5th ed. Pearson International.

Zhang, L.H., Chen, Y.N., Zhao, R.F., Li, W.H., 2010. Significance of temperature and soil water content on soil respiration in three desert ecosystems in Northwest China. Journal of Arid Environments 74, 1200–1211.

General Conclusions

This research purposes a series of studies aiming at detecting patterns of vegetation recovery, environmental constraints and assessing the impact of post-fire management on seedling establishment. The studies were carried out in two different forests in the Alps where the analysis of vegetation recovery and the consequences of restoration activities were evaluated at short and medium-term.

Recovery processes resulted strongly influenced by fire severity. Regeneration establishment of *P. nigra* and *P. sylvestris* (dominant species in pre-fire conditions) resulted clearly greater in areas where fire severity was lower, with surviving seed-trees. Distance from seed source arises as a relevant constraint in the recovery process of *P. nigra* and *P. sylvestris.*

Together with seed availability, a necessary condition for seedling establishment and survival is the preservation of sufficient levels of soil water throughout the growing season (Hille and den Ouden, 2004). Under stressful environmental conditions, in terms of solar radiation and availability of soil water, a strong relationship between regeneration and standing or lying deadwood was highlighted. Pine regeneration seems to have taken benefit of the shelter effect provided by deadwood elements. The presence of burnt wood was decisive in influencing soil temperature and moisture, reducing the extreme values and buffering micro-climatic fluctuations. The facilitative effect produced by deadwood on regeneration recovery was identified at different scales. Analysis ranging from a broad scale to the microsite, highlighted that the presence of deadwood elements provides amelioration of recruitment conditions promoting the early establishment of regeneration.

Restoration activities showed a strong effect in altering microclimate conditions. Extreme values of micro-environmental parameters have been detected in salvage logged area, while milder conditions were encountered in treatments characterized by retention of burnt wood material. These latter proved to be more effective in reducing diurnal variations, keeping low values of radiation and maximum soil temperatures, and preserving soil water during summer months. Management type influenced also species composition in the regeneration layer. Obligate seeders were more abundant in absence of any intervention, while facoltative sprouters were detected mostly in salvage logged areas. Under mixed levels of fire severity, where high severity zones were unevenly surrounded by medium-low ones, the effects of restoration activities in a medium-term context appear negligible in relation to the regeneration improvements. At this purpose, slopes with high insolation in a dry environment appear exacerbated by salvage logging which reduces the establishment and survival of seedlings. Conversely, facultative sprouters, confirmed the higher performances of these species in dry post-fire conditions due to their main regeneration strategy.

Under these specific environmental constraints, salvage logging management may counteract seedling establishment, by loading the process of recovery mainly in the regeneration ability of sprouting species.

A contest of increasing frequency of climate extremes seems to drive significant changes in fire regimes worldwide (Running, 2006; Westerling et al., 2006; Pausas and Fernández-Muñoz, 2011) growing the chances of high-severity events. This study confirms the difficulty of these ecosystems in recovering the pre-fire conditions following large fire events. As a consequence, the overall distribution of these pine species may decrease (Retana et al., 2002; Vilà-Cabrera et al., 2012).
In this scenario, post-fire interventions properly applied, may affect the temporal and spatial restoration of tree cover playing a crucial role in preserving biodiversity. Aiming at promoting the seedling establishment, post-fire restoration of *P.nigra* and *P.sylvestris* forests, should consider the fundamental presence of living trees as seed dispersers. Areas affected by low severity of the fire allow the survival of seed-trees and improve the establishment of seedlings, reducing understory competition. The harsh conditions of the slopes, where soil water availability is often a limiting factor for the regeneration, should discourage a widespread logging. Planning for interventions favoring the release of burnt wood, or patches of standing dead trees, reduces the environmental stress promoting regeneration establishment, saves biological legacies improving species richness.

References

Hille, M., Den Ouden, J., 2004. Improved recruitment and early growth of Scots pine (*Pinus sylvestris* L.) seedlings after fire and soil scarification. European Journal of Forest Research 123, 213–218.

Nuñez, M.R., Bravo, F., Calvo, L., 2003. Predicting the probability of seed germination in *Pinus sylvestris* L. and four competitor shrub species after fire. Annals of forest science 60, 75–81.

Pausas, J.G., Fernández-Muñoz, S., 2011. Fire regime changes in the Western Mediterranean Basin: from fuel-limited to drought-driven fire regime. Climatic Change 110, 215–226.

Retana, J., Espelta, J.M., Habrouk, A., Ordonez, J.L., De Sola-Morales, F., 2002. Regeneration patterns of three Mediterranean pines and forest changes after a large wildfire in northeastern Spain. Ecoscience 9, 89–97.

Running, S.W., 2006. Climate change. Is global warming causing more, larger wildfires? Science (New York, N.Y.) 313, 927–8.

Tapias, R., Gil, L., Fuentes-Utrilla, P., Pardos, J.A., 2001. Canopy seed banks in Mediterranean pines of south- • eastern Spain: a comparison between *Pinus halepensis* Mill., P. pinaster Ait., P. nigra Arn. and P. pinea L. Journal of Ecology 89, 629–638.

Vilà-Cabrera, A., Rodrigo, A., Martínez-Vilalta, J., Retana, J., 2012. Lack of regeneration and climatic vulnerability to fire of Scots pine may induce vegetation shifts at the southern edge of its distribution. Journal of Biogeography 39, 488–496.

Westerling, a L., Hidalgo, H.G., Cayan, D.R., Swetnam, T.W., 2006. Warming and earlier spring increase western U.S. forest wildfire activity. Science (New York, N.Y.) 313, 940–3.

Abstract

Forest fires in the Alps are increasing both in frequency and size, especially on southern slopes where environmental conditions are more suitable for fire ignition and spread. Post-fire restoration activities are often applied without considering the large heterogeneity and variability of ecological constraints. Fire severity, species composition and site characteristics heavily affect vegetation recovery dynamics.

The main objectives of this study were to test the hypothesis that post-fire burned wood management may greatly affect forest recovery and to identify the main environmental variables affecting seedling establishment and survival.

We investigated restoration dynamics following high severity crown fire in two forests located in Western (Bourra site - Aosta Valley) and Eastern (Barcis site - Friuli Venezia Giulia) Italian Alps. Fires burnt large area of pine forests (*P. sylvestris, P. nigra*) located on southern slopes, characterized by harsh conditions (dry environment with high solar radiation exposure). In both sites active restoration strategies were adopted in the following years. These practices consisted in Salvage logging (cut and deadwood removal) followed by plantation or not, and Cut and release (living deadwood on site). Passive management area (remnants of burnt stand trees, where no intervention occurred) was also considered and compared.

The recovery processes of vegetation were explored through methods of integrated analysis, using different spatial- and temporal-scale approaches. Field-data measures on regeneration, shelter elements and environmental variables were analyzed at microsite scale. Maps of fire severity were created by means of change-detection techniques on Landsat TM/ETM+ images. A scan through the time of forest recovery was performed associating regeneration and environmental data with Vegetation Indices (VIs) derived from a chronosequence of multispectral images. The evaluation of post-fire recovery dynamics, their relationships with fire severity and restoration activities are analyzed at a landscape scale, combining field-data, VIs, topographic and vegetation parameters extracted from LiDAR data. The influence of post-fire management on microclimate was investigated by means of instrumental measurements of environmental parameters affecting the regeneration dynamics. Measurements of soil temperature and moisture together with estimates of near-ground solar radiation were carried during a whole growing season within areas subjected to different restoration practices.

Differences in species composition were found in the study sites among treatments. Regeneration density and diversity were positively associated with deadwood presence. Early establishment of pine seedlings was associated with the presence of standing or lying deadwood. Conversely, *Populus tremula*, regenerating mostly vegetatively, showed a different behaviour from the other tree species.

Ground cover conditions contributed to patterns of seedling occurrence.

The strong spatial association of seedlings with deadwood suggests that this latter produces microsites that enhance the establishment of regeneration. The relationship between nurse deadwood elements and regeneration was found to be highly anisotropic, as a consequence of the

higher protection from radiation and lower soil moisture loss in the shady sides of the shelter element. Marked differences in incoming solar radiation, soil moisture and temperature were detected among treatments, in particular, salvaged areas resulted strongly associated with severe environmental conditions. Higher fire severity diminishes seed availability reducing the seeders, thus the distance from seed source has emerged as an important constraint for pine regeneration establishment.

In relation to different spatio-temporal scales of analysis, this research reports a significant impact of the post-fire management actions on forest recovery. Restoration practices may significantly affect environmental parameters, particularly in stressful conditions,. The presence of burnt wood provides an amelioration of microsite reducing the extreme values, buffering microclimatic fluctuations thus favoring the establishment of regeneration. Standing and lying deadwood, also resulting from active management, should be leaved *in situ* during restoration activities.

Riassunto

Gli incendi boschivi nelle Alpi presentano negli ultimi decenni un trend di crescita sia in frequenza che per superficie, in particolare sui versanti meridionali dove l'eventuale innesco e la rapida diffusione dell'incendio sono favorite dalle condizioni ambientali. Le attività di ripristino post-incendio vengono condotte spesso senza considerare le peculiarità dell'ambiente montano e la grande eterogeneità e variabilità dei principali parametri ecologico-ambientali. La severità dell'incendio, le caratteristiche del sito e la composizione specifica delle foreste coinvolte influiscono significativamente sulle dinamiche di ricostituzione della vegetazione.

Gli obiettivi principali di questo studio consistono nel verificare l'ipotesi che la gestione post-incendio della necromassa legnosa possa significativamente influire sulle dinamiche di ricostituzione della foresta, e di individuare le principali variabili ambientali che condizionano l'insediamento e la sopravvivenza della rinnovazione.

Per verificare tali ipotesi, le dinamiche di ricostituzione a seguito di incendi ad alta severità sono state analizzate in due foreste situate una nelle Alpi occidentali (sito di Bourra - Valle d'Aosta) e una in quelle orientali (sito di Barcis - Friuli Venezia Giulia). L'incendio ha interessato, in entrambi i siti, una estesa superficie di pineta (*P. sylvestris, P. nigra*), soprattutto su versanti aridi esposti a Sud (con elevata esposizione alle radiazioni solari e scarsa disponibilità idrica). In entrambi i casi, negli anni successivi all'incendio, sono stati effettuati interventi (trattamenti) di ricostituzione attiva: "Salvage logging" (taglio ed esbosco del materiale legnoso, talvolta seguito da rimboschimenti localizzati) e "Cut and release" (taglio e rilascio a terra del materiale legnoso). A tali tipologie si sono contrapposte e comparate aree a "Passive management" (ricostituzione passiva, aree in cui non si sono effettuati interventi).

Le dinamiche di ricostituzione della vegetazione sono state valutate integrando differenti metodi di analisi applicati a diverse scale sia spaziali che temporali. A scala di microsito si sono rilevati, per ogni semenzale, i principali parametri ambientali e l'eventuale presenza nelle vicinanze di necromassa e/o massi. Applicando tecniche di *change-detection* a opportuni indici di stato della vegetazione (Vegetation Indices - VIs), derivati da immagini Landsat TM/ETM+ (pre- e post-incendio), si sono definite delle cartografie di severità dell'incendio per ciascun sito. Associando i VIs estratti da una crono-sequenza di immagini multispettrali con i rilievi dei dati ambientali e della rinnovazione, si sono individuate le dinamiche di ricostituzione della vegetazione. Si sono inoltre valutate, a scala di paesaggio, le relazioni fra la severità dell'incendio e i patterns della rinnovazione associati ai diversi trattamenti. A tale scopo, sono stati utilizzati dati topografici e strutturali della vegetazione estratti da dati LiDAR. L'influenza dei trattamenti sui principali parametri microclimatici è stata valutata per mezzo di misure strumentali di campo. In tale campagna di misure si sono monitorate la temperatura e l'umidità del suolo, unitamente alla stima della radiazione solare al suolo.

Differenze significative si sono evidenziate nella composizione specifica della rinnovazione tra i trattamenti. Densità di rinnovazione e diversità specifica sono risultate positivamente correlate con la presenza di necromassa legnosa. Un precoce insediamento della rinnovazione di pino si è

evidenziato nelle aree ove vi fosse presenza di materiale legnoso a terra o piante morte in piedi. Il pioppo tremolo, specie rinnovatasi prevalentemente per via vegetativa, ha invece evidenziato una dinamica di ricolonizzazione diversa dalle altre specie arboree. Anche le condizioni di copertura del suolo hanno contribuito alla definizione dei patterns di ricostituzione della copertura vegetale.

L'evidente associazione spaziale fra semenzali della rinnovazione ed elementi di necromassa conferma l'ipotesi che quest'ultima contribuisca in maniera determinante alla creazione di micrositi idonei all'insediamento della rinnovazione stessa. L'effetto di facilitazione prodotto dalla necromassa legnosa, nei riguardi dell'insediamento dei semenzali, è risultato altamente anisotropo; ciò sembra associato all'ombreggiamento prodotto dallo *shelter* legnoso sul semenzale, che proteggendo il microsito dall'eccessivo carico radiativo consente anche la conservazione di adeguati livelli di umidità nel terreno. Notevoli differenze di radiazione solare, di umidità e temperatura del suolo sono stati riscontrati tra i trattamenti, in particolare, le aree gestite a salvage logging risultano essere associate a condizioni microclimatiche piuttosto critiche per la rinnovazione. Nelle aree percorse dal fuoco ad alta severità, la disponibilità di seme è diminuita consistentemente a causa della drastica riduzione di piante porta-seme. Ciò ha permesso di individuare la distanza dalle piante porta-seme quale fattore determinante per l'insediamento della rinnovazione di *Pinus*. In relazione alle diverse scale spazio-temporali di analisi, questa ricerca evidenzia un impatto significativo dei trattamenti nei riguardi delle dinamiche di ricostituzione della vegetazione forestale. La gestione del post-incendio può incidere in maniera significativa sulle condizioni del microclima, in particolare in situazioni ambientali critiche per la rinnovazione (p.es aridità dei versanti). La presenza di necromassa legnosa consente la formazione di micrositi nei quali i valori estremi e le fluttuazioni dei parametri microclimatici si riducono, creando condizioni favorevoli per l'insediamento e la sopravvivenza dei semenzali. Per tale motivo, risulta opportuno il rilascio di piante morte in piedi o di materiale legnoso a terra durante le operazioni di ricostituzione attiva post-incendio.

Acknowledgements

A huge debt of gratitude goes to Emanuele Lingua and Raffaella Marzano for the patience in driving me through this adventure and Matteo Garbarino for the logistical help during the field-work in Aosta valley.
Thanks to the Forest Service of Barcis station (Friuli Venezia Giulia) for the logistic support to the field-activities in Cellina valley.
Thanks to Mario Pividori, Tommaso Anfodillo and the other colleagues of TeSAF department, with whom I had positive interactions.
Thanks to Francesco Pirotti for the advices concerning the RS approach.
Thanks to my daughter Gloria for spelling corrections.
Finally, I'm grateful for the availability in the review of this work and the advices to Ioannis Gitas and Jorge Castro, whose patience, suggestions and warm hospitality meant a lot to me.

Part of this project was funded by the University of Padova (Progetto di Ricerca di Ateneo 2009 – CPDA097420).